

STRESS AND DISPLACEMENT ANALYSIS
OF PLANAR STIFFENED SHELL
STRUCTURES

By

GORDON CAMPBELL STONE

Bachelor of Science
Southern Methodist University
Dallas, Texas
1960

Master of Science
Oklahoma State University
Stillwater, Oklahoma
1963

Submitted to the Faculty of the Graduate College
of the Oklahoma State University
in partial fulfillment of the requirements
for the Degree of
DOCTOR OF PHILOSOPHY
May, 1967

JAN 18 1968

STRESS AND DISPLACEMENT ANALYSIS
OF PLANAR STIFFENED SHELL
STRUCTURES

Thesis Approved:

R.E. Chapel

Thesis Adviser

Sydislaus J. Fila

R. L. Lowery

E. K. McFadden

D. D. Durbin

Dean of the Graduate College

660193

ACKNOWLEDGMENTS

The author wishes to express his appreciation to the Thesis Adviser, Associate Professor R. E. Chapel, for his advice and encouragement during the course of this study. In addition, the efforts of Associate Professor L. J. Fila, Graduate Study Committee Chairman, and those of Dr. R. L. Lowery and Dr. E. K. McLachlan, committee members, are appreciated.

Likewise, the author is grateful to his colleagues, Dr. M. U. Ayres and Mr. John Levosky, and wishes to thank his associates, Mr. Steve Burchett, Mr. Don Kinsey, Mr. John Wallace, Mr. Everett Smiley, Mr. Everett Cook, and Mr. Bill Accola, for their cooperation throughout his graduate program. The aid of the Mechanical Engineering School Staff is also recognized.

With deep gratitude, the author recognizes his wife, Martha, for her continued encouragement, understanding, and her numerous sacrifices for the completion of this undertaking.

Miss Velda Davis is thanked for her assistance rendered while typing the final manuscript.

The Army Research Office - Durham is recognized for its sponsorship of this research effort under contract Number DA-31-124-ARO-D-235.

TABLE OF CONTENTS

Chapter	Page
I. INTRODUCTION	1
II. MATRIX FORCE METHOD OF ANALYSIS	8
Basic Equations	9
Analysis of the Test Structure by the Matrix Force Method	15
Effective Area	19
Calculations of the [GIM], [GIR], and [FORCE] Matrices	22
A Flexibility Matrix Which Incorporates Poisson's Ratio and Sweep Effects	35
Transformation Into Oblique Coordinates	36
Component Energy Terms	38
Inclusion of [ALPIJ] _{prs} Into the Matrix Force Method for Analysis of the Test Structure	47
III. ANALYTICAL INVESTIGATION	53
Generation of the Matrices: [QI], [STRESS], [DELTAM], and [ARNTR]	54
Analysis by the Direct Stiffness Method	66
Analysis of the Test Structure: Structural Idealization	68
Generation of Node Point Displacements; Forces and Element Stresses	71
IV. EXPERIMENTAL ANALYSIS	78
Test Apparatus and Instrumentation	81
V. COMPARISON OF ANALYTICAL AND EXPERIMENTAL RESULTS	98
VI. CONCLUSION AND RECOMMENDATIONS	113
Recommendations for Future Work	116
A SELECTED BIBLIOGRAPHY	118

Chapter	Page
APPENDIX A - BASIC EQUATIONS, DERIVATION OF ELEMENT STIFFNESS MATRICES FOR THE DIRECT STIFFNESS METHOD	120
Basic Equations	120
Development of a Stiffness Matrix for the Planar Bar Element	121
Derivation of the Stiffness Matrix for the Triangular Plate Element	123
Determination of Deflections	128
Calculation of Stresses in the Bar Element	130
Calculation of Stresses in the Triangular Plate Element	131
APPENDIX B - STRESS ANALYSIS SYSTEM	132
Example Listing	139
APPENDIX C - A DIGITAL COMPUTER PROGRAM FOR IMPLEMENTING THE MATRIX FORCE METHOD	148
Modifications of RMATNZ	148
Modifications of WRTMAT	149
Additional Matrix Designations	149
Program Description	150
Example Listing	152
APPENDIX D - A DIGITAL COMPUTER PROGRAM FOR CALCULATING [GIM] AND [GIR]	157
APPENDIX E - TREATMENT OF EXPERIMENTAL DATA	164
Correlation of Experimental Data	166
Stress-Strain Relations	172
Data Reduction Computer Program	175
APPENDIX F - LIST OF MAJOR INSTRUMENTATION	178
APPENDIX G - CALIBRATION OF STRAIN GAGE SYSTEMS	179
Calibration of Load Recording Equipment	181
APPENDIX H - CALIBRATION OF DIAL INDICATORS	185

LIST OF TABLES

Table	Page
I. [ALPIJ] Matrix	20
II. [AREINV] Column Vector	21
III. [ALPIJ] Matrix ("WAL")	23
IV. [AREINV] Column Vector ("WAL")	24
V. [COEF] Matrix, RDC-1	25
VI. [CONST] Matrix, RDC-1	30
VII. [COEF] Matrix, RDC-2	31
VIII. [CONST] Matrix, RDC-2	32
IX. [GIM] Matrix for RDC-1	33
X. [GIM] Matrix for RDC-2	33
XI. [GIR] Matrix for RDC-1	34
XII. [GIR] Matrix for RDC-2	34
XIII. Composite [ALPIJ] _{prs}	51
XIV. [DELTAM] Matrix	62
XV. [ARNTR] Matrix	62
XVI. [DELTAM] Matrix From Extended Force Analysis	65
XVII. Load Point Displacements	73
XVIII. Force Values	92
XIX. Comparison of Deflections for LC-1	110
XX. Comparison of Deflections for LC-2	111
XXI. Comparison of Deflections for LC-3	112

Table	Page
XXII. Fortran Program for Stress Analysis System	140
XXIII. Fortran Program for Implementing the Matrix Force Method	153
XXIV. A Fortran Program for Determining the Matrices [GIM] and [GIR]	159
XXV. Correlation Coefficients	171
XXVI. Sample Data Sheet	176
XXVII. Axial and Rosette Strain Gage Data Reduction Program	177
XXVIII. Typical Indicator Readings During Calibration Tests	181
XXIX. Calibration of 5000 LB BLH U-3G1 Type Load Cell	183
XXX. Calibration of 10,000 LB BLH U-3G1 Type Load Cell	184
XXXI. Calibration of Starrett Dial Indicators	185

LIST OF FIGURES

Figure	Page
1. Possible Constraints in Panel Idealization	14
2. Structural Idealization of the Panel of Figure 13 Illustrating the Choice of Generalized Forces to be Used	17
3. Redundants Choice Number 1, "RDC-1" Redundants: Q4, Q5, Q6, Q7, Q8, Q9	25
4. Redundants Choice Number 2, "RDC-2" Redundants: Q13, Q14, Q15, Q19, Q20, Q21	25
5. Generalized Freebody and Resulting Equation of Equilibrium	26
6. Transformation of Stress Components	37
7. Sign Convention and a Typical Trapezoidal Panel	44
8. The Matrix $[S]$	45
9. The Flexibility Matrix, $[ALPIJ]_{prs}$	46
10. Second Structural Idealization Illustrating 51 Generalized Forces	48
11. Sign Convention for Section 2	49
12. Sign Convention for Section 3	50
13. Test Panel and Its Geometry	55
14. $[QI]$ Values for RDC-1, LC-1, LC-2, and LC-3	58
15. $[QI]$ Values for RDC-2, LC-1, LC-2, and LC-3	59
16. $[STRESS]$ Values for RDC-1, LC-1, LC-2, and LC-3	60
17. $[STRESS]$ Values for RDC-2, LC-1, LC-2, and LC-3	61
18. $[QI]$ Values for $[ALPIJ]_{prs}$, RDC-1, LC-1, LC-2, and LC-3	63

Figure	Page
19. [STRESS] Values for [ALPIJ] _{PRS} , RDC-1, LC-1, and LC-3	64
20. Structural Idealization Choices	69
21. Internal Forces Acting on Externally Loaded and Reaction Nodes for IDC-3	74
22. Element Stresses for IDC-3, LC-1	75
23. Element Stresses for IDC-3, LC-2	76
24. Element Stresses for IDC-3, LC-3	77
25. Experimental Facility and Structural Skin Panel	79
26. Floor Plan of Experimental Facility	80
27. Portable Strain Gage Instrumentation	82
28. Experimental Tapered Reinforced Skin Panel	83
29. Mechanical Loading System	85
30. Support System	87
31. Gage Numbering System	89
32. Gage Locations	90
33. Load Configurations	91
34. Stress Values for LC-1, Test No. 2	93
35. Stress Values for LC-2, Test No. 3	94
36. Stress Values for LC-3, Test No. 1	95
37. Axial Stresses for LC-1	102
38. Axial Stresses for LC-2	103
39. Axial Stresses for LC-3	104
40. Top Stringer Stresses for LC-1	105
41. Stringer Stresses for LC-1	106
42. Stringer Stresses for LC-2	107
43. Stringer Stresses for LC-3	108

Figure	Page
44. Shear Stresses for LC-3	109
45. Planar Bar Element	122
46. Element Dimensions	124
47. Assumed Displacement Pattern	124
48. Triangular Plate Nomenclature	125
49. Stress Resultants for Triangular Plate	127
50. Equation (A-17) Featuring the Triangular Stiffness Matrix	129
51. Deflection Diagram of Bar Element	130
52. Typical Experimental Data	166
53. Scattering of Data Points	168
54. Leg Locations and Reading Sequence	173
55. Strain Gage Bridge With Calibration Resistor	179

CHAPTER I

INTRODUCTION

The fundamental problem in the elastic analysis of aircraft structures is the determination of the distribution of stresses and displacements under prescribed loads and constraints. This problem can be readily solved for certain types of structures by direct solution of the differential equations of elasticity describing the elastic behavior of the structure. A good example of such a solution is the Engineering Theory of Bending applied to box beam structures. However, these direct solutions are usually based on certain simplifying assumptions which are too restrictive particularly when applied to structures as complex as the present day aircraft structures. Consequently, either numerical or quasi numerical methods must invariably be used in aircraft structural analysis to include the various structural effects which could not conveniently be accounted for in the direct solution type methods.

The numerical and quasi numerical methods fall basically into two groups: the first being strictly numerical methods in which the differential equations describing the deflections and/or stresses in the structure are solved by numerical procedures, and the second in which the structure is idealized into an assembly of discrete structural elements having an assumed form of stress or displacement distribution. The complete solution is then obtained by combining these individual

approximate stress or displacement distributions in a manner which satisfies the force equilibrium and displacement compatibility at the junctions of these elements. Both these groups of methods involve appreciable quantities of linear algebra which must be organized into a systematic sequence of operations and to this end the use of matrix algebra is a convenient method of defining the various processes involved in the analysis without the necessity of writing out the complete operations in full.

The rapid development of the digital computer during recent years has immensely enhanced the popularity of this second group of methods, generally referred to as finite element methods or matrix methods. Probably the most important reason for this lies in the fact that the finite element methods readily lend themselves to matrix algebra which is ideally suited for subsequent solution via the digital computer.

Finite element methods have been used extensively for the analysis of aircraft structures. However, elementary theories are often insufficient in the prediction of the stress and deformation characteristics of modern airframe configurations. Consequently, finite element methods are topics of numerous current research efforts, with new analysis capabilities being developed in terms of matrix operations of algebraic equations.

The two most widely used finite element methods are referred to as the force method and the direct stiffness or displacement method primarily due to the assumption of the initial unknown quantities. Both methods require the mathematical development of systems of finite elements, which are joined to form the idealized structure and to develop the necessary algebraic equations. The equations are generally solved by

either semi automatic or completely automatic sequence of computer operations originating with the definition of the structural configuration and terminating with the calculation of the structural response for the applied external load configurations.

The purpose of this research effort is to improve the capability for the analysis of stiffened shell structural skin panels and to demonstrate this improved capability by the comparison of experimental and analytical results. The approach taken toward this improved capability is via one of the two previously mentioned finite element methods: the matrix force method. The matrix force method is described and illustrated in Chapter II. This improved capability is verified theoretically by the direct stiffness method which is described in Chapter III. The matrix force method is implemented by digital computer programs given in Appendices C and D, respectively. The basis for ascertaining this improved capability is provided by comparison of the analytical results with those from an experimental investigation, which is described in Chapter IV.

The structure considered in this dissertation is limited to a planar oblique configuration. The structure is a monolithic semi-monocoque trapezoidal shaped panel with thin webs and integral reinforcements. This type of structure has a significant relationship with aircraft structural analysis. The words "monolithic" and "semi-monocoque" mean "being made of one integrated piece" and "stiffened shell", respectively. Until recently, airplane skin panels or "skin" type structures consisted of a very thin sheet of material to which was attached various shaped extrusions. For the purpose of analysis, these extrusions were theoretically replaced by a slender bar of circular cross section equal to that of the actual extrusion. This slender bar

element or stringer, as it later became commonly referred to, was then theoretically integrated into the thin sheet such that its centroid coincided with that of the sheet. Presently, due to the perfection of the chemical milling process, aircraft interior bulkhead and rib structures are integrated with the thin sheet -- agreeing exactly with the theoretical idealization of the older "assembled" skin type structures.

The structure under consideration is idealized as an array of rib and stringer elements transmitting axial loads and thin web elements transmitting shear and axial loads. The web elements may occasionally be referred to as plate elements in the text of this work but they are visualized as capable of carrying only loads applied within their planes. The term, plate, is commonly applied to planar structural elements which carry loads applied normal to their plane. The tapered panel is oriented to lie in the xy plane, and the deflections and stresses are produced by loads in both the x and y directions.

Finite element methods of analysis as they are presently known have many origins and no single author can be recognized for contributing entirely to their present form. Langefors (2) recognized that there is a certain resemblance between the analysis of an elastic structure and that of an electrical network. In both cases, simple members are coupled together to constitute more or less complex systems. The problem of analysis is that of finding the physical state or internal energy level of each element, in which this state is a consequence of the introduction of certain disturbances into some parts of the structure. Solution results from minimizing the potential or strain energy of the structure. Argyris (4) described in matrix form the schematic analysis of structures composed of discrete structural elements. He compiled

a number of special analysis methods which were used for structural analysis and demonstrated the similiarity among many of the analysis methods by using matrix notation to abbreviate the mathematics. Argyris bases his work mainly on simple physical arguments in contrast to Langefors' work which is based upon the concept of strain energy for deriving flexibility or stiffness expressions for individual elements.

From the background provided by Langefors, Argyris, and many others, such as Wehle and Lansing (5), Turner, et al. (6), published their work in 1956 and developed the direct stiffness method to its present form. They extended matrix methods of structural analysis to plate-type elements and described the analysis of plane stress problems with the use of finite elements. Their derivations allow the stress element to deform in a combination of certain assumed patterns. This concept eliminates the necessity for knowing the behavior of an element before its stiffness can be developed.

The version of the matrix force method of analysis used in this research effort was introduced by Wehle and Lansing (5) when they first published their work in 1952. They used the concept of strain energy and Castigliano's Second Theorem to compile a library of flexibility matrices for various individual elements and developed and extended the techniques embodied in the classical redundant force method to matrix algebra. Bruhn (7) further extended the work of Wehle and Lansing (5) and presented it in a readily usable form.

These developments in the finite element approach to the approximate analysis of reinforced panels form the basis for this investigation. The structural behavior of a panel is determined by analyzing the group behavior of small elastic elements connected at common joints to

form an idealized structure which approximates the actual panel. The structural behavior is determined by element idealizations using both the force and stiffness methods of analysis and assuming a different stress behavior for the plate elements.

In order to achieve the desired improved capability for analyzing planar, tapered stiffened shell structures, this dissertation has undertaken four distinct tasks. These tasks are:

1. A new flexibility matrix has been derived for trapezoidal shaped plate elements. This new flexibility matrix takes into account both the effects due to Poisson's ratio coupling and those due to sweep. In essence, the idealization is based upon the lumping concept. The direct-stress-carrying capacity of the structural material is concentrated along the stringers and ribs surrounding a given plate while shear carrying capacity is assigned to the panel areas contained within the plate. This derivation appears in Chapter II.
2. The matrix force method has been modified for the inclusion of the new flexibility matrix of item one, above, for analysis purposes. Analysis by this new flexibility matrix of a planar stiffened shell structure such as the one used in this investigation requires that the matrix force method be modified. This modification is comprised mainly of "building up", by special means, the flexibility matrix for the composite structure. The details for this development are given in Chapter II.
3. A digital computer program has been developed which will

implement both the modified and unmodified versions of the matrix force method. The concept employed in developing this digital computer program is that of writing a "main" program which, in turn, calls upon existing sub-routines to perform required matrix operations. Appendix D contains a detailed description of this program.

4. A regimented approach has been formulated for the determination of $[GIM]$, the matrix which contains the internal generalized load distribution due to a given external load and $[GIR]$, the matrix containing the internal generalized load distribution due to a given redundant load. This technique is based upon the writing of generalized freebody equations and the solution of these equations in a manner peculiar to the determination of $[GIM]$ and $[GIR]$. This procedure is described in detail in Chapter II.

The application of existing techniques contained within the matrix force method enhanced by the tasks given above provide an improved analysis capability for planar, tapered monolithic semi-monocyclic structures.

CHAPTER II

MATRIX FORCE METHOD OF ANALYSIS

The matrix force method is a finite element method of structural analysis which considers a structure to be an array of idealized elastic elements which are considered to be joined along their common edges. In this method of analysis, the internal generalized forces acting upon the idealized elements of the structure are considered to be the initial unknowns. In essence, the matrix force method is based upon the supposition that a large number of internal force distributions acting on the idealized elements can be in equilibrium. The correct distribution of internal forces is the one for which the mutual deformations of the elements are also compatible.

In contrast to other finite element methods, the matrix force method raises the question of statical redundancy. The degree of redundancy for the idealized structure must be determined, since the problem is directed toward the solution for redundant forces (or groups of forces). The equations of equilibrium in terms of forces are inadequate in number to determine all the internal forces and they must, therefore, be supplemented by the equations of deflection compatibility.

Although the idea of determining the degree of redundancy for the idealized structure may seem cumbersome, the force method, in general, requires a smaller number of unknowns than other finite element methods and, in turn, does not require intricate and complex computer programs

for its implementation as do other finite element methods. Also, the smaller number of unknowns required by the force method does not place such large memory requirements upon the digital computer and subsequently, in certain cases, larger and more complex structures may be analyzed on a given size computer. Even more important is the fact that the force method is a culmination of classical, established principles and theories which can be readily visualized. This gives the researcher a good "feel" for what is actually happening throughout a structural analysis by the matrix force method. From an academic standpoint, the force method of analysis may be broken down into component operations and the contribution of each operation to the final result can be distinctly identified and monitored.

The version of the matrix force method used in this analytical investigation is that which is presented by Bruhn (7). It is a special adaptation of the redundant force method to the use of the high speed digital computer.

The redundant force method is fully developed and is applied to the analysis of the planar stiffened shell tapered skin panel used in this research program. The remainder of this chapter covers new assumptions for the stress behavior for a given trapezoidal shaped plate and the surrounding stringers and ribs and the subsequent development of a new flexibility matrix based upon these assumptions.

Basic Equations

The internal forces of a statically indeterminate structure can be expressed as

$$\{q_i\} = [g_{im}]\{P_m\} + [g_{ir}]\{q_r\}, \quad (2-1)$$

where

$\{q_i\}$ = column matrix of internal forces,

$\{q_r\}$ = column matrix of redundant forces,

$\{P_m\}$ = column matrix of external loads,

$[g_{im}]$ = rectangular matrix of internal loads due to unit values of the external loads in the stable statically determinate structure or S.S.D.S.,

$[g_{ir}]$ = rectangular matrix of internal loads due to unit values of the redundants.

The redundant forces can be expressed in terms of the applied loads by requiring compatibility of deformations throughout the structure.

The internal forces can be written as

$$\{q_i\} = [G_{im}] \{P_m\}, \quad (2-2)$$

where

$$[G_{im}] = [g_{im}] - [g_{ir}] \left([g_{ri}] [\alpha_{ij}] [g_{ir}] \right)^{-1} [g_{ri}] [\alpha_{ij}] [g_{im}], \quad (2-3)$$

and

$[\alpha_{ij}]$ = square symmetric matrix of element flexibility coefficients, deflection at point i for a unit force at point j .

The two matrix triple products in Equation (2-3) may be written as

$$[g_{ri}] [\alpha_{ij}] [g_{ir}] = [a_{rs}],$$

$$[g_{ri}][\alpha_{ij}][g_{jr}] = [a_{rn}].$$

Then, Equation (2-3) may be rewritten as

$$[G_{im}] = [g_{im}] - [g_{jr}][a_{rs}]^{-1}[a_{rn}]. \quad (2-4)$$

If the product $[a_{rs}]^{-1}[a_{rn}]$ be given the symbol $[G_{sn}]$ and

the product $[g_{jr}][G_{sn}]$ be given the symbol $[G_{mp}]$, then Equation (2-4)

can be simplified to the form

$$[G_{im}] = [g_{im}] - [G_{mp}]. \quad (2-5)$$

Stress for the bar element is given by

$$\sigma_b = \frac{q_{ib}}{A_{ib}}, \quad (2-6)$$

where

q_{ib} = internal force in the bar element,

A_{ib} = cross sectional area of the bar element.

Stress for the web element is given by

$$\sigma_w = \frac{q_{iw}}{t_{iw}}, \quad (2-7)$$

where

q_{iw} = assumed constant average shear flow,

t_{iw} = thickness of web.

Deflections at the load points of the structure are given by

$$\{\delta_m\} = [A_{mn}]\{P_n\}, \quad (2-8)$$

where

$$\{\delta_m\} = \text{column of deflections,}$$

$$[A_{mn}] = [a_{mn}] - [G_{nn}] \quad = \text{square symmetric matrix of influence coefficients for the complete redundant structure, deflection at external loading point } m \text{ for a unit applied load, } P_n = 1.$$

$$[a_{mn}] = [g_{mi}] [\alpha_{ij}] [g_{im}],$$

$$[G_{nn}] = [a_{rn}] [G_{sn}].$$

In order to check the final results of a redundant force calculation after obtaining the final true forces $[G_{im}]$, the product

$$[a_{rn}]_{\text{true}} = [g_{ri}] [\alpha_{ij}] [G_{im}], \quad (2-9)$$

can be formed and compared element-by-element with the matrix previously computed,

$$[a_{rn}] = [g_{ri}] [\alpha_{ij}] [g_{im}].$$

The "true-matrix" elements (elements of $[a_{rn}]_{\text{true}}$) should be zero, or nearly so, if $[G_{im}]$ is error free.

Degree of Redundancy

If the panel in Figure 13 is built in along the root rib

and is free along the other other edges, and if there are no unstiffened cut-outs, the number of redundants, N , is given by (This constraint appears in the upper configuration of Figure 1.)

$$N = \sum_{\text{BAYS}} (\beta - 2), \quad (2-10)$$

where

β is the number of longitudinal effective stringer flanges which are continuous across a rib junction and "2" is a constant.

The number of bays is the number of transverse sections defined in the structural idealization. If a certain number of the stringer flanges are not held at the root section, the number of redundants reduces accordingly.

The degree of redundancy is illustrated for the two-dimensional panel. The number of redundants or degree of redundancy is the number of unknown forces minus the number of independent equilibrium equations which can be written for the structure.

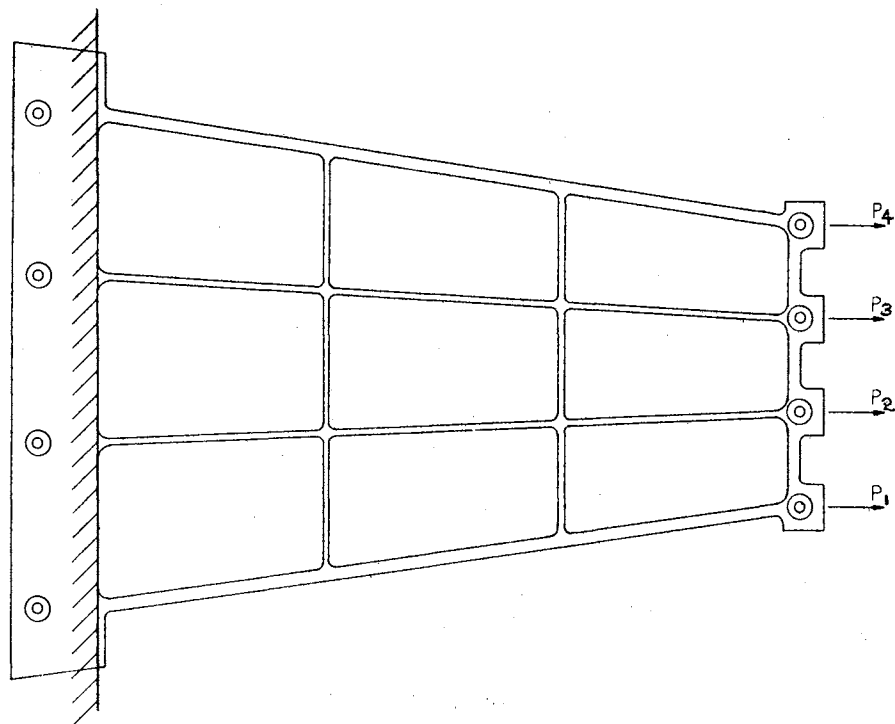
From Figure 1, the unknown forces are:

Unknown forces in longitudinal stringers	12
Unknown forces in transverse ribs	6
Unknown forces in the webs	9
	Total 27.

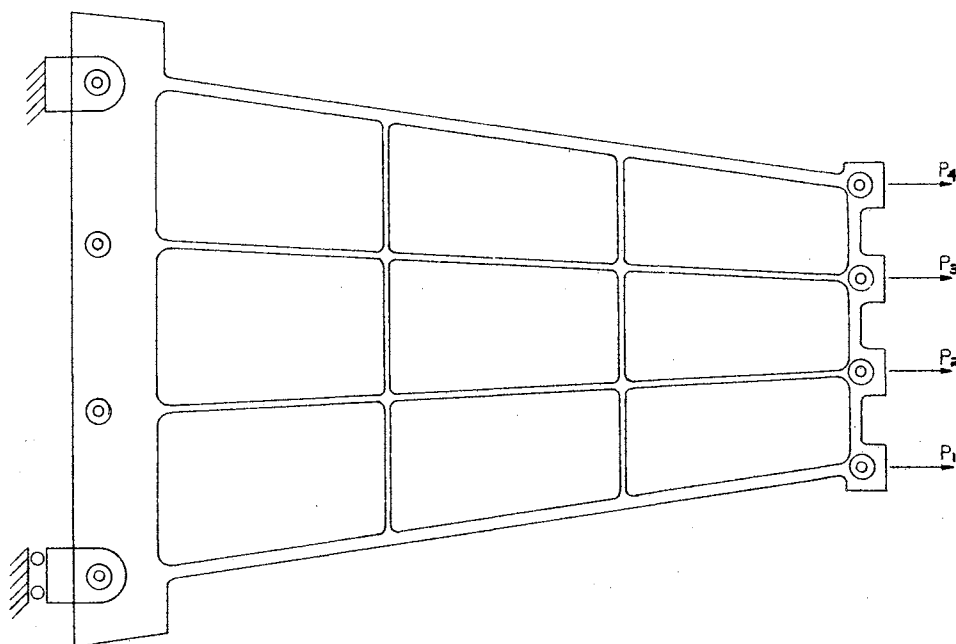
The equations of equilibrium which can be written are:

Equilibrium between the stringers and webs	12
Equilibrium between ribs and webs	9
	Total 21.

Thus, the number of redundants is: $27 - 21 = 6$.



Built-In Constraint



Statically Determinant Constraint

Figure 1. Possible Constraints in Panel Idealization

Equation (2-10) may be evaluated for N, the number of redundants, to give

$$N = \sum_{\text{BAYS}} (\beta - 2) = 3(4 - 2) = 6.$$

Therefore, it is necessary to remove six of the unknown internal forces by the use of fictitious cuts. The structure is then stable and statically determinant.

To demonstrate the change in redundancy resulting from the use of a statically determinant support system, the lower configuration shown in Figure 1 is considered.

The unknown forces are as follows:

Unknown forces in longitudinal stringers	10
Unknown forces in the transverse ribs	9
Unknown forces in the webs	9
	<u> </u>
	Total 28.

The equations of equilibrium which can be written are:

Equilibrium between stringers and webs	12
Equilibrium between ribs and webs	12
	<u> </u>
	Total 24.

The number of redundants is then: 28 - 24 = 4.

Equation (2-10) may again be evaluated for N to give

$$N = \sum_{\text{BAYS}} (\beta - 2) = 2(4 - 2) = 4.$$

Analysis of the Test Structure
by the Matrix Force Method

The Matrix Force Method is applied in the analysis of a tapered

integrally reinforced panel which is described in the experimental investigation, Chapter IV. A sketch of this panel and its geometry is shown in Figure 2.

The first step in the analysis of the test structure is to calculate the matrix $[\alpha_{ij}]$ which appears in Equation (2-3) and the terms $\frac{1}{A_{ib}}$ in Equation (2-6) and $\frac{1}{t_{iw}}$ in Equation (2-7).

The given structure was idealized into an assembly of bar and trapezoidal shaped web elements with the choice of internal generalized forces as shown in Figure 2. Each bar element was theoretically constrained to carry only a linearly varying axial load, while each web element was allowed to carry only an average constant shear flow value.

For ease of handling by the digital computer and for brevity, the matrix $[\alpha_{ij}]$ has been designated $[ALPIJ]$, and the terms $\frac{1}{A_{ib}}$ and $\frac{1}{t_{iw}}$ have been arranged to form $[AREINV]$, a column vector.

The basic strain energy equations for the bar and trapezoidal web elements are given along with sample calculations for coefficients of $[ALPIJ]$.

For a bar element with generalized loads q_i and q_j applied at each end the elements of $[ALPIJ]$ are

$$\alpha_{ii} = \frac{L}{3AE} = \alpha_{jj}, \quad (2-11)$$

$$\alpha_{ij} = \frac{L}{6AE} = \alpha_{ji}, \quad (2-12)$$

where

L = length of the bar element,

A = cross sectional area of the bar element,

E = modulus of elasticity.

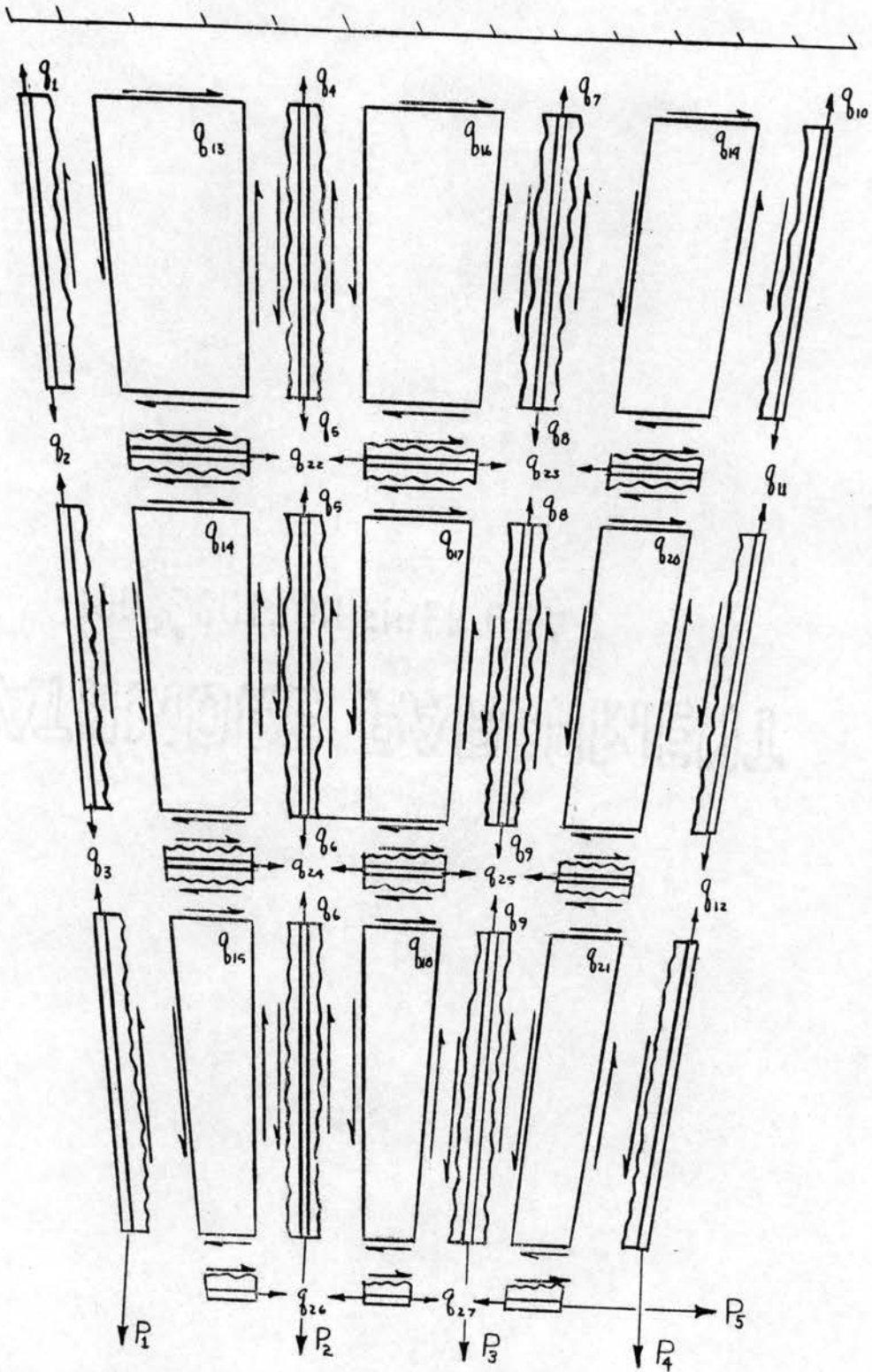


Figure 2. Structural Idealization of the Panel of Figure 13, Illustrating the Choice of Generalized Forces to be Used

For a trapezoidal shaped web element with a generalized average shear flow q_i applied along its edges, the elements of $[ALPIJ]$ are:

$$\alpha_{ij} = \frac{S}{Gt}, \quad (2-13)$$

where

S = planform area of the web element,

t = thickness of the web element,

G = modulus of rigidity.

From the theory of elasticity, the modulus or rigidity is

$$G = \frac{E}{[2(1+\nu)]}, \quad (2-14)$$

where

ν = Poisson's ratio.

ν is assumed to have a value of 0.325 which corresponds to $G = 4.0 \times 10^6$ psi, and $E = 10.6 \times 10^6$ psi. (This value of ν is shown in Table 30, p. 103, Reference 17). Therefore, Equation (2-14) becomes

$$G = \frac{E}{[2(1+0.325)]} = \frac{E}{2.65}. \quad (2-15)$$

The result of Equation (2-15) may be substituted into Equation (2-13)

to give
$$G = \frac{[(2.65)S]}{Et}. \quad (2-16)$$

The finite element distribution shown in Figure 2 may be used to determine the coefficients of $[ALPIJ]$. A few sample calculations are

$$\alpha_{44} = \frac{L}{3AE} = \frac{10.111873}{(3)(0.25)E} = \left(\frac{1}{E}\right)(13.482497),$$

$$\alpha_{2,2} = \frac{2L}{3AE} = \frac{(2)(10.111873)}{(3)(0.25)(E)} = \left(\frac{1}{E}\right)(26.964994),$$

$$\alpha_{1,2} = \frac{L}{6AE} = \frac{10.111873}{(6)(0.25)(E)} = \left(\frac{1}{E}\right)(6.741249),$$

$$\alpha_{16,16} = \frac{(2.65)S}{Et} = \frac{(2.65)(65.000)}{(0.05)(E)} = \left(\frac{1}{E}\right)(3445.000000),$$

$$\alpha_{22,22} = \frac{2L}{3AE} = \frac{(2)(6)}{(3)(0.125)(E)} = \left(\frac{1}{E}\right)(32.000000),$$

$$\alpha_{23,23} = \frac{L}{6AE} = \frac{6}{(6)(0.125)(E)} = \left(\frac{1}{E}\right)(8.000000).$$

The non-zero coefficients of the [ALPIJ] matrix are listed in Table I. The [AREINV] column vector consists of reciprocal cross sectional area values for the ends of the bar elements and reciprocal thickness values for the web elements. Sample calculations would be

$$\text{TERM } 1,1 = \frac{1}{0.25} = 4.000000,$$

$$\text{TERM } 13,1 = \frac{1}{0.05} = 20.000000,$$

$$\text{TERM } 22,1 = \frac{1}{0.125} = 8.000000.$$

The values of the [AREINV] column vector are listed in Table II.

Effective Area

An assumption widely used in aircraft design is to account for the axial load carrying capability of the web by lumping the cross-sectional area of the web with the stringers and ribs. The original cross-sectional area of the bar element, plus the appropriate web cross-sectional area, is usually referred to as effective flange area.

The amount of web area added to the stringer and/or rib area depends on the stress level, type of material, and type of loading. For

TABLE I

[ALPIJ] MATRIX

Non-Zero Values Listed

NOTE: Each Coefficient Must be Multiplied by $\frac{1}{E}$

Row	Column	Coefficient	Row	Column	Coefficient
1	1	13.4824973	12	11	6.7412485
1	2	6.7412485	12	12	26.9649940
2	1	6.7412485	13	13	3445.0000000
2	2	26.9649940	14	14	2915.0000000
2	3	6.7412485	15	15	2385.0000000
3	2	6.7412485	16	16	3445.0000000
3	3	26.9649940	17	17	2915.0000000
4	4	26.6996933	18	18	3285.0000000
4	5	13.3498465	19	19	3445.0000000
5	4	13.3498465	20	20	2915.0000000
5	5	53.3993860	21	21	3285.0000000
5	6	13.3498465	22	22	32.0000000
6	5	13.3498465	22	23	8.0000000
6	6	53.3993860	23	22	8.0000000
7	7	26.6996933	23	23	32.0000000
7	8	13.3498465	24	24	26.6666667
8	7	13.3498465	24	25	6.6666667
8	8	53.3993860	25	24	6.6666667
8	9	13.3498465	25	25	26.6666667
9	8	13.3498465	26	26	10.6666667
9	9	53.3993860	26	27	2.6666667
10	10	13.4824973	27	26	2.6666667
11	11	26.9649940	27	27	10.6666667
11	12	6.7412485			

TABLE II
 [AREINV] COLUMN VECTOR

Row	Column	Value	Row	Column	Coefficient
1	1	4.0000000	15	1	20.0000000
2	1	4.0000000	16	1	20.0000000
3	1	4.0000000	17	1	20.0000000
4	1	8.0000000	18	1	20.0000000
5	1	8.0000000	19	1	20.0000000
6	1	8.0000000	20	1	20.0000000
7	1	8.0000000	21	1	20.0000000
8	1	8.0000000	22	1	8.0000000
9	1	8.0000000	23	1	8.0000000
10	1	4.0000000	24	1	8.0000000
11	1	4.0000000	25	1	8.0000000
12	1	4.0000000	26	1	4.0000000
13	1	20.0000000	27	1	4.0000000
14	1	20.0000000			

example, by neglecting Poisson's ratio effect and assuming the same material for stringers and flat plates, one-sixth to one-half of the web cross-sectional area should be added to the stringer area. The former value applies when the field is in pure bending within its own plane, and the latter value applies when it is under uniform axial stress.

In this investigation, one-half of the web cross-sectional area has been lumped into that of the stringers and webs. The resulting effective area of each stringer varies linearly along the axis of the element while the effective area of each rib remains constant. The $[ALPIJ]$ terms for the ribs are calculated from the "unlumped" formula in the past section, but those terms for the stringers must be calculated by different means.

The $[ALPIJ]$ terms for the stringers were calculated with the use of Figures A7.34b and A7.34c of reference (7).

The non-zero elements of $[ALPIJ]$, "WAL" (web area lumped) are shown listed in Table III and the values of $[AREINV]$, "WAL" are listed in Table IV.

Calculations of the $[GIM]$, $[GIR]$, and $[FORCE]$ Matrices

Two choices of redundants were made to render the structure of Figure 13 stable and statically determinant.

Redundants choice number 1, or "RDC-1", by which the generalized forces Q_4 , Q_5 , Q_6 , Q_7 , Q_8 , and Q_9 are assumed to be redundant, is shown in Figure 3.

Redundants choice number 2, or "RDC-2", by which the generalized forces Q_{13} , Q_{14} , Q_{15} , Q_{19} , Q_{20} , and Q_{21} are assumed to be redundant, is shown in Figure 4.

TABLE III

$$\left[\begin{array}{c} \text{ALPIJ} \\ \text{("WAL")} \end{array} \right] \text{ MATRIX}$$

NOTE: Each Coefficient Must be Multiplied by $\frac{1}{E}$

Row	Column	Coefficient	Row	Column	Coefficient
1	1	7.685023	11	12	4.323387
1	2	3.939410	12	11	4.323387
2	1	3.939410	12	12	18.002341
2	2	16.712673	13	13	3445.000000
2	3	4.323387	14	14	2915.000000
3	2	4.323387	15	15	2385.000000
3	3	18.002341	16	16	3445.000000
4	4	7.224624	17	17	2915.000000
4	5	3.671207	18	18	2385.000000
5	4	3.671207	19	19	3445.000000
5	5	15.755438	20	20	2915.000000
5	6	4.138452	21	21	2385.000000
6	7	4.138452	22	22	6.400000
6	8	17.875103	22	23	1.600000
7	7	7.224624	23	22	1.600000
7	8	3.671207	23	23	6.400000
8	7	3.671207	24	24	5.333333
8	8	15.755438	24	25	1.333333
8	9	4.138452	25	24	1.333333
9	8	4.138452	25	25	5.333333
9	9	17.875103	26	26	5.333333
10	10	7.685023	26	27	1.333333
10	11	3.939417	27	26	1.333333
11	10	3.939417	27	27	5.333333
11	11	16.712673			

TABLE IV

$$\left[\text{AREINV} \right]_{(\text{WAL})}$$

COLUMN VECTOR

Row	Column	Value	Row	Column	Value
1	1	2.352941	15	1	20.000000
2	1	2.500000	16	1	20.000000
3	1	2.666667	17	1	20.000000
4	1	2.105263	18	1	20.000000
5	1	2.352941	19	1	20.000000
6	1	2.666667	20	1	20.000000
7	1	2.105263	21	1	20.000000
8	1	2.352941	22	1	1.600000
9	1	2.666667	23	1	1.600000
10	1	2.352941	24	1	1.600000
11	1	2.500000	25	1	1.600000
12	1	2.666667	26	1	2.000000
13	1	20.000000	27	1	2.000000
14	1	20.000000			

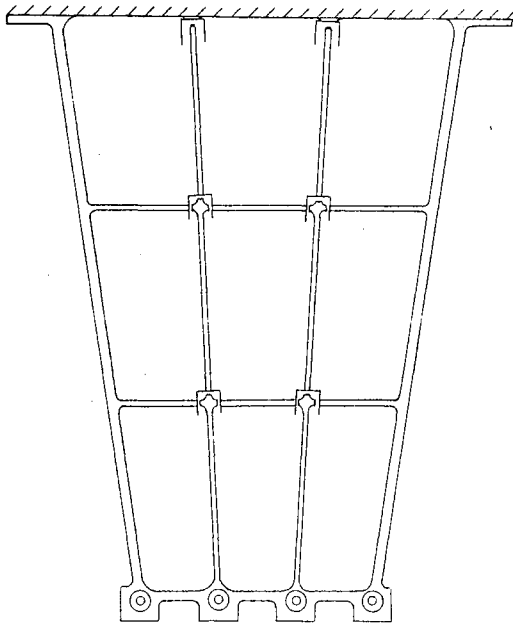


Figure 3. Redundants Choice
Number 1, "RDC-1"
Redundants: q_4 ,
 q_5 , q_6 , q_7 , q_8 , q_9 .

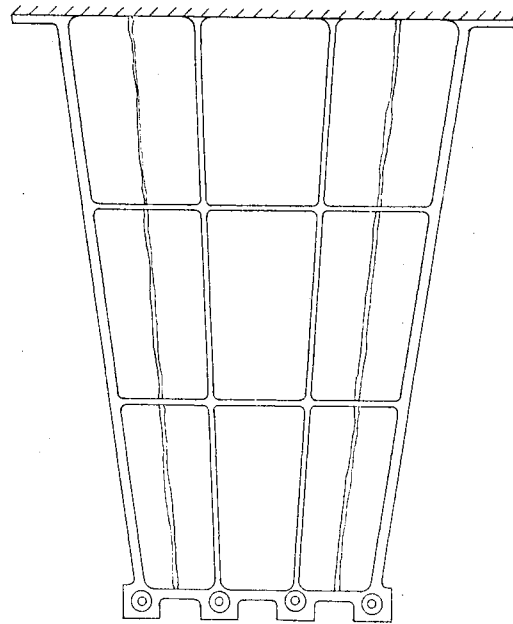


Figure 4. Redundants Choice
Number 2, "RDC-2"
Redundants: q_{13} , q_{14} ,
 q_{15} , q_{19} , q_{20} , q_{21} .

As in the case of the $[ALPIJ]$ matrix and the $[AREINV]$ column vector, the matrices $[g_{im}]$ and $[g_{ir}]$ appearing in Equation (2-1) have been designated $[GIM]$ and $[GIR]$, respectively.

The $[GIM]$ matrix is calculated by allowing each external load to have a value of 1 lb and determining the resulting internal load distribution assuming the values of the internal redundant loads to be zero.

The $[GIR]$ matrix is calculated by allowing each internal redundant load to have a value of 1 lb, assuming that the values of the external loads are zero.

The calculation of the $[GIM]$ and $[GIR]$ matrices for a structure as complex as the one under consideration becomes quite lengthy and tedious.

If local freebodies are drawn in a random manner, much repetition results and there is a high chance for error.

A more regimented and precise approach can be developed. From the degree of redundancy section, the development for the wall constraint yields a precise approach to solve for the terms of [GIM] and [GIR] in a general manner. By the use of generalized forces shown in Figure 2, twenty-one freebodies can be drawn. Twelve freebodies can be drawn containing a stringer and a web which produces twelve equations of equilibrium between the stringer and webs. Then, nine freebodies can be drawn containing a rib and a web which produces the remaining nine equations of equilibrium. An example of a freebody and resulting equilibrium equation is shown in Figure 5.

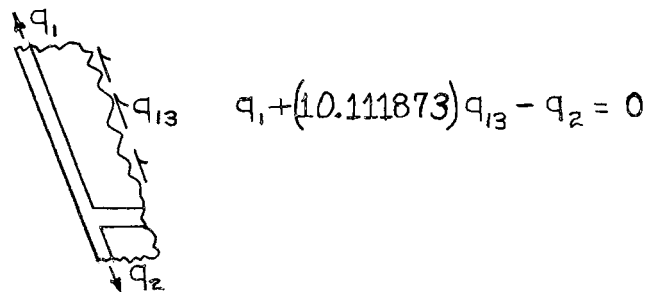


Figure 5. Generalized Freebody and Resulting Equation of Equilibrium

The twenty-one equations in twenty-seven unknowns are listed as follows:

$$q_1 - q_2 + (10.111873)q_{13} = 0,$$

$$q_2 - q_3 + (10.111873)q_{14} = 0,$$

$$q_3 + (10.111873)q_{15} = (1.0111873)P_1,$$

$$q_4 - q_5 - (10.012385)q_{13} + (10.012385)q_{16} = 0,$$

$$q_5 - q_6 - (10.012385)q_{14} + (10.012385)q_{17} = 0,$$

$$q_6 - (10.012385)q_{15} + (10.012385)q_{18} = (1.0012385)P_2,$$

$$q_7 - q_8 - (10.012385)q_{16} + (10.012385)q_{19} = 0,$$

$$q_8 - q_9 - (10.012385)q_{17} + (10.012385)q_{20} = 0,$$

$$q_9 - (10.012385)q_{18} + (10.012385)q_{21} = (1.0012385)P_3,$$

$$q_{10} - q_{11} - (10.111873)q_{19} = 0,$$

$$q_{11} - q_{12} - (10.111873)q_{20} = 0,$$

$$q_{12} - (10.111873)q_{21} = (1.0111873)P_4,$$

$$(7)q_{13} - (5)q_{14} + q_{22} = 0,$$

$$(6)q_{14} - (4)q_{15} + q_{24} = 0,$$

$$(5)q_{15} + q_{26} = P_8 + (0.5)P_7 + (0.15)P_2 + (0.025)P_2,$$

$$(7)q_{16} - (5)q_{17} - q_{22} + q_{23} = 0,$$

$$(6)q_{17} - (4)q_{18} - q_{24} + q_{25} = 0,$$

$$(5)q_{18} - q_{26} + q_{27} = (0.5)P_7 - (0.5)P_6 - (0.025)P_3 + (0.025)P_2,$$

$$(7)q_{19} - (5)q_{20} - q_{23} = 0,$$

$$(6)q_{20} - (4)q_{21} - q_{25} = 0,$$

$$-(5)q_{21} + q_{27} = P_8 + (0.15)P_4 + (0.025)P_3 + (0.5)P_6.$$

It is to be noted that all input data were read into the digital computer with six digits to the right of the decimal point regardless of their appearance in any figure, table, or example listing.

It has been established that six of the unknowns are redundant. When a choice of redundants is made, the appropriate "q" values can be transferred to the right side of the equal sign with the external loads. Now, there are twenty-one unknowns since the redundant "q" values are either one or zero, depending upon whether the elements of $[GIM]$ or those of $[GIR]$ are sought. Twenty-one linear simultaneous equations are the result. These equations can be transformed into a matrix equation consisting of a matrix of coefficients, a column vector representing the unknowns and a matrix of constants. The coefficients matrices for RDC-1 and RDC-2 are shown in Tables V and VII and the matrices of constants for both choices of redundants are shown in Tables VI and VIII.

A digital computer program was developed for solving the two sets of equations and determining $[GIM]$ and $[GIR]$ automatically. An explanation of that program is given in Appendix D. $[GIM]$, "RDC-1", "RDC-2", and $[GIR]$, "RDC-1", "RDC-2", are listed in Tables IX, X, XI, and XII, respectively.

The $\{P_m\}$ column matrix of Equation (2-1) has been designated $[FORCE]$ and it consists of the actual values of the external loads.

Three load configurations (see Figure 33, Chapter IV) were used in this investigation, and $[FORCE]$ matrices corresponding to these configurations are shown in Table XVIII of Chapter IV.

TABLE V
 [COEF] MATRIX, RDC-1
 Non-Zero Elements Listed

Row	Col	Coeff	Row	Col	Coeff
1	1	1.000000	10	4	1.000000
1	2	-1.000000	10	5	-1.000000
1	7	10.111873	10	13	-10.111873
2	2	1.000000	11	1	1.000000
2	3	-1.000000	11	6	-1.000000
2	8	10.111873	11	14	-10.111873
3	3	1.000000	12	6	-1.000000
3	9	10.111873	12	15	-10.111873
4	7	-10.012385	13	7	7.000000
4	10	10.012385	13	8	-5.000000
5	8	-10.012385	13	16	1.000000
5	11	10.012385	14	8	6.000000
6	9	-10.012385	14	9	-4.000000
6	12	10.012385	14	18	1.000000
7	10	-10.012385	15	9	5.000000
7	13	10.012385	15	20	1.000000
8	11	-10.012385	16	10	7.000000
8	14	10.012385	16	11	-5.000000
9	12	-10.012385	16	16	-1.000000
9	15	10.012385	16	17	1.000000
17	11	6.000000	19	14	-5.000000
17	12	-4.000000	19	14	-5.000000
17	18	-1.000000	20	14	6.000000
17	19	1.000000	20	15	-4.000000
18	12	5.000000	20	19	-1.000000
18	20	-1.000000	21	15	-5.000000
18	21	1.000000	21	21	1.000000
19	13	7.000000			

TABLE VI
 [CONST] MATRIX

RDC-1

Non-Zero Values Listed

Row	Column	Coefficient	Row	Column	Coefficient
3	1	1.0111873	8	11	1.0000000
4	6	-1.0000000	12	4	1.0111873
4	7	1.0000000	15	1	0.1500000
5	7	-1.0000000	15	2	0.0250000
5	8	1.0000000	18	2	0.0250000
6	2	1.0012385	18	3	-0.0250000
6	8	-1.0000000	21	3	0.0250000
7	9	-1.0000000	21	4	0.1500000
7	10	1.0000000	21	5	1.0000000
8	10	-1.0000000			

TABLE VII
 [COEF] MATRIX, RDC-2
 Non-Zero Values Listed

Row	Col	Coeff	Row	Col	Coeff
1	1	1.000000	10	11	-1.000000
1	2	-1.000000	11	11	1.000000
2	2	1.000000	11	12	-1.000000
2	3	-1.000000	12	12	1.000000
3	3	1.000000	13	16	1.000000
4	4	1.000000	14	18	1.000000
4	5	-1.000000	15	20	1.000000
4	13	10.012385	16	13	7.000000
5	5	1.000000	16	14	-5.000000
5	6	-1.000000	16	16	-1.000000
5	14	10.012385	16	17	1.000000
6	6	-1.000000	17	14	6.000000
6	15	10.012385	17	15	-4.000000
7	7	1.000000	17	18	-1.000000
7	8	-1.000000	17	18	-1.000000
7	13	-10.012385	17	19	1.000000
8	8	1.000000	18	15	5.000000
8	9	-1.000000	18	20	-1.000000
8	14	-10.012385	18	21	1.000000
9	9	1.000000	19	17	-1.000000
9	15	-10.012385	20	19	-1.000000
10	10	1.000000	20	21	1.000000

TABLE VIII

[CONST] MATRIX, RDC-2

Non-Zero Values Listed

Row	Col	Coeff	Row	Col	Coeff
1	6	-10.1118730	13	7	5.0000000
2	7	-10.1118730	14	7	-6.0000000
3	1	1.0111873	14	8	4.0000000
3	8	-10.1118730	15	1	0.1500000
4	6	10.0123850	15	2	0.0250000
5	7	10.0123850	15	8	-5.0000000
6	2	1.0012385	18	2	0.0250000
6	8	10.0123850	18	3	-0.0250000
7	9	-10.0123850	19	9	-7.0000000
8	10	-10.0123850	19	10	5.0000000
9	3	1.0012385	20	10	-6.0000000
9	11	-10.0123850	20	11	4.0000000
10	9	10.1118730	21	3	0.0250000
11	10	10.1118730	21	4	0.1500000
12	4	1.0118730	21	5	1.0000000
12	11	10.1118730	21	11	5.0000000
13	6	-7.0000000			

TABLE IX

[GIM] MATRIX FOR RDC-1

i \ m	P ₁ =1	P ₂ =1	P ₃ =1	P ₄ =1	P ₅ =1
1	0.7746	0.6003	0.4084	0.2143	1.4450
2	0.8223	0.6164	0.3923	0.1667	1.1240
3	0.8889	0.6388	0.3699	0.1000	0.6741
4	0	0	0	0	0
5	0	0	0	0	0
6	0	0	0	0	0
7	0	0	0	0	0
8	0	0	0	0	0
9	0	0	0	0	0
10	0.2143	0.4084	0.6003	0.7746	-1.4450
11	0.1667	0.3923	0.6164	0.0223	-1.1240
12	0.1000	0.3699	0.6388	0.8889	-0.6741
13	0.0047	0.0016	-0.0016	-0.0047	-0.0318
14	0.0066	0.0022	-0.0022	-0.0066	-0.0444
15	0.0099	-0.0621	-0.0366	-0.0099	-0.0667
16	0.0047	0.0016	-0.0016	-0.0047	-0.0318
17	0.0066	0.0022	-0.0022	-0.0066	-0.0444
18	0.0099	0.0366	-0.0366	-0.0099	-0.0667
19	0.0047	-0.0016	-0.0016	-0.0047	-0.0318
20	0.0066	0.0022	-0.0022	-0.0066	-0.0444
21	0.0099	0.0366	0.0632	-0.0099	-0.0667
22	0	0	0	0	0
23	0	0	0	0	0
24	0	-0.2660	-0.1330	0	0
25	0	-0.1330	-0.2660	0	0
26	0.0989	0.3408	0.1829	0.0495	0.3333
27	0.0495	0.1829	0.3406	0.0989	0.6667

TABLE X

[GIM] MATRIX FOR RDC-2

i \ m	P ₁ =1	P ₂ =1	P ₃ =1	P ₄ =1	P ₅ =1
1	1.0112	0	0	0	0
2	1.0112	0	0	0	0
3	1.0112	0	0	0	0
4	-0.6457	0.7867	0.2146	0.6437	4.2910
5	-0.5006	0.8344	0.1669	0.5006	3.3370
6	-0.3004	0.9011	0.1001	0.3004	2.0020
7	0.6437	0.2146	0.7867	-0.6437	-4.2910
8	0.5006	0.1669	0.8344	-0.5006	-3.3370
9	0.3004	0.1001	0.9011	-0.3004	-2.0020
10	0	0	0	1.0110	0
11	0	0	0	1.0110	0
12	0	0	0	1.0110	0
13	0	0	0	0	0
14	0	0	0	0	0
15	0	0	0	0	0
16	0.0143	0.0048	-0.0048	-0.0143	-0.0952
17	0.0200	0.0067	-0.0067	-0.0200	-0.1333
18	0.0300	0.0100	-0.0100	-0.0300	-0.2000
19	0	0	0	0	0
20	0	0	0	0	0
21	0	0	0	0	0
22	0	0	0	0	0
23	0	0	0	0	0
24	0	0	0	0	0
25	0	0	0	0	0
26	0.1500	0.0250	0	0	0
27	0	0	0.0250	0.1500	1.0000

TABLE XI

[GIR] MATRIX FOR RDC-2

i \ r	q ₄ =1	q ₅ =1	q ₆ =1	q ₇ =1	q ₈ =1	q ₉ =1
1	0	0	-0.3366	-0.3366	0	0
2	0	-0.6733	0	0	-0.3366	0
3	0	0	-0.6733	0	0	-0.3366
4	1.0000	0	0	0	0	0
5	0	1.0000	0	0	0	0
6	0	0	1.0000	0	0	0
7	0	0	0	1.0000	0	0
8	0	0	0	0	1.0000	0
9	0	0	0	0	0	1.0000
10	-0.3366	0	0	-0.6733	0	0
11	0	-0.3366	0	0	-0.6733	0
12	0	0	-0.3366	0	0	-0.6733
13	0.0666	-0.0666	0	0.0333	-0.0333	0
14	0	0.0666	-0.0666	0	0.0333	-0.0333
15	0	0	0.0666	0	0	0.0333
16	-0.0333	0.0333	0	0.0333	-0.0333	0
17	0	-0.0333	0.0333	0	0.0333	-0.0333
18	0	0	-0.0333	0	0	0.0333
19	-0.0333	0.0333	0	-0.0666	0.0666	0
20	0	-0.0333	0.0333	0	-0.0666	0.0666
21	0	0	-0.0333	0	0	-0.0666
22	-0.4661	0.7990	-0.3333	-0.2330	0.3995	-0.1665
23	-0.2330	0.3995	-0.1665	-0.4661	0.7990	-0.3329
24	0	-0.3995	0.6658	0	-0.1998	0.3329
25	0	-0.1998	0.3329	0	-0.3995	0.6658
26	0	0	-0.3329	0	0	0.1665
27	0	0	-0.1665	0	0	-0.3329

TABLE XII

[GIR] MATRIX FOR RDC-2

i \ r	q ₁₃ =+1	q ₁₄ =+1	q ₁₅ =+1	q ₁₉ =+1	q ₂₀ =+1	q ₂₁ =+1
1	-10.1120	-10.1120	0	0	0	0
2	0	-10.1120	-10.1120	0	0	0
3	0	0	-10.1120	0	0	0
4	20.0200	20.0200	20.0200	10.0100	10.0100	10.0100
5	0	20.0200	20.0200	0	10.0100	10.0100
6	0	0	20.0200	0	0	10.0100
7	-10.0100	-10.0100	-10.0100	-20.0200	-20.0200	-20.0200
8	0	-10.0100	-10.0100	0	-20.0200	-20.0200
9	0	0	-10.0100	0	0	-20.0200
10	0	0	0	10.1100	10.1100	10.1100
11	0	0	0	0	10.1100	10.1100
12	0	0	0	0	0	10.1100
13	1.0000	0	0	0	0	0
14	0	1.0000	0	0	0	0
15	0	0	1.0000	0	0	0
16	-1.0000	0	0	-1.0000	0	0
17	0	-1.0000	0	0	-1.0000	0
18	0	0	-1.0000	0	0	-1.0000
19	0	0	0	1.0000	0	0
20	0	0	0	0	1.0000	0
21	0	0	0	0	0	1.0000
22	-7.0000	5.0000	0	0	0	0
23	0	0	0	7.0000	-5.0000	0
24	0	-6.0000	4.0000	0	0	0
25	0	0	0	0	6.0000	-4.0000
26	0	0	-5.0000	0	0	0
27	0	0	0	0	0	5.0000

A Flexibility Matrix Which Incorporates
Poisson's Ratio and Sweep Effects

The standard approach to analyzing stiffened shell structures has been shown. The structure was idealized into an array of bar and plate elements. The stringers and ribs were assumed to carry only a linearly varying axial stress while the plates were assumed to carry only a constant average shear stress. In order to account for the axial stress carrying capacity of the plates, a discrete amount of plate cross sectional area was added to that of the bar elements bordering a particular plate. Two $[ALPIJ]$ matrices were developed. One $[ALPIJ]$ matrix allowed for no lumping of plate areas while the other $[ALPIJ]$ matrix contained terms which allowed for one-half of the plate cross sectional area to be lumped into the adjacent bar element.

This method is approximately correct for rectangular or nearly rectangular panels, but in its present form neglects two couplings which impose a restriction on its application:

1. The coupling between direct stresses which is referred to as Poisson's ratio coupling.
2. The coupling between shear stresses and the direct stresses existing in oblique panels.

In a recent paper, Grjedzielski (8) showed that both Poisson's ratio and sweep in coupling can be accounted for in a rational manner. In essence, the idealization is based upon the lumping concept, wherein the direct-stress-carrying capacity of the structural material is concentrated along the stringers and ribs surrounding a given plate and shear carrying capacity is assigned to the panel areas contained within

the plate. Although this has the appearance of the axial-force-member, shear panel idealization, the Poisson's ratio and sweep effects are taken into account by incorporating them into the flexibility matrix.

Subsequently a new flexibility matrix for a trapezoidal shaped plate is derived which takes into account effects due to Poisson's ratio and sweep.

The strain energy of a plate can be given by

$$U = \frac{1}{2} \frac{t}{E} \iint [\sigma_x^2 + \sigma_y^2 - 2\nu\sigma_x\sigma_y + 2(1+\nu)\tau_{xy}^2] dA. \quad (2-17)$$

Here, the integrals of σ_x^2 and σ_y^2 are interpreted as strain energy of the stringers and ribs bordering a web, respectively, and the integral of τ_{xy}^2 as the energy of panels and webs. The integral of $\sigma_x\sigma_y$ represents the cross coupling due to Poisson's ratio.

Transformation Into Oblique Coordinates

To change from rectangular coordinates x, y to trapezoidal ones u, ψ , the following transformation holds (This transformation is shown in Figure 6.):

$$x = u, \quad y = u \tan \psi. \quad (2-18)$$

The stress components will be used as follows:

- (a) Stress components of the system u, ψ : $\sigma_u, \sigma_\psi, \tau_{u\psi}$,
- (b) Stress components of the auxiliary system x, y : $\sigma_x, \sigma_y, \tau_{xy}$,
- (c) Stress components of the grid system: $\sigma_s, \sigma_r, \tau_p$,

where σ_s and σ_r are the direct stress of the stringer and rib caps, respectively, and τ_p is the average panel shearing stress.

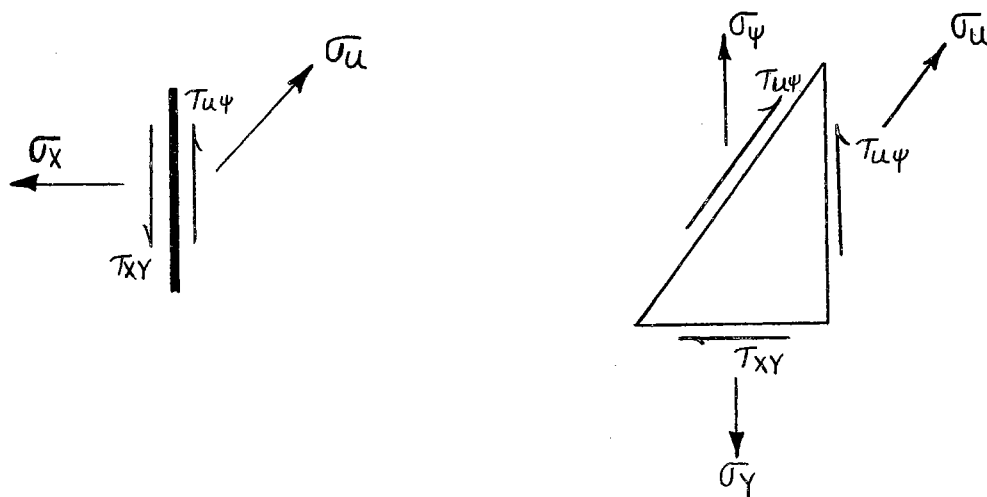
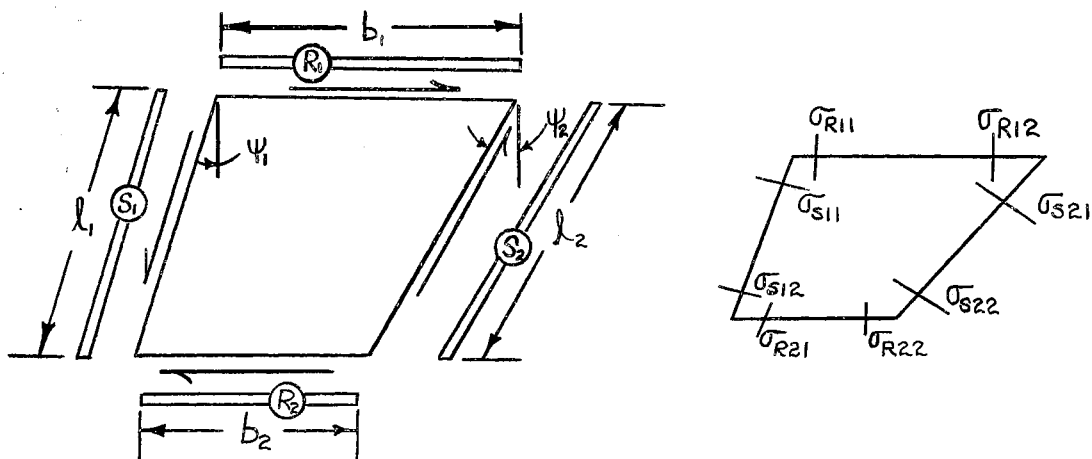


Figure 6. Transformation of Stress Components

From the consideration of equilibrium of stresses at a point, the following transformation equations between the stress components (a) and (b) may be written (These equations are written from Figure 6.):

$$\begin{aligned} \tau_{xy} &= \tau_{u\psi} + \sigma_u \sin\psi, \\ \sigma_x &= \sigma_u \cos\psi, \\ \sigma_y &= \sigma_\psi \sec\psi + 2\tau_{u\psi} \tan\psi + \sigma_u \sin\psi \tan\psi. \end{aligned} \quad (2-19)$$

Strain energy of the panels in terms of the trapezoidal coordinates is obtained by substitution of Equation (2-19) into Equation (2-17). After replacing the integration element $dx dy$ by $u du \cdot d\psi \sec^2\psi$, there results

$$\begin{aligned} U = \frac{t}{2E} \iint & \left[\sigma_u^2 + \sigma_\psi^2 - 2(\sqrt{3} \cos^2\psi - \sin^2\psi) \sigma_u \sigma_\psi \right. \\ & \left. + 4 \sin\psi (\sigma_u + \sigma_\psi) \tau_{u\psi} + \left(\frac{E}{G} \cos^2\psi + 4 \sin^2\psi \right) \tau_{u\psi}^2 \right] \frac{u du d\psi}{\cos^4\psi}. \end{aligned} \quad (2-20)$$

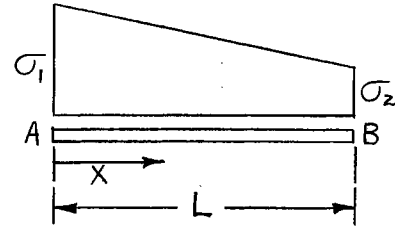
For lumping theory, the particular terms have the following meaning: The $\tau_{u\psi}^2$ term represents the shear energy of the panel. The σ_u^2 and σ_ψ^2 terms are interpreted as bending energy of stringers and ribs. The term containing $\sigma_u \sigma_\psi$ introduces the Poisson's ratio coupling. Finally, the term $4 \sin\psi (\sigma_u + \sigma_\psi) \tau_{u\psi}$ takes care of the coupling due to the sweep angle.

Component Energy Terms

For the contribution of the flange stresses to the total strain energy, a flange AB with stresses σ_1 and σ_2 at the ends A and B, respectively, is considered. There results

$$\sigma_x = \frac{\sigma_1(L-x)}{L} + \sigma_2\left(\frac{x}{L}\right),$$

$$\sigma_x^2 = \frac{\sigma_1^2(L-x)^2}{L^2} + \frac{\sigma_2^2 x^2}{L^2} + \frac{2\sigma_1\sigma_2(xL-x^2)}{L^2}.$$



Hence, the energy possessed by the flanges can be stated as

$$\begin{aligned} U &= \frac{AL}{2E} \int_0^L \sigma^2 dx \\ &= \frac{AL}{2E} \int_0^L \left[\frac{\sigma_1^2(L-x)^2}{L^2} + \frac{\sigma_2^2 x^2}{L^2} + \frac{2\sigma_1\sigma_2(xL-x^2)}{L^2} \right] dx \\ &= \frac{AL}{2E} (\sigma_1^2 + \sigma_2^2 + \sigma_1\sigma_2), \end{aligned}$$

where σ_1 , σ_2 are the direct stresses at each end of a lumped flange and will be equal to the node force divided by the corresponding lumped area.

Strain energy U_p corresponding to the state of shear T_p is evaluated by integration. Thus U_p is given up

$$U_p = \frac{1}{2E} \iint \left[\frac{E}{G} \cos^2\psi + 4\sin^2\psi \right] T_{u\psi}^2 \frac{u du d\psi}{\cos^4\psi}.$$

An expression for τ_{ux} is

$$T_{u\psi} = T_p \frac{u_1 u_2}{u^2},$$

$$U_p = \frac{1}{2E} \int_{\psi_1}^{\psi_2} \int_{u_1}^{u_2} \left[\frac{E}{G} \frac{1}{\cos^2\psi} + \frac{4\sin^2\psi}{\cos^4\psi} \right] \frac{u_1^2 u_2^2}{u^3} T_p^2 du d\psi,$$

$$\begin{aligned}
&= \frac{+}{2G} \int_{\psi_1}^{\psi_2} \left[\frac{1}{\cos^2 \psi} + \frac{4G}{E} \frac{\sin^2 \psi}{\cos^4 \psi} \right] \left(\frac{u_2^2 - u_1^2}{2} \right) T_P^2 d\psi \\
&= \frac{+T_P^2}{2G} \left(\frac{u_2^2 - u_1^2}{2} \right) \left[\tan \psi_2 - \tan \psi_1 + \frac{4G}{3E} (\tan^3 \psi_2 - \tan^3 \psi_1) \right] \\
&= \left(\frac{u_2^2 - u_1^2}{2} \right) (\tan \psi_2 - \tan \psi_1) \left[\frac{+T_P^2}{2G} \left[1 + \frac{4G}{3E} (\tan^2 \psi_2 + \tan \psi_1 \tan \psi_2 + \tan^2 \psi_1) \right] \right] \\
&= A_P \frac{+T_P^2}{2G} \left[1 + \frac{4G}{3E} (\tan^2 \psi_1 + \tan \psi_1 \tan \psi_2 + \tan^2 \psi_2) \right],
\end{aligned}$$

where $A_P = \frac{u_2^2 - u_1^2}{2} (\tan \psi_2 - \tan \psi_1)$

= area of the plate.

Strain energy corresponding to Poisson's ratio and shear couplings vis. $\sigma_u \sigma_\psi$, $\sigma_u \tau_{u\psi}$ and $\sigma_\psi \tau_{u\psi}$ is obtained by taking the value of each product due to the four node values, summing them up and taking the average to represent the plate.

The total strain energy for the four flanges and the plate is given by

$$\begin{aligned}
U &= \frac{A_1 b_1}{6E} (\sigma_{R11}^2 + \sigma_{R12}^2 + \sigma_{R11} \sigma_{R12}) \\
&+ \frac{A_2 b_2}{6E} (\sigma_{R21}^2 + \sigma_{R22}^2 + \sigma_{R21} \sigma_{R22}) \\
&+ \frac{A_3 l_1}{6E} (\sigma_{S11}^2 + \sigma_{S12}^2 + \sigma_{S11} \sigma_{S12}) \\
&+ \frac{A_4 l_2}{6E} (\sigma_{S21}^2 + \sigma_{S22}^2 + \sigma_{S21} \sigma_{S22})
\end{aligned}$$

$$\begin{aligned}
& -\frac{1}{2E} \cdot 2(\sqrt{\cos^2\psi_1 - \sin^2\psi_1}) \frac{\cos\psi_1}{4} (l_1 b_1 \sigma_{S11} \sigma_{R11} + l_1 b_2 \sigma_{S12} \sigma_{R21}) \\
& -\frac{1}{2E} \cdot 2(\sqrt{\cos^2\psi_2 - \sin^2\psi_2}) \frac{\cos\psi_2}{4} (l_2 b_1 \sigma_{R12} \sigma_{S21} + l_2 b_2 \sigma_{R22} \sigma_{S22}) \\
& + \frac{1}{2E} \cdot 4 \sin\psi_1 \cdot \frac{TP}{4} [l_1 b_1 (\sigma_{S11} + \sigma_{R11}) + l_1 b_2 (\sigma_{S12} + \sigma_{R21})] \\
& + \frac{1}{2E} \cdot 4 \sin\psi_2 \cdot \frac{TP}{4} [l_2 b_1 (\sigma_{R12} + \sigma_{S21}) + l_2 b_2 (\sigma_{R22} + \sigma_{S22})] \\
& + \frac{b_1 + b_2}{2} \cdot \frac{l_1 \cos\psi_1}{G} \cdot \frac{1}{2} \left[1 + \frac{4G}{3E} (\tan^2\psi_1 + \tan\psi_1 \tan\psi_2 + \tan^2\psi_2) \right].
\end{aligned}$$

Castigliano's second theorem states that a displacement δ_i can be derived from the strain energy U , expressed in terms of the applied loads P , as

$$\delta_i = \frac{\partial U}{\partial P_i},$$

where P_i is the loading in the direction of the displacement δ_i . The expression for δ_i may be written as

$$\delta_i = \frac{\partial U}{\partial P_i} = \frac{\partial U}{\partial \sigma_j} \cdot \frac{\partial \sigma_j}{\partial P_i} = \frac{\partial \sigma_j}{\partial P_i} [S] \{\sigma\}.$$

But the expression for stress, σ_j , is

$$\sigma_j = \frac{P_j}{A_j}.$$

Therefore, the partial derivative of σ_j with respect to P_i is

$$\frac{\partial \sigma_j}{\partial P_i} = \delta_{ij} \cdot \frac{1}{A_j},$$

where δ_{ij} is the Kronecker delta. Then the expression for δ_i may be written as

$$\delta_i = \left[\frac{1}{A} \right] [S] \{\sigma\} = \left[\frac{1}{A} \right] [S] \left[\frac{1}{A} \right] \{P\},$$

where the expression for the flexibility matrix $[\alpha_{ij}]$ is

$$\left[\frac{1}{A}\right][S]\left[\frac{1}{A}\right] = [\alpha_{ij}].$$

$[S]$ can be obtained by differentiating the strain energy with respect to each stress term separately. Differentiating

$$\begin{aligned} \frac{\partial U}{\partial \sigma_{R11}} &= \frac{A_1 b_1}{6E} (2\sigma_{R11} + \sigma_{R22}) - \frac{t}{E} (\sqrt{\cos^2 \psi_1 - \sin^2 \psi_1}) \frac{\cos \psi_1}{4} (l_1 b_1 \sigma_{S11}) \\ &\quad + \frac{t}{2E} \sin \psi_1 T_P(l_1 b_1), \end{aligned}$$

$$\begin{aligned} \frac{\partial U}{\partial \sigma_{R12}} &= \frac{A_1 b_1}{6E} (2\sigma_{R12} + \sigma_{R11}) - \frac{t}{E} (\sqrt{\cos^2 \psi_2 - \sin^2 \psi_2}) \frac{\cos \psi_2}{4} (l_2 b_1 \sigma_{S21}) \\ &\quad + \frac{t}{2E} \sin \psi_2 T_P(l_2 b_1), \end{aligned}$$

$$\begin{aligned} \frac{\partial U}{\partial \sigma_{R21}} &= \frac{A_2 b_2}{6E} (2\sigma_{R21} + \sigma_{R22}) - \frac{t}{E} (\sqrt{\cos^2 \psi_1 - \sin^2 \psi_1}) \frac{\cos \psi_1}{4} (l_1 b_2 \sigma_{S12}) \\ &\quad + \frac{t}{2E} \sin \psi_1 T_P(l_1 b_2), \end{aligned}$$

$$\begin{aligned} \frac{\partial U}{\partial \sigma_{R22}} &= \frac{A_2 b_2}{6E} (2\sigma_{R22} + \sigma_{R21}) - \frac{t}{E} (\sqrt{\cos^2 \psi_2 - \sin^2 \psi_2}) \frac{\cos \psi_2}{4} (l_2 b_2 \sigma_{S22}) \\ &\quad + \frac{t}{2E} \sin \psi_2 T_P(l_2 b_2), \end{aligned}$$

$$\begin{aligned} \frac{\partial U}{\partial \sigma_{S11}} &= \frac{A_3 l_1}{6E} (2\sigma_{S11} + \sigma_{S12}) - \frac{t}{E} (\sqrt{\cos^2 \psi_1 - \sin^2 \psi_1}) \frac{\cos \psi_1}{4} (l_1 b_1 \sigma_{R11}) \\ &\quad + \frac{t}{2E} \sin \psi_1 T_P(l_1 b_1), \end{aligned}$$

$$\begin{aligned} \frac{\partial U}{\partial \sigma_{S12}} &= \frac{A_3 l_1}{6E} (2\sigma_{S12} + \sigma_{S11}) - \frac{t}{E} (\sqrt{\cos^2 \psi_1 - \sin^2 \psi_1}) \frac{\cos \psi_1}{4} (l_1 b_2 \sigma_{R21}) \\ &\quad + \frac{t}{2E} \sin \psi_1 T_P(l_1 b_2), \end{aligned}$$

$$\frac{\partial U}{\partial \sigma_{S21}} = \frac{A_4 l_2}{6E} (2\sigma_{S21} + \sigma_{S22}) - \frac{t}{E} (\sqrt{\cos^2 \psi_2 - \sin^2 \psi_2}) \frac{\cos \psi_2}{4} (l_2 b_1 \sigma_{R12})$$

$$+ \frac{t}{2E} \sin \psi_2 T_P (l_2 b_1),$$

$$\frac{\partial U}{\partial \sigma_{S22}} = \frac{A_4 l_2}{6E} (2\sigma_{S22} + \sigma_{S21}) - \frac{t}{E} (\sqrt{\cos^2 \psi_2 - \sin^2 \psi_2}) \frac{\cos \psi_2}{4} (l_2 b_2 \sigma_{R22})$$

$$+ \frac{t}{2E} \sin \psi_2 T_P (l_2 b_2),$$

$$\frac{\partial U}{\partial T_P} = \frac{t}{2E} \sin \psi_1 \left[l_1 b_1 (\sigma_{S11} + \sigma_{R11}) + l_1 b_2 (\sigma_{S12} + \sigma_{R21}) \right]$$

$$+ \frac{t}{2E} \sin \psi_2 \left[l_2 b_1 (\sigma_{R12} + \sigma_{S21}) + l_2 b_2 (\sigma_{R22} + \sigma_{S22}) \right]$$

$$+ (b_1 + b_2) \frac{l_1 \cos \psi_1}{G} + T_P \left[1 + \frac{4G}{3E} (\tan^2 \psi_1 + \tan \psi_1 \tan \psi_2 + \tan^2 \psi_2) \right],$$

where A_1 , A_2 , A_3 , and A_4 are the total lumped areas in sections normal to ribs R_1 , R_2 , and stringers S_1 and S_2 . The equations above may now be transformed into matrix notation such that

$$\frac{\partial U}{\partial \sigma_i} = [S] \{ \sigma \}.$$

The $[S]$ matrix is shown in Figure 8.

The matrix triple product $\left[\frac{1}{A}\right][S]\left[\frac{1}{A}\right]$ may now be formed, the result of which is the final flexibility matrix which incorporates the effects of Poisson's ratio and sweep. Henceforth, this matrix will be referred to as $[ALPIJ]_{\text{prs}}$. $[ALPIJ]_{\text{prs}}$ is shown in Figure 9.

The sign convention for $[ALPIJ]_{\text{prs}}$ for a typical trapezoidal panel is shown in Figure 7.

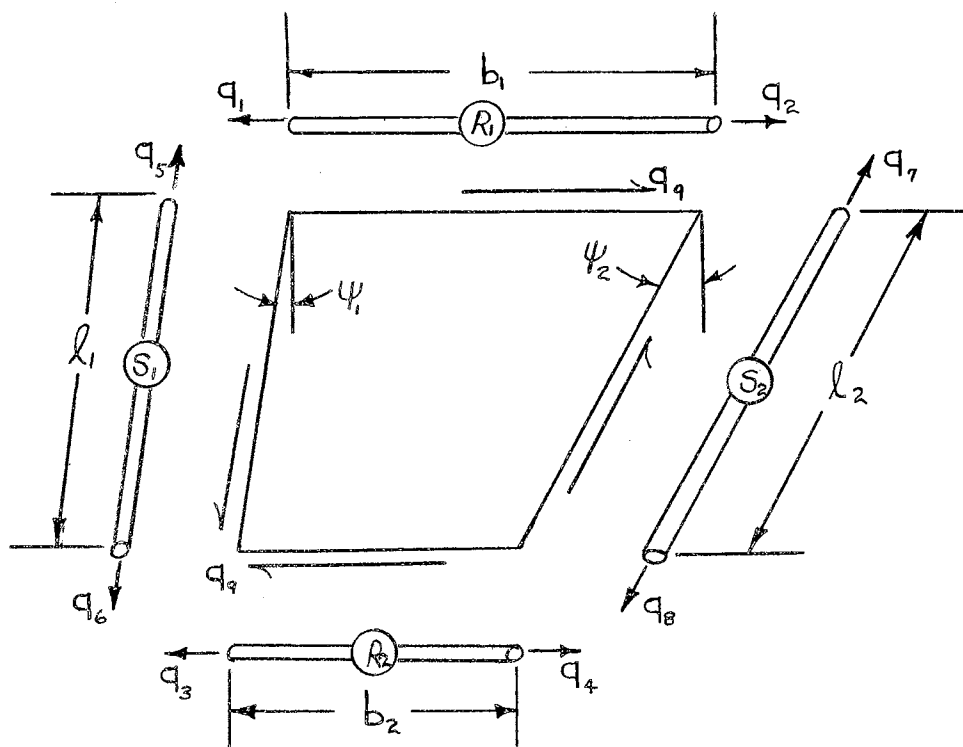


Figure 7. Sign Convention and a Typical Trapezoidal Panel

$\frac{A_1 b_1}{3E}$	$\frac{A_1 b_1}{6E}$			$\frac{l_1 b_1 t}{4E}$				$\frac{l_1 b_1 t \sin \psi_1}{2E}$
$\frac{A_1 b_1}{6E}$	$\frac{A_1 b_1}{3E}$					$\frac{l_2 b_1 t \phi_2}{4E}$		$\frac{l_2 b_1 t \sin \psi_2}{2E}$
		$\frac{A_2 b_2}{3E}$	$\frac{A_2 b_2}{6E}$		$\frac{l_1 b_1 t \phi_1}{4E}$			$\frac{l_1 b_1 t \sin \psi_1}{2E}$
		$\frac{A_2 b_2}{6E}$	$\frac{A_2 b_2}{3E}$				$\frac{l_2 b_2 t \phi_2}{4E}$	$\frac{l_2 b_2 t \sin \psi_2}{2E}$
$\frac{l_1 b_1 \phi_1}{4E}$				$\frac{A_3 l_1}{3E}$	$\frac{A_3 l_1}{6E}$			$\frac{l_1 b_1 t \sin \psi_1}{2E}$
		$\frac{l_1 b_1 t \phi_1}{4E}$		$\frac{A_3 l_1}{6E}$	$\frac{A_3 l_1}{3E}$			$\frac{l_1 b_1 t \sin \psi_1}{2E}$
	$\frac{l_2 b_1 t \phi_2}{4E}$					$\frac{A_4 l_2}{3E}$	$\frac{A_4 l_2}{6E}$	$\frac{l_2 b_1 t \sin \psi_2}{2E}$
			$\frac{l_2 b_2 t \phi_2}{4E}$			$\frac{A_4 l_2}{6E}$	$\frac{A_4 l_2}{3E}$	$\frac{l_2 b_2 t \sin \psi_2}{2E}$
$\frac{l_1 b_1 t \sin \psi_1}{2E}$	$\frac{l_2 b_1 t \sin \psi_2}{2E}$	$\frac{l_1 b_1 t \sin \psi_1}{2E}$	$\frac{l_2 b_2 t \sin \psi_2}{2E}$	$\frac{l_1 b_1 t \sin \psi_1}{2E}$	$\frac{l_1 b_2 t \sin \psi_1}{2E}$	$\frac{l_2 b_1 t \sin \psi_2}{2E}$	$\frac{l_2 b_2 t \sin \psi_2}{2E}$	$\frac{A_1 t \phi_3}{E}$

$$\phi_1 = (\sqrt{1 - \tan^2 \psi_1}) \cos^3 \psi_1$$

$$\phi_2 = (\sqrt{1 - \tan^2 \psi_2}) \cos^3 \psi_2$$

$$\phi_3 = \left[2 + 2\sqrt{1 - \frac{3}{4} (\tan^2 \psi_1 + \tan \psi_1 \tan \psi_2 + \tan^2 \psi_2)} \right]$$

Figure 8. The Matrix [S]

$\frac{b_1}{3A_1E}$									
$\frac{b_1}{6A_1E}$	$\frac{b_1}{3A_1E}$								
		$\frac{b_2}{3A_2E}$							
		$\frac{b_2}{6A_2E}$	$\frac{b_2}{3A_2E}$						
				$\frac{l_1}{3A_3E}$					
$\frac{l_1 b_1 t \phi}{4A_1 A_3 E}$				$\frac{l_1}{6A_3 E}$	$\frac{l_1}{3A_3 E}$				
		$\frac{l_1 b_2 t \phi}{4A_2 A_3 E}$							
	$\frac{l_2 b_1 t \phi_2}{4A_1 A_4 E}$					$\frac{l_2}{3A_4 E}$			
			$\frac{l_2 b_2 t \phi_2}{4A_2 A_4 E}$			$\frac{l_2}{6A_4 E}$	$\frac{l_2}{3A_4 E}$		
$\frac{l_1 b_1 \sin \psi_1}{2A_1 E}$	$\frac{l_2 b_1 \sin \psi_2}{2A_1 E}$	$\frac{l_1 b_2 \sin \psi_1}{2A_2 E}$	$\frac{l_2 b_2 \sin \psi_2}{2A_2 E}$	$\frac{l_1 b_1 \sin \psi_1}{2A_3 E}$	$\frac{l_1 b_2 \sin \psi_1}{2A_3 E}$	$\frac{l_2 b_1 \sin \psi_2}{2A_4 E}$	$\frac{l_2 b_2 \sin \psi_2}{2A_4 E}$	$\frac{A_p \phi_3}{Et}$	

SYMM

$$\phi_1 = (\sqrt{1 - \tan^2 \psi_1}) \cos^3 \psi_1$$

$$\phi_2 = (\sqrt{1 - \tan^2 \psi_2}) \cos^3 \psi_2$$

$$\phi_3 = \left[2 + 2\sqrt{1 - \tan^2 \psi_1} + \frac{4}{3} (\tan^2 \psi_1 + \tan \psi_1 \tan \psi_2 + \tan^2 \psi_2) \right]$$

Figure 9. The Flexibility Matrix, $[ALPIJ]_{prs}$

Inclusion of $[\text{ALPIJ}]_{\text{prs}}$ Into the Matrix Force Method
for Analysis of the Test Structure

In order to apply the Matrix Force Method with $[\text{ALPIJ}]_{\text{prs}}$ included, to an analysis of the test structure of Figure 13, the $[\text{ALPIJ}]$ matrix for the composite structure must be "built up" by special means.

The use of $[\text{ALPIJ}]_{\text{prs}}$ implies that the test structure be idealized in a different manner. The given structure was idealized into the same basic assembly of bar and trapezoidal shaped web elements, but, now, with a choice of fifty-one internal generalized forces, instead of the twenty-seven forces shown in Figure 2. Each bar element is still theoretically constrained to carry only a linearly varying axial load, while each web element is still only allowed to carry an average constant shear flow value, but, now, both the bar element load and web shear flow will include the effects of Poisson's ratio and sweep. The fifty-one unknown idealization of the test structure is shown in Figure 10.

For "building up" the composite $[\text{ALPIJ}]_{\text{prs}}$ matrix, the idealized version of the test structure can be divided into three sections. The first section consists of the top stringer, the upper center stringer, and the enclosed ribs and webs. The second section consists of the upper center stringer, lower center stringer and the ribs and webs enclosed within these two stringers. The third section is made up of the remaining lower center stringer, the bottom stringer and the ribs and webs enclosed within these two stringers. For the contribution of the second section to the composite $[\text{ALPIJ}]$, Figure 7 can be modified to the form shown in Figure 11. Figure 7 can be modified to that shown

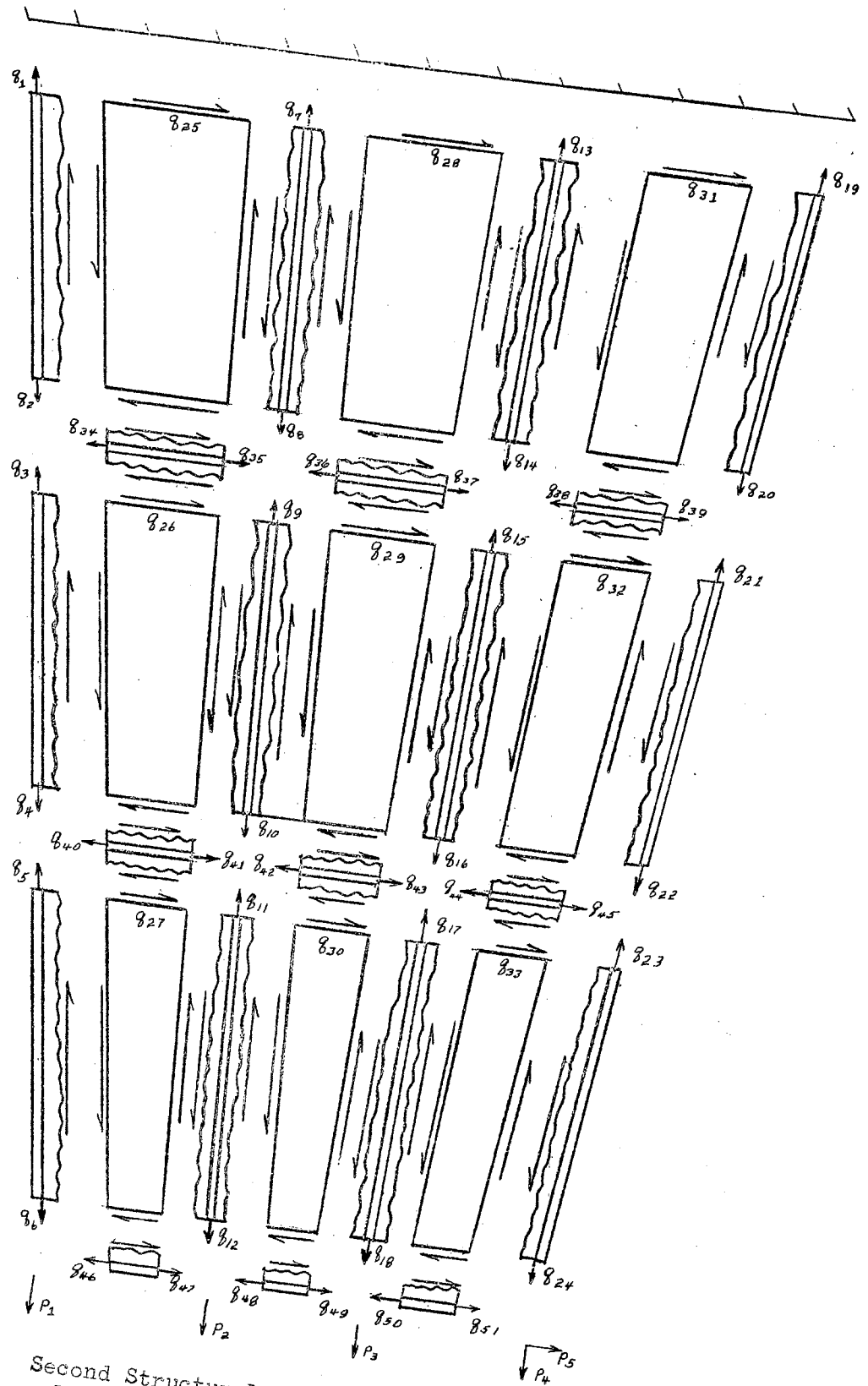


Figure 10. Second Structural Idealization Illustrating Fifty-one Generalized Forces

in Figure 12 for the contribution of the third section. Figure 7 can be applied directly for the contribution of the first section.

The modification of the original sign convention for a typical trapezoidal "cell" requires slight modification of $[\text{ALPIJ}]_{\text{prs}}$. With the use of a simple reindexing system, the composite $[\text{ALPIJ}]_{\text{prs}}$ may now be evaluated. The coefficients of the composite $[\text{ALPIJ}]_{\text{prs}}$ are listed in Table XIII.

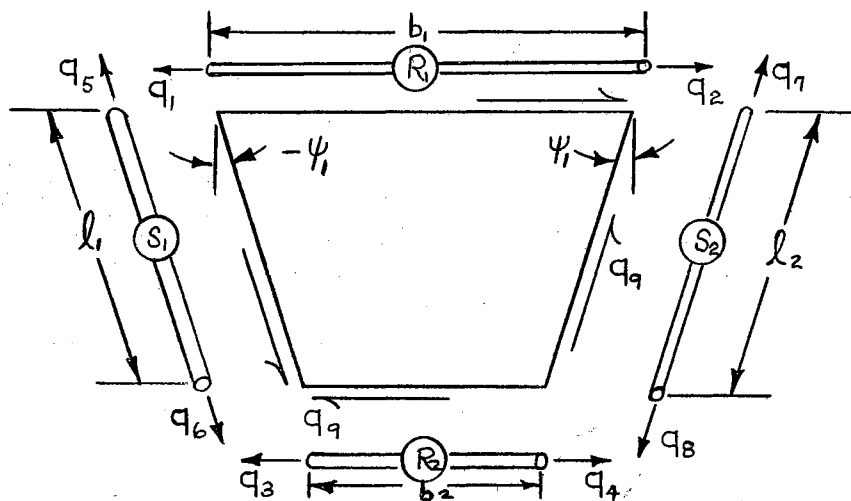


Figure 11. Sign Convention for Section 2

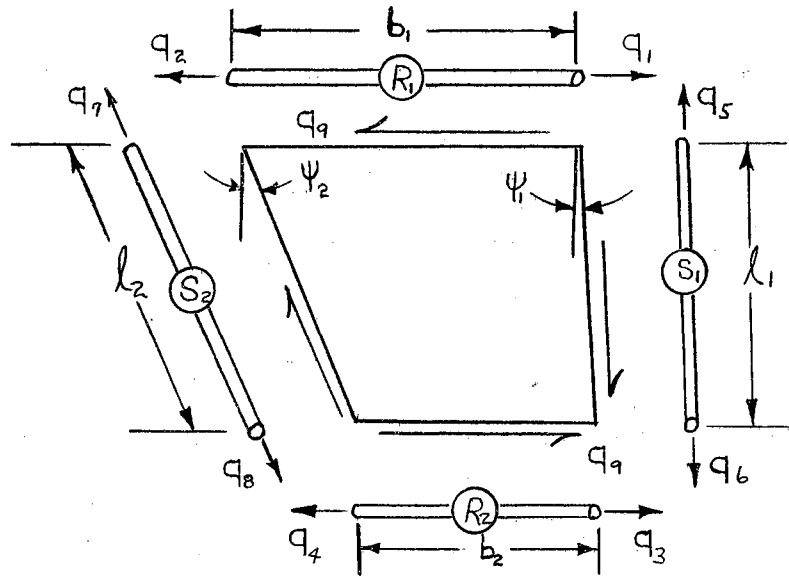


Figure 12. Sign Convention for Section 3

Finally, in order to be compatible with the composite $[ALPIJ]_{prs}$, the matrices $[GIM]$ and $[GIR]$ and the column vector $[AREINV]$ must be redeveloped in terms of fifty-one unknowns instead of twenty-seven unknowns.

TABLE XIII

COMPOSITE $[ALPIJ]_{prs}$

Non-Zero Term Consisting of Nonsymmetrical Terms and
 One-Half of the Symmetrical Terms are Listed

Row	Col	Coeff	Row	Col	Coeff
1	1	8.171000	25	1	12.730000
2	1	4.086000	25	2	10.910000
2	2	8.171000	25	7	3.889000
3	3	8.698000	25	8	3.333333
4	3	4.349000	25	25	3501.333333
4	4	8.698000	26	3	11.610000
5	5	9.298000	26	4	9.677000
6	5	4.649000	26	9	3.750000
6	6	9.298000	26	10	3.125000
7	7	7.417000	26	26	2962.666667
8	7	3.708000	27	5	10.340000
8	8	7.417000	27	6	8.276000
9	9	8.344000	27	11	3.571000
10	9	4.172000	27	12	2.857000
10	10	8.344000	27	27	2484.666667
11	11	9.536000	28	7	-3.889000
12	11	4.768000	28	8	-3.333333
12	12	9.536000	28	13	3.889000
13	13	7.417000	28	14	3.333333
14	13	3.708000	28	28	3471.000000
14	14	7.417000	29	9	-3.750000
15	15	8.344000	29	10	-3.125000
16	15	4.172000	29	15	3.750000
16	16	8.344000	29	16	3.125000
17	17	9.536000	29	29	2964.000000
18	17	4.768000	30	11	-3.571000
18	18	9.536000	30	12	-2.857000
19	19	8.171000	30	17	3.571000
20	19	4.086000	30	18	2.857000
20	20	8.171000	30	30	2462.666667
21	21	8.698000	31	13	3.889000
22	21	4.349000	31	14	3.333333
22	22	8.698000	31	19	12.730000
23	23	9.298000	31	20	10.910000
24	23	4.649000	31	31	3501.333333
24	24	9.298000	32	15	3.750000

TABLE XIII (Continued)

Row	Col	Coeff	Row	Col	Coeff
32	16	3.125000	41	11	-0.919200
32	21	11.610000	41	26	2.000000
32	22	9.677000	41	27	2.000000
32	32	2962.666667	41	40	1.333333
33	17	3.571000	41	41	2.666667
33	18	2.857000	42	10	-0.804300
33	23	10.340000	42	11	-0.919200
33	24	8.276000	42	29	-2.000000
33	33	2484.600000	42	30	-2.000000
34	2	-0.860600	42	42	2.666667
34	3	-0.916200	43	16	-0.804300
34	25	7.200000	43	17	-0.919200
34	26	7.200000	43	29	2.000000
34	34	3.200000	43	30	2.000000
35	8	-0.857900	43	42	1.333333
35	9	-0.965100	43	43	2.666667
35	25	2.400000	44	16	-0.804300
35	26	2.400000	44	17	-0.919200
35	34	1.600000	44	32	2.000000
35	35	3.200000	44	33	2.000000
36	8	-0.857900	44	44	2.666667
36	9	-0.965100	45	22	-0.763500
36	28	-2.400000	45	23	-0.816100
36	29	-2.400000	45	32	6.000000
37	14	-0.857900	45	44	1.333333
37	15	-0.965100	45	45	2.666667
37	28	2.400000	46	6	-0.816100
37	29	2.400000	46	27	6.000000
37	36	1.600000	46	46	2.666667
37	37	3.200000	47	12	-0.919200
38	14	-0.857900	47	27	2.000000
38	15	-0.965100	47	46	1.333333
38	31	2.400000	47	47	2.666667
38	32	2.400000	48	12	-0.919200
38	38	3.200000	48	30	-2.000000
39	20	-0.860600	48	48	2.666667
39	21	-0.916200	49	18	-0.919200
39	31	7.200000	49	30	2.000000
39	32	7.200000	49	48	1.333333
39	38	1.600000	49	49	2.666667
39	39	3.200000	50	18	-0.919200
40	4	-0.763500	50	33	2.000000
40	5	-0.816100	50	50	2.666667
40	26	6.000000	51	24	-0.816100
40	27	6.000000	51	33	6.000000
40	40	2.667000	51	50	1.333333
41	10	-0.804300	51	51	2.666667

CHAPTER III

ANALYTICAL INVESTIGATION

The structural panel used in this investigation was designed so that the idealization used in the force analysis corresponded as precisely as possible to the actual test model. In the case of complex structural configurations, the analysis problem should be divided into two phases: the idealization of the complex structure; the analysis of the idealized structure.

In the first phase, large errors may occur due to computer size limitations because it is necessary to approximate large structural configurations with a relatively few number of structural elements. In addition, thick panels are idealized as thin panels which carry no out-of-plane loads; and tapered bar elements are idealized into constant area sections that carry constant loads. These discrepancies occur in the idealization phase of the analysis.

The second phase, the comparison between the structural behavior of the panel and the mathematical analysis of the idealized panel, is hopefully limited to errors in the mathematical representation of the characteristics of the structural elements. It is first necessary to prove that an idealized structural configuration behaves in a manner similar to an actual structural configuration of approximately the same geometric characteristics. After this comparison is made, the errors resulting from idealization procedures can be more accurately

investigated.

The design of the research model shown in Figure 13 is based on the idealization of actual structural configurations that are commonly encountered in aerospace structural analysis. This structural configuration results in a convenient idealization for the force method of analysis.

An extensive analysis of the structure was performed using the matrix force method described in Chapter II. A complete analysis of the structure was performed using each of the flexibility matrices described in Chapter II for each of the load configurations performed in the experimental investigation. Load condition No. 1 consists of four equivalent loads applied at the forward edge of the panel of Figure 13. Load condition No. 2 consists of a "shear" load applied at the upper forward edge of the panel in a direction perpendicular to those of LC-1. Load condition No. 3 is similar to LC-1 but consists of only two equivalent loads applied in the "axial" direction. LC-1, LC-2, and LC-3 are shown in Figure 33. The array of load values for each load condition are shown in Table XVIII:

The first analysis is illustrated in detail to show how the matrices $\{q_i\}$, $\{\sigma_b\}$, $\{\sigma_w\}$, $\{\delta_m\}$, and $[a_{rn}]_{true}$ are determined.

Generation of the Matrices: $[QI]$, $[STRESS]$,
 $[DELTAM]$, and $[ARNTR]$

The matrices of $\{q_i\}$ of Equation (2-1), $\{\sigma_b\}$ and $\{\sigma_w\}$, of Equations (2-6) and (2-7), $\{\delta_m\}$ on page 11, and $[a_{rn}]_{true}$ of Equation (2-9), have each been designated as follows:

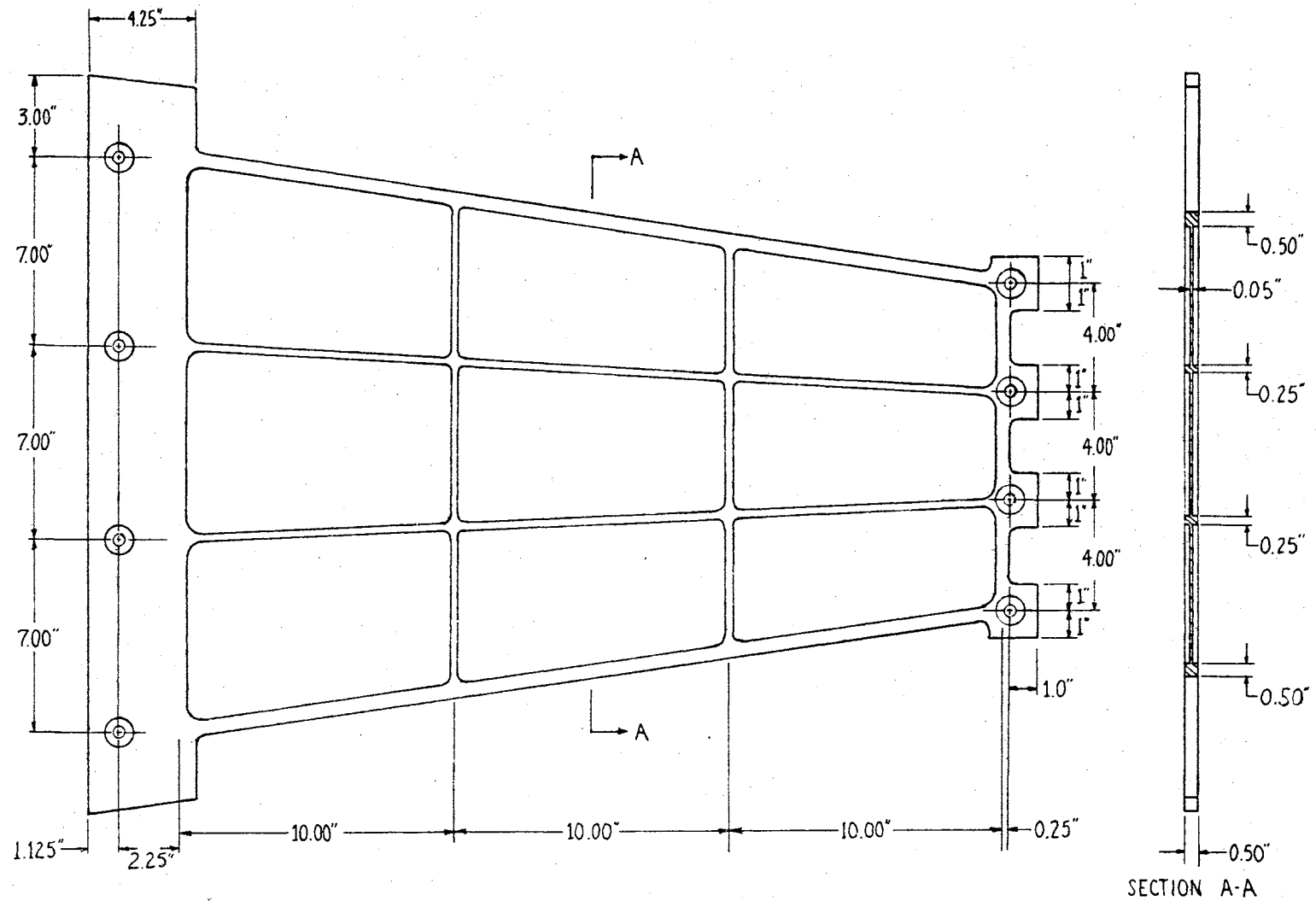


Figure 13. Test Panel and Its Geometry

$$\begin{aligned} \{q_i\} &= [QI] \\ [G_b, \sigma_w] &= [STRESS] \\ \{\delta_m\} &= [DELTAM] \\ [a_{rn}]_{true} &= [ARNTR] \end{aligned}$$

The digital computer program described and illustrated in Appendix C was used to calculate six sets of values for the above four matrices. Three sets of values or runs were made for each, the RDC-1 assumption and the RDC-2 assumption.

The combination of the input matrices $[ALPIJ]$, $[AREINV]$, $[GIM]$, $[GIR]$, and $[FORCE]$ for each run is shown as follows:

$$\begin{aligned} \text{Run No. 1: } & [ALPIJ] ; [AREINV] ; \\ & [GIM], \text{ RDC-1} ; [GIR], \text{ RDC-1} ; \\ & [FORCE]_{LC-1} \\ \text{Run No. 2: } & [ALPIJ] ; [AREINV] ; \\ & [GIM], \text{ RDC-1} ; [GIR], \text{ RDC-1} ; \\ & [FORCE]_{LC-2} \\ \text{Run No. 3: } & [ALPIJ] ; [AREINV] ; \\ & [GIM], \text{ RDC-1} ; [GIR], \text{ RDC-1} ; \\ & [FORCE]_{LC-3} \end{aligned}$$

Run No. 4: $[ALPIJ]$; $[AREINV]$;
 $[GIM]$, RDC-2 ; $[GIR]$, RDC-2 ;
 $[FORCE]_{LC-1}$

Run No. 5: $[ALPIJ]$; $[AREINV]$;
 $[GIM]$, RDC-2 ; $[GIR]$, RDC-2 ;
 $[FORCE]_{LC-2}$

Run No. 6: $[ALPIJ]$; $[AREINV]$;
 $[GIM]$, RDC-2 ; $[GIR]$, RDC-2 ;
 $[FORCE]_{LC-3}$

The values of $[QI]$ are shown in Figures 14 and 15 the values of $[STRESS]$ are shown in Figures 16 and 17 and the values of $[DELTAM]$ are shown in Table XIV.

The products of Equation (2-9) were performed and these values which make up $[ARNTR]$ are shown in Table XV. The magnitude of these values indicates that the matrix $[GIM]$ is almost error-free. This serves as a good check on the accuracy of values of $[QI]$, $[STRESS]$, and $[DELTAM]$.

Since the two redundant choices produce results which are so similar, only RDC-1 was used in the analysis containing $[ALPIJ]_{prs}$.

The values of $[QI]$, $[STRESS]$, and $[DELTAM]$ produced by $[ALPIJ]_{prs}$ analysis are shown in Figures 18 and 19 and Table XVI.

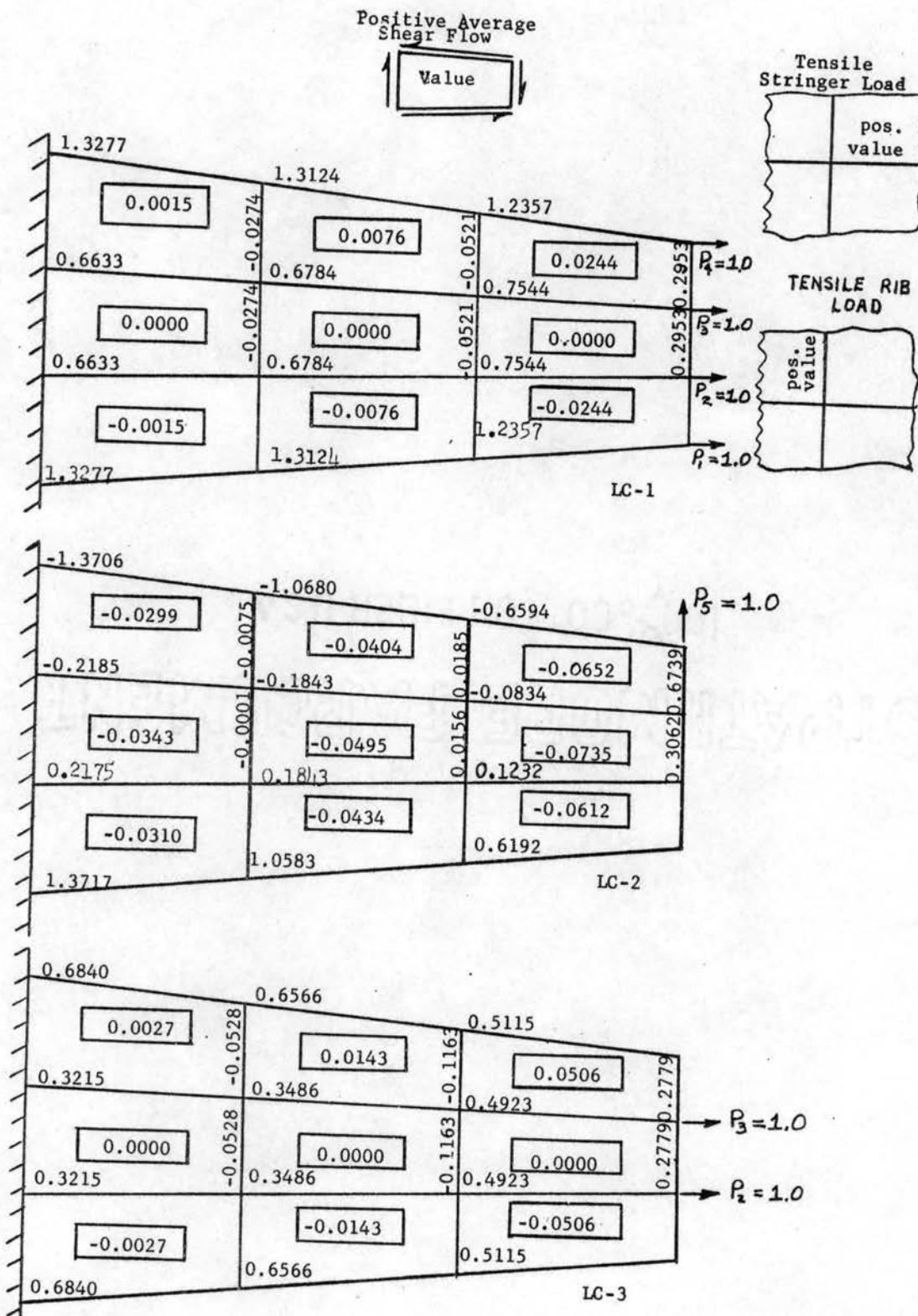


Figure 14. [QI] Values for RDC-1, LC-1, LC-2, and LC-3

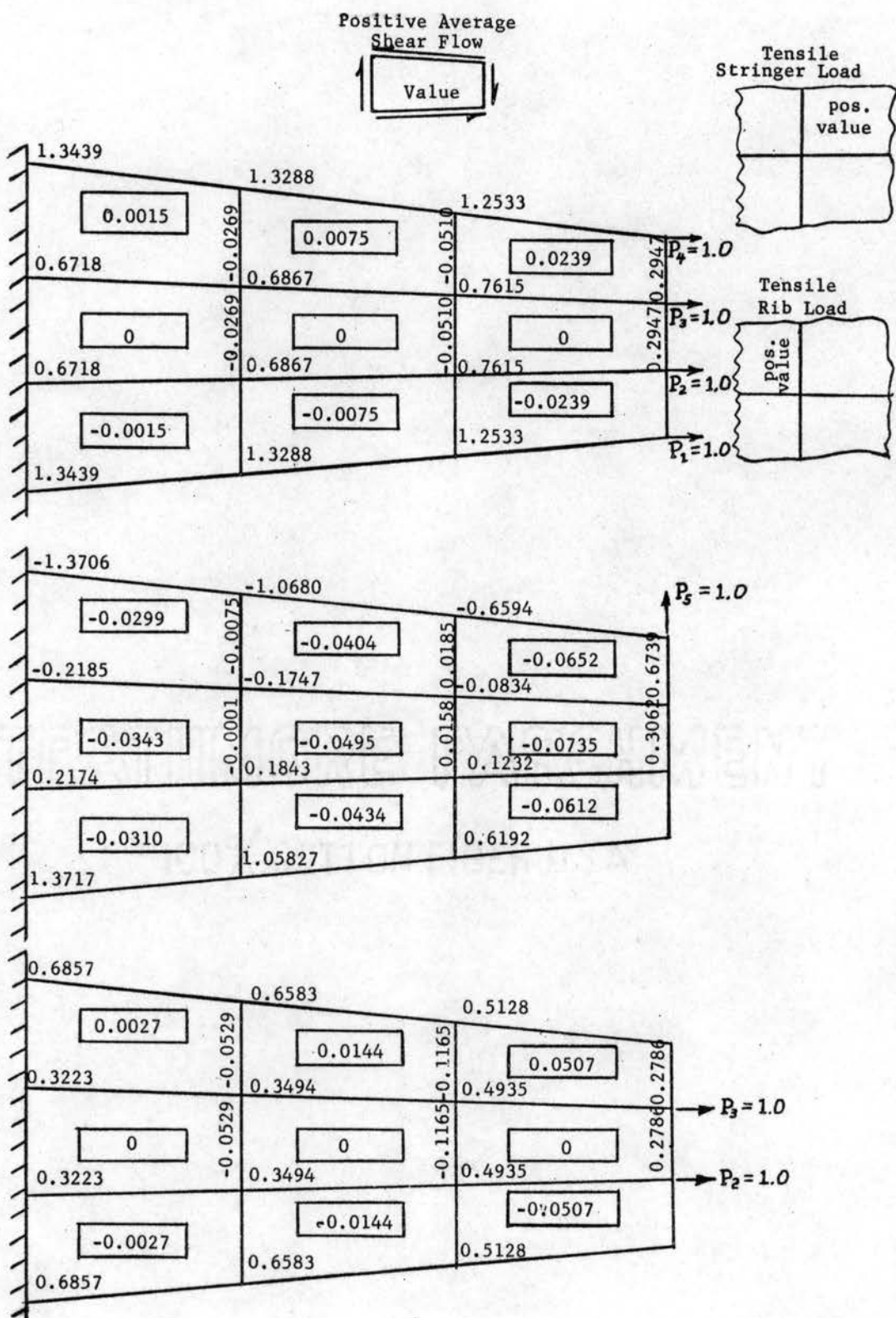


Figure 15. [QI] Values for RDC-2, LC-1, LC-2, and LC-3

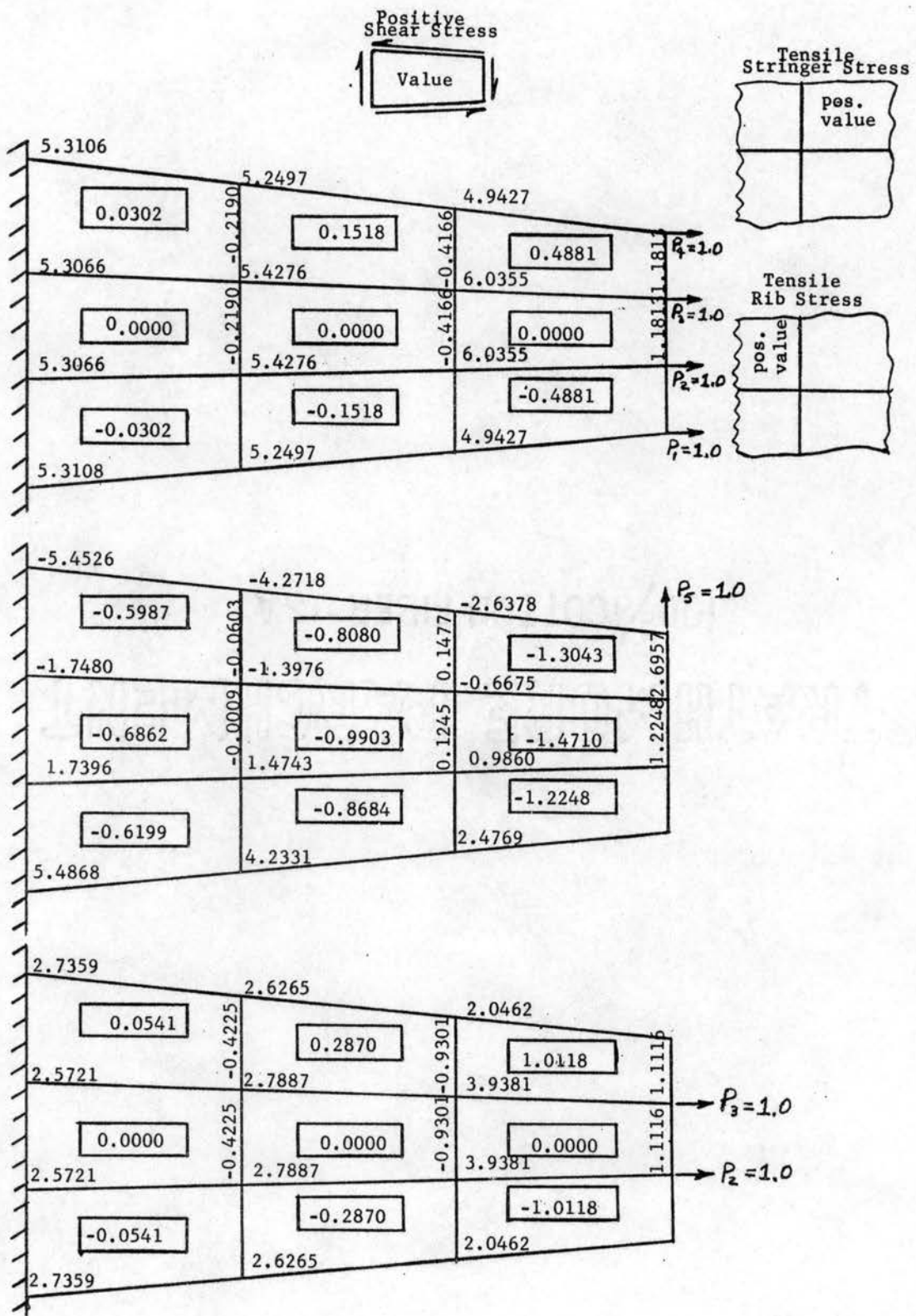


Figure 16. [STRESS] Values for RDC-1, LC-1, LC-2, and LC-3

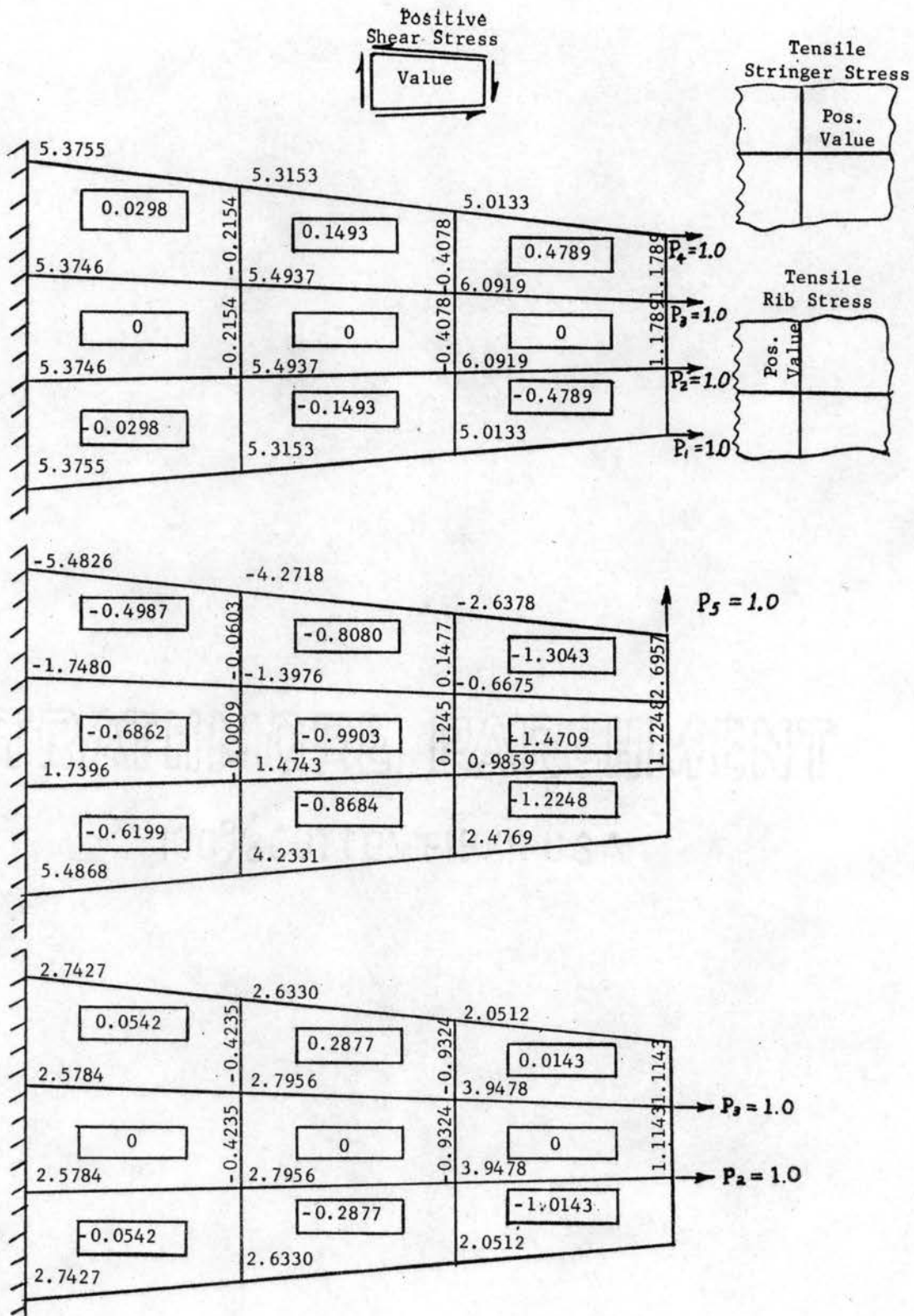


Figure 17. [STRESS] Values for RDC-2, LC-1, LC-2, and LC-3

TABLE XIV

[DELTAM] MATRIX

NOTE: All values must be multiplied by 1/E

	LC-1 $P_1=P_2=P_3=P_4=1.0$	LC-2 $P_5=1.0$	LC-3 $P_2=P_3=1.0$
	120.8230	52.5279	57.5455
	131.2030	18.7801	73.6570
RDC-1	131.2030	-15.0746	73.6570
	120.8230	-52.2956	57.5455
	3.9377	268.4080	3.7055
	125.1380	54.1391	58.9804
	133.0030	18.8426	74.0224
RDC-2	133.0030	-15.1283	74.0224
	125.1380	-53.9236	58.9804
	3.9300	268.4080	3.7143

TABLE XV

[ARNTR] MATRIX

	RDC-1	RDC-2
	1	-1.35601 E-06
	2	-1.84588 E-06
For all	3	-1.54250 E-06
Load	4	-8.12133 E-07
Configurations	5	-6.07102 E-07
	6	-7.07102 E-07
		-1.60279 E-05
		-4.26322 E-05
		-3.86368 E-05
		-1.70259 E-05
		1.29342 E-05
		8.41729 E-05

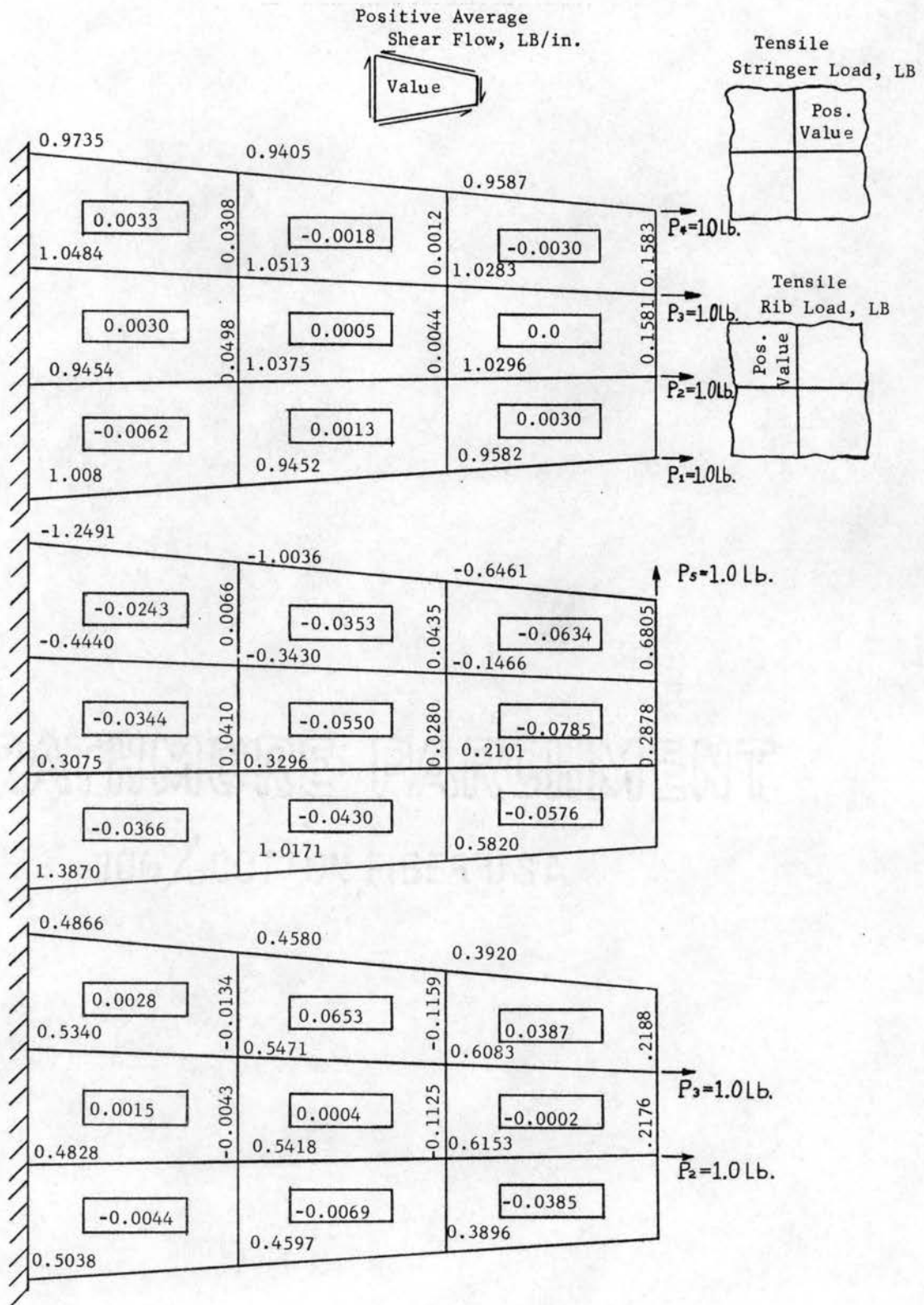


Figure 18. [QI] Values for [ALPIJ]_{prs}, RDC-1, LC-1, LC-2, and LC-3

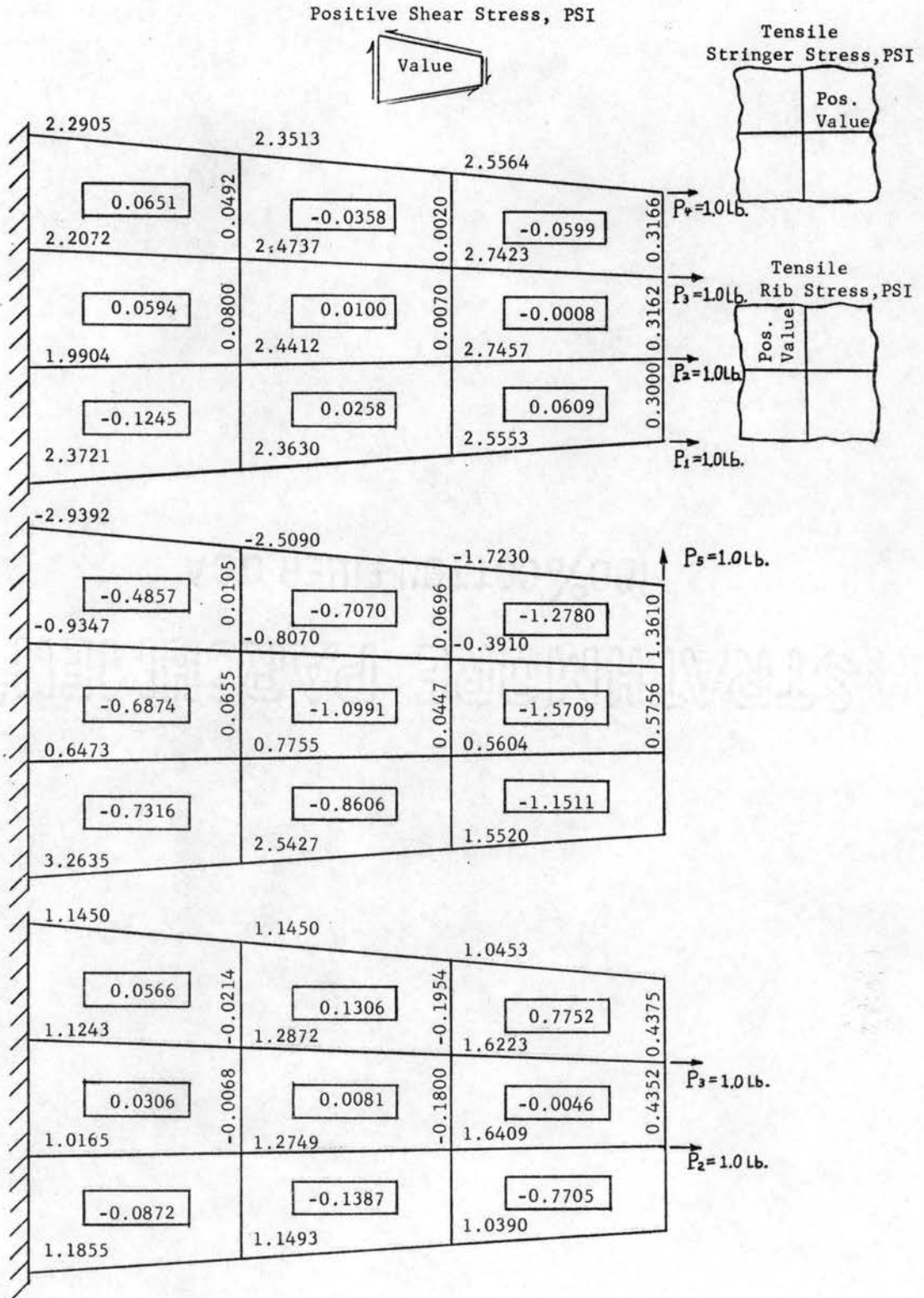


Figure 19. [STRESS] Values for [ALPIJ]_{prS}, RDC-1, LC-1, LC-2, and LC-3

TABLE XVI

[DELTAM] MATRIX FROM EXTENDED FORCE ANALYSIS

NOTE: All values must be multiplied by $1/E$

	LC-1 $P_1=P_2=P_3=P_4=1.0$	LC-2 $P_5=1.0$	LC-3 $P_2=P_3=1.0$
	76.4964	28.7230	27.6396
	76.7557	7.3656	48.8485
RDC-1	77.5933	-11.2631	49.6506
	73.8320	-32.9868	28.2103
	-8.1613	188.1140	-3.8975

Analysis by the Direct Stiffness Method

The direct stiffness method has been employed in three separate analyses of the test structure in order to provide theoretical results with which those of the matrix force method may be compared. Also, the description and subsequent application of the direct stiffness method illustrates its basic characteristics in contrast to those of the matrix force method.

The direct stiffness method is a finite element method of structural analysis which considers a structure to be an assembly of idealized elastic elements which are assumed to be joined only at discrete points called nodes. The stiffness method is a contrast to the force method, which is described in Chapter II, in that displacements, not forces, are the initial unknown quantities. The problem is directed toward the solution for unknown displacements at the joints, and the resulting stress distribution is calculated subsequently from the displacements. In these terms, there are always as many equations of equilibrium available as there are unknowns. The relationship of forces and of displacements is defined for the node points on the structure by the stiffness matrix. The stiffness matrix for the complete structure is obtained by adding the stiffness coefficients for common degrees of freedom of adjacent elements at each node on the structure. The summed stiffness coefficients define the coefficients for the linear algebraic equations relating the nodal forces and the nodal displacements of the complete structure. The general stiffness coefficient K_{jn} is the force in the direction j due to the unit displacement in the direction h , while all other displacements are zero. As a result of equilibrium conditions, the stiffness matrix is a positive definite, symmetric matrix; and the sum of the coefficients along any row or column of the stiffness matrix is equal

to zero.

The forces and deflections in each element of the structure are related by an assumed stress-strain relationship for the idealized element. The displacements of the nodes in a structure are considered as the initial unknown quantities. A large number of mutually compatible deformations of the elements are possible; the correct pattern of displacements of the elements is the one for which the equations of equilibrium are satisfied.

If the idealized structural elements, for which the stiffness coefficients are known, are combined for a continuous structure, the composite stiffness matrix for the total structure is assembled as

$$\begin{bmatrix} K_{11} & K_{12} & \cdot & K_{1n} & K_{1m} \\ K_{21} & K_{22} & \cdot & \cdot & \cdot \\ \cdot & \cdot & \cdot & \cdot & \cdot \\ K_{ji} & \cdot & \cdot & K_{jh} & K_{jm} \\ K_{mi} & \cdot & \cdot & K_{mh} & K_{mm} \end{bmatrix}$$

Where each K_{jh} term is the stiffness coefficient representing the total force component produced at node j due to a corresponding unit displacement component at node h .

With the use of these ideas, the basic equations of the direct stiffness method can be summarized. These equations appear in Appendix A.

Two theoretical elements are used in the direct stiffness analysis of the test structure of Figure 13. They are the planar bar element and the planar triangular element. The derivation of the stiffness matrices for each of these elements is given and follows mainly from the work of

Turner et al. (6). These matrices have been derived in a manner which is applicable to this particular application of the direct stiffness method to an analysis. These derivations appear in Appendix A.

The stresses in each element may now be evaluated from the node point displacements. The equations for these quantities are given in Appendix A.

Analysis of the Test Structure:

Structural Idealization

Three choices of structural idealization were used in this investigation. Each employs the constant stressed bar element and the constant stressed triangular element. These three choices of idealization are shown in Figure 20.

Idealization choice number one or IDC-1 breaks the original structure into an array of bar and triangular plate elements, each original web being divided into two triangular elements.

Idealization choice number two or IDC-2 is identical to IDC-1 except the triangular plate elements replacing each original web are oriented in a different direction.

Idealization choice number three or IDC-3 breaks each original web into four triangular plates and introduces a new hypothetical node at the intersection of the diagonals connecting the corners of each web.

Calculation of the element stiffness matrices and the buildup of the stiffness matrix for the composite structure are implemented by the Stress Analysis System of Reference (11). A more detailed description and example listing of the Stress Analysis System is given in Appendix B.

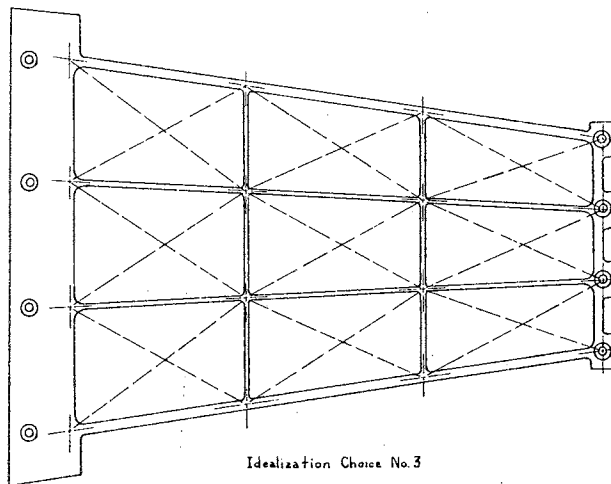
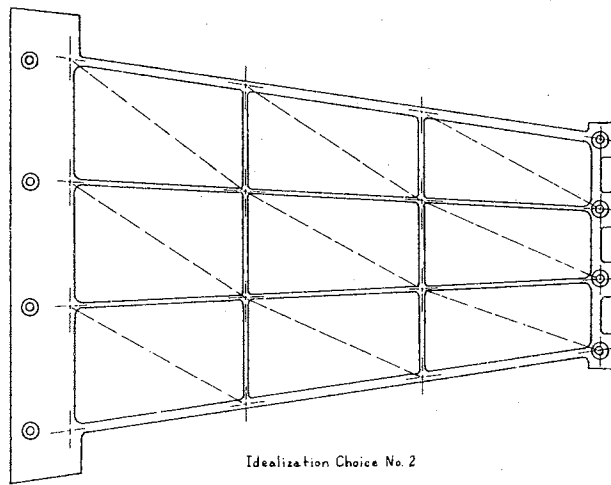
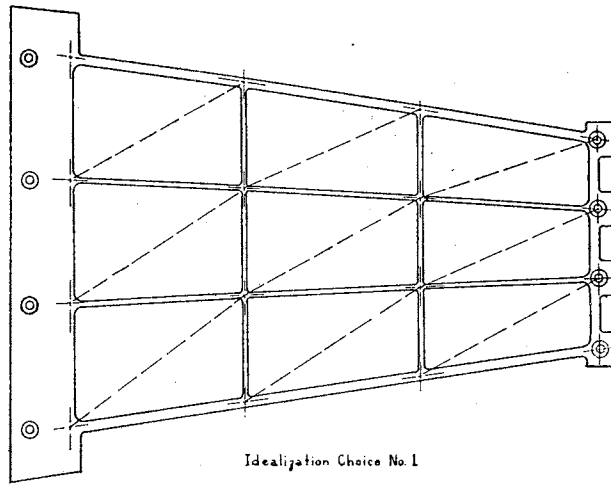


Figure 20. Structural Idealization Choices

Three separate analyses of the panel shown in Figure 13 are conducted. The first analysis will utilize the two triangle web makeup of IDC-1. The second analysis will utilize IDC-2 which is also a two triangle web makeup, but oriented in a different direction. The third analysis employs IDC-3 and is a four triangle web makeup.

The three load conditions used in the matrix force method analysis are used in each stiffness analysis. These various load conditions appear in Chapter IV and have been described earlier in this chapter.

The input data required for the Stress Analysis System consists of node numbers, element numbers and geometric descriptions of the idealized structure. Therefore, the first step for preparing input data for an analysis is to establish nodes, node numbers, idealized elements, and idealized element numbers.

The idealized structure is then defined in terms of the number of the node point, the coordinates of the node point, the external load condition and load values acting on the node point, and the definition of the boundary condition at the node point.

The idealized panel must also be defined in terms of the structural data. The structural data consist of the location of the idealized elements relative to the node points, the type of structural element, and the description of its material properties.

The node data and the structural data are then employed in evaluating the stiffness matrix of the appropriate element. If the element is a bar, $[K]$ of Equation (A-7) is evaluated; if the element is a triangular plate, $[K]$ of Equation (A-17) is evaluated.

The content of the stiffness matrix for each bar and plate element may now be combined into a composite stiffness matrix for the entire

structure by tabulating the contribution of the elements to the various modes of the structure.

Generation of Node Point Displacements;

Forces and Element Stresses

As described in Appendix A, the unconstrained node point displacements are the result of the product of the inverse of the partitioned composite stiffness matrix and the external forces acting on the structure. Nodal displacements for IDC-1, IDC-2, and IDC-3 are shown in Table XVII.

If $\{\delta\}$ in Equation (A-18) are set equal the nodal displacements, the internal forces acting at each node may now be calculated with the use of $[K_c] = [K]$, the composite stiffness matrix. Forces acting on externally loaded and reaction nodes are shown in Figure 21 for the third idealization choice and each load condition.

The stresses in each bar element may be calculated with the use of Equation (A-23) by employing the end point displacements of each bar. Plate element stresses may be calculated by evaluating Equation (A-24). Element stresses for the third idealization choice and each of the load conditions are shown in Figures 22, 23, and 24.

This chapter has included the explanation of and the results of analyses of the test structure by both the matrix force method and the direct stiffness method. A more detailed and extensive analysis was performed with the matrix force method while an abbreviated analysis was conducted with the direct stiffness method.

The test structure was first analyzed with the matrix force method in its unmodified form. Two choices of redundants were used along with

the unmodified $[ALPIJ]$ matrix. A second analysis was performed with the new $[ALPIJ]_{prs}$ matrix, which accounts for Poisson's ratio and sweep effects, included in the modified version of the matrix force method. The final analysis of the test structure was performed with the direct stiffness method to provide a theoretical comparison with the results of the second analysis utilizing the new $[ALPIJ]_{prs}$ matrix.

The results of the analysis by the unmodified matrix force method indicate that the two redundant choices, RDC-1 and RDC-2, produce values of internal forces, element stresses and load point displacements which are quite similar. This shows, among other things, that the input matrices were accurately calculated.

A general comparison of the results of the analysis with the modified version of the matrix force method including the new $[ALPIJ]_{prs}$ matrix with those of the unmodified matrix force method shows that all results: internal forces, element stresses and load point displacements, of the modified method are significantly smaller in value than those of the unmodified version.

Finally, a comparison of the results of the analysis with the modified matrix force method with those of the direct stiffness method indicates favorable agreement of the element stresses and the load point displacements.

TABLE XVII
LOAD POINT DISPLACEMENTS

	LC1	LC2	LC3
IDC-1	0.7259×10^{-5}	$+0.2785 \times 10^{-5}$	0.3117×10^{-5}
	0.7554×10^{-5}	$+0.9220 \times 10^{-6}$	0.4481×10^{-5}
	0.7548×10^{-5}	-0.7852×10^{-6}	0.4506×10^{-5}
	0.7212×10^{-5}	-0.2874×10^{-5}	0.2998×10^{-5}
	0.4784×10^{-5}	0.1738×10^{-4}	0.1367×10^{-6}
IDC-2	0.7212×10^{-5}	0.2843×10^{-5}	0.2998×10^{-5}
	0.7548×10^{-5}	0.8577×10^{-6}	0.4506×10^{-5}
	0.7554×10^{-5}	-0.9252×10^{-6}	0.4481×10^{-5}
	0.7259×10^{-5}	-0.3106×10^{-5}	0.3117×10^{-5}
	-0.3303×10^{-6}	0.1749×10^{-4}	-0.6749×10^{-7}
IDC-2	0.7237×10^{-5}	0.3270×10^{-5}	0.2892×10^{-5}
	0.7615×10^{-5}	0.1054×10^{-5}	0.4723×10^{-5}
	0.7615×10^{-5}	-0.9497×10^{-6}	0.4723×10^{-5}
	0.7237×10^{-5}	-0.3448×10^{-5}	0.2892×10^{-5}
	-0.7390×10^{-7}	0.1879×10^{-4}	0.1046×10^{-6}

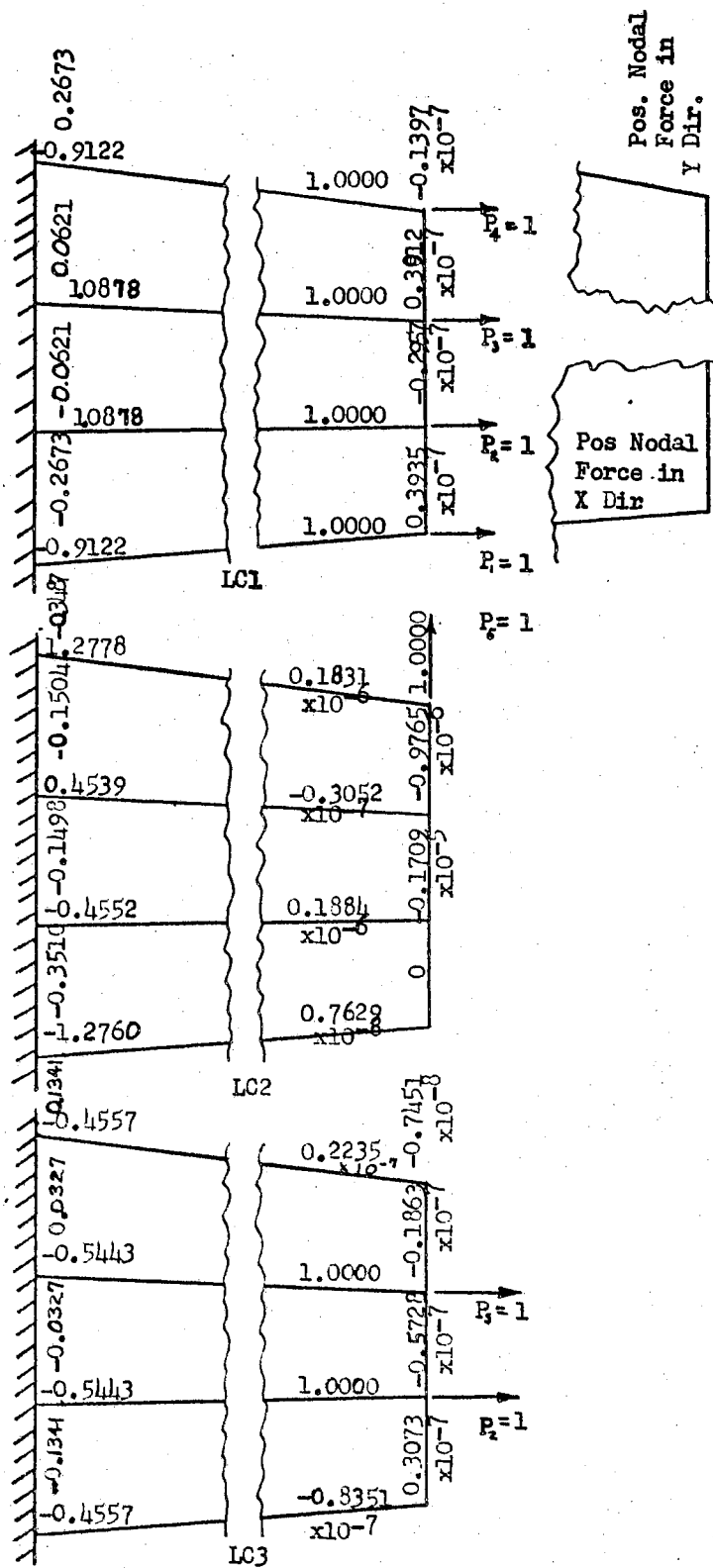


Figure 21. Internal Forces Acting on Externally Loaded and Reaction Nodes for IDC-3

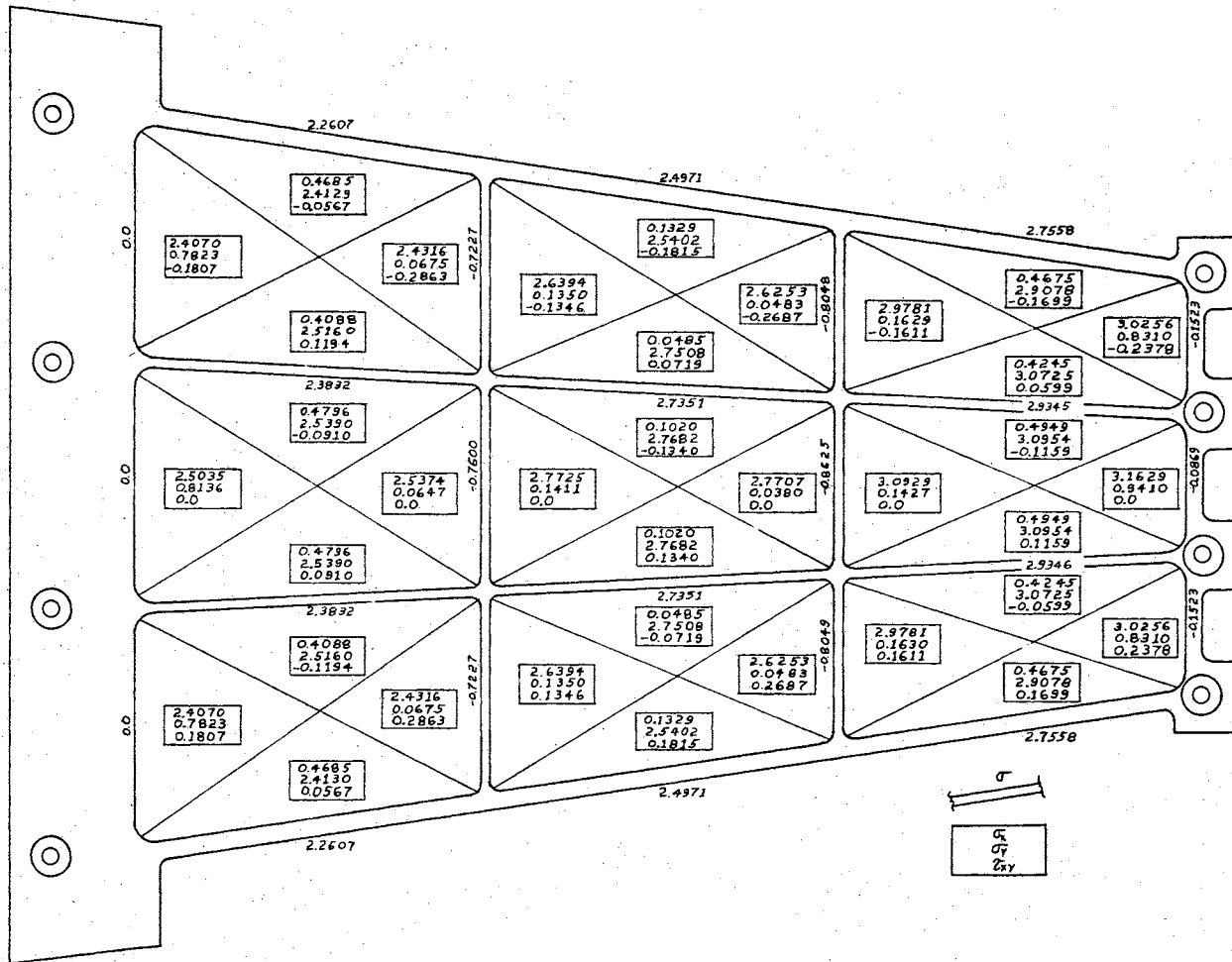


Figure 22. Element Stresses for IDC-3, LC-1

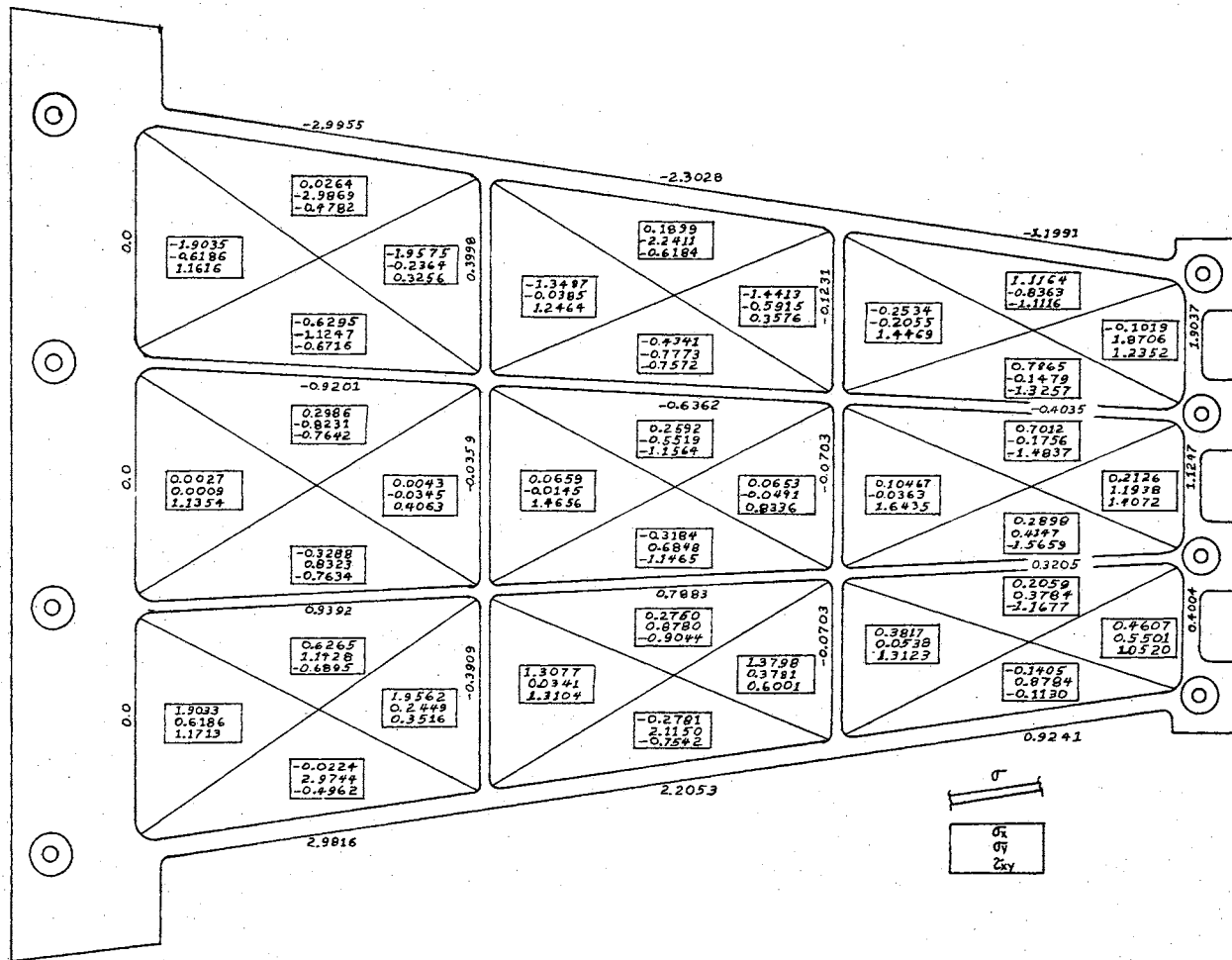


Figure 23. Element Stresses for IDC-3, LC-2

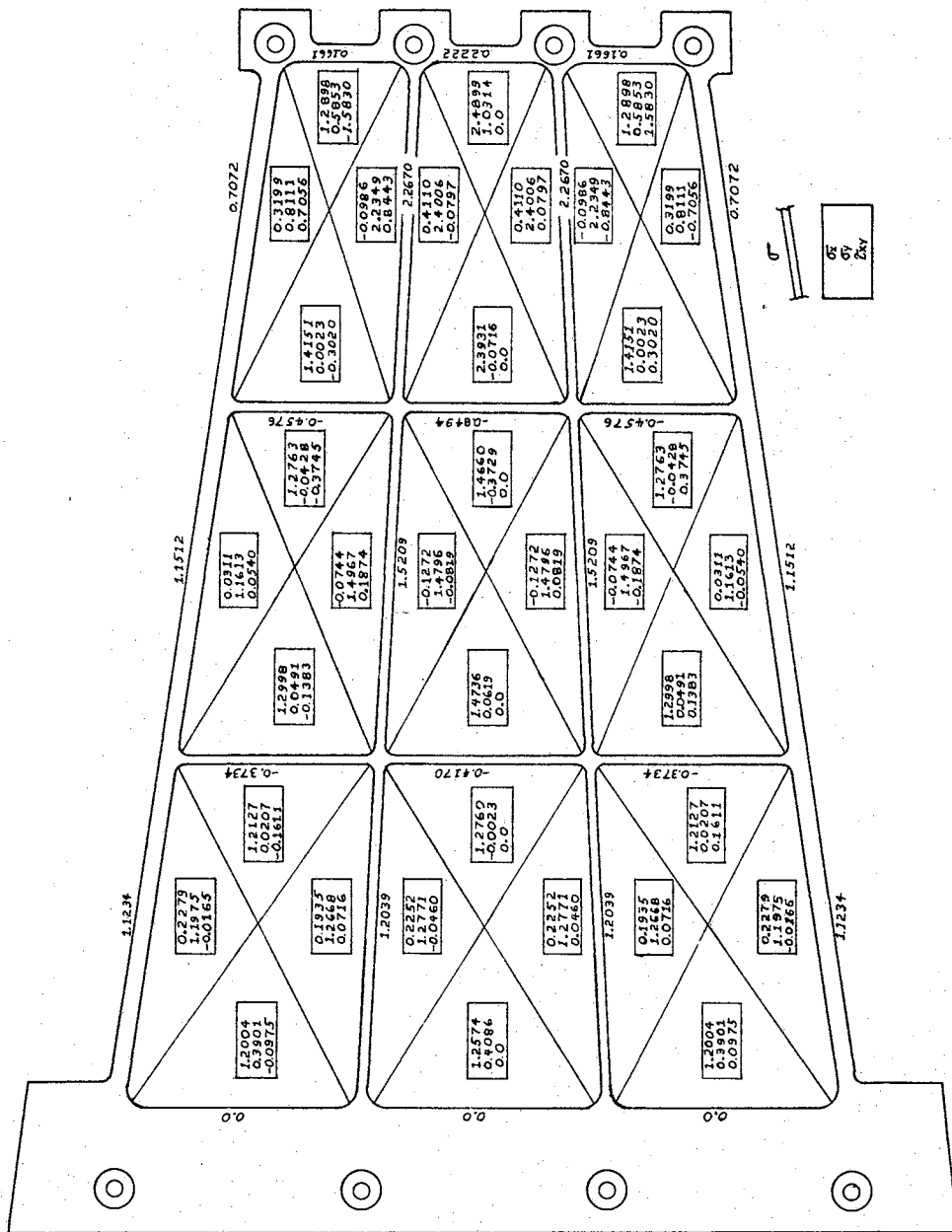


Figure 24. Element Stresses for IDC-3, LC-3

CHAPTER IV

EXPERIMENTAL ANALYSIS

The purpose of this experimental investigation is to provide data for direct comparison to the analytical methods. Since the structural idealization techniques provide a unique and somewhat unrealistic structural configuration, prior experimental data are unavailable for comparison purposes. The experimental facility and the structural skin panel that were developed for this investigation are shown in Figure 25 and a general floor plan of the facility is given in Figure 26.

One objective of the experimental investigation is the determination of the complete state of strain at various points in the model for three conditions of external loading. The strain gages are positioned on the panel at points which correspond with points easily selected for the analytical solutions. These locations of the strain gages reduce any errors that might occur as a result of extrapolating either the analytical or the experimental data.

The research model was mechanically milled from $\frac{5}{8}$ " x 36" x 96 aluminum 2024-T351 bare plate, QQ A 250/4C, by Northwest Engineering Company, Oklahoma City, Oklahoma. This material was selected because of its high utilization in current aircraft programs. The panel was machined from one-half inch thick plate to eliminate joints. The panel and its geometry are shown in Figure 13.

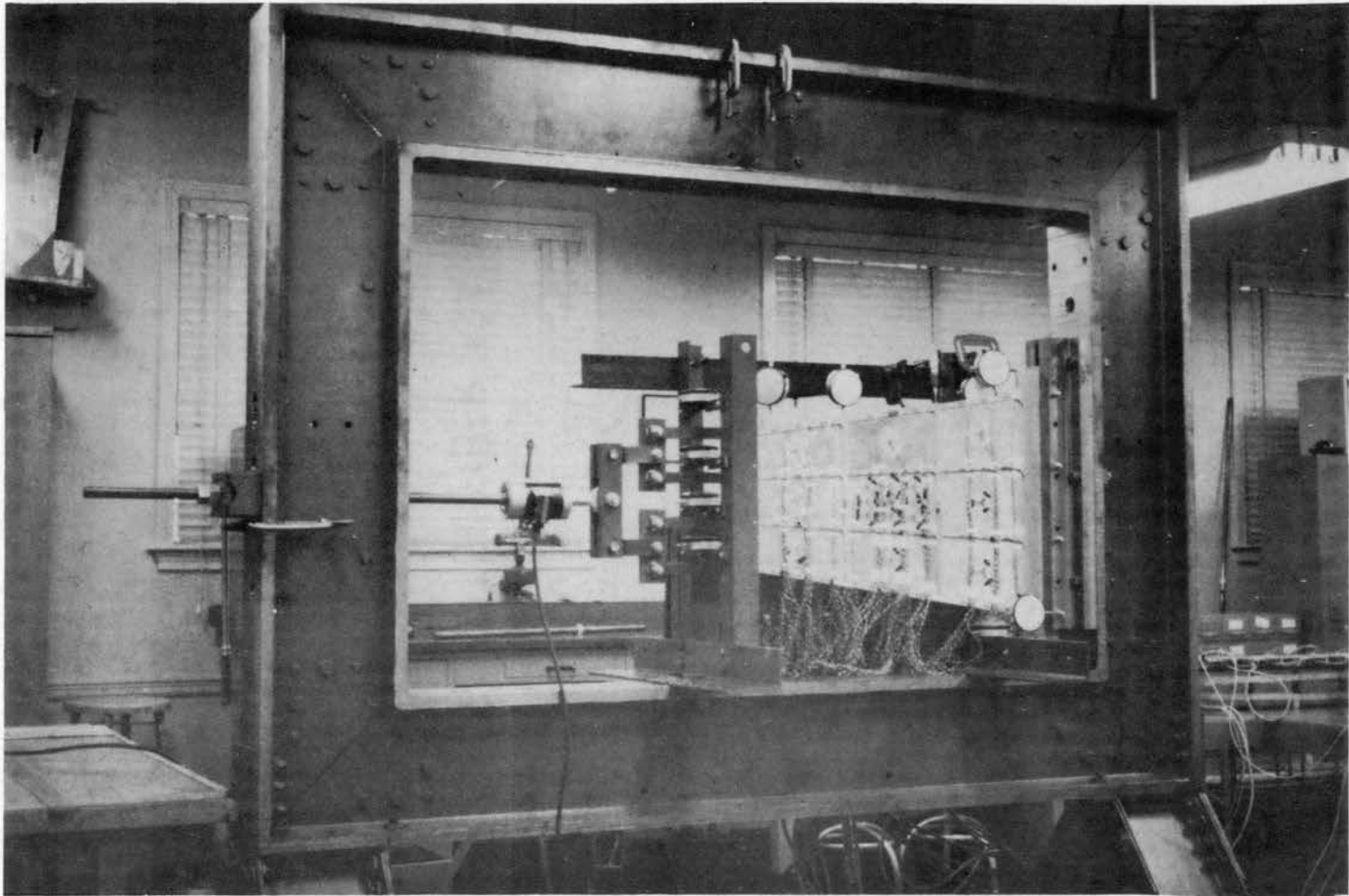


Figure 25. Experimental Facility and Structural Skin Panel

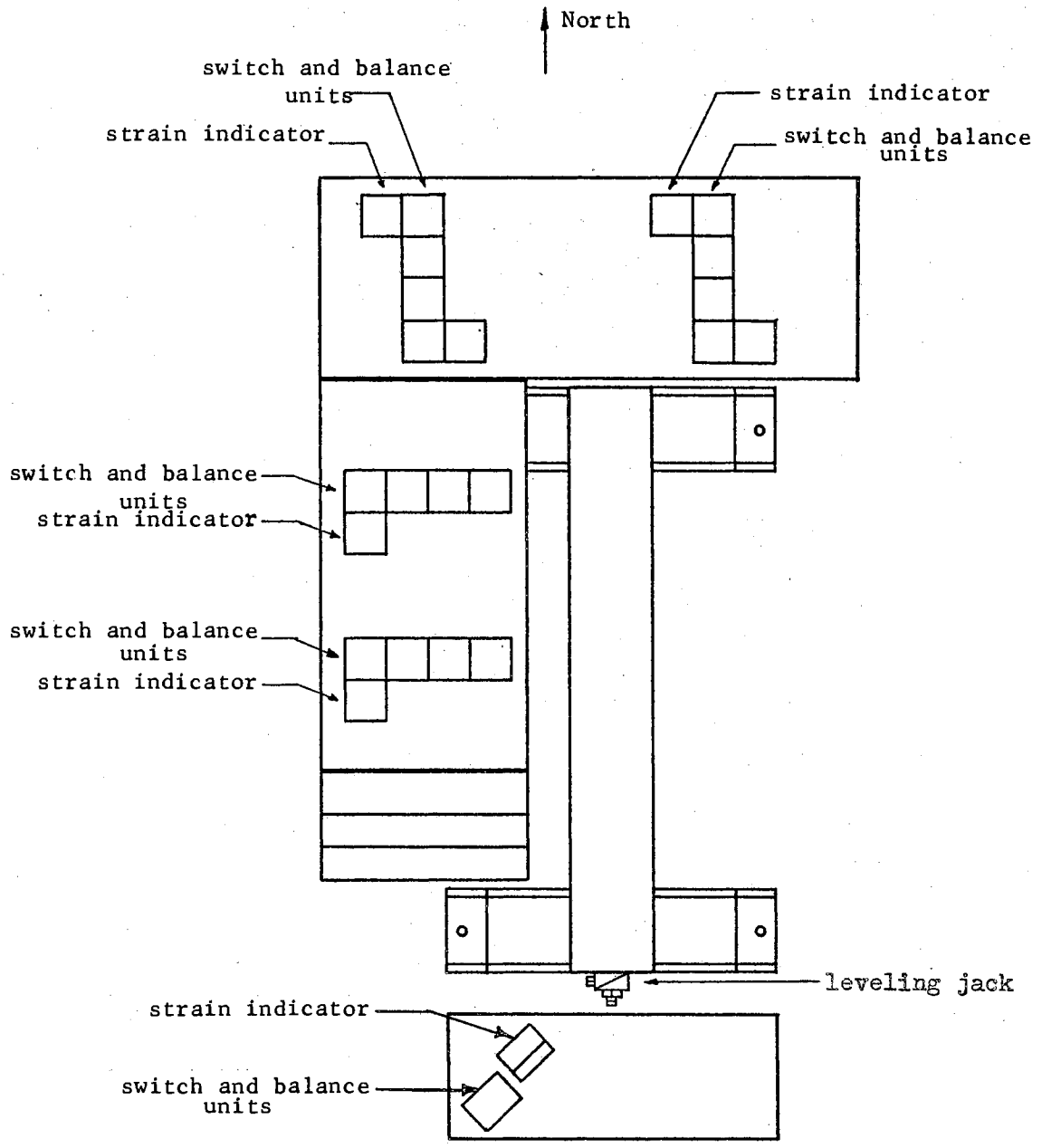


Figure 26. Floor Plan of Experimental Facility

Test Apparatus and Instrumentation

A list of the major equipment in this test program is given in Appendix F.

The types of strain gages selected for this experimental program were:

	<u>Axial</u>	<u>Rosette</u>
Manufacturer	The Budd Co.	The Budd Co.
Type	C12-121-A	C12-121D-R3Y
Gage Factor	$2.07 \pm \frac{1}{2}\%$	$2.03 \pm \frac{1}{2}\%$
Resistance	120 ± 0.2 ohms	120 ± 0.2 ohms

Eastman 910 cement was used to bond the strain gages to the surface of the model after the surface of the model had been prepared using sandpaper, trichlorethylene, and an acid neutralizer. A three-wire system was used to connect the strain gages to the read out instrumentation in order to cancel the effect of changes of wire resistance encountered due to changes in room temperature.

The strain gage data recording instrumentation consists of Budd Model P 350 Strain Indicators and Budd Model SB-1 Switch and Balance Units. These portable strain indicators and switch and balance units, shown in Figure 27 were used to record a total of 188 channels of strain data.

Deflections were measured with Starrett Dial Indicators. The indicators have a range of 0.4 inches and a graduation of 0.0001 inch. The dial indicators were located at the boundary of the panel as shown in Figure 28. Data from these dial indicators were used to determine the deflected shape of the panel. Appendix F contains a detailed

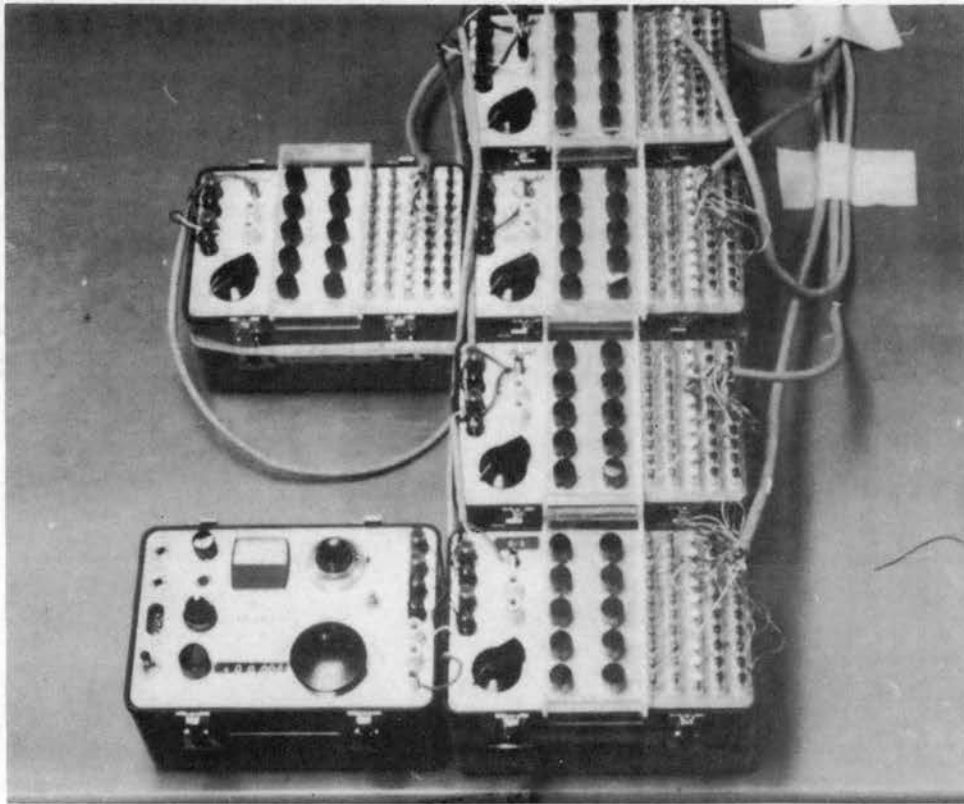


Figure 27. Portable Strain Gage Instrumentation

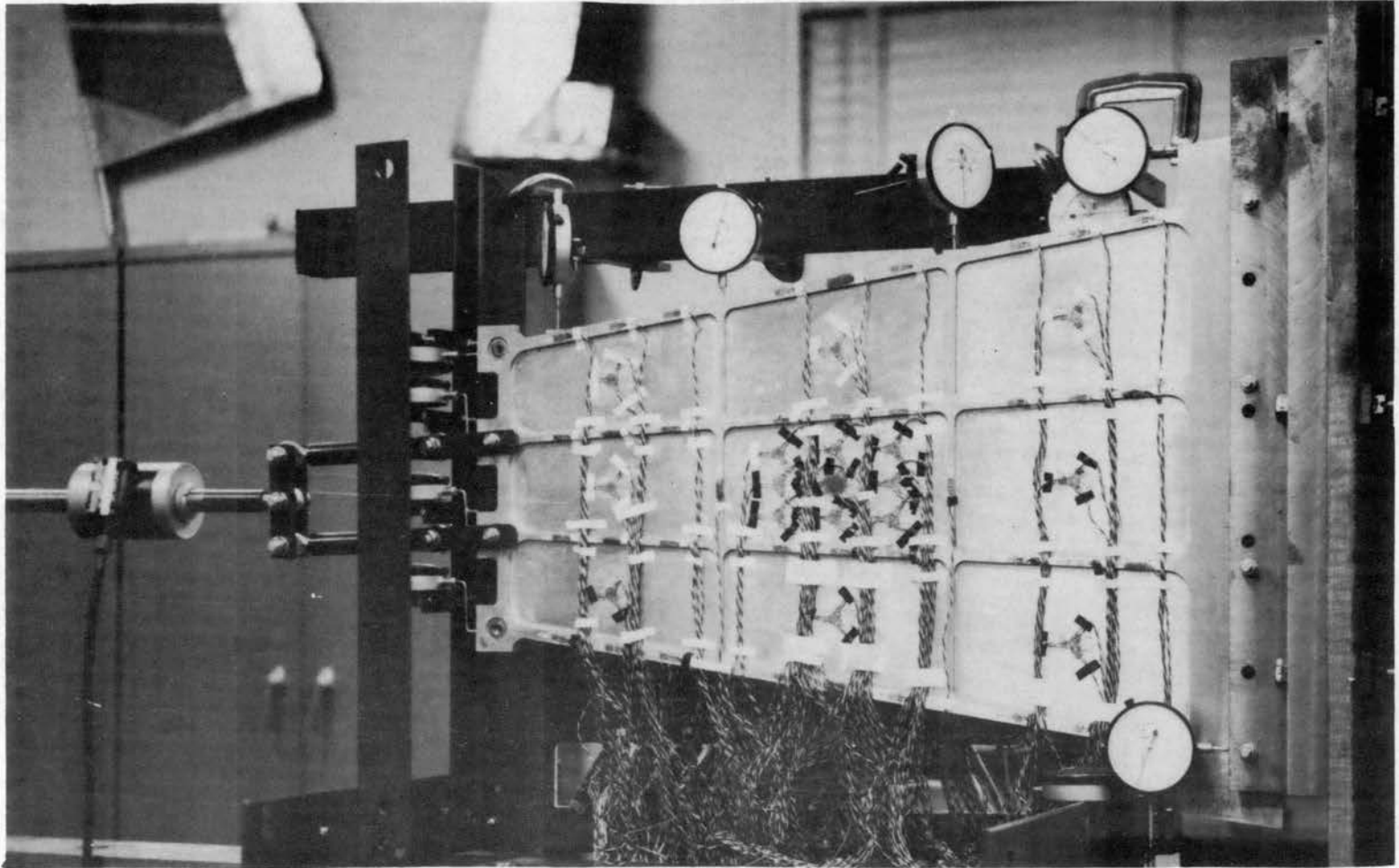


Figure 28. Experimental Tapered Reinforced Skin Panel

explanation of the calibration of the dial gages.

The loads were applied with an Empco Vertical Motion Jack Style JH-20, purchased from the Enterprise Machine Parts Corporation. Preliminary tests indicated that these mechanical load devices were satisfactory for this type of static testing. BLH SR-4 Load Cells were used to monitor the external loads on the panel. The loading system is shown in Figure 29. These load cells were calibrated by the manufacturer for an accuracy of ± 0.25 percent of full scale load value.

In order to read both load cells on the BLH SR-4 Indicator, the load cells were connected to the indicator through the BLH Switch and Balance Unit, and the system calibrated for a gage factor of 2.0. The SR-4 Load Cells were used to calibrate the BLH, Type N, Indicator against the Budd portable indicators based on the calibration factors specified by The Budd Company. The system was also calibrated with test equipment at the Halliburton Oil Company, Duncan, Oklahoma. A more detailed explanation of this calibration is given in Appendix E.

The loading system is shown in Figure 29. Load-divider systems shown in Figures 25 and 28 were used to divide the load symmetrically to the various load points for load configuration numbers one and three.

The basic loading fixture for the experimental investigation, Figure 25, was designed, fabricated, and used in previous experimental programs at Oklahoma State University (11), (12).

One of the most critical aspects of testing these small structural configurations for deflection and stress characteristics is the manner in which the model is supported in the loading fixture. The support system must not contribute effects at the supports which cannot be

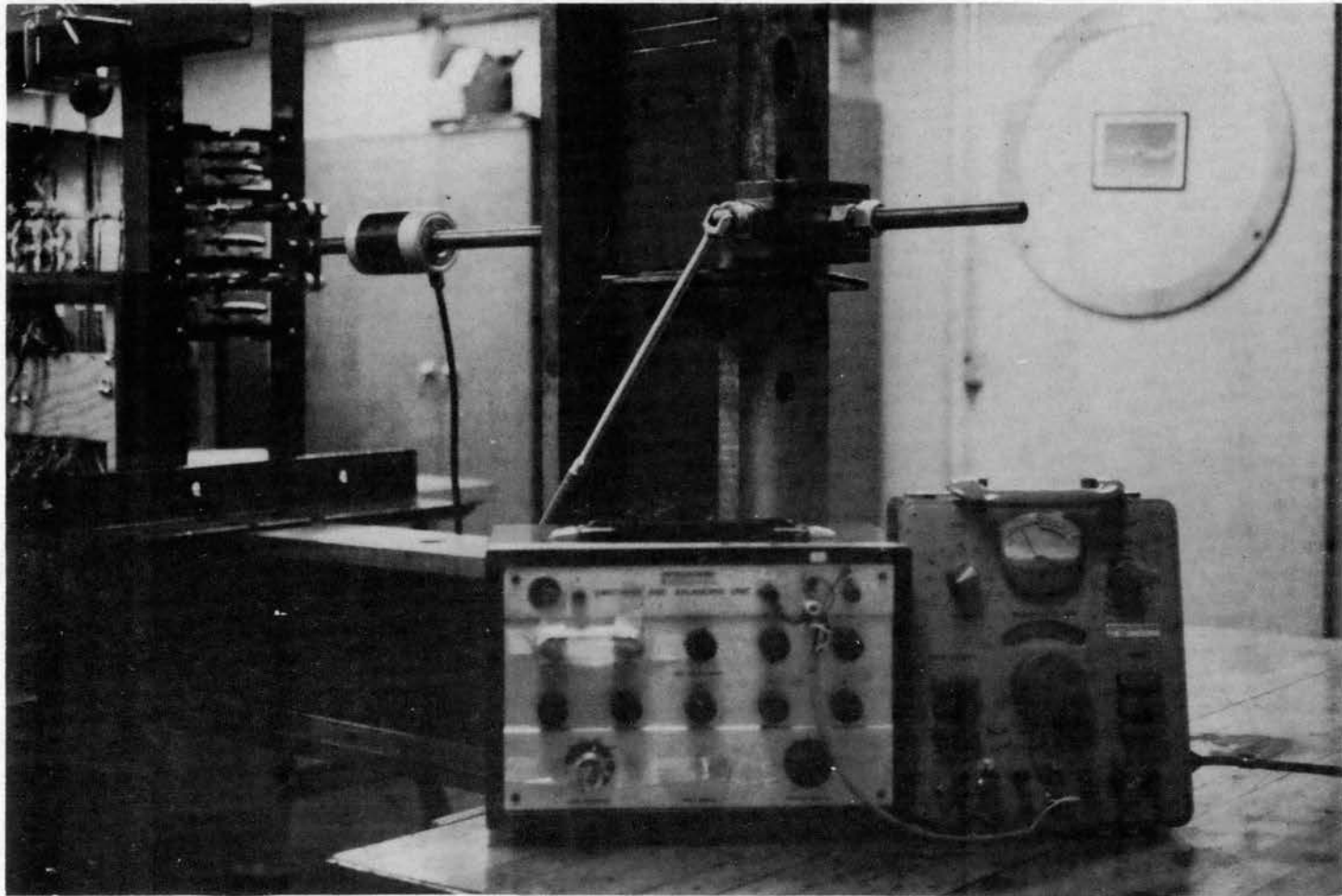


Figure 29. Mechanical Loading System.

represented accurately as boundary conditions. The support system should be rigid enough to minimize the contributions to the panel deflections for maximum loads. Two types of support configurations were considered: a simple support configuration, and a fixed-base configuration. Either of these support configurations could be handled accurately in the analysis; however, due to the results of Ayres' (12) work, the fixed support system, Figure 30 was chosen. A large factor affecting this choice was a result of friction in the sliding support which must be assumed friction free.

Preliminary tests were conducted on the panel with twenty strain gages to determine the panel alignment characteristics and to verify the design and application of the related test equipment. The objectives of the preliminary tests were:

1. To ascertain out-of-plane bending and torsion effects;
2. To ascertain the linearity of the load deflection relationships;
3. To determine hysteresis effects;
4. To determine the amount of preload required to remove the initial joint slippage in the model.

The results of these preliminary tests indicated that hysteresis effects were negligible for the load conditions to be investigated. In addition, the model yielded linear results with strains of sufficient magnitude to be recorded easily from the available equipment for the desired load levels. Stress concentration effects were observed from both the load divider system and the support system. These unavoidable effects were not excessive and, hence, did not prejudice the experimental data.

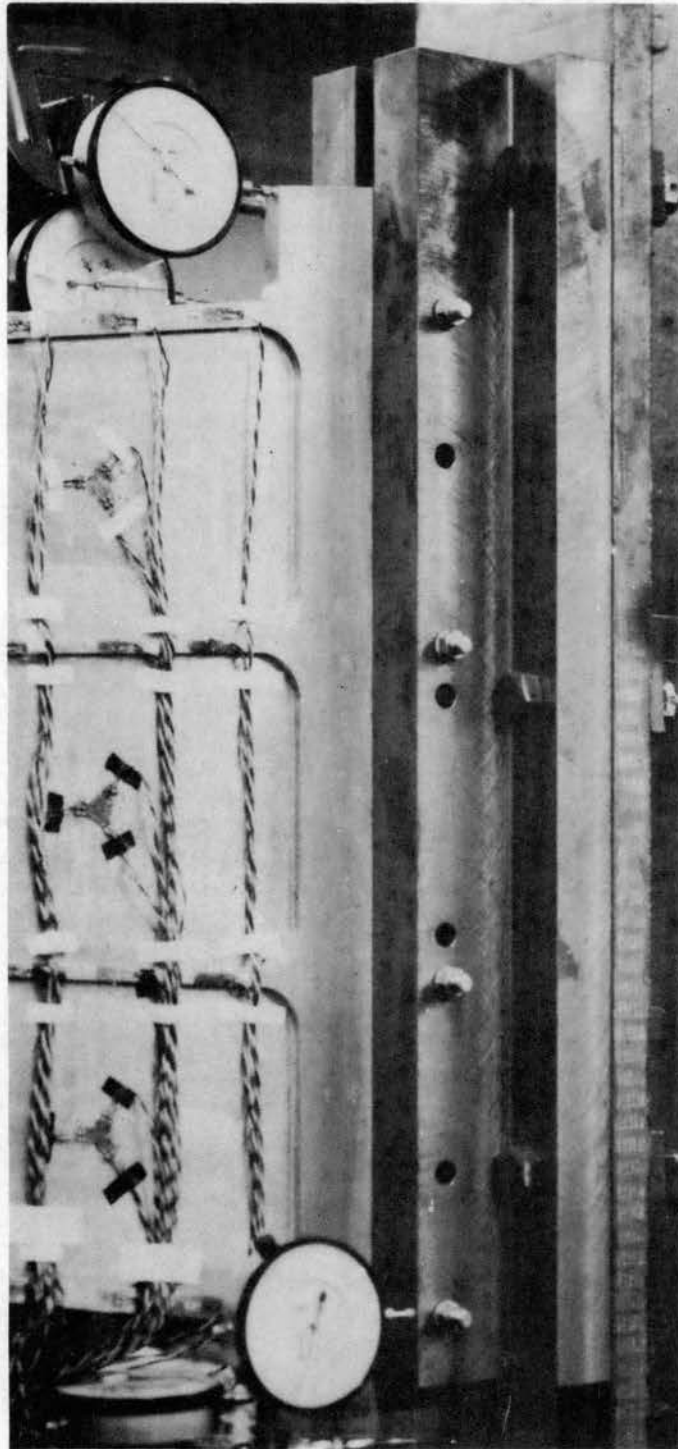


Figure 30. Support System

The preliminary tests did indicate that a small amount of out-of-plane deformation was present in the model as a result of the machining operation. This initial deformation had a significant effect on strain measured at the surface of the stringers and ribs. The strain gages on the stringers and ribs were actually one-fourth inch from the center plane of the model. However, good results were obtained by using strain gages located opposite each other on the ribs and stringers and by using the average of the two readings.

The initial shape of the model also had a significant effect for the shear load configuration. The initial eccentricity resulted in less load capacity than would have been present for a perfect model. This difficulty was overcome by using a 10,000-pound uniform preload to straighten the model for the shear load configuration. Since the combined load was still in the linear load-deformation range, the effect of the 10,000-pound uniform load was easily segregated from the shear load effects.

Subsequent to the completion of the preliminary tests, an additional 168 strain gage legs were applied to the model at the typical locations shown in Figure 31. In many cases, redundant gage locations were used to check the symmetry of load distribution. The axial and rosette gages were numbered as shown in Figure 31. All axial gage numbers begin with "1" signifying one leg, while all rosette leg numbers begin with "3", signifying three legs. All even numbered legs are located on the side shown in Figure 31 and all odd numbered legs with the "0" designation are mounted on the opposite side, "mating" with the appropriate even numbered legs. The numbering system was designed to provide maximum flexibility in the adding or in the changing of

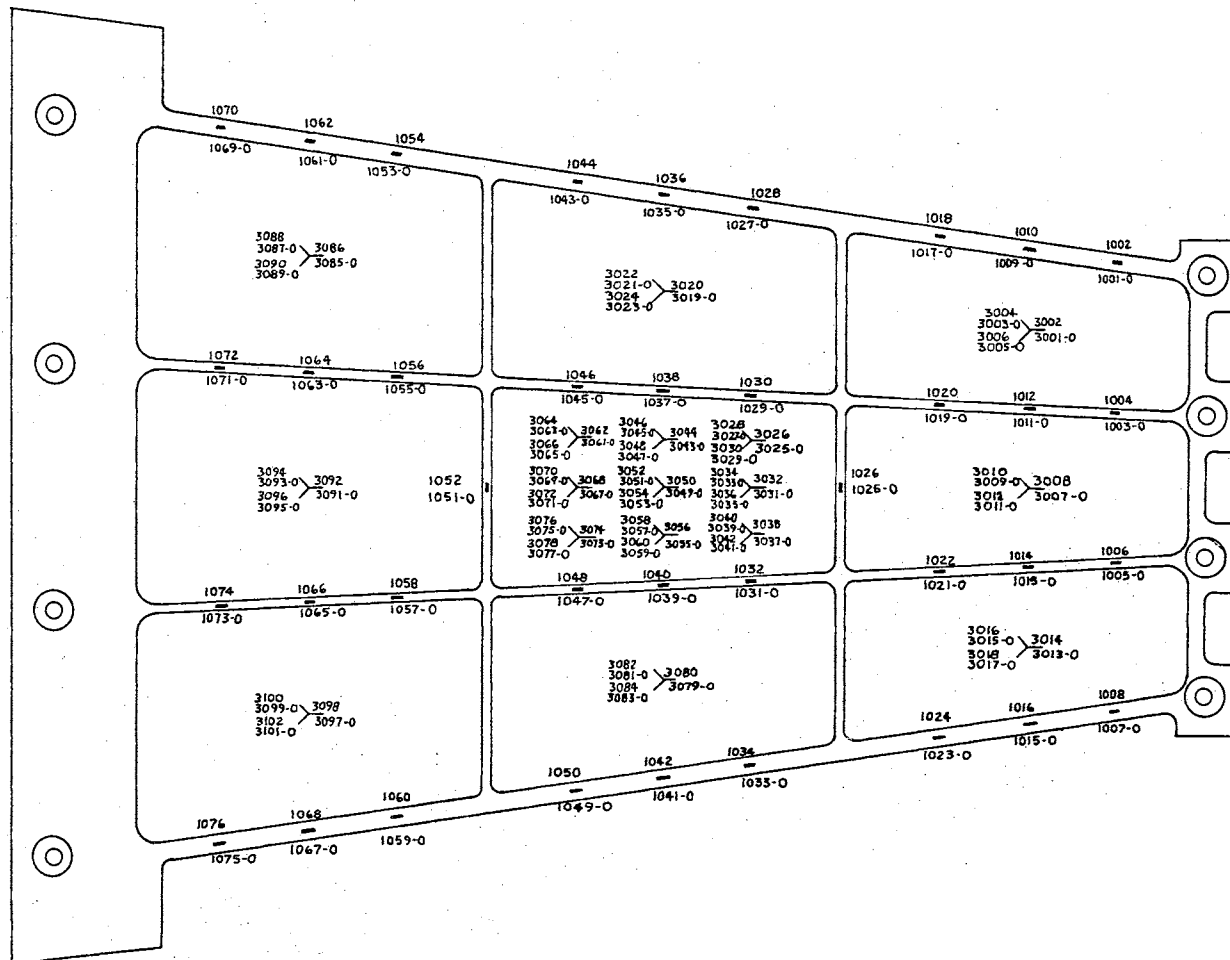


Figure 31. Gage Numbering System

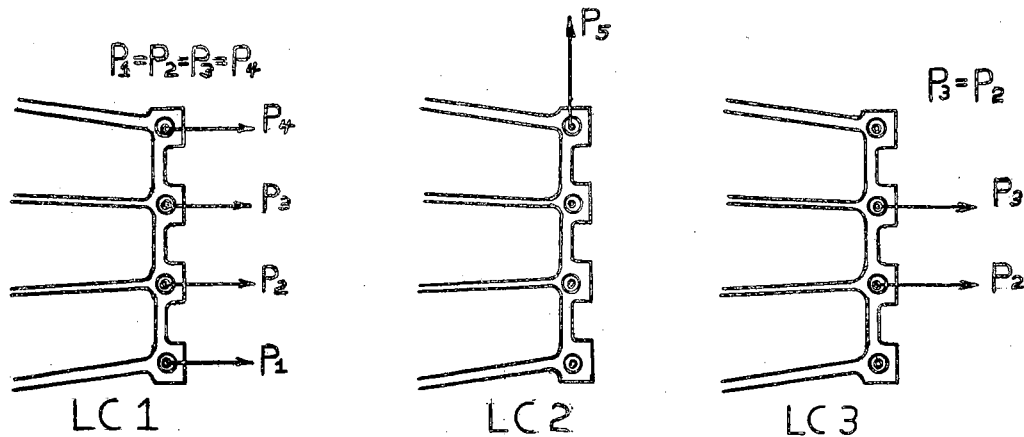


Figure 32. Load Configurations

gages. The gage locations are shown in Figure 33.

Deflections and internal load distributions were determined experimentally for the fundamental types of applied loads that are found on actual aircraft structural skin panel configurations. The test configurations are divided into three load conditions. These three load conditions are shown in Figure 32. The force values corresponding to the configurations are shown in Table XVIII. Data for each test configuration were obtained after a check out of the test equipment.

Three tests corresponding to the appropriate load conditions were conducted. These tests are shown in Table XVIII. All strain gages were monitored during each test. All experimental strain data were reduced to final values of stress by techniques explained in Appendix E. Deflection data were obtained for the magnitudes of external loads shown in Table XVIII. Since hysteresis effects were demonstrated to be small in the preliminary test, data were recorded for increasing loads

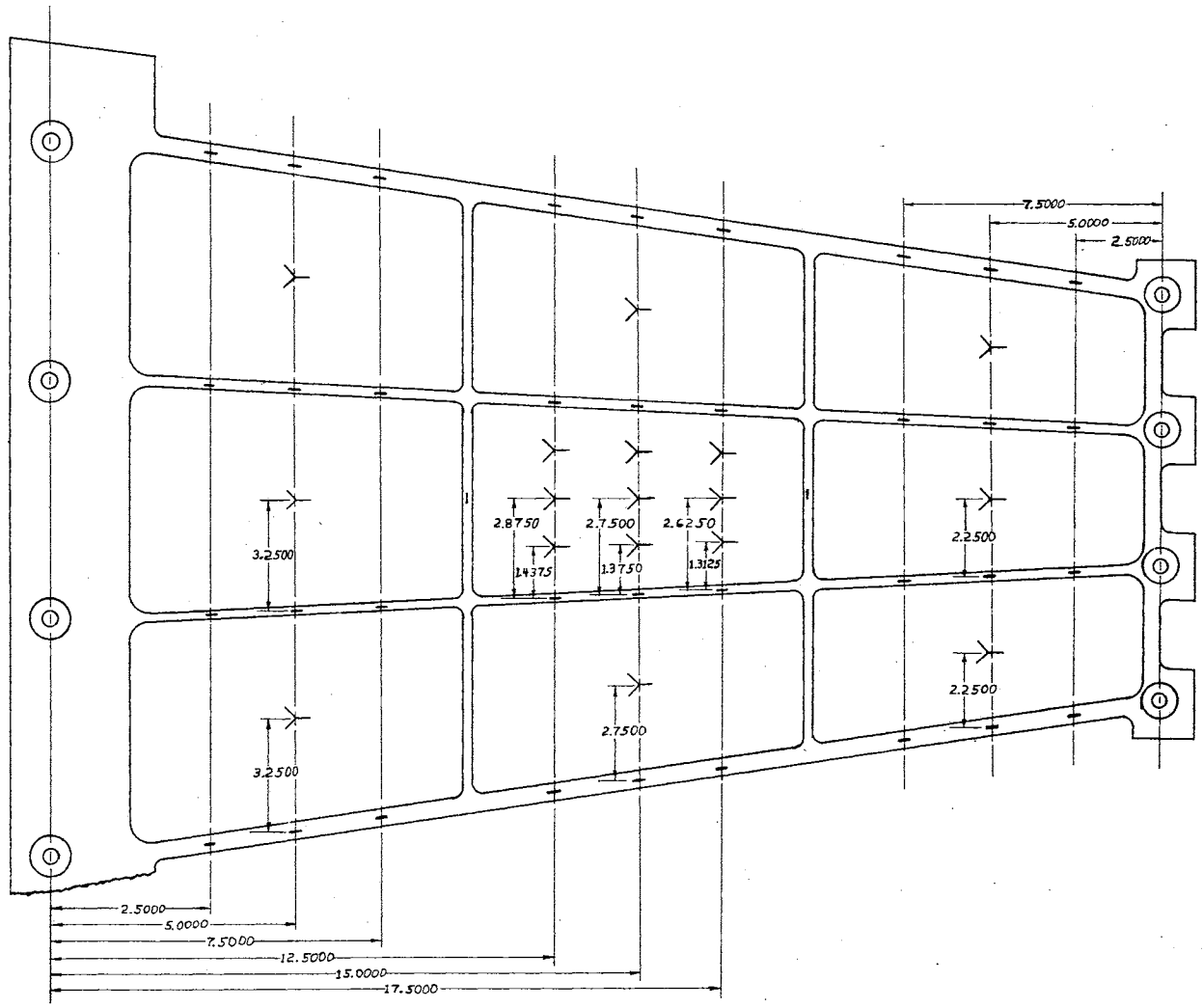


Figure 33. Gage Locations

TABLE XVIII
FORCE VALUES

Pi \ Value		1	2	3	4	5	6	7	8	9	10	11
LC1 TEST 2	P ₁	1	250	500	750	1000	1250	1500	1750	2000	2250	2500
	P ₂	1	250	500	750	1000	1250	1500	1750	2000	2250	2500
	P ₃	1	250	500	750	1000	1250	1500	1750	2000	2250	2500
	P ₄	1	250	500	750	1000	1250	1500	1750	2000	2250	2500
	P ₅	0	0	0	0	0	0	0	0	0	0	0
LC2 TEST 3	P ₁	0	0	0	0	0	0	0	0	0	0	0
	P ₂	0	0	0	0	0	0	0	0	0	0	0
	P ₃	0	0	0	0	0	0	0	0	0	0	0
	P ₄	0	0	0	0	0	0	0	0	0	0	0
	P ₅	1	200	400	600	800	1000	1200	1400	1600	1800	2000
LC3 TEST 1	P ₁	0	0	0	0	0	0	0	0	0	0	0
	P ₂	1	250	500	750	1000	1250	1500	1750	2000	2250	2500
	P ₃	1	250	500	750	1000	1250	1500	1750	2000	2250	2500
	P ₄	0	0	0	0	0	0	0	0	0	0	0
	P ₅	0	0	0	0	0	0	0	0	0	0	0

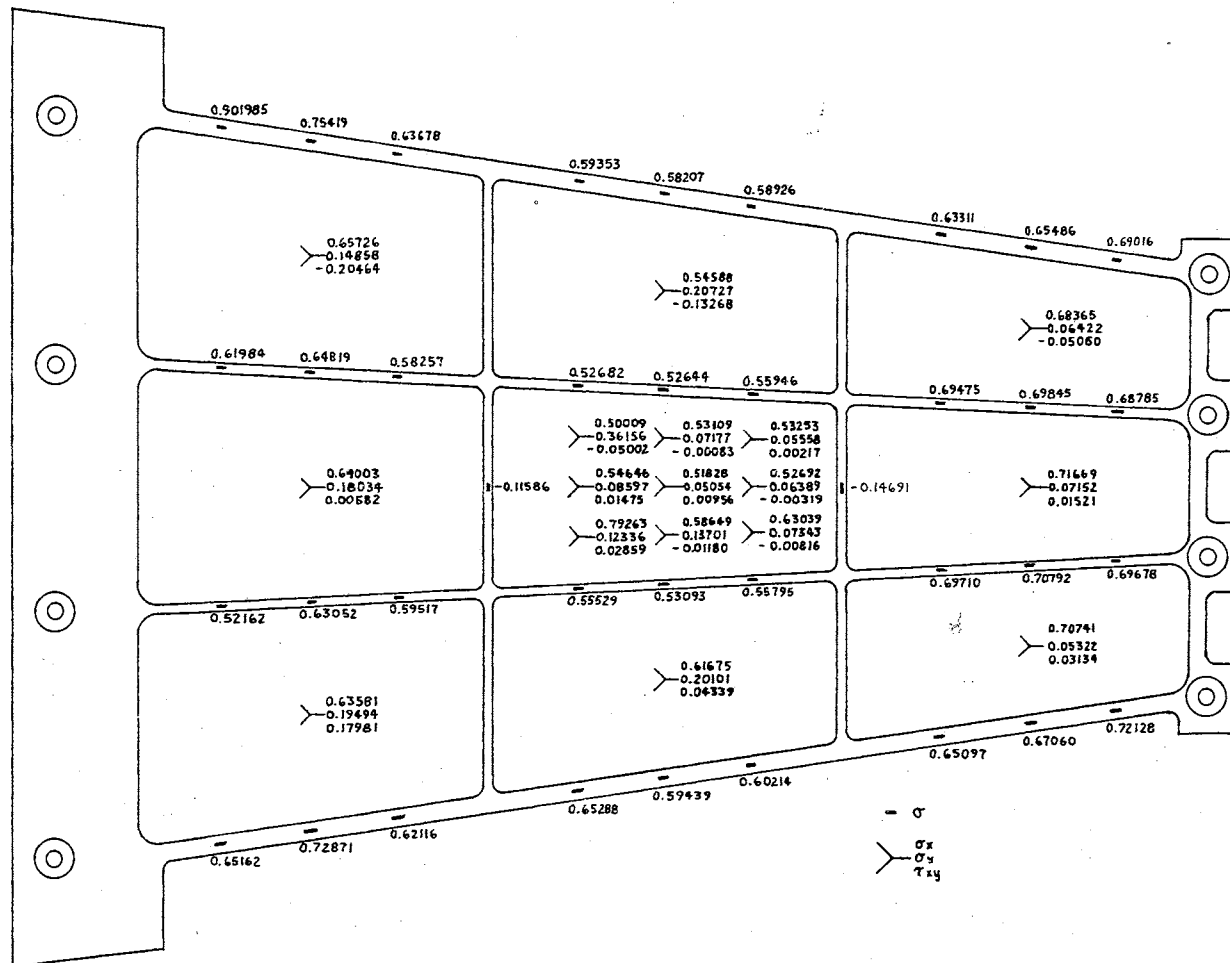


Figure 34. Stress Values for LC-1, Test No. 2

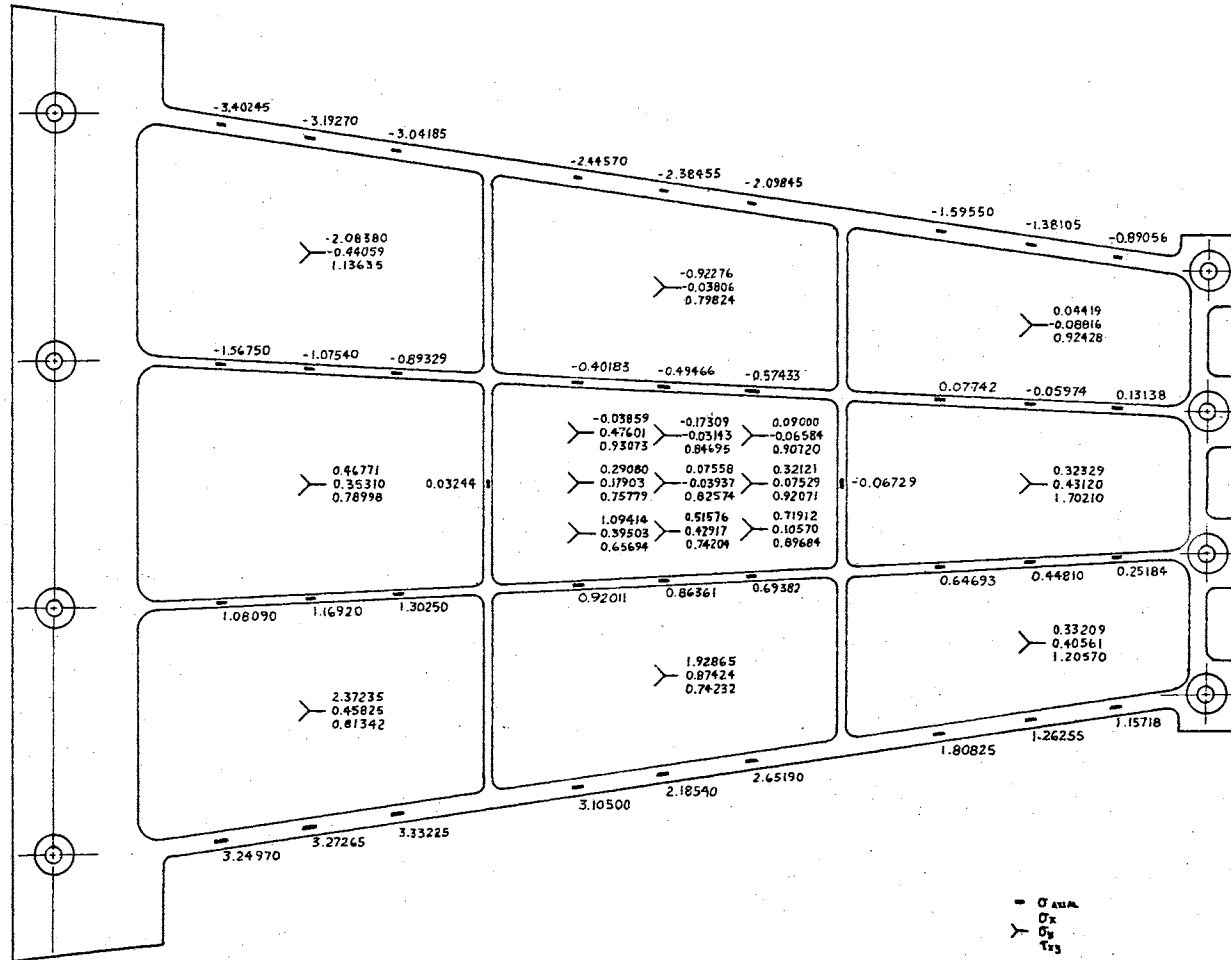


Figure 35. Stress Values for LC-2, Test No. 3

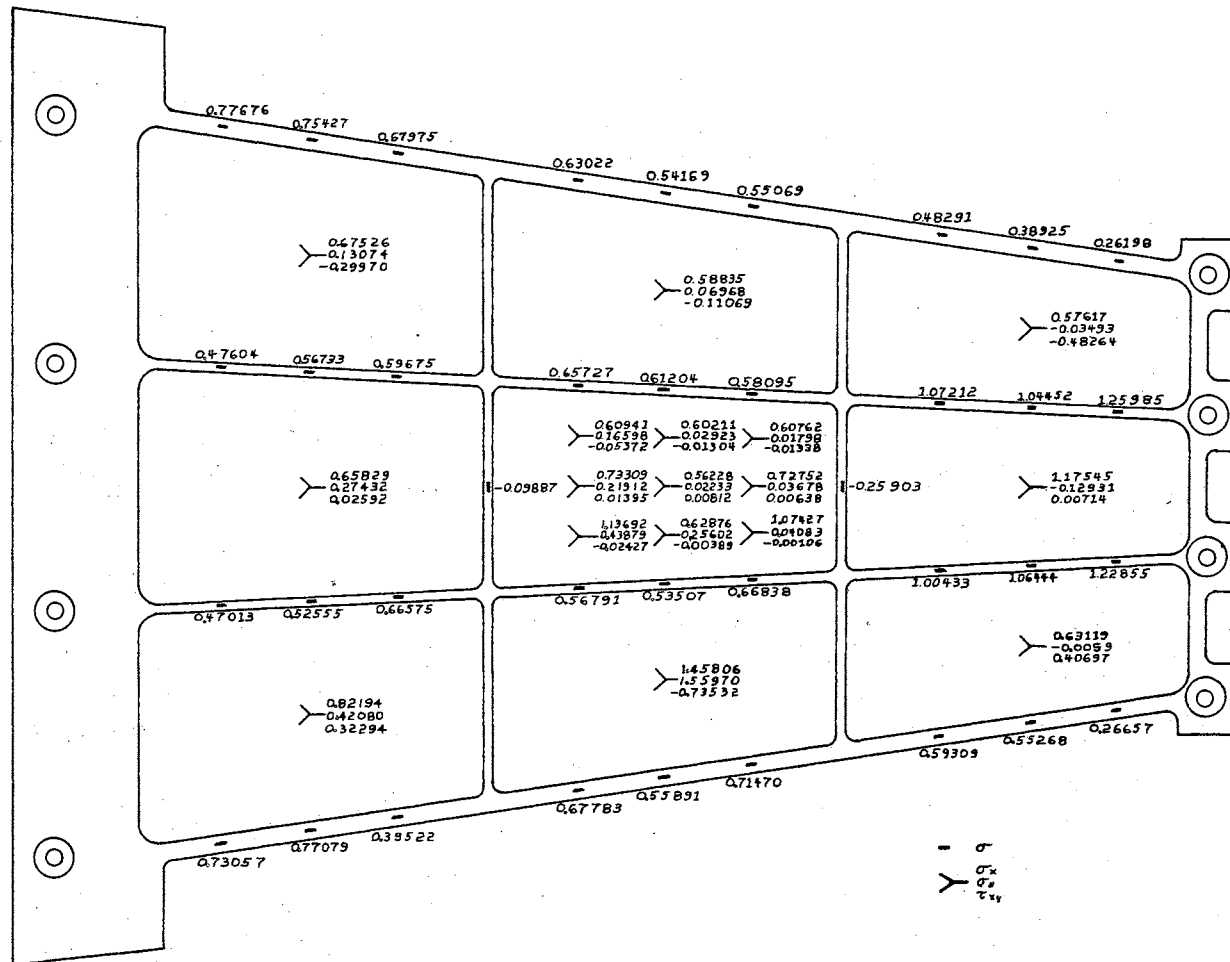


Figure 36. Stress Values for LC-3, Test No. 1

at equal intervals for the number of observations during each test condition as shown in Table XVIII. The deflection data are shown in the experimental portions of Tables XIX, XX, and XXI of Chapter V.

The stress data for each load condition are shown in Figures 34, 35, and 36. In these figures, the stress values are given in terms of PSI per pound of load cell load. For example: to obtain the correct values for LC-1, the values of Figure 34, should be multiplied by 4.

This chapter has provided a detailed explanation of the experimental analysis conducted on the test structure. The purpose of and the main objective of this experimental investigation have each been outlined. The construction of the test structure itself was described including details of the material employed, the manufacturer, etc.

The testing facility and all load application equipment, strain measuring apparatus, and deflection measuring equipment have been presented. The calibration of all pertinent equipment was given. The representative load configurations used were illustrated along with the force values corresponding to each configuration.

All stress data were calculated from strain data measured directly by the portable strain gage instrumentation. The strain data were reduced from ten observations at each strain gage leg location to a representative value of strain per unit load cell load by the least squares fit criterion of statistical theory. This treatment of the experimental strain data is explained in Appendix E.

All experimental deflection data were reduced by hand and verified to a certain extent by comparing the deflection values of loaded points in the axial direction with those values determined by summing the strain data at representative points along the axis of each stringer.

This comparison showed good agreement between the experimentally measured deflection data and the approximate integration of the axial strain values along the stringers.

The above comparison and the result of the calibration of all critical measuring equipment indicate that all experimental data are correct within a reasonable amount of accuracy.

CHAPTER V

COMPARISON OF ANALYTICAL AND EXPERIMENTAL RESULTS

The objective of this research effort is to develop the capability for the analytical and experimental investigation of integrally reinforced tapered skin panels with finite element methods of structural analysis. The analytical capabilities, which are developed, include both the force and direct stiffness methods of structural analysis.

The stiffness method of analysis demonstrates how a structure with complicated geometry can be analyzed with relatively simple theoretical elements through idealization. All three analyses were performed with the digital computer specifying only the geometric and structural configuration of the skin panel. The analysis capability is described in Chapter III and Appendices A and B. The results of the stiffness method analysis serve as both a check and theoretical comparison for the results of the analysis by the matrix force method.

The matrix force method of analysis was used for the more extensive investigations of the structural skin panel. It demonstrates the redundant load paths that are possible in the analysis of complex skin structures. The accuracy of the matrix force analysis is influenced by the choice of the idealized statically determinate system. The idealized systems used in this investigation satisfactorily represent the principal load paths throughout the structure. The idealization resulted in well-conditioned matrices preserving computational accuracy and stress

variations that represent the actual structural behavior. Consequently, good results are obtained from the matrix force method of analysis. The analysis capability is available for further study of any class of two dimensional structural configurations. The scope of these problems is too broad to be mentioned here.

The experimental capabilities developed during this and previous investigations have provided fundamental procedures and equipment that are applicable for numerous future research programs. Some of these possibilities are suggested in Chapter VI.

A total of three tests were performed with the integrally reinforced tapered panel, using three load conditions applicable for this type of structure. These three load conditions have been described in Chapters III and IV. Only the basic data required for comparison to the analytical results are reported in this thesis. Data from additional tests would only duplicate the basic information given in this chapter. The basic data reported here are sufficient to indicate the good agreement between the analytical and experimental results. This agreement demonstrates the applicability of the finite elements methods of structural analysis for planar stiffened shell structural skin panels.

The comparisons of the analytical and experimental stress results at typical points on the panel are shown in Figures 37 through 44. The comparisons of the analytical and experimental deflection results for points on the edge of the panel are shown in Tables IX, X, and XI.

The deflections representing the corner point where the shear load is applied are actually shown for two different points located as close as possible to each other. The analytical data are obtained for the exact point where the shear load is applied. Due to the loading system,

it was not possible to place a dial indicator at the same point.

Therefore, the experimental data are obtained for a point approximately two inches from the point where the shear load is applied.

The experimental deflection data shown in Tables IX, X, and XI are corrected based on the measured deflections of the supporting system.

Figures 37, 38, and 39 show axial stress values produced by load conditions 1, 2, and 3, respectively. The stress values are oriented in the x direction and are plotted at the strain gage locations along the center point of the center bay of the test structure. The reference point for plotting is the longitudinal centerline of the test structure. Distances to the left of the centerline are negative while those to the right are positive. A "best fit" straight line has been drawn by hand through the experimental data points. The dimensions of the test structure are shown in Figure 13 and the strain gage locations are shown in Figure 32. Figure 44 is very similar to Figures 37, 38, and 39 except that it shows values of shear stress produced by load condition 3. These shear stress values were plotted at the strain gage locations along the center point of center bay of the test structure. Only those locations resting on the surface of the webs are applicable since only single legged axial gages are mounted on the surface of the stringers and, furthermore, the modified or extended matrix force method contains no assumption that the idealized bar elements carry shear stress.

Figures 40, 41, 42, and 43 show values of axial stress produced by load conditions 1, 2, and 3. These stress values are plotted along the axes of the stringers. The experimental values appear opposite the strain gage locations on each stringer while the values from the extended matrix force method which contains the new flexibility matrix

$[ALPIJ]_{prs}$ appear at the "idealized junctions" of the bar elements making up each stringer.

Tables XIX, XX, and XXI show experimental values of load point deflection versus theoretical values. The theoretical values are those produced by the extended matrix force method with the new $[ALPIJ]_{prs}$ matrix included. The experimental values from two representative tests were averaged and normalized for measured base deflection.

Figures 37 and 40 contain stress results produced by each of the four analyses of the test structure: the experimental analysis, the extended matrix force analysis which contains the new $[ALPIJ]_{prs}$ matrix, the unmodified version of the matrix force method employing redundants choice number 1 and the direct stiffness method. As can be readily seen from these two figures, a very definite improvement in the axial stress results has been made by the use of the new flexibility matrix, $[ALPIJ]_{prs}$ included in the extended version of the matrix force method over those of the unmodified version of the matrix force method. This fact is born out by Figures 38, 39, 41, 42, and 43. Furthermore, the results of the extended matrix force method agree quite favorably with those of the direct stiffness method.

As can be seen from Tables XIX, XX, and XXI, the values of load point deflection produced by the extended matrix force method agree very well with the normalized average of the experimental values.

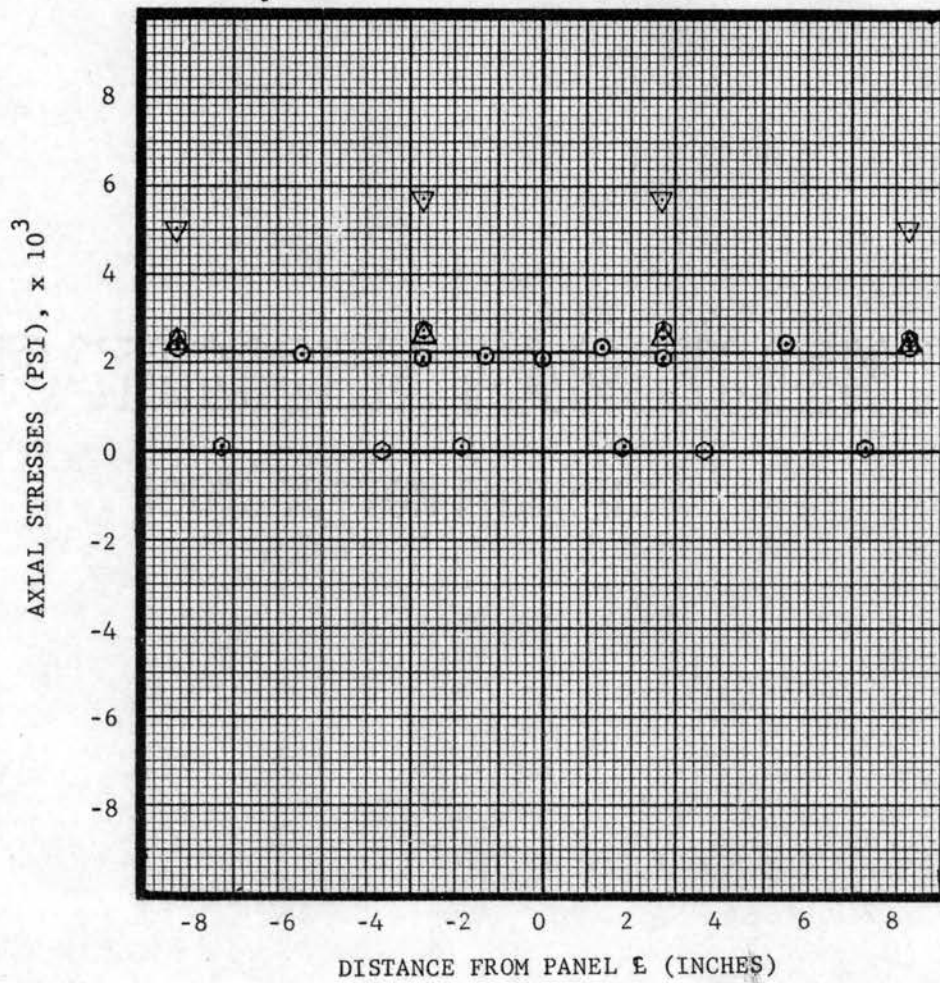
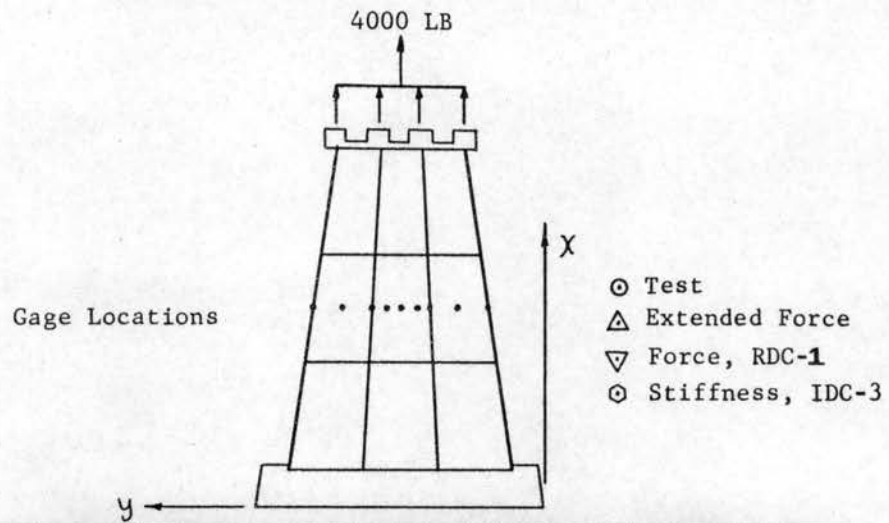


Figure 37. Axial Stresses for LC-1

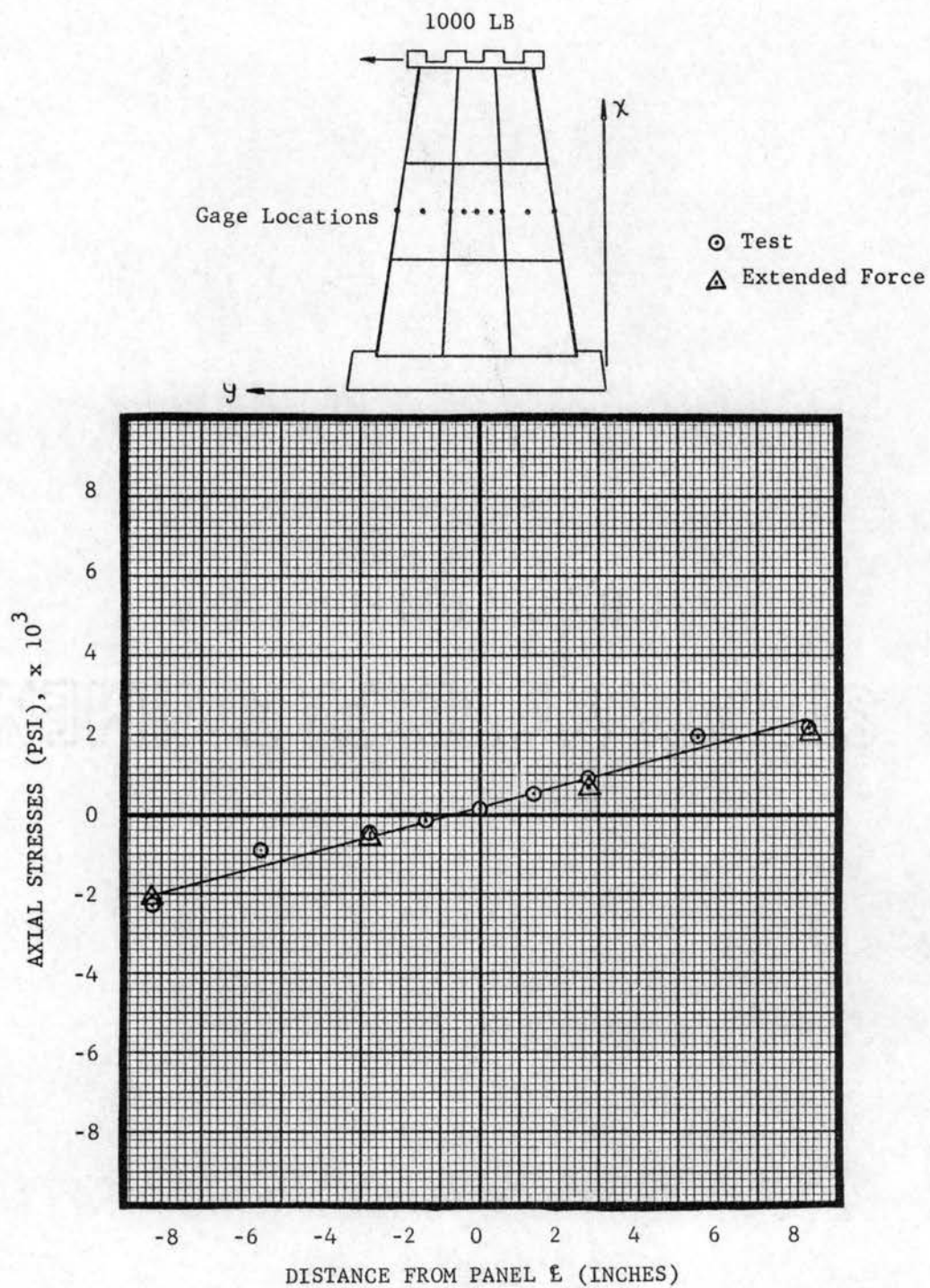


Figure 38. Axial Stresses for LC-2

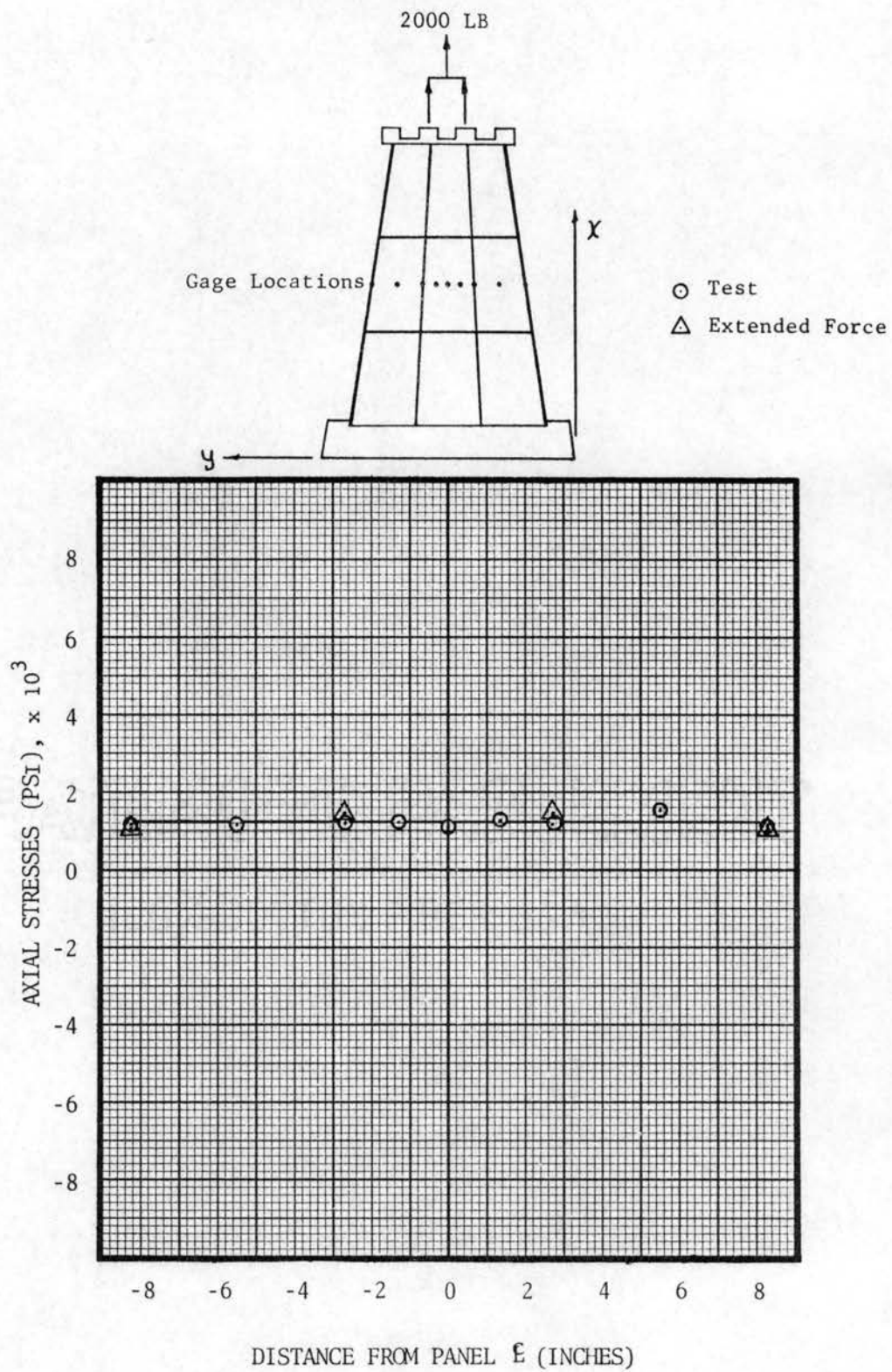


Figure 39. Axial Stresses for LC-3

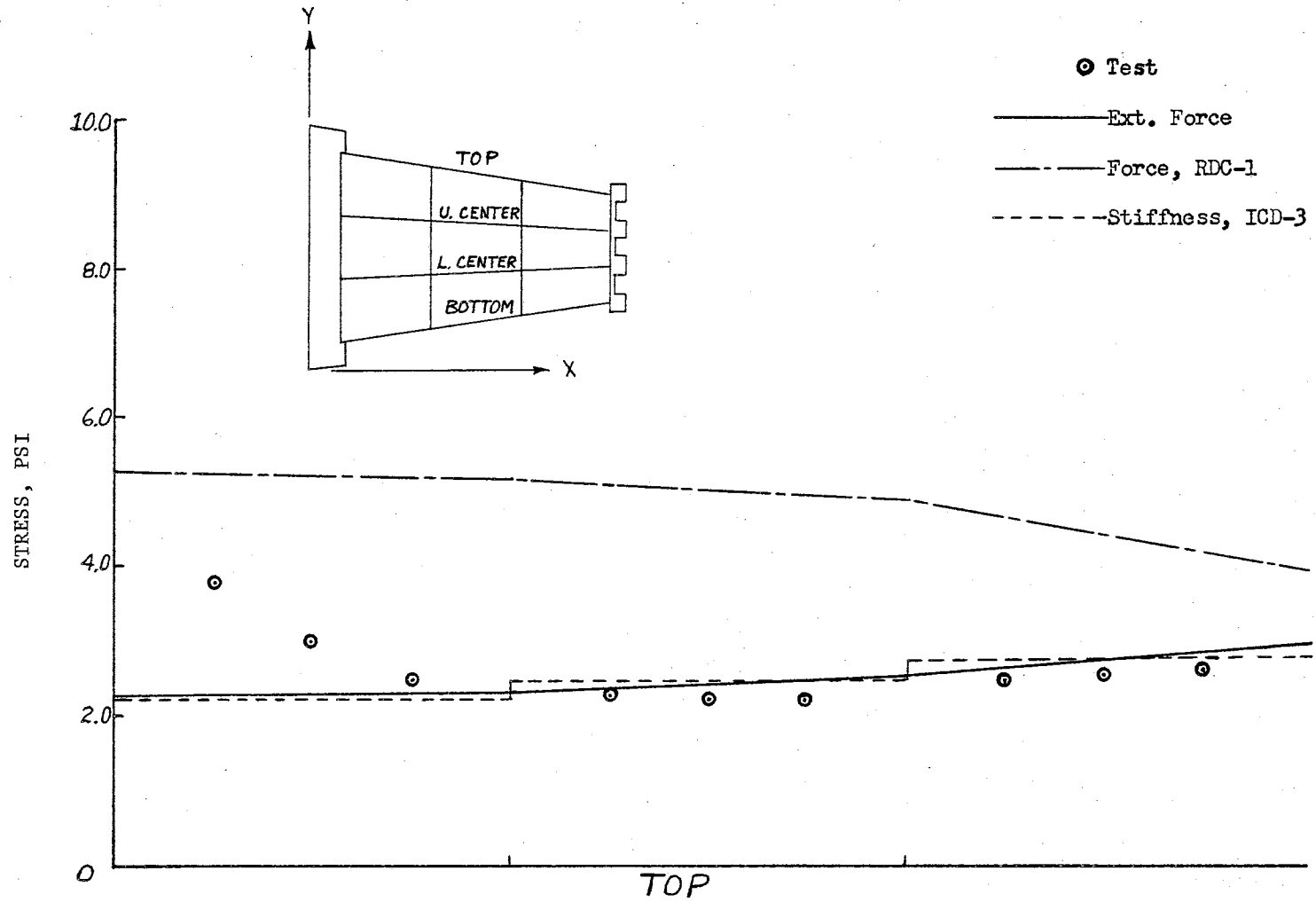


Figure 40. Top Stringer Stresses for LC-1

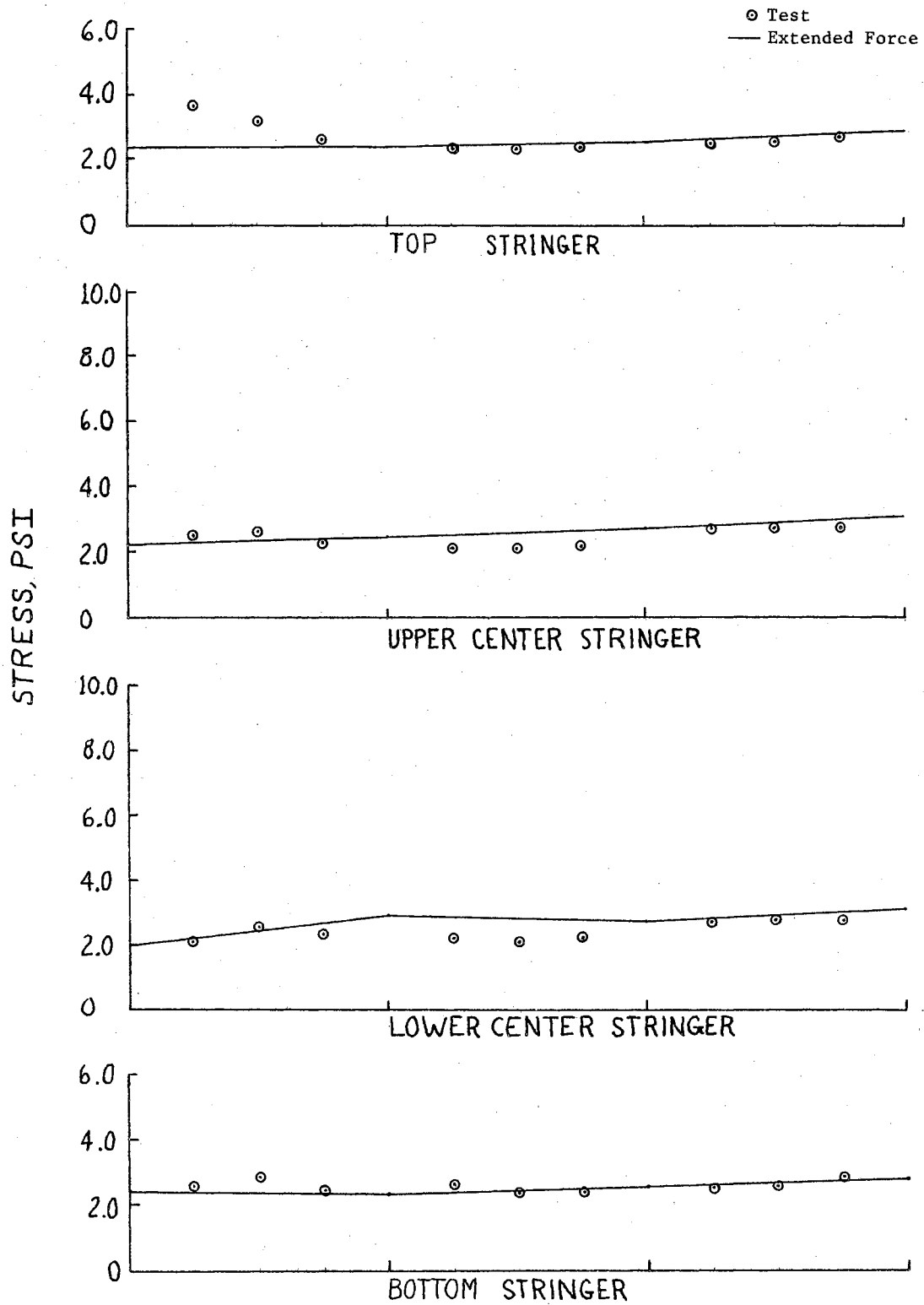


Figure 41. Stringer Stresses for LC-1

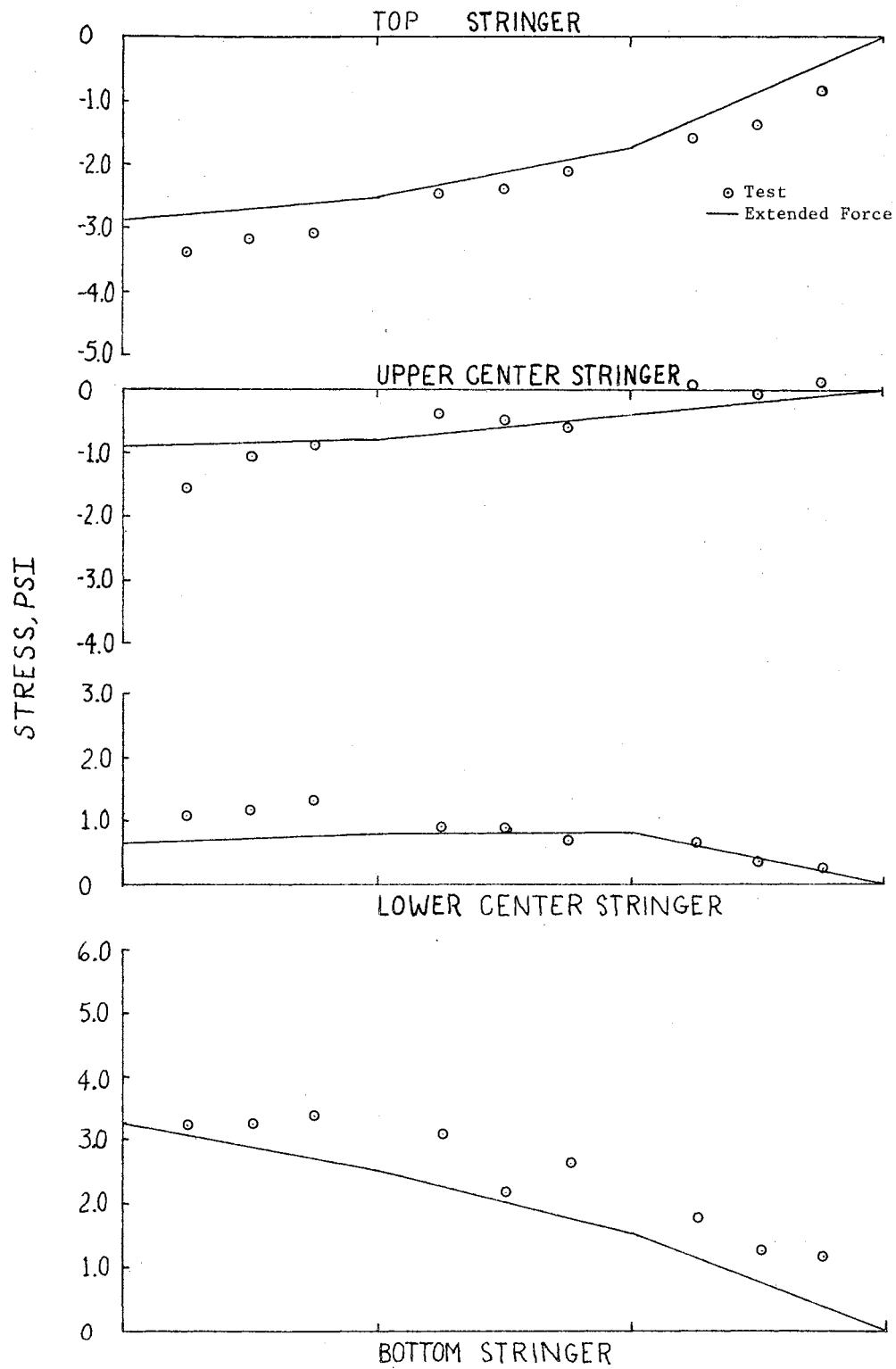


Figure 42. Stringer Stresses for LC-2

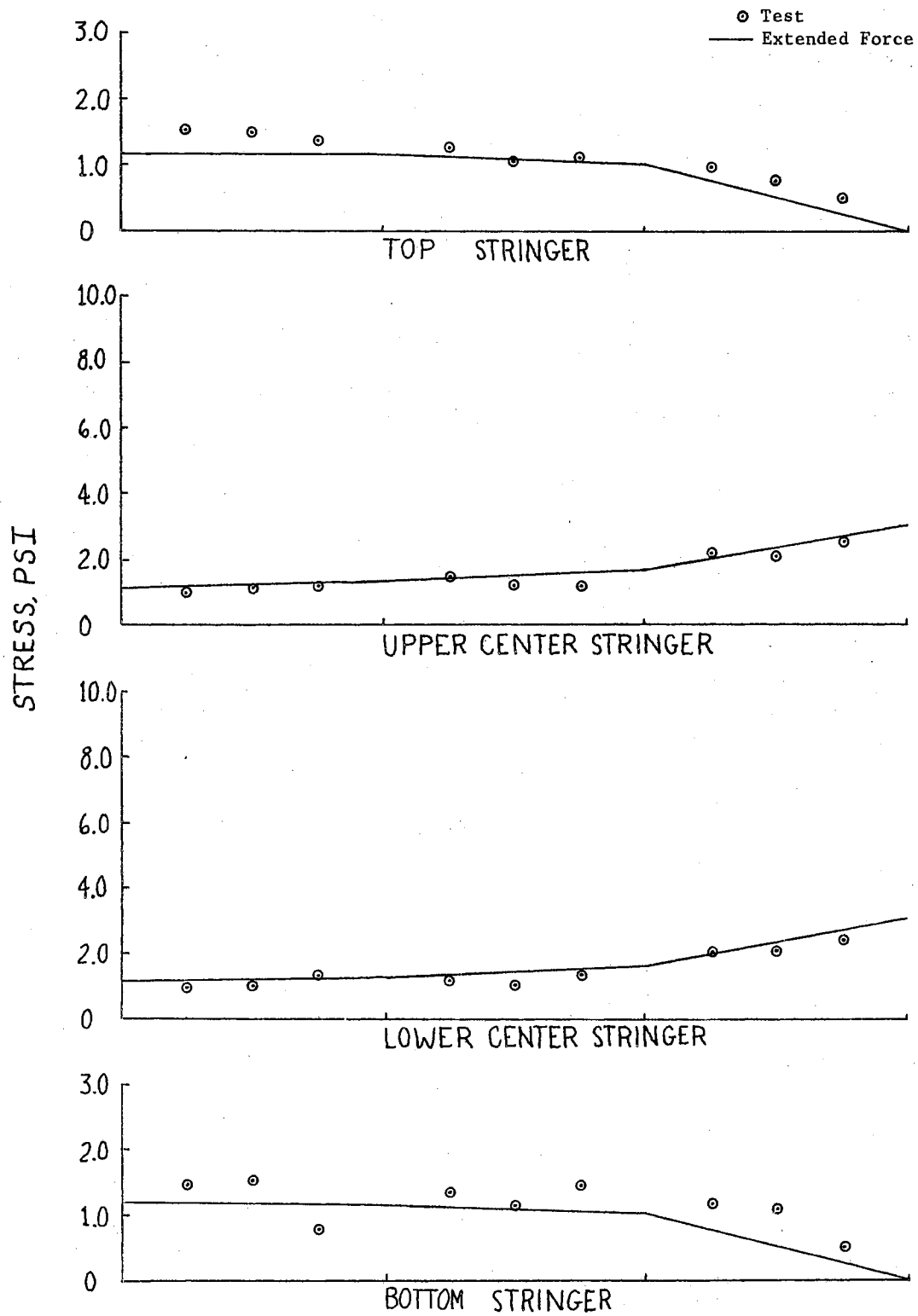


Figure 43. Stringer Stresses for LC-3

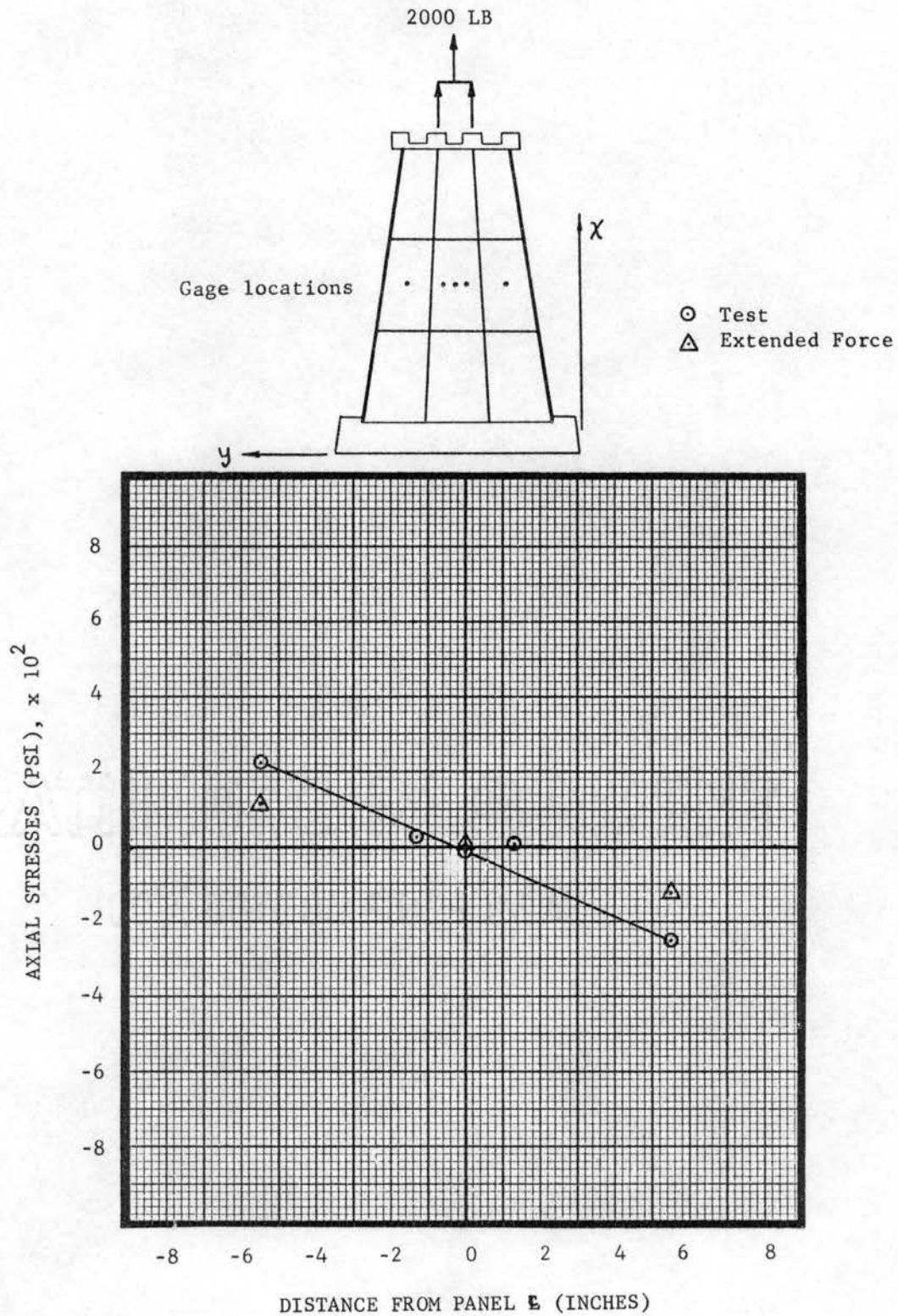
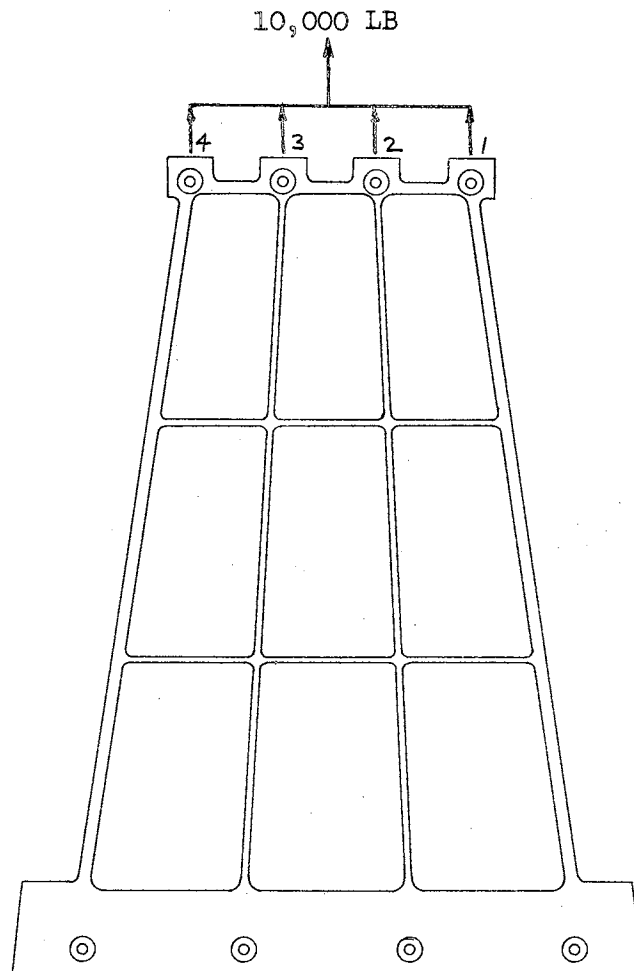


Figure 44. Shear Stresses for LC-3

TABLE XIX

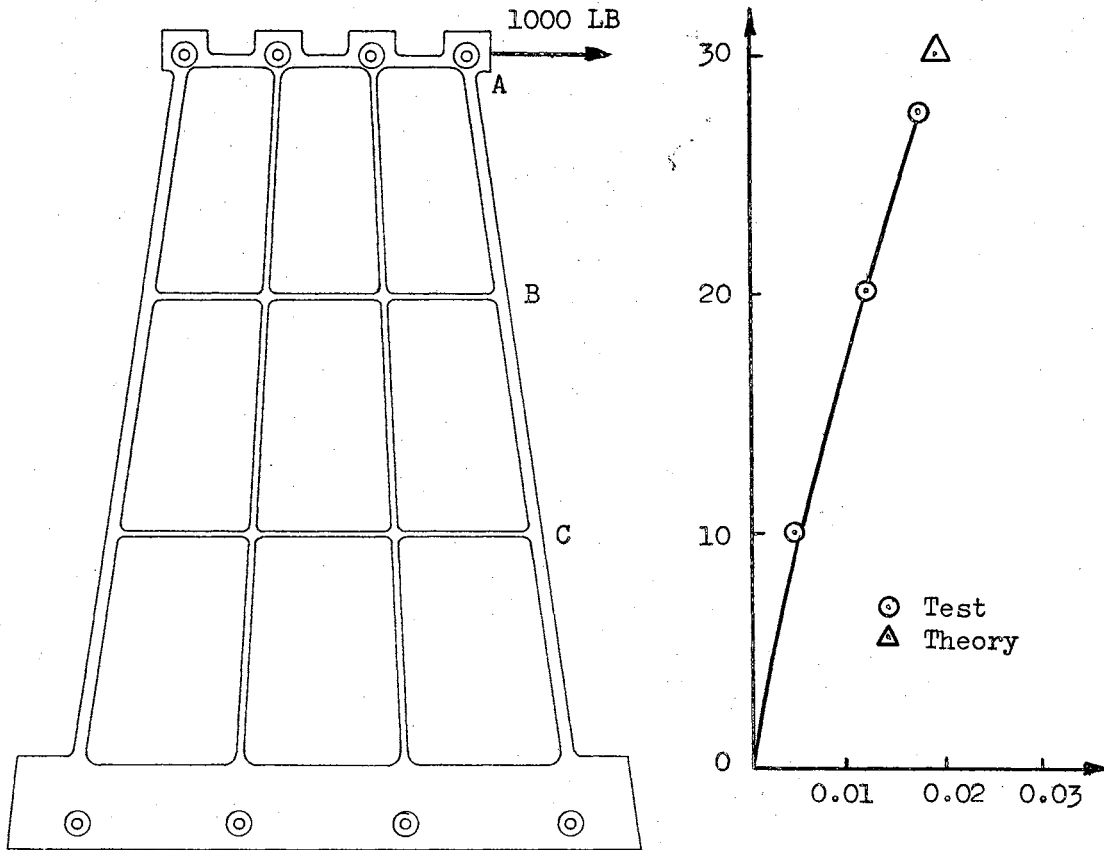
COMPARISON OF DEFLECTIONS FOR LC-1



Point of Deflection	EXPERIMENTAL			THEORETICAL
	Test 1	Test 2	Normalized Average	
1	0.0275	0.0281	0.0188	0.0180
2	0.0274	0.0287	0.0188	0.0181
3	0.0255	0.0261	0.0177	0.0183
4	0.0259	0.0267	0.0194	0.0174

*Normalized Average deflection are adjusted for measured base deflection.

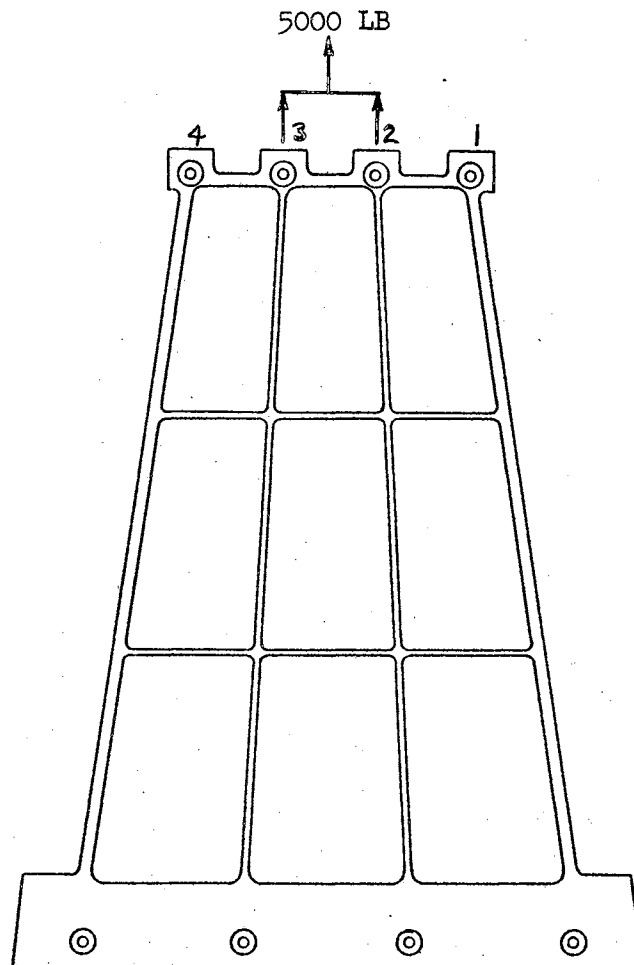
TABLE XX
COMPARISON OF DEFLECTIONS FOR LC-2



Point of Deflection	EXPERIMENTAL		*Normalized Average	THEORETICAL
	Test 1	Test 2		
A	0.0257	0.0273	0.0174	0.0177
B	0.0179	0.0185	0.0117	
C	0.0074	0.0084	0.0044	

*Normalized Average deflections are adjusted for measured base deflection.

TABLE XXI
COMPARISON OF DEFLECTIONS FOR LC-3



Point of Deflection	EXPERIMENTAL			THEORETICAL
	Test 1	Test 2	Normalized Average	
1	0.0120	0.0122	0.0081	0.0065
2	0.0156	0.0171	0.0118	0.0115
3	0.0165	0.0189	0.0120	0.0117
4	0.0106	0.0118	0.0079	0.0067

*Normalized Average deflections are adjusted for measured base deflection.

CHAPTER VI

CONCLUSIONS AND RECOMMENDATIONS

At the outset, it was stated that the purpose and goal of this research effort was to develop an improved capability for the analysis of stiffened shell structural skin panels and to demonstrate this improved capability by the comparison of experimental and analytical results. Furthermore, it was stated that in order to first develop this improved capability for the analysis of stiffened shell structural skin panels and then to demonstrate it, four distinct tasks were undertaken. These tasks were:

1. To derive a new flexibility matrix for trapezoidal shaped plate elements. This new flexibility matrix would take into account both the effects due to Poisson's ratio coupling and those due to sweep.
2. To modify the matrix force method for the inclusion of the new flexibility matrix from item one for analysis purposes.
3. To develop a digital computer program which would implement both the modified and unmodified versions of the matrix force method.
4. To formulate a regimented approach to the determination of $[GIM]$, the matrix which contains the internal generalized load distribution due to a given external load and

$[GIR]$, the matrix containing the internal generalized load distribution due to a given redundant load.

The test structure was first analyzed by the unmodified version of the matrix force method. Then, the new $[ALPIJ]_{prs}$ matrix was derived and the matrix force method was modified for its inclusion. The test structure was analyzed with the extended force method containing $[ALPIJ]_{prs}$. To provide a theoretical check and comparison for the results of the extended force method, the test structure was analyzed with the existing form of the direct stiffness method. The results from all of the above analytical investigations were compiled and presented. In order to provide a basis for ascertaining improvement of the capability for theoretically analyzing stiffened shell structural skin panels, an experimental investigation was conducted of the test structure. The results of this investigation were compiled and presented. Then, the results of the analysis with the unmodified matrix force method, the results of the analysis with the extended matrix force method, the results of analysis with the direct stiffness method and the results of the experimental analysis were all brought into sharp comparison.

The subsequent conclusions have been reached as a consequence of the previous effort.

1. A very definite improvement in the prediction of stress and displacement characteristics of planar, tapered stiffened shell structures has been produced by the use of the extended version of the matrix force method which contains the new $[ALPIJ]_{prs}$. This matrix applies to all planar, trapezoidal shaped plates except those for which two corners approach one point. The analysis of a

complete family of trapezoidal plates to determine a critical value of the angle ϕ , above which $[ALPIJ]_{prs}$ would not apply, would require a very expensive experimental program.

2. The results of the analysis with the extended matrix force method agree well with those of the analysis with the direct stiffness method. This enhances and reinforces the first conclusion, above. The characteristics of the direct stiffness method have been contrasted with those of the matrix force method and, as a result, better insight into the application of these two methods has been provided.
3. A good capability for analyzing planar, tapered stiffened shell structures by experimental means has been established. The experimental facilities as outlined in Chapter IV are capable of providing correct results within a reasonable amount of accuracy. The development of techniques for statistically reducing the strain data provides a valuable tool for future researchers in this area.
4. The matrix force method having been modified for the inclusion of $[ALPIJ]_{prs}$ becomes a well developed vehicle within which other idealizations may be included for subsequent analyses of planar, tapered stiffened shell skin panels. This method has been developed from a general standpoint and, consequently, is applicable to a broad class of structural configurations.
5. The digital computer program which implements the extended matrix force method is an important companion to the extended matrix force method. Having been developed with

the concept in mind of writing a "main" program, which, in turn, calls upon existing subroutines to perform required matrix operations, this computer program is quite flexible and is also applicable to a broad array of force analyses.

6. The regimented approach to the determination of the $[GIM]$ and $[GIR]$ matrices is a very definite improvement over the haphazard writing of overlapping freebodies and the involved solution of the resulting freebody equations. This approach enhances and broadens the applicability of the extended matrix force method to say nothing of the reduction of the chance for human error involved in developing $[GIM]$ and $[GIR]$.

Recommendations for Future Work

In addition to the conclusions just mentioned, this study precipitated many topics for future study and scrutiny. The current investigation could be advanced to deal with planar stiffened shell structures of arbitrary geometry such as the quadrilateral. The extension of the present development of the $[ALPIJ]_{prs}$ to a quadrilaterally shaped "cell" of stringers and ribs bordering a plate of this same configuration and its subsequent application to an analysis would be a very interesting topic for future consideration.

The current investigation could be continued for a cutout in the center section of the planar skin panel described in Chapter IV. The capabilities developed in this program can be used for direct application to the problem of cutout sections. Extending the analysis capability for arbitrary cutout configurations would be valuable for practical

aircraft design considerations.

A broad extension of the present capability would be the analysis of three dimensional structures beginning with various shapes of box structures containing components which could be idealized into an array of bar and plate elements of arbitrary configuration.

Another topic for future investigation would be the development of a fully automatic digital computer program to implement the matrix force method. The flexibility matrices of various theoretical elements could be combined in a symbolic manner within this program such that a given flexibility matrix could be "built up" automatically. Also, the scheme for writing generalized freebody equations could be programmed such that $[GIM]$ and $[GIR]$ would be calculated automatically as soon as a choice of redundants was made. These two features combined with the main matrix force program given in Appendix C would allow the researcher to obtain results automatically with a choice of redundants.

As a result of the broad class of problems encountered in this investigation, it is recommended that future studies make full use of the current computing capabilities. In addition, a study of idealization techniques and computational procedures would be a valuable contribution, providing significant reductions in computer running time.

A SELECTED BIBLIOGRAPHY

- (1) Timoshenko, S., and J. N. Goodier. Theory of Elasticity. 2nd ed. New York, N. Y.: McGraw-Hill Book Company, Inc., 1951.
- (2) Langefors, B. "Analysis of Elastic Structures by Matrix Transformation With Special Regard to Semimonocoque Structures," Journal of the Aeronautical Sciences, Vol. 19 (1952), pp. 451-458.
- (3) Argyris, J. H. "Die Matrizentheorie Der Statik," Ingenieur-Archiv. Vol. 25 (1957), pp. 174-192.
- (4) Argyris, J. H., and S. Kelsey. Energy Theorems of Structural Analysis. London: Butterworths, 1960.
- (5) Wehle, L., and W. Lansing. "A Method for Reducing the Analysis of Complex Redundant Structure to a Routine Procedure," Journal of the Aeronautical Sciences, Vol. 19 (1952).
- (6) Turner, M. J., R. W. Clough, H. C. Martin, and L. J. Topp. "Stiffness and Deflection Analysis of Complex Structures," Journal of the Aerospace Sciences, Vol. 23 (1956), pp. 805-823.
- (7) Bruhn, E. F. Analysis and Design of Flight Vehicle Structures. Cincinnati, Ohio: Tri-State Offset Company, 1965.
- (8) Grzedzielski, A. L. M. "Organization of a Large Computation in Aircraft Stress Analysis," Aeronautical Report LR 297, National Research Council of Canada (1959).
- (9) Borg, S. F., and J. J. Gennaro. Advanced Structural Analysis. Princeton, New Jersey: D. Van Nostrand Company, Inc., 1960.
- (10) Chapel, R. E., and E. L. Cook. The Boeing Company Structures Project No. 204607. Progress Report, April 1, 1964.
- (11) Cook, E. L. "An Analytical and Experimental Investigation of Amonolithic Trapezoidal Shear Panel Subjected to Mechanical Loading" (unpub. Ph.D. thesis, Oklahoma State University, 1966).

- (12) Ayres, M. U. "Theoretical and Experimental Comparison of Matrix Methods for Structural Analysis" (unpub. Ph.D. thesis, Oklahoma State University, July, 1966).
- (13) Mood, Alexander M., and Franklin A. Graybill. Introduction to the Theory of Statistics. New York, N. Y.: McGraw-Hill Book Company, Inc., 1963.
- (14) Freund, J. E., P. E. Livermore, and Irwin Miller. Manuel of Experimental Statistics. Englewood Cliffs, New Jersey: Prentice-Hall, Inc., 1960.
- (15) Beers, Y. Theory of Error. Reading, Massachusetts: Addison-Wesley Publishing Company, Inc., 1962.
- (16) Young, H. D. Statistical Treatment of Experimental Data. New York, N. Y.: McGraw-Hill Book Company, Inc., 1962.
- (17) Perry, C. C., and H. R. Lissner. The Strain Gage Primer. New York, N. Y.: McGraw-Hill Book Company, Inc., 1962.
- (18) Angermayer, Karl. Structural Aluminum Design. Richmond, Virginia: Reynolds Metals Company, 1964.

APPENDIX A

BASIC EQUATIONS, DERIVATION OF ELEMENT STIFFNESS MATRICES FOR THE DIRECT STIFFNESS METHOD

Basic Equations

The nodal forces on a structural element can be expressed in terms of the nodal displacements by the equation

$$\{f\} = [K]\{\delta\}, \quad (\text{A-1})$$

where

$\{f\}$ = column matrix of nodal forces on an element,

$\{\delta\}$ = column matrix of nodal displacements of an element,

$[K]$ = square, symmetric matrix of stiffness coefficients for an element.

The stiffness coefficient matrix for the complete structure can be obtained by superposing the element stiffness matrices. The resulting matrix equation is of the form

$$\{F\} = [K_c]\{\delta\}, \quad (\text{A-2})$$

where

$\{F\}$ = column matrix of external forces at the nodes of the

structure (including reactions),

$\{\delta_c\}$ = column matrix of nodal displacements (including boundary displacements),

$[K_c]$ = square, symmetric matrix of stiffness coefficients of the entire structure.

Once the displacements have been obtained, the internal forces can be calculated for each element from its force-displacement equation (Equation (A-1)); or, since the stresses in an element can be expressed in terms of the nodal forces, stress-displacement equations can be derived for the elements, and the stresses can be determined without first finding the nodal forces.

Development of a Stiffness Matrix for the Planar Bar Element

If loads are applied at points (nodes) 1 and 2, each node can experience two components of displacement. Therefore, prior to the introduction of boundary conditions (supports) the stiffness matrix, $[K]$ will be 4×4 .

In order to develop the terms in the $[K]$ matrix, each deformation component must be considered singularly, i.e.,

u_1, u_2 = deflection in the X direction,

v_1, v_2 = deflection in the Y direction,

then, the results are superimposed.

From a consideration of the bar element in Figure 45, it is assumed that $u_2 \neq 0$ as shown with $u_1 = v_1 = v_2 = 0$, i.e., end "1" fixed.

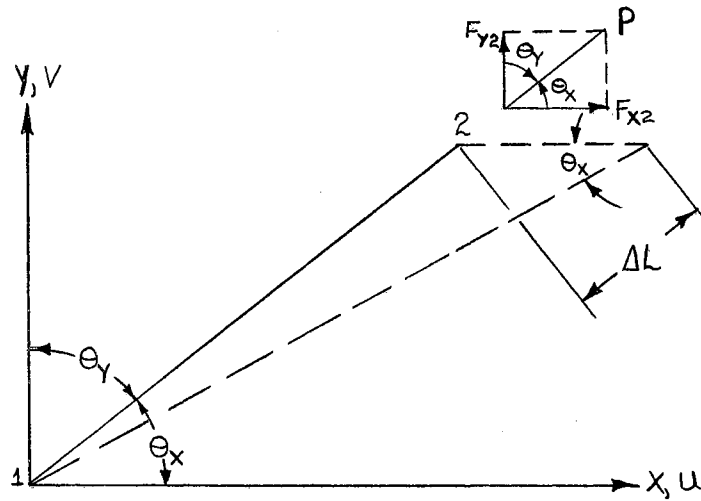


Figure 45. Planar Bar Element

From Figure 45, the expression for ΔL is

$$\Delta L = u_2 \cos \theta_x.$$

If the expressions for $\cos \theta_x$ and $\cos \theta_y$, are

$$\cos \theta_x = \lambda,$$

$$\cos \theta_y = \mu,$$

then the expression for ΔL is

$$\Delta L = u_2 \lambda.$$

Then the (F-s) relation for an axially loaded member is

$$\Delta L = \frac{PL}{AE} \Rightarrow P = \frac{(\Delta L)AE}{L} = \frac{AE(\lambda u_2)}{L}.$$

The components of the force P at node "2" are

$$F_{x2} = P \cos \theta_x = \frac{AE}{L} (\lambda u_2) \cos \theta_x = \frac{AE}{L} \lambda^2 u_2, \quad (A-3)$$

$$F_{Y_2} = P \cos \theta_Y = \frac{AE}{L} (\lambda u_2) \cos \theta_Y = \frac{AE}{L} \lambda \mu u_2. \quad (\text{A-4})$$

From static equilibrium of the member, i.e., $\sum F_x = 0$; $\sum F_y = 0$, the expressions for the forces are

$$F_{X_1} = -F_{X_2} = -\left(\frac{AE}{L}\right) \lambda^2 u_2, \quad (\text{A-5})$$

$$F_{Y_1} = -F_{Y_2} = -\left(\frac{AE}{L}\right) \lambda \mu u_2. \quad (\text{A-6})$$

From a similar analysis for v_2 , u_1 , and v_1 , the forces are expressed as

$$\begin{Bmatrix} F_{X_1} \\ F_{Y_1} \\ F_{X_2} \\ F_{Y_2} \end{Bmatrix} = \frac{AE}{L} \begin{bmatrix} \lambda^2 & & & \\ \lambda \mu & \mu^2 & \text{SYMM} & \\ -\lambda^2 & -\lambda \mu & \lambda^2 & \\ -\lambda \mu & -\mu & \lambda \mu & \mu^2 \end{bmatrix} \begin{Bmatrix} u_1 \\ v_1 \\ u_2 \\ v_2 \end{Bmatrix}, \quad (\text{A-7})$$

or the forces are expressed as

$$\{F\} = [K] \{\delta\}.$$

Derivation of the Stiffness Matrix for the Triangular Plate Element

The first step in the development of the triangular plate stiffness matrix is to express the three components of the strain within each element in terms of the six corner displacement. The geometry of a typical triangular plate element is defined in Figure 46.

The assumed displacement pattern is shown in Figure 47.

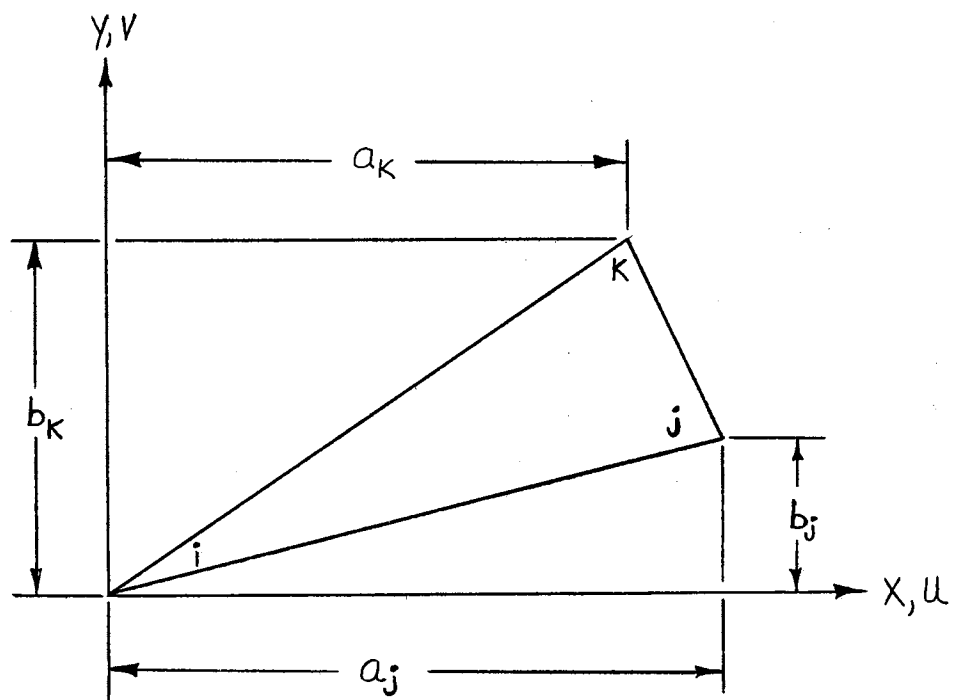


Figure 46. Element Dimensions

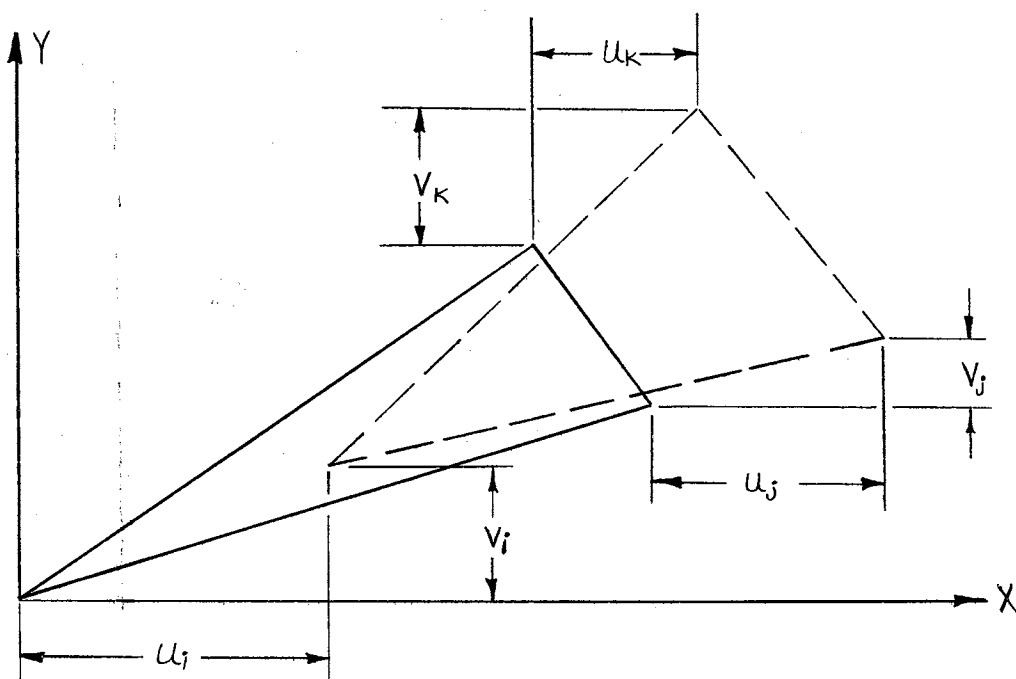


Figure 47. Assumed Displacement Pattern

The strains within each element are obtained from the displacement pattern by considering the basic definitions of strain.

$$\begin{aligned}\epsilon_x &= \frac{\partial u}{\partial X}, \\ \epsilon_y &= \frac{\partial v}{\partial Y}, \\ \gamma_{xy} &= \frac{\partial u}{\partial Y} + \frac{\partial v}{\partial X}.\end{aligned}\tag{A-8}$$

If each component of strain is set equal to a constant, linear displacements of the following form may be solved for. They are

$$u(X, Y) = C_1 + C_2 X + C_3 Y,\tag{A-9}$$

$$v(X, Y) = C_4 + C_5 X + C_6 Y.$$

Since each node of the triangular plate, Figure 48, can undergo displacement in two directions, Equation (A-9) may be evaluated in terms

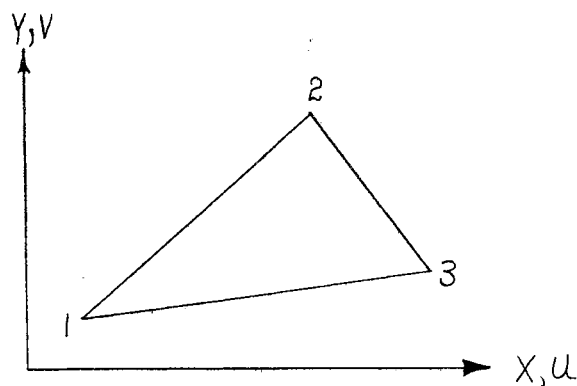


Figure 48. Triangular Plate Nomenclature

of the coordinates and displacements of the three nodes. This provides six equations from which the six unknown constants $C_1, C_2, C_3, C_4, C_5,$ and C_6 may be found.

Now, Equation (A-8) may be evaluated in terms of the constants C_i and in matrix form is

$$\{\epsilon\} = [A]\{\delta\}, \quad (\text{A-10})$$

where $[A]$ is a transformation matrix in terms of the coordinate and displacements of each of the three nodes.

For isotropic materials which obey Hooke's Law

$$\begin{aligned} \epsilon_x &= \frac{1}{E}(\sigma_x - \nu\sigma_y), \\ \epsilon_y &= \frac{1}{E}(\sigma_y - \nu\sigma_x), \\ \gamma_{xy} &= \frac{\tau_{xy}}{G} = \frac{2(1+\nu)\tau_{xy}}{E}, \end{aligned} \quad (\text{A-11})$$

where

ν = Poisson's ratio.

If Equation (A-11) is solved for $\sigma_x, \sigma_y,$ and τ_{xy} and the results put in matrix form, they would appear as

$$\begin{Bmatrix} \sigma_x \\ \sigma_y \\ \tau_{xy} \end{Bmatrix} = \frac{E}{1-\nu^2} \begin{bmatrix} 1 & \nu & 0 \\ \nu & 1 & 0 \\ 0 & 0 & \frac{1-\nu}{2} \end{bmatrix} \begin{Bmatrix} \epsilon_x \\ \epsilon_y \\ \gamma_{xy} \end{Bmatrix}, \quad (\text{A-12})$$

or, in symbolic form

$$\{\sigma\} = [B]\{\epsilon\}, \quad (\text{A-13})$$

The stress from the three assumed load states shown in Figure 49 are now transformed into resultant forces acting at the corners of the element.

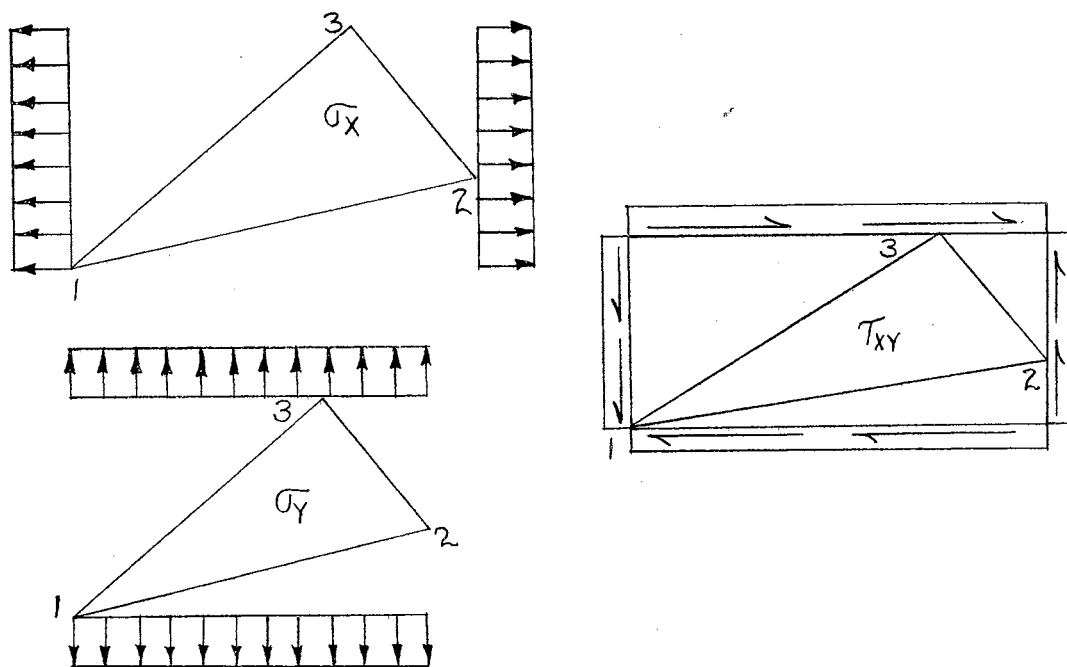


Figure 49. Stress Resultants for the Triangular Plate

Then an expression for the forces can be written as

$$\{F\} = [C]\{\delta\}, \quad (\text{A-14})$$

where $\{F\}$ is the set of resultant forces at the nodes of the plate.

The element stresses can be expressed in terms of corner displacements by substituting Equation (A-10) into Equation (A-13) to give

$$\{G\} = [B][A]\{\delta\}. \quad (A-15)$$

The substitution of Equation (A-15) into Equation (A-14) yields

$$\{F\} = [C][B][A]\{\delta\}. \quad (A-16)$$

Equation (A-16), which is an expression for corner forces in terms of corner displacements, can be written in the following form

$$\{F\} = [K]\{\delta\}, \quad (A-17)$$

with the expression for $[K]$ being

$$[K] = [C][B][A],$$

where $[K]$ is the 6 x 6 stiffness matrix for the triangular plate element and is given in Figure 50.

Determination of Deflections

The content of the stiffness matrix for each bar and plate element may now be combined into a composite stiffness matrix for the entire structure by tabulating the contribution of the elements to the various nodes of the structure. The expression for the forces is

$$\{F\} = [K_c]\{\delta\}, \quad (A-18)$$

where $[K_c]$ is the composite stiffness matrix of the structure.

The application of the constraints of fixity (also thought of as boundary conditions) will render a certain subset of $\{\delta\}$ equal to zero. If $\{F\}$, $[K_c]$ and $\{\delta\}$ are each permuted such that the zero subset of $\{\delta\}$ appears in the lower half of the column, then the equation

F_{x_1}	$y_{23}^2 + \left(\frac{1-\nu}{2}\right) x_{32}^2$						u_1
F_{y_1}	$\left(\frac{1+\nu}{2}\right) x_{32} y_{23}$	$x_{32}^2 + \left(\frac{1-\nu}{2}\right) y_{23}^2$				-SYMMETRIC-	v_1
F_{x_2}	$y_{31} y_{23}$ $+ \left(\frac{1-\nu}{2}\right) x_{13} x_{32}$	$\nu x_{32} y_{31}$ $+ \left(\frac{1-\nu}{2}\right) x_{13} y_{23}$	$y_{31}^2 + \left(\frac{1-\nu}{2}\right) x_{13}^2$				u_2
F_{y_2}	$\nu x_{13} y_{23}$ $+ \left(\frac{1-\nu}{2}\right) y_{31} x_{32}$	$x_{13} x_{32}$ $+ \left(\frac{1-\nu}{2}\right) y_{31} y_{23}$	$\left(\frac{1+\nu}{2}\right) x_{13} y_{13}$	$x_{13}^2 + \left(\frac{1-\nu}{2}\right) y_{31}^2$			v_2
F_{x_3}	$y_{12} y_{23}$ $+ \left(\frac{1-\nu}{2}\right) x_{21} x_{32}$	$\nu y_{12} x_{32}$ $+ \left(\frac{1-\nu}{2}\right) x_{21} y_{23}$	$y_{12} y_{31}$ $+ \left(\frac{1-\nu}{2}\right) x_{21} x_{13}$	$\nu y_{12} x_{13}$ $+ \left(\frac{1-\nu}{2}\right) x_{21} y_{31}$	$y_{12}^2 + \left(\frac{1-\nu}{2}\right) x_{21}^2$		u_3
F_{y_3}	$\nu x_{21} y_{23}$ $+ \left(\frac{1-\nu}{2}\right) y_{12} x_{32}$	$x_{21} x_{32}$ $+ \left(\frac{1-\nu}{2}\right) y_{12} y_{23}$	$\nu x_{21} y_{31}$ $+ \left(\frac{1-\nu}{2}\right) y_{12} x_{13}$	$x_{21} x_{13}$ $+ \left(\frac{1-\nu}{2}\right) y_{12} y_{31}$	$\nu x_{21} y_{12}$ $+ \left(\frac{1-\nu}{2}\right) y_{12} x_{21}$	$x_{21}^2 + \left(\frac{1-\nu}{2}\right) y_{12}^2$	v_3

Figure 50. Equation (A-17) Featuring the Triangular Stiffness Matrix

$$\{F\} = [K_c] \{\delta\},$$

can be partitioned such that

$$\{F_a\} = [K_{ca}] \{\delta_a\}, \quad (\text{A-19})$$

where

$\{\delta_a\}$ is the nonzero subset of $\{\delta\}$.

Then, the required deflections are given by the expression

$$\{\delta_a\} = [K_{ca}]^{-1} \{F_a\}, \quad (\text{A-20})$$

where $\{F_a\}$ is the set of external forces and $\{\delta_a\}$ deflection at each unconstrained node due to $\{F_a\}$.

Calculation of Stresses in the Bar Element

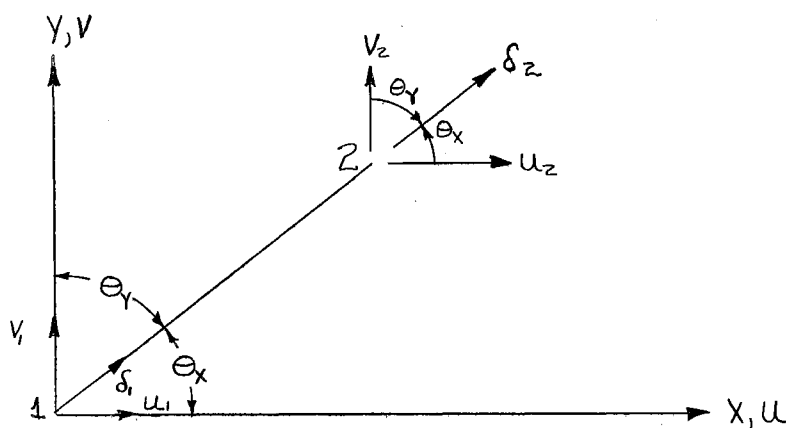


Figure 51. Deflection Diagram of Bar Element

From Figure 51, the expression for stress is

$$\sigma = \frac{P}{A} = \frac{E}{L} [\delta_2 - \delta_1], \quad (\text{A-21})$$

where

A = area of the element.

But δ_1 and δ_2 may be expressed as

$$\delta_2 = u_2 \cos \theta_x + v_2 \cos \theta_y = u_2 \lambda + v_2 \mu, \quad (\text{A-22})$$

$$\delta_1 = u_1 \cos \theta_x + v_1 \cos \theta_y = u_1 \lambda + v_1 \mu.$$

Then, substituting for δ_1 and δ_2 , Equation (A-21) becomes

$$\sigma = \frac{P}{A} = \frac{E}{L} [(u_2 \lambda + v_2 \mu) - (u_1 \lambda + v_1 \mu)],$$

or, in matrix form, the expression for σ becomes

$$\sigma_{1-2} = \frac{P}{A} = \frac{E}{L} \begin{bmatrix} -\lambda & -\mu & \lambda & \mu \end{bmatrix} \begin{Bmatrix} u_1 \\ v_1 \\ u_2 \\ v_2 \end{Bmatrix}. \quad (\text{A-23})$$

Calculation of Stresses in the Triangular Plate Element

The set of deflections $\{\delta_a\}$ may be substituted back into Equation (A-15) to give

$$\{\sigma_a\} = [B][A]\{\delta_a\}, \quad (\text{A-24})$$

where the product $[B][A]$ depends on nodal coordinates, Young's modulus and Poisson's ratio.

APPENDIX B

STRESS ANALYSIS SYSTEM

The Stress Analysis System is a digital computer program using matrix methods based on discrete element idealization for two-dimensional structures. The complete solution for deflections and stresses requires only that the structure be defined in terms of its geometrical characteristics and types of structural elements. The structure is first idealized as an assemblage of discrete structural elements. Each structural element has an assumed form of displacement or stress distribution. The complete solution is obtained by satisfying the force equilibrium and displacement compatibility at the junctions of the elements. Thus, the conditions of equilibrium and compatibility are satisfied at only a finite number of points which do not necessarily imply any appreciable loss of accuracy. When the size of the element is sufficiently small in relation to the over-all size of the structure and the variations of stresses within the structure do not exceed those allowed in the mathematical model, the discrete element methods give good approximations to the exact solutions.

The displacement method is the basis for developing this digital computer program for analyzing two-dimensional rectangular panel configurations for arbitrary load and support conditions. The system provides solutions for displacements and internal or external forces at the structural node points and stresses at any stress node points defined

for the structural element.

The input data required for the Stress Analysis System consist of node numbers, element numbers, and geometric descriptions of the idealization structure and locations of desired stress results on the elements. The program is divided into the following categories:

1. Geometric description of the structure.
2. Idealized description of the structure.
3. Generation of stiffness matrices.
4. Generation of stress matrices.
5. Deflection solution.
6. Reaction force solution.
7. Generalized stress calculations.
8. Printing of analysis results.

The first step for preparing the input data for the analysis is to simulate the actual structure as an assemblage of idealized elements, which is commonly referred to as the idealized structure.

The structure is formed from available elements, i.e., stringers and triangular plates, so that it is capable of representing the deflection behavior of the actual structure. The idealized structure is described in terms of the node data and the structural data. The node data consist of the number of the node point, the coordinates of the node point, the external forces acting on the node point, and the definition of the boundary condition at the node point. The structural data consist of the location of the idealized elements relative to the node points, the type of structural element, and the description of its material properties.

The location of the node points is given relative to a

two-dimensional rectangular coordinate system. The n node points are numbered consecutively from 1 to n in the direction of the minimum width.

The boundary conditions are specified by restricting the displacement of the supported node point in the directions of the intended supports. This is achieved by placing a 1 in column 80 of each node data card for the degrees of freedom which are to be restrained. If insufficient boundary conditions are defined, the stiffness of the general structure is zero in that direction. Consequently, the stiffness matrix is singular and the analysis cannot be completed.

The loading conditions are given as part of the node data. Three loading conditions can be considered in each analysis. The loads are entered by listing the x and y components of the applied load in the x and y rows of the node points on which the loads are acting. The actual external loads acting on the real structure are represented by concentrated loads acting at the node points of the idealized structure.

The locations of the idealized elements are given relative to the node points in the structural data. The idealized elements are numbered consecutively. No specific grouping is required between stringer or triangular plate elements. If an integer is assigned to a stringer, the next integer can be assigned to a triangular plate. For stringer elements, the connecting node point numbers are given in columns 6 through 9 and 10 through 13 of the structural data cards and are called nodes P and Q. For triangular plates, the nodes are called P, Q, and R, and are listed in consecutive order clockwise around the triangular plate. The implication in listing the corner node point numbers is that it automatically assigns a local xy coordinate system for the triangle. The

local x axis extends from node P to node R; the local y axis extends from node P to node Q.

The stress components are calculated and printed out relative to the local coordinate system. For example, if the structure has grid lines parallel to the x and y axis of the general coordinate system, a PQR sequence is chosen so that the coordinate axes for each triangular plate have directions identical to those of the general coordinate axes. In this case, the stresses are then relative to the external coordinate axes and are the same for all triangular plates. The stress results for the stringer elements are given relative to the axis of the stringers. As additional elements are added to this program, the common element coordinate system should be maintained.

The type of idealized element is specified in the structural data by entering the type number in column 24.

The elastic properties of the material are defined in the structural data and consist of modulus of elasticity and Poisson's ratio.

Stresses are calculated for the stress node points defined for each element relative to the local coordinate system of the element. The characteristic dimensions of the idealized elements are defined by the coordinates of their end or corner node points. The coordinates of the stress node points are given in inches relative to the local coordinate system for the element. A maximum of five stress nodes can be used in each analysis. If no stress nodes are specified, stresses are automatically computed for the coordinates of the centroid of the element.

Node numbers, element numbers, element-type numbers, and support conditions are always entered as integers. All other data are entered with a decimal point in the proper place.

Once the idealized structure and the loading conditions are defined, the computational sequence follows from the stiffness method. The stiffness and stress matrices are generated for each element using the structural material properties and the dimensions obtained from the node data. The rows and columns of the stiffness matrix and stress and load matrices are in the order of x and y for each node point on the structure. In general, if P is the number of the node point, the x and y degrees of freedom at P are labeled $2P-1$ and $2P$, respectively. These numbers are then used as indices to denote a displacement or force component acting at node P in either x or y direction.

The matrix \bar{K} (BARK) is the stiffness matrix of the idealized structure in lower symmetric form. It is obtained by simply summing up the contributions of the various element stiffness coefficients in the direction of each displacement. To facilitate this summation, the MPQRS numbering scheme is used to denote the x and y directions of each of the nodes.

Once the element stiffness matrices have been computed based on the stiffness properties and the node locations of each element, the coefficients of the stiffness matrix are assigned indices according to the MPQRS scheme. The indices designate the position of the stiffness matrix for the individual composite stiffness matrix for the total structure. The total stiffness matrix \bar{K} is obtained by summing the stiffness matrix elements with common indices obtained by the MPQRS scheme. As the stiffness matrix for each element is generated, it is added to the large \bar{K} matrix.

The output data are presented in two forms, an abbreviated form containing only the basic results of the analysis and an extended form

including all of the individual plate and stringer stiffness and stress.

The coefficients of \bar{K} are the forces generated at the node points in the x and y directions, when one node is displaced a unit distance in the x or y direction and all other displacements are restrained. The sum of the coefficients in every row and column is zero since the forces generated at restrained node points and the force developed due to the unit displacement are in equilibrium. If the structure is restrained from rotation and translation degrees of freedom by removing the rows and columns of the \bar{K} matrix that represent the displacement of boundary conditions, the matrix is subsequently nonsingular. Removing these rows and columns decreases the size of the matrix and consequently changes the indices of the coefficients of \bar{K} . Consequently, one has the choice of using the reduced matrix and changing the indices of the rows and column designations or removing the rows and columns except on the diagonal. The diagonal element is replaced by a 1. The result is that the stiffness matrix will contain a unit matrix which will not effect the solution of the simultaneous equations obtained by performing the inverse operation. This technique does save the numbering scheme but, of course, retains the size of the stiffness matrix. This method of modification rather than reduction of the stiffness matrix is utilized in this program because it simplifies the bookkeeping problems throughout the calculations; and, for these types of structures, the decrease in the size of the stiffness matrix obtained by reducing the matrix for the boundary conditions is not a significant advantage.

After the stiffness matrices for each element have been added to the total stiffness matrix \bar{K} , the matrix \bar{K} is modified, as mentioned in the previous paragraph, according to the defined boundary conditions.

The modified stiffness matrix is then inverted and the node point deflections are calculated from the equation

$$\{\delta\} = [K]^{-1}\{F\}.$$

The deflection matrix $\{\delta\}$ is a complete listing of the node displacements, including the zero displacements at the boundaries.

The stresses in each idealized element are calculated from the deflections $\{\delta\}$ for the element, which must be obtained from the total $\{\delta\}$ matrix. The stresses are computed by generating the stress matrix for the coordinates of the stress node point and postmultiplying the element stress matrix by the element displacements. The stresses within the idealized element are based on the assumptions made for deriving the stiffness and stress matrices. Consequently, the stresses at any number of points in a single plate may be obtained through the stress coefficient matrix and the corner displacements of the plate or stringer element. The components of the stress tensor at the stress node points defined in the stress node data are calculated relative to the local coordinate system of the plate element.

The reaction forces at the boundary node points are computed from the equation

$$\{F\} = [\bar{K}]\{\delta\}$$

by evaluating the right-hand side of the equation where \bar{K} is the original stiffness matrix before boundary conditions are applied. The reaction forces are used for checking the original input data or the accumulation of numerical errors in the computing process and do

provide a solution for the reactions in the directions of the specified boundary conditions.

The output is controlled by placing a numeral 1 in column 30 of the program control card. If no parameter is used in column 30, the abbreviated form of the analysis will be printed.

Example Listing

A complete listing of the main program and required subroutines is given in Table XXII. (Table XXII is shown on the next page.)

TABLE XXII

FORTRAN PROGRAM FOR THE STRESS ANALYSIS SYSTEM (12)

```

C SAS PROGRAM BY G. STONE
DIMENSION AL(2),AL2(2),AL3(2),IPQRS(4),MPQRS(8),DSK(8,8),STR(3,8),
100RU(8,5),STRESS(3,5),R(12),BARK(180),NBC(60),X(60),Y(60),
2UBAR(60,5),FORCE(60,5),QBAR(60,5),XN(60,5),YN(60,5)
EQUIVALENCE (IPQRS(4),IS),(IPQRS(3),IR),(IPQRS(2),IQ),(IPQRS(1),IP)
101 FORMAT ( 2X, 1P6E16.3) SAS001
102 FORMAT ( 2X, 1P4E16.3) SAS002
103 FORMAT (1H0, 7HK BAR I , 1X) SAS003
104 FORMAT (2X,15) SAS004
105 FORMAT ( 6HO I = , 15, 13H IPQRS(I) = , 15) SAS005
106 FORMAT ( 6HO K = , 15, 13H MPQRS(K) = , 15) SAS006
107 FORMAT ( 6HOLA = , 15, 19H KI = MPQRS(LA) = , 15) SAS007
109 FORMAT ( 6HOKJ = , 15) SAS008
110 FORMAT ( 6HOBARK( , 15, 9H ) = DSK( , 15, 2H , , 15, 2H ) ) SAS009
111 FORMAT ( 6HO I = , 15) SAS010
112 FORMAT ( 6HOIJ = , 15, 12H NBC(IJ) = , 15) SAS011
113 FORMAT ( 7HO LA = , 15, 7H I = , 15, 17H BARK(I) = 1.0 ) SAS012
114 FORMAT ( 41HO NUMBER OF ROWS AND COLS TO BE ZEROED = , 15) SAS013
115 FORMAT ( 6HO I = , 15, 15H BARK(I) = 0.0 ) SAS014
116 FORMAT (2X, 15,5X,3E14.8,5X, 15,5X, 4E14.8, / 2X, 8110, SAS015
1 / 2X, 4110) SAS016
200 FORMAT ( 25HO ELEMENT STRESS MATRIX ) SAS017
201 FORMAT(8HONODE , 2(8X,7HTYPE OF),49X,8HSTRESSES) SAS018
202 FORMAT(1X,6HNUMBER,9X,7HELEMENT,8X,6HSTRESS,10X,6HCASE 1,11X,6HCAS SAS019
1E 2 ,11X,6HCASE 3,11X,6HCASE 4,11X,6HCASE 5) SAS020
203 FORMAT (25H1 GENERALIZED STRESS CALCULATIONS ) SAS021
204 FORMAT (33H1 DEFLECTIONS FOR ELEMENT NUMBER , 15 ) SAS022
205 FORMAT(//43H1 STRESSES AT THE CENTROID OF THE ELEMENT//) SAS023
206 FORMAT (30HO STRESSES FOR ELEMENT NUMBER , 13, 6H TYPE ,13) SAS024
210 FORMAT(1HO,14,9X,15,14X,2HXX,9X,5E17.8) SAS025
221 FORMAT(33X,2HXY, 9X,5(2X,E15.8)) SAS026
222 FORMAT(33X,2HY, 9X,5(2X,E15.8)) SAS027
251 FORMAT (15,1X,5F12.4) SAS028
252 FORMAT( 44H1 STRESS NODE COORDINATES , / SAS029
1 52H ELEMENT NODE 1 NODE 2 NODE 3 NODE 4 NODE 5 ) SAS030
253 FORMAT( 1X, 13, 2H X, 5F12.4, ) SAS031
254 FORMAT (15,1X,5F12.4) SAS032
255 FORMAT(1X,13,2H Y,5F12.4) SAS033
256 FORMAT(1X,30HNO STRESS MATRIX FOR TYPE ,13,2X,7HELEMENT) SAS034
257 FORMAT(1X,30HNO STIFFNESS MATRIX FOR TYPE ,13,2X,7HELEMENT) SAS035
258 FORMAT ( 8H ELEMENT, 25X, 16HCOORDINATES FOR, / SAS036
1 7H NUMBER, 4X,54HNODE 1 NODE 2 NODE 3 NODE 4
2 NODE 5 ) SAS037
259 FORMAT(1HO,27HNORMALIZED COORDINATES X = ,F12.4,10X,4HY = ,F12.4) SAS038
603 FORMAT(1O16) SAS039
612 FORMAT(6E13.0) SAS040
687 FORMAT(1X,4HDET=,E14.2,10X,2HL=,13) SAS041
800 FORMAT(1H1) SAS042
801 FORMAT(1HO,10HNODE POINT,5 X,11HCOORDINATES,47X, SAS043
125HDEFLECTION OF NODE POINTS) SAS044
802 FORMAT(1X,6HNUMBER,40X,6HCASE 1,11X , SAS045
16HCASE 2,11X,6HCASE 3,11X,6HCASE 4,11X,6HCASE 5 ) SAS046
804 FORMAT(1HO,2X,12,13X,1HX,24X,5E17.8) SAS047
805 FORMAT(18X,1HY,24X,5E17.8) SAS048
809 FORMAT( 11H1NODE POINT,3X,11HCOORDINATES,63X,6HFORCES ) SAS049
992 FORMAT(2O14) SAS050
993 FORMAT(6X,6F12.0,I2) SAS051
994 FORMAT(15,4I4,13,1X,E10.6,2F6.0) SAS052
995 FORMAT(1H1,12A6) SAS053
8629 FORMAT(19HAMATRIX IS SINGULAR) SAS054
8798 FORMAT (7H1 K BAR /1X) SAS055
8799 FORMAT(16H1 K BAR INVERSE/1X) SAS056
SAS057
SAS058
SAS059
SAS060
SAS061
SAS062
9603 FORMAT( 7H NODES=,15,5X,9HELEMENTS=,15,5X,6HCASES=,12,5X SAS063
1,13HSTRESS NODES= ,12/ SAS064
2 89H NODE COORDINATE LOAD 1 LOAD 2 LOAD 3 SAS065
3 LOAD 4 LOAD 5 SUPPORT/1X) SAS066
9993 FORMAT(1X,13,2H X,F12.3,1X,5F12.3,6X,11/1X,13,2H Y,F12.3,1X,5F12. SAS067
13,6X,11) SAS068
9994 FORMAT(1X,15,4I4,13,4X,E11.4,F11.4,F13.4 ) SAS069
9995 FORMAT(114H1 ELEM P O R S TYPE E PR TH SAS070
1 THICKNESS-AREA ) SAS071
31009 FORMAT(1X,3HROW,14,71X,(1P10E13.4)) SAS072
99999 FORMAT(1H1,23HEXECUTION COMPLETED FOR,12A6) SAS073
839 CONTINUE SAS074
REWIND 3 SAS075
REWIND 4 SAS076
C READ IN TITLE SAS077
READ(5,995) (R(J),J=1,12) SAS078
WRITE(6,995) (R(J),J=1,12) SAS079
C READ IN PARAMETERS SAS080
READ(5,603) NNODES,NELEM,NC,NSN,IWRITE SAS081
WRITE(6,9603) NNODES,NELEM,NC,NSN SAS082
N2=2 *NNODES SAS083
NUM=(N2*(N2+1))/2 SAS084
C READ IN NODE LOCATIONS, FORCE, AND BOUNDARY CONDITIONS SAS085
DO 7777 I=1,NNODES SAS086
12=2*I SAS087
READ(5,993) X(I), (FORCE(12-I,J), J=1,5 ),BARK(12-I), SAS088
1 Y(I), (FORCE (12,J), J=1,5), BARK(12) SAS089
7777 WRITE (6,9993) 1,X(I), (FORCE(12-I,J), J=1,5), BARK(12-I), SAS090
1 Y(I), (FORCE (12 , J), J=1,5),BARK(12) SAS091
C THE NCROSS ROWS AND COLS. TO BE STRUCK FROM K-BAR ,AS DICTATED BY SAS092
C BOUNDARY CONDITIONS, ARE STORED IN ARRAY NBC(I). SAS093
C BARK IS USED TO READ THE INDEX OF FIXED BOUNDARY NODES SAS094
IJ=0 SAS095
DO 7778 I=1,N2 SAS096
IF(BARK(I))7779,7778,7779 SAS097
7779 IJ=I+1 SAS098
NBC(IJ)=I SAS099
IF(IWRITE,EQ.0) GO TO 7778 SAS100
WRITE (6,111) I SAS101
WRITE (6,112) IJ, I SAS102
7778 CONTINUE SAS103
NCROSS=IJ SAS104
DO 320 I=1,NUM SAS105
BARK (I)=0.0 SAS106
320 CONTINUE SAS107
C READ NODE NUMBER TYPE ELEMENT MODULUS PR AREA SAS108
WRITE(6,9995) SAS109
DO 236 NN=1,NELEM SAS110
READ(5,994) IE,IP,IO,IR,IS,NTYPE,E,PR,A SAS111
IF(IWRITE,EQ.0) GO TO 513 SAS112
WRITE (6,9995) SAS113
513 CONTINUE SAS114
WRITE(6,9994) IF,IP,IO,IR,IS,NTYPE,E,PR,A SAS115
GO TO (1,2,3,4,5,6,7,8,9),NTYPE SAS116
1 CONTINUE SAS117
C*****STRINGER AND RIB CALCULATIONS***** SAS118
JLAM=4 SAS119
DO 10004 I=1,4 SAS120
DO 10004 J=1,4 SAS121
10004 DSK(I,J)=0.0 SAS122
CALCULATE THE PQ DIRECTION COSINES. SAS123
XOP=X(IO)-X(IP) SAS124

```

TABLE XXII (Continued)

YQP=Y(IQ)-Y(IP)	SAS125	Y2=Y(IR)-Y(IQ)	SAS187
D1=SQRT (XQP**2+YQP**2)	SAS126	D2=SQRT (X2**2+Y2**2)	SAS188
D2 = D1	SAS127	AL(1)=XQP/D1	SAS189
AL(1)=XQP/D1	SAS128	AL(2)=YQP/D1	SAS190
AL(2)=YQP/D1	SAS129	AL2(1)=X2/D2	SAS191
AE=A*E	SAS130	AL2(2)=Y2/D2	SAS192
DO239I=1,2	SAS131	BETA=D1/D2	SAS193
DO239J=1,2	SAS132	ET1=AE/(1.-PR**2)	SAS194
DSK (I,J) = AL(I)*AL(J)*AE/D1	SAS133	ET2=AE/(2.+2.*PR)	SAS195
DSK(I+2,J) = -DSK(I,J)	SAS134	CALCULATE THE KD+KS MATRIX	SAS196
DSK (I,J+2) = -DSK(I,J)	SAS135	PR2=PR**2	SAS197
DSK(I+2,J+2) = DSK(I,J)	SAS136	DSK (1,1)= ET1*BETA/3.+ET2/(3.*BETA)	SAS198
239 CONTINUE	SAS137	DSK (2,1)=(ET1*PR+ET2)/4.	SAS199
IF(IWRITE.EQ.0) GO TO 500	SAS138	DSK (3,1)=ET1*BETA/6.-ET2/(3.*BETA)	SAS200
WRITE (6,205) NTYPE	SAS139	DSK (4,1)=(-ET1*PR+ET2)/4.	SAS201
WRITE (6,103)	SAS140	DSK (5,1)=-ET1*BETA/6.-ET2/(6.*BETA)	SAS202
WRITE (6,102) ((DSK(I,J),I=1,4), J=1,4)	SAS141	DSK (7,1)=-ET1*BETA/3.+ET2/(6.*BETA)	SAS203
500 CONTINUE	SAS142	DSK (2,2)=ET1/(3.*BETA)+ET2*BETA/3.	SAS204
GO TO 235	SAS143	DSK (4,2)=-ET1/(3.*BETA)+ET2*BETA/6.	SAS205
2 CONTINUE	SAS144	DSK (6,2)=-ET1/(6.*BETA)-ET2*BETA/6.	SAS206
C *****STRINGER WITH LINEAR STRESS FUNCTION *****	SAS145	DSK (8,2)=ET1/(6.*BETA)-ET2*BETA/3.	SAS207
JLAM=4	SAS146	DSK (3,3)=ET1*BETA/3.+ET2/(3.*BETA)	SAS208
DO 10005 I=1,4	SAS147	DSK (5,3)=-ET1*BETA/3.+ET2/(6.*BETA)	SAS209
DO 10005 J=1,4	SAS148	DSK (6,1)=-DSK (2,1)	SAS210
10005 DSK(I,J)=0.0	SAS149	DSK (8,1)=-DSK (4,1)	SAS211
CALCULATE THE PO DIRECTION COSINES.	SAS150	DSK (3,2)=-DSK (4,1)	SAS212
XQP=X(IQ)-X(IP)	SAS151	DSK (5,2)=-DSK (2,1)	SAS213
YQP=Y(IQ)-Y(IP)	SAS152	DSK (7,2)= DSK (4,1)	SAS214
D1=SQRT (XQP**2+YQP**2)	SAS153	DSK (4,3)=-DSK (2,1)	SAS215
D2 = D1	SAS154	DSK (6,3)= DSK (4,1)	SAS216
AL(1)=XQP/D1	SAS155	DSK (7,3)= DSK (5,1)	SAS217
AL(2)=YQP/D1	SAS156	DSK (8,3)= DSK (2,1)	SAS218
AE=A*E	SAS157	DSK (4,4)= DSK (2,2)	SAS219
DO 240 I=1,2	SAS158	DSK (5,4)= DSK (3,2)	SAS220
DO 240 J=1,2	SAS159	DSK (6,4)= DSK (8,2)	SAS221
DSK(I,J)=AL(I)*AL(J)*(AE/D1)*4.0/ 3.0	SAS160	DSK (7,4)= DSK (2,1)	SAS222
DSK(I+2,J)=-DSK(I,J)	SAS161	DSK (8,4)= DSK (6,2)	SAS223
DSK (I,J+2)=-DSK(I,J)	SAS162	DSK (5,5)= DSK (1,1)	SAS224
DSK(I+2,J+2) = DSK(I,J)	SAS163	DO 8620 I=2,4	SAS225
240 CONTINUE	SAS164	DSK (1+4,5)=DSK (1,1)	SAS226
IF(IWRITE.EQ.0) GO TO 511	SAS165	8620 DSK (1+4,6)=DSK (1,2)	SAS227
WRITE (6,205) NTYPE	SAS166	DSK (7,7)= DSK (1,1)	SAS228
WRITE (6,103)	SAS167	DSK (8,7)=-DSK (2,1)	SAS229
WRITE (6,102) ((DSK(I,J),I=1,4), J=1,4)	SAS168	DSK (8,8)= DSK (2,2)	SAS230
511 CONTINUE	SAS169	DO 302 J=1,8	SAS231
GO TO 235	SAS170	DO 302 I=1,8	SAS232
3 CONTINUE	SAS171	302 DSK(J,I) = DSK(I,J)	SAS233
4 CONTINUE	SAS172	IF(IWRITE.EQ.0) GO TO 502	SAS234
WRITE(6,257) NTYPE	SAS173	WRITE (6,205) NTYPE	SAS235
GO TO 839	SAS174	WRITE (6,103)	SAS236
5 CONTINUE	SAS175	WRITE (6,101) ((DSK(I,J),I=1,8), J=1,8)	SAS237
C*****RECTANGULAR*PLATE*CALCULATIONS*****	SAS176	502 CONTINUE	SAS238
C*****ASSUMED DISPLACEMENT FUNCTION*****	SAS177	GO TO 235	SAS239
DO 10003 I = 1,8	SAS178	6 CONTINUE	SAS240
DO 10003 J=1,8	SAS179	C*****RECTANGULAR*PLATE*CALCULATIONS*****	SAS241
10003 DSK (I,J) = 0.0	SAS180	C*****ASSUMED STRESS FUNCTION WITH FIVE COEFFICIENTS*****	SAS242
JLAM=8	SAS181	DO 10002 I = 1,8	SAS243
XQP=X(IQ)-X(IP)	SAS182	DO 10002 J = 1,8	SAS244
YQP=Y(IQ)-Y(IP)	SAS183	10002 DSK (I,J) = 0.0	SAS245
D1=SQRT (XQP**2+YQP**2)	SAS184	JLAM=8	SAS246
AE=A*E	SAS185	XQP=X(IQ)-X(IP)	SAS247
X2=X(IR)-X(IO)	SAS186	YQP=Y(IQ)-Y(IP)	SAS248

TABLE XXII (Continued)

D1=SQRT (XQP**2+YQP**2)	SAS249	JLAM=8	SAS311
AE=A*E	SAS250	XQP=X(IQ)-X(IP)	SAS312
X2=X(IR)-X(IQ)	SAS251	YQP=Y(IQ)-Y(IP)	SAS313
Y2=Y(IR)-Y(IQ)	SAS252	BY=SQRT (XQP**2+YQP**2)	SAS314
D2=SQRT (X2**2+Y2**2)	SAS253	D1 = BY	SAS315
AL(1)=XQP/D1	SAS254	AE=A*E	SAS316
AL(2)=YQP/D1	SAS255	AL(1)=XQP/D1	SAS317
AL2(1)=X2/D2	SAS256	AL(2)=YQP/D1	SAS318
AL2(2)=Y2/D2	SAS257	X2=X(IR)-X(IQ)	SAS319
BETA=D1/D2	SAS258	Y2=Y(IR)-Y(IQ)	SAS320
ET1=AE/(1.-PR**2)	SAS259	AX=SQRT (X2**2+Y2**2)	SAS321
ET2=AE/(2.+2.*PR)	SAS260	D2 = AX	SAS322
PR2=PR**2	SAS261	ALP = (3.0*AX*AX) + (BY*BY)	SAS323
C CALCULATE THE KD+KS MATRIX	SAS262	BET = (AX*AX) + (3.0 * BY*BY)	SAS324
DSK (1,1)= (2.*(4.-PR2)*BETA/3.+(1.-PR)/BETA)*ET1/8.	SAS263	DSK(1,1)=+(35.*BY*BY*ALP*BET)+((BY**4)*BET)-(6.*AX*AX*BY*BY*BET)+(SAS325
DSK (2,1)= (1.+PR)*ET1/8.	SAS264	19.*AX*AX*ALP*BET)+(9.*(AX**4)*BET)	SAS326
DSK (3,1)= (2.*(2.+PR2)*BETA/3.-(1.-PR)/BETA)*ET1/8.	SAS265	DSK(2,1)=18.*AX*BY*ALP*BET	SAS327
DSK (4,1)= (1.-3.*PR)*ET1/8.	SAS266	DSK(3,1)=+(19.*BY*BY*ALP*BET)-((BY**4)*BET)+(6.*AX*AX*BY*BY*BET)-(SAS328
DSK (5,1)= (-2.*(2.+PR2)*BETA/3.-(1.-PR)/BETA)*ET1/8.	SAS267	19.*AX*AX*ALP*BET)-(9.*(AX**4)*BET)	SAS329
DSK (7,1)= (-2.*(4.-PR2)*BETA/3.+(1.-PR)/BETA)*ET1/8.	SAS268	DSK(5,1)=-(19.*BY*BY*ALP*BET)+((BY**4)*BET)-(6.*AX*AX*BY*BY*BET)-(SAS330
DSK (2,2)= (2.*(4.-PR2)/(3.*BETA)+(1.-PR)*BETA)*ET1/8.	SAS269	19.*AX*AX*ALP*BET)+(9.*(AX**4)*BET)	SAS331
DSK (4,2)= (-2.*(4.-PR2)/(3.*BETA)+(1.-PR)*BETA)*ET1/8.	SAS270	DSK(7,1)=-(35.*BY*BY*ALP*BET)-((BY**4)*BET)+(6.*AX*AX*BY*BY*BET)+(SAS332
DSK (6,2)= (-2.*(2.+PR2)/(3.*BETA)-(1.-PR)*BETA)*ET1/8.	SAS271	19.*AX*AX*ALP*BET)-(9.*(AX**4)*BET)	SAS333
DSK (8,2)= (2.*(2.+PR2)/(3.*BETA)-(1.-PR)*BETA)*ET1/8.	SAS272	DSK(2,2)=+(35.*AX*AX*ALP*BET)+((AX**4)*ALP)-(6.*AX*AX*BY*BY*ALP)+(SAS334
DSK (3,3)= (2.*(4.-PR2)*BETA/3. +(1.-PR)/BETA)*ET1/8.	SAS273	19.*BY*BY*ALP*BET)+(9.*(BY**4)*ALP)	SAS335
DSK (5,3)= (-2.*(4.-PR2)*BETA/3.+(1.-PR)/BETA)*ET1/8.	SAS274	DSK(4,2)=-(35.*AX*AX*ALP*BET)-((AX**4)*ALP)+(6.*AX*AX*BY*BY*ALP)+(SAS336
DSK (6,1)=-DSK (2,1)	SAS275	19.*BY*BY*ALP*BET)-(9.*(BY**4)*ALP)	SAS337
DSK (8,1)=-DSK (4,1)	SAS276	DSK(6,2)=-((19.*AX*AX*ALP*BET)+((AX**4)*ALP)-(6.*AX*AX*BY*BY*ALP)-(SAS338
DSK (3,2)=-DSK (4,1)	SAS277	19.*BY*BY*ALP*BET)+(9.*(BY**4)*ALP)	SAS339
DSK (5,2)=-DSK (2,1)	SAS278	DSK(8,2)=+(19.*AX*AX*ALP*BET)-((AX**4)*ALP)+(6.*AX*AX*BY*BY*ALP)-(SAS340
DSK (7,2)= DSK (4,1)	SAS279	19.*BY*BY*ALP*BET)-(9.*(BY**4)*ALP)	SAS341
DSK (4,3)=-DSK (2,1)	SAS280	DSK(6,1)=-DSK(2,1)	SAS342
DSK (6,3)= DSK (4,1)	SAS281	DSK(5,2) = DSK(6,1)	SAS343
DSK (7,3)= DSK (5,1)	SAS282	DSK(3,3) = DSK(1,1)	SAS344
DSK (8,3)= DSK (2,1)	SAS283	DSK(4,3) = DSK(6,1)	SAS345
DSK (4,4)= DSK (2,2)	SAS284	DSK(3,3) = DSK(7,1)	SAS346
DSK (5,4)= DSK (3,2)	SAS285	DSK(7,3) = DSK(5,1)	SAS347
DSK (6,4)= DSK (8,2)	SAS286	DSK(8,3) = DSK(2,1)	SAS348
DSK (7,4)= DSK (2,1)	SAS287	DSK(4,4) = DSK(2,2)	SAS349
DSK (8,4)= DSK (6,2)	SAS288	DSK(6,4) = DSK(8,2)	SAS350
DSK (5,5)= DSK (1,1)	SAS289	DSK(7,4) = DSK(2,1)	SAS351
DO 8621 I=2,4	SAS290	DSK(8,4) = DSK(6,2)	SAS352
DSK (I+4,5)=DSK (I,1)	SAS291	DSK(5,5) = DSK(1,1)	SAS353
8621 DSK (I+4,6)=DSK (I,2)	SAS292	DSK(6,5) = DSK(2,1)	SAS354
DSK (7,7)= DSK (1,1)	SAS293	DSK(7,5) = DSK(3,1)	SAS355
DSK (8,7)=-DSK (2,1)	SAS294	DSK(6,6) = DSK(2,2)	SAS356
DSK (8,8)= DSK (2,2)	SAS295	DSK(8,6) = DSK(4,2)	SAS357
DN 301 J=1,8	SAS296	DSK(7,7) = DSK(1,1)	SAS358
DO 301 I=1,8	SAS297	DSK(8,7) = DSK(6,1)	SAS359
301 DSK(J,I) = DSK(I,J)	SAS298	DSK(8,8) = DSK(2,2)	SAS360
IF(IWRITE.EQ.0) GO TO 501	SAS299	DO 402 J=1,8	SAS361
WRITE (6,205) NTYPE	SAS300	DO 402 I=1,8	SAS362
WRITE (6,103)	SAS301	402 DSK(J,I) = DSK (I,J)	SAS363
WRITE (6,101) ((DSK(I,J),I=1,8), J=1,8)	SAS302	DO 403 I=1,8	SAS364
501 CONTINUE	SAS303	DO 403 J=1,8	SAS365
GO TO 235	SAS304	403 DSK(I,J) = DSK(I,J) * ((E*A)/(96.*ALP*BET*AX*BY))	SAS366
7 CONTINUE	SAS305	IF(IWRITE.EQ.0) GO TO 512	SAS367
C*****RECTANGULAR*PLATF*CALCULATIONS*****	SAS306	WRITE (6,205) NTYPE	SAS368
C*****ASSUMED STRFSS FUNCTION WITH SEVEN COEFFICIENTS*****	SAS307	WRITE (6,103)	SAS369
DO 10006 I = 1,8	SAS308	WRITE (6,101) ((DSK(I,J),I=1,8), J=1,8)	SAS370
DO 10006 J = 1,8	SAS309	512 CONTINUE	SAS371
10006 DSK (I,J) = 0.0	SAS310	GO TO 235	SAS372

TABLE XXII (Continued)

```

8 CONTINUE
C*****TRIANGULAR*PLATE*CALCULATIONS*****
JLAM=6
XRP=X(1R)-X(1P)
YRP=Y(1R)-Y(1P)
XRO=X(1R)-X(1Q)
YRO=Y(1R)-Y(1Q)
XQP=X(1Q)-X(1P)
YQP=Y(1Q)-Y(1P)
D1=SQRT(XQP**2+YQP**2)
AL(1)=XQP/D1
AL(2)=YQP/D1
AE=A*E
RR=AL(1)*XRP+AL(2)*YRP
X2=XRP-AL(1)*RR
Y2=YRP-AL(2)*RR
D2=SQRT(X2**2+Y2**2)
AL2(1)=X2/D2
AL2(2)=Y2/D2
C CHANGE FROM DATUM TO LOCAL COORDINATES
X21=XQP*AL2(1)+YQP*AL2(2)
Y21=XQP*AL(1)+YQP*AL(2)
X31=XRP*AL2(1)+YRP*AL2(2)
Y31=XRP*AL(1)+YRP*AL(2)
X32=XRO*AL2(1)+YRO*AL2(2)
Y32=XRO*AL(1)+YRO*AL(2)
A123=(X32*Y21-X21*Y32)/2.
ET1=AE/(4.*A123*(1.-PR**2))
ET2=AE/(8.*A123*(1.+PR))
C CALCULATE THE K SUB (D) + K SUB (S) MATRIX.
DSK (1,1)= ET1* Y32**2 +ET2* X32**2
DSK (2,1)= -ET1* PR*Y32*X32 -ET2* X32*Y32
DSK (2,2)= ET1* X32**2 +ET2* Y32**2
DSK (3,1)= -ET1* Y32*Y31 -ET2* X32*X31
DSK (3,2)= ET1* PR*X32*Y31 +ET2* Y32*X31
DSK (3,3)= ET1* Y31**2 +ET2* X31**2
DSK (4,1)= ET1* PR*Y32*X31 +ET2* X32*Y31
DSK (4,2)= -ET1* X32*X31 -ET2* Y32*Y31
DSK (4,3)= -ET1* PR*Y31*X31 -ET2* X31*Y31
DSK (4,4)= ET1* X31**2 +ET2* Y31**2
DSK (5,1)= ET1* Y32*Y21 +ET2* X32*X21
DSK (5,2)= -ET1* PR*X32*Y21 -ET2* Y32*X21
DSK (5,3)= -ET1* Y31*Y21 -ET2* X31*X21
DSK (5,4)= ET1* PR*X31*Y21 +ET2* Y31*X21
DSK (5,5)= ET1* Y21**2 +ET2* X21**2
DSK (6,1)= -ET1* PR*Y32*X21 -ET2* X32*Y21
DSK (6,2)= ET1* X32*X21 +ET2* Y32*Y21
DSK (6,3)= ET1* PR*Y31*X21 +ET2* X31*Y21
DSK (6,4)= -ET1* X31*X21 -ET2* Y31*Y21
DSK (6,5)= -ET1* PR*Y21*X21 -ET2* X21*Y21
DSK (6,6)= ET1* X21**2 +ET2* Y21**2
DO I17 J=1,6
DO I17 I=1,6
DSK(J,I)=DSK(I,J)
IF(IWRITE.EQ.0) GO TO 118
WRITE(6,205) NTYPE
WRITE(6,103)
WRITE(6,101) ((DSK(1,J),I=1,6),J=1,6)
118 CONTINUE
GO TO 235
9 CONTINUE
WRITE (6,257)

```

SAS373
SAS374
SAS375
SAS376
SAS377
SAS378
SAS379
SAS380
SAS381
SAS382
SAS383
SAS384
SAS385
SAS386
SAS387
SAS388
SAS389
SAS390
SAS391
SAS392
SAS393
SAS394
SAS395
SAS396
SAS397
SAS398
SAS399
SAS400
SAS401
SAS402
SAS403
SAS404
SAS405
SAS406
SAS407
SAS408
SAS409
SAS410
SAS411
SAS412
SAS413
SAS414
SAS415
SAS416
SAS417
SAS418
SAS419
SAS420
SAS421
SAS422
SAS423
SAS424
SAS425
SAS426
SAS427
SAS428
SAS429
SAS430
SAS431
SAS432
SAS433
SAS434

```

GO TO 839
C MPQRS(I) CONTAINS THE SCHEME FOR PLACING THE ELEMENT MATRICES INTO
C THERE LARGER COUNTERPARTS.
235 CONTINUE
K=0
JROW = JLAM / 2
DO 39 I=1,JROW
DO 39 J=1,2
K=K+1
MPQRS(K)=2*IPQRS(I)-2+J
IF(IWRITE.EQ.0) GO TO 504
WRITE (6,106) K, MPQRS(K)
504 CONTINUE
39 CONTINUE
C ADD KBAR I INTO KBAR
38 DO 37 LA=1,JLAM
KI=MPQRS(LA)
DO 37 I=1,JLAM
KL=MPQRS(I)
IF(KI-KL)37,374,374
374 KJ=(I*(KI-1))/2+KL
BARK(KJ)=BARK(KJ)+DSK (LA,I)
IF(IWRITE.EQ.0) GO TO 505
WRITE (6,107) LA, KI
WRITE (6,110) KJ, LA, I
505 CONTINUE
37 CONTINUE
C*****WRITE TAPE 4 FOR STRESS CALCULATIONS.*****
WRITE (4) NTYPE,E,PR,A,JLAM,D1,D2,AL(1),AL(2),MPQRS, IPQRS
IF(IWRITE.EQ.0) GO TO 506
WRITE(6,8798)
CALL WRT ( BARK, N2)
506 CONTINUE
236 CONTINUE
C*****WRITE COMPLETE STIFFNESS MATRIX ON TAPE 3 FOR FORCE CALCULATION*
WRITE(3) (BARK(I),I=1,NUM)
WRITE(6,8798)
NF=0
NS=0
DO 31007 J=1,N2
NS=NF+1
NF=NF+J
31007 WRITE (6,31009) J,(BARK(I), I=NS,NF)
C REMOVE SINGULARITIES FROM K-BAR BY PLACING 1 ON DIAGONAL AND ZERO
C ELSEWHERE ON DUPLICATED ROWS AND COLUMNS.
WRITE (6,114) NCROSS
DO 316 LC=1,NCROSS
LA=NBC(LC)
DO 315 I=1,N2
L=MAX0(LA,I)
KA=(LA+I)+(L*(L-3))/2
IF(IWRITE.EQ.0) GO TO 507
WRITE (6,115) KA
507 CONTINUE
315 BARK(KA)=0
KB=(LA*(LA+1))/2
IF(IWRITE.EQ.0) GO TO 508
WRITE (6,113) LA, KB
508 CONTINUE
BARK(KB)=1.
316 CONTINUE
IF(IWRITE.EQ.0) GO TO 509

```

SAS435
SAS436
SAS437
SAS438
SAS439
SAS440
SAS441
SAS442
SAS443
SAS444
SAS445
SAS446
SAS447
SAS448
SAS449
SAS450
SAS451
SAS452
SAS453
SAS454
SAS455
SAS456
SAS457
SAS458
SAS459
SAS460
SAS461
SAS462
SAS463
SAS464
SAS465
SAS466
SAS467
SAS468
SAS469
SAS470
SAS471
SAS472
SAS473
SAS474
SAS475
SAS476
SAS477
SAS478
SAS479
SAS480
SAS481
SAS482
SAS483
SAS484
SAS485
SAS486
SAS487
SAS488
SAS489
SAS490
SAS491
SAS492
SAS493
SAS494
SAS495
SAS496

TABLE XXII (Continued)

```

WRITE(6,8798)
CALL WRT ( BARK, N2)
509 CONTINUE
CALCULATE K-BAR-INVERSE. IF ISING IS 0 ON RETURN THE MATRIX IS SINGULA
CALL SYMINV (N2, BARK, ISING)
WRITE(6,8799)
NS=0
NF=0
DO 31008 J=1,N2
NS=NF+1
NF=NF+J
31008 WRITE(6,31009) J,(BARK(I),I=NS,NF)
30001 IF(ISING)317,8623,317
8623 WRITE(6,8629)
GO TO 839
317 CONTINUE
C ZERO DIAGONAL ELEMENTS OF BARK INVERSE
DO 319 LC=1,NCROSS
LA=(NBC(LC)*(NBC(LC)+1))/2
319 BARK(LA)=0
IF(IWRITE.EQ. 0) GO TO 510
WRITE(6,8799)
CALL WRT ( BARK, N2)
510 CONTINUE
CALL SMMPY(BARK,FORCE,UBAR,N2,NC)
WRITE(6,800)
WRITE(6,801)
900 WRITE(6,802)
K=0
DO 638 I=1,N2*2
K=K+1
WRITE(6,804) K,(UBAR(I,J),J=1,NC)
638 WRITE(6,805) (UBAR(I+1,J),J=1,NC)
637 CONTINUE
C*****WRITE FORCES ACTING ON THE STRUCTURE*****
WRITE(6,809)
WRITE(6,802)
K=0
DO 701 I=1,N2*2
K=K+1
WRITE(6,804) K,(FORCE(I,J),J=1,NC)
701 WRITE(6,805)(FORCE(I+1,J),J=1,NC)
C CALCULATE THE FORCE MATRIX = KBAR * UBAR
REWIND 3
READ(3)(BARK(I),I=1,NUM)
CALL SMMPY (BARK,UBAR ,QBAR,N2,NC)
WRITE(6,809)
WRITE(6,802)
K=0
DO 640 I=1,N2*2
K=K+1
WRITE (6,804) K, (QBAR(I,J), J=1,NC)
640 WRITE(6,805)(QBAR(I+1,J),J=1,NC)
C*****ELEMENT GENERALIZED STRESS CALCULATIONS*****
IF(NSN.EQ.0) GO TO 642
WRITE (6,203)
642 CONTINUE
REWIND 4
DO 370 NN=1,NELEM
READ (4) NTYPE,E,PR,A,JLAM,D1,D2,AL(1),AL(2),MPQRS ,IPQRS
IF(IWRITE.EQ.0) GO TO 641
WRITE (6,116) NTYPE,E,PR,A,JLAM,D1,D2,AL(1),AL(2),MPQRS ,IPQRS
SAS497
SAS498
SAS499
SAS500
SAS501
SAS502
SAS503
SAS504
SAS505
SAS506
SAS507
SAS508
SAS509
SAS510
SAS511
SAS512
SAS513
SAS514
SAS515
SAS516
SAS517
SAS518
SAS519
SAS520
SAS521
SAS522
SAS523
SAS524
SAS525
SAS526
SAS527
SAS528
SAS529
SAS530
SAS531
SAS532
SAS533
SAS534
SAS535
SAS536
SAS537
SAS538
SAS539
SAS540
SAS541
SAS542
SAS543
SAS544
SAS545
SAS546
SAS547
SAS548
SAS549
SAS550
SAS551
SAS552
SAS553
SAS554
SAS555
SAS556
SAS557
SAS558
641 CONTINUE
C*****
C SELECT U-BAR-I FROM U-BAR AND STORE IT IN QORU(I,J)
DO 220 I=1,JLAM
KI=MPQRS(I)
DO 220 J=1,NC
220 QORU(I,J)=UBAR(KI,J)
WRITE (6,204) NN
WRITE (6,801)
WRITE (6,802)
K=0
DO 223 I = 1,JLAM, 2
K=K+1
WRITE (6,804) IPQRS(K), (QORU(I,J),J=1,NC)
WRITE(6,805) (QORU(I+1, J),J=1,NC)
223 CONTINUE
C*****
IF(NSN.EQ.0) GO TO 379
WRITE (6,258)
IF(NTYPE.GE. 5) GO TO 375
READ(5,251) I,(XN(NN,J),J=1,NSN)
WRITE(6,253) I,(XN(NN,J),J=1,NSN)
GO TO 376
375 CONTINUE
READ (5,251)I, (XN(NN,J),J=1,NSN)
READ(5,254) I,(YN(NN,J),J=1,NSN)
WRITE(6,253)I, (XN(NN,J),J=1,NSN)
WRITE(6,255) I,(YN(NN,J),J=1,NSN)
GO TO 376
379 CONTINUE
IF(NSN.EQ.0) NSN1=1
IF(NSN.NE.0) NSN1=NSN
XN(NN,1)=D2/2.
YN(NN,1)=D1/2.
WRITE(6,205)
376 CONTINUE
DO 237 NNSN=1,NSN1
DO 377 I=1,3
DO 377 J=1,8
377 STR (I,J) = 0.0
DO 378 I=1,3
DO 378 J=1,5
378 STRESS (I,J) = 0.0
GO TO (11,22,33,44,55,66,77,88,99),NTYPE
11 CONTINUE
C*****STRESS MATRIX STRINGER ELEMENT*****
WRITE (6,200)
STR (1,1) = -(AL(1)*E) / D1
STR (1,2) = -(AL(2)*E) / D1
STR (1,3) = AL(1)*E / D1
STR (1,4) = AL(2)*E / D1
WRITE (6,101) (STR (1,J),J=1,4)
CALL MXM (STR,QORU,STRESS,NC)
GO TO 30
C*****STRINGER STRESS MATRIX ASSUMED STRESS FUNCTION*****
22 CONTINUE
XX = XN(NN,NNSN) / D2
WRITE(6,101) XX
STR (1,1)=- (AL(1)*E)*(1.0-XX) / D1
STR (1,2)=- (AL(2)*E)*(1.0-XX) / D1
STR (1,3)=AL(1)*E*XX / D1
STR (1,4)=AL(2)*E*XX / D1
SAS559
SAS560
SAS561
SAS562
SAS563
SAS564
SAS565
SAS566
SAS567
SAS568
SAS569
SAS570
SAS571
SAS572
SAS573
SAS574
SAS575
SAS576
SAS577
SAS578
SAS579
SAS580
SAS581
SAS582
SAS583
SAS584
SAS585
SAS586
SAS587
SAS588
SAS589
SAS590
SAS591
SAS592
SAS593
SAS594
SAS595
SAS596
SAS597
SAS598
SAS599
SAS600
SAS601
SAS602
SAS603
SAS604
SAS605
SAS606
SAS607
SAS608
SAS609
SAS610
SAS611
SAS612
SAS613
SAS614
SAS615
SAS616
SAS617
SAS618
SAS619
SAS620

```

TABLE XXII (Continued)

```

WRITE(6,200)
WRITE(6,101)((STR (I,J),J=1,4)
CALL MXM (STR,QORU,STRESS,NC)
GO TO 30
33 CONTINUE
44 CONTINUE
WRITE (6,256)
GO TO 839
55 CONTINUE
C*****STRESS MATRIX ASSUMED DISPLACEMENTS*****
XX = XN(NN,NNSN) / D2
YY = YN(NN,NNSN) / D1
WRITE(6,259) XX,YY
XA = D2
YB = D1
EPRO=1.0-PR**2
EPR1=E/EPRO
STR(1,1)=-EPR1*(1.0-YY)/XA
STR(1,2)=-EPR1*PR*(1.0-XX)/YB
STR(1,3)=-EPR1*XX/XA
STR(1,4)= -(STR(1,2))
STR(1,5)= -(STR(1,3))
STR(1,6)=EPR1*PR*XX/YB
STR(1,7)= -(STR(1,1))
STR(1,8)= -(STR(1,6))
STR(2,1)=-EPR1*PR*(1.0-YY)/XA
STR(2,2)=-EPR1*(1.0-XX)/YB
STR(2,3)=-EPR1*PR*YY/XA
STR(2,4)= -(STR(2,2))
STR(2,5)= -(STR(2,3))
STR(2,6)=EPR1*XX/YB
STR(2,7)= -(STR(2,1))
STR(2,8)= -(STR(2,6))
STR(3,1)=-EPR1*(1.0-PR)*(1.0-XX)/(2.0*YB)
STR(3,2)=-EPR1*(1.0-PR)*(1.0-YY)/(2.0*XA)
STR(3,3)= -(STR(3,1))
STR(3,4)=-EPR1*YY*(1.0-PR)/(2.0*XA)
STR(3,5)=EPR1*XX*(1.0-PR)/(2.0*YB)
STR(3,6)= -(STR(3,4))
STR(3,7)= -(STR(3,5))
STR(3,8)= -(STR(3,2))
WRITE (6,200)
WRITE (6,101)((STR(I,J),J=1,8),I=1,3)
CALL MXM (STR,QORU,STRESS,NC)
GO TO 30
66 CONTINUE
C*****STRESS MATRIX ASSUMED STRESS FUNCTION WITH 5 COEFFICIENTS*****
XX = XN(NN,NNSN) / D2
YY = YN(NN,NNSN) / D1
WRITE(6,259) XX,YY
XA = D2
YB = D1
EPRO=1.0-PR**2
EPR1=E/EPRO
EPR2=2.0*YY-1.0
EPR3=1.0-2.0*YY
EPR4=2.0*XX-1.0
EPR5=1.0-2.0*XX
STR(1,1)=EPR1*((EPRO*EPR2)-1.0)/(2.0*XA)
STR(1,2)=-EPR1*PR/(2.0*YB)
STR(1,3)=EPR1*((EPRO*EPR2)-1.0)/(2.0*XA)
STR(1,4)=EPR1*PR/(2.0*YB)
SAS621
SAS622
SAS623
SAS624
SAS625
SAS626
SAS627
SAS628
SAS629
SAS630
SAS631
SAS632
SAS633
SAS634
SAS635
SAS636
SAS637
SAS638
SAS639
SAS640
SAS641
SAS642
SAS643
SAS644
SAS645
SAS646
SAS647
SAS648
SAS649
SAS650
SAS651
SAS652
SAS653
SAS654
SAS655
SAS656
SAS657
SAS658
SAS659
SAS660
SAS661
SAS662
SAS663
SAS664
SAS665
SAS666
SAS667
SAS668
SAS669
SAS670
SAS671
SAS672
SAS673
SAS674
SAS675
SAS676
SAS677
SAS678
SAS679
SAS680
SAS681
SAS682
STR(1,5)=EPR1*((EPRO*EPR2)+1.0)/(2.0*XA)
STR(1,6)=STR(1,4)
STR(1,7)=EPR1*((EPRO*EPR3)+1.0)/(2.0*XA)
STR(1,8)=-STR(1,4)
STR(2,1)=-EPR1*PR/(2.0*XA)
STR(2,2)=EPR1*((EPRO*EPR4)-1.0)/(2.0*YB)
STR(2,3)=STR(2,1)
STR(2,4)=EPR1*((EPRO*EPR5)+1.0)/(2.0*YB)
STR(2,5)=-STR(2,1)
STR(2,6)=EPR1*((EPRO*EPR4)+1.0)/(2.0*YB)
STR(2,7)=STR(2,5)
STR(2,8)=EPR1*((EPRO*EPR5)-1.0)/(2.0*YB)
STR(3,1) = -(EPR1*(1.0-PR)/(4.0 * YB))
STR(3,2) = -(EPR1*(1.0-PR)/(4.0 * XA))
STR(3,3)=-STR(3,1)
STR(3,4)=STR(3,2)
STR(3,5)=STR(3,3)
STR(3,6)=-STR(3,2)
STR(3,7)=STR(3,1)
STR(3,8)=STR(3,6)
WRITE(6,200)
WRITE(6,101)((STR(I,J),J=1,8),I=1,3)
CALL MXM (STR,QORU,STRESS,NC)
GO TO 30
77 CONTINUE
C*****STRESS MATRIX - WITH SEVEN COEFFICIENTS*****
BY = D1
AX = D2
XX = XN(NN,NNSN)
YY = YN(NN,NNSN)
WRITE(6,259) XX,YY
ALP = (3.*D2*D2 + D1*D1)
BET = (3.*D1*D1)+(D2*D2)
DO 371 I=1,3
DO 371 J=1,8
371 STR(I,J) = 0.0
STR(1,1) = -(102.*BY*ALP*BET)-(6.*(BY**3)*BET)+(18.*AX*AX*BY*BET)
1+YY*((96.*ALP*BET)+(12.*BY*BY*BET)-(36.*AX*AX*BET))
STR(2,1) = -(18.*BY*ALP*BET)-(18.*(BY**3)*BET)+(54.*AX*AX*BY*BET)
1+YY*((36.*BY*BY*BET) - (108.*AX*AX*BET))
STR(3,1) = -(18.*AX*ALP*BET)-(54.*(AX**3)*BET)+(18.*AX*BY*BY*BET)
1-XX*((36.*BY*BY*BET) - (108.*AX*AX*BET))
STR(1,2) = -(18.*AX*ALP*BET)-(18.*(AX**3)*ALP)+(54.*AX*BY*BY*ALP)
1+XX*((36.*AX*AX*ALP) - (108.*BY*BY*ALP))
STR(2,2) = -(102.*AX*ALP*BET)-(6.*(AX**3)*ALP)+(18.*AX*BY*BY*ALP)
1+XX*((96.*ALP*BET) - (36.*BY*BY*ALP) + (12.*AX*AX*ALP))
STR(3,2) = -(18.*BY*ALP*BET)-(54.*(BY**3)*ALP)+(18.*AX*AX*BY*ALP)
1-YY*((36.*AX*AX*ALP) - (108.*BY*BY*ALP))
STR(1,3) = -(6.*BY*ALP*BET)+(6.*(BY**3)*BET)-(18.*AX*AX*BY*BET)
1+YY*((-96.*ALP*BET)-(12.*BY*BY*BET)+(36.*AX*AX*BET))
STR(2,3) = -(18.*BY*ALP*BET)+(18.*(BY**3)*BET)-(54.*AX*AX*BY*BET)
1+YY*((-36.*BY*BY*BET) + (108.*AX*AX*BET))
STR(3,3) = +(18.*AX*ALP*BET)+(54.*(AX**3)*BET)-(18.*AX*BY*BY*BET)
1-XX*((-36.*BY*BY*BET) + (108.*AX*AX*BET))
STR(1,4) = +(18.*AX*ALP*BET)+(18.*(AX**3)*ALP)-(54.*AX*BY*BY*ALP)
1+XX*((-36.*AX*AX*ALP) + (108.*BY*BY*ALP))
STR(2,4) = +(102.*AX*ALP*BET)+(6.*(AX**3)*ALP)-(18.*AX*BY*BY*ALP)
1+XX*((-96.*ALP*BET)+(36.*BY*BY*ALP)-(12.*AX*AX*ALP))
STR(3,4) = -(18.*BY*ALP*BET)+(54.*(BY**3)*ALP)-(18.*AX*AX*BY*ALP)
1-YY*((-36.*AX*AX*ALP) + (108.*BY*BY*ALP))
STR(1,5) = +(6.*BY*ALP*BET)-(6.*(BY**3)*BET)+(18.*AX*AX*BY*BET)
1+YY*((96.*ALP*BET)+(12.*BY*BY*BET)-(36.*AX*AX*BET))
SAS683
SAS684
SAS685
SAS686
SAS687
SAS688
SAS689
SAS690
SAS691
SAS692
SAS693
SAS694
SAS695
SAS696
SAS697
SAS698
SAS699
SAS700
SAS701
SAS702
SAS703
SAS704
SAS705
SAS706
SAS707
SAS708
SAS709
SAS710
SAS711
SAS712
SAS713
SAS714
SAS715
SAS716
SAS717
SAS718
SAS719
SAS720
SAS721
SAS722
SAS723
SAS724
SAS725
SAS726
SAS727
SAS728
SAS729
SAS730
SAS731
SAS732
SAS733
SAS734
SAS735
SAS736
SAS737
SAS738
SAS739
SAS740
SAS741
SAS742
SAS743
SAS744

```

TABLE XXII (Continued)

STR(2,5)= (18.*BY*ALP*BET)-(18.*(BY**3)*BET)+(54.*AX*AX*BY*BET)	SAS745	CALL MXM (STR,QORU,STRESS,NC)	SAS807
1+YY*((36.*BY*BY*BET) - (108.*AX*AX*BET))	SAS746	GO TO 30	SAS808
STR(1,5)= +(18.*AX*ALP*BET)-(54.*(AX**3)*BET)+(18.*AX*BY*BY*BET)	SAS747	99 CONTINUE	SAS809
1-XX*((36.*BY*BY*BET) - (108.*AX*AX*BET))	SAS748	WRITE (6,256)	SAS810
STR(1,6)= +(18.*AX*ALP*BET)-(18.*(AX**3)*ALP)+(54.*AX*BY*BY*ALP)	SAS749	GO TO 839	SAS811
1+XX*((36.*AX*AX*ALP) - (108.*BY*BY*ALP))	SAS750	30 CONTINUE	SAS812
STR(2,6)= +(6.*AX*ALP*BET)-(6.*(AX**3)*ALP)+(18.*AX*BY*BY*ALP)	SAS751	WRITE(6,206) NN,NTYPE	SAS813
1+XX*((96.*ALP*BET) - (36.*BY*BY*ALP) + (12.*AX*AX*ALP))	SAS752	WRITE (6,201)	SAS814
STR(3,6)= (18.*BY*ALP*BET)-(54.*(BY**3)*ALP)+(18.*AX*AX*BY*ALP)	SAS753	WRITE (6,202)	SAS815
1-YY*((+36.*AX*AX*ALP) - (108.*BY*BY*ALP))	SAS754	WRITE (6,219) NNSN, NTYPE, (STRESS(1,I), I=1,NC)	SAS816
STR(1,7)= (102.*BY*ALP*BET)+(6.*(BY**3)*BET)-(18.*AX*AX*BY*BET)	SAS755	IF(NTYPE.LE.4) GO TO 237	SAS817
1+YY*((-96.*ALP*BET)-(12.*BY*BY*BET)+(36.*AX*AX*BET))	SAS756	WRITE (6,222) (STRESS(2,I), I=1,NC)	SAS818
STR(2,7)= (18.*BY*ALP*BET)+(18.*(BY**3)*BET)-(54.*AX*AX*BY*BET)	SAS757	WRITE (6,221) (STRESS(3,I), I=1,NC)	SAS819
1+YY*((-36.*BY*BY*BET) + (108.*AX*AX*BET))	SAS758	237 CONTINUE	SAS820
STR(3,7)= -(18.*AX*ALP*BET)+(54.*(AX**3)*BET)-(18.*AX*BY*BY*BET)	SAS759	370 CONTINUE	SAS821
1-XX*((-36.*BY*BY*BET) + (108.*AX*AX*BET))	SAS760	REWIND 3	SAS822
STR(1,8)= -(18.*AX*ALP*BET)+(18.*(AX**3)*ALP)-(54.*AX*BY*BY*ALP)	SAS761	REWIND 4	SAS823
1+XX*((-36.*AX*AX*ALP) + (108.*BY*BY*ALP))	SAS762	WRITE(6,99999)(R(J),J=1,12)	SAS824
STR(2,8)= -(6.*AX*ALP*BET)+(6.*(AX**3)*ALP)-(18.*AX*BY*BY*ALP)	SAS763	19999 GO TO 839	SAS825
1+XX*((-96.*ALP*BET)+(36.*BY*BY*ALP)-(12.*AX*AX*ALP))	SAS764	11999 CALL EXIT	SAS826
STR(3,8)= (18.*BY*ALP*BET)+(54.*(BY**3)*ALP)-(18.*AX*AX*BY*ALP)	SAS765	END	SAS827
1-YY*((-36.*AX*AX*ALP) + (108.*BY*BY*ALP))	SAS766	\$IBFTC SYMINV	
DO 404 I=1,3	SAS767	SUBROUTINE SYMINV (IO, A, ISING)	SMINV001
DO 404 J=1,8	SAS768	DIMENSION A(1830),COL(60)	SMINV002
404 STR(I,J)= STR(I,J)*(E/(96.*ALP*BET *AX*BY))	SAS769	IF(10-1)800,810,97	SMINV003
WRITE(6,200)	SAS770	----INVERSE OF 2X2----	SMINV004
WRITE(6,101)((STR(I,J),J=1,8),I=1,3)	SAS771	97 C=A(1)*A(3)-A(2)*A(2)	SMINV005
CALL MXM (STR,QORU,STRESS,NC)	SAS772	IF(C)98,900,98	SMINV006
GO TO 30	SAS773	A(2)=-A(2)/C	SMINV007
88 CONTINUE	SAS774	COL(1)=A(1)/C	SMINV008
DO 377 I=1,3	SAS775	A(1)=A(3)/C	SMINV009
DO 377 J=1,8	SAS776	A(3)=COL(1)	SMINV010
377 STR (I,J) = 0.0	SAS777	IF(10-2)800,720,99	SMINV011
DO 378 I=1,3	SAS778	99 K=1	SMINV012
DO 378 J=1,5	SAS779	M=10-1	SMINV013
378 STRESS (I,J) = 0.0	SAS780	DO7001011=2,M	SMINV014
DO 119 I=1,3	SAS781	K=K+1011	SMINV015
DO 119 J=1,6	SAS782	C ----L.L.H.OFSYMMETRICMATRIX*COLUMN----	SMINV016
119 STR(I,J)=0.0	SAS783	N=0	SMINV017
STR(1,1)=Y32	SAS784	DO1001=1,1011	SMINV018
STR(1,2)=-PR*X32	SAS785	COL(I)=0	SMINV019
STR(1,3)=-Y31	SAS786	DO3001=1,1011	SMINV020
STR(1,4)=PR*X31	SAS787	IA=K+I	SMINV021
STR(1,5)=Y21	SAS788	DO300J=1,I	SMINV022
STR(1,6)=-PR*X21	SAS789	N=N+1	SMINV023
STR(2,1)=PR*Y32	SAS790	COL(J)=COL(J)+A(N)*A(IA)	SMINV024
STR(2,2)=-X32	SAS791	IF(J-1)200,300,800	SMINV025
STR(2,3)=-PR*Y31	SAS792	18=K+J	SMINV026
STR(2,4)=X31	SAS793	COL(I)=COL(I)+A(N)*A(18)	SMINV027
STR(2,5)=PR*Y21	SAS794	300 CONTINUE	SMINV028
STR(2,6)=-X21	SAS795	C ----COMPUTE B22----	SMINV029
STR(3,1)=-((1.-PR)/2.)*X32	SAS796	C=0	SMINV030
STR(3,2)=-((1.-PR)/2.)*Y32	SAS797	DO4001=1,1011	SMINV031
STR(3,3)=-((1.-PR)/2.)*X31	SAS798	IA=K+I	SMINV032
STR(3,4)=-((1.-PR)/2.)*Y31	SAS799	400 C=C+A(IA)*COL(I)	SMINV033
STR(3,5)=-((1.-PR)/2.)*X21	SAS800	IA=IA+1	SMINV034
STR(3,6)=-((1.-PR)/2.)*Y21	SAS801	C=A(IA)-C	SMINV035
DO 120 I=1,3	SAS802	IF(C)410,900,410	SMINV036
DO 120 J=1,6	SAS803	C=1.0/C	SMINV037
120 STR(I,J)=(E/(2.*0.5*(X32*Y21-X21*Y32)*(1.-(PR**2))))*STR(I,J)	SAS804	A(IA)=C	SMINV038
WRITE(6,200)	SAS805	C ----COMPUTE B21----	SMINV039
WRITE(6,101)((STR(I,J),J=1,8),I=1,3)	SAS806	DO5001=1,1011	SMINV040

TABLE XXII (Continued)

	IA=K+1	SMINV041
500	A(IA)=-C*COL(I)	SMINV042
C	----COMPUTE B11----	SMINV043
	N=0	SMINV044
	DO600I=1,I011	SMINV045
	DO600J=1,I	SMINV046
	N=N+1	SMINV047
	IA=K+J	SMINV048
600	A(N)=A(N)-A(IA)*COL(I)	SMINV049
700	CONTINUE	SMINV050
720	ISING=1	SMINV051
710	RETURN	SMINV052
900	ISING=0	SMINV053
	GOTO710	SMINV054
810	A(1)=1.0/A(1)	SMINV055
	GO TO 720	SMINV056
800	ISING = 2	SMINV057
	RETURN	SMINV058
	END	SMINV059
\$IBFTC	SMMPY	
	SUBROUTINE SMMPY(A,B,C,N3,NC)	SMMPY001
C	(KINVERSE)*(FORCE)**DEFLECTIONS****NO OF ROWS****NO OF FORCES	SMMPY002
	DIMENSION A(1830),B(60,5),C(60,5)	SMMPY003
	DO 100 I=1,N3	SMMPY004
	DO 100 J=1,NC	SMMPY005
	C(I,J)=0	SMMPY006
	DO 100 K1=1,N3	SMMPY007
	L=MAX0(I,K1)	SMMPY008
	K=(L*(L-3))/2+(I+K1)	SMMPY009
100	C(I,J)=A(K)*B(K1,J)+C(I,J)	SMMPY010
	RETURN	SMMPY011
	END	SMMPY012
\$IBFTC	WRT	
	SUBROUTINE WRT(A, N3)	WRT001
	DIMENSION A(3)	WRT002
31009	FORMAT(1X,3HROW,I4,1X,(1P10E13.4))	WRT003
	NF=0	WRT004
	NS=0	WRT005
	DO 31010 J=1,N3	WRT006
	NS=NF+1	WRT007
	NF=NF+J	WRT008
31010	WRITE (6,31009) J,(A(I), I=NS,NF)	WRT009
	RETURN	WRT010
	END	WRT011
\$IBFTC	MXM	
	SUBROUTINE MXM (A, B, C, NC)	MXM001
	DIMENSION A(3*8),B(8*5),C(3*5)	MXM002
	DO 20 I=1,3	MXM003
	DO 20 J=1,NC	MXM004
20	C(I,J) = 0.0	MXM005
	DO 10 I=1,3	MXM006
	DO 10 J=1,NC	MXM007
	DO 10 N=1,8	MXM008
10	C(I,J) = C(I,J) + A(I,N) * B(N,J)	MXM009
	RETURN	MXM010
	END	MXM011

APPENDIX C

A DIGITAL COMPUTER PROGRAM FOR IMPLEMENTING THE MATRIX FORCE METHOD

(Mr. Bill Accola of the University Computing Center, Oklahoma State University, rendered very able and valuable assistance to the planning of this program and had a major role in its development.)

The following computer program is developed from the concept set forth by Reference (12); namely, that of building up a main program from a set of matrix subroutines with each subroutine performing some matrix manipulation (multiplication, inversion, addition, etc.). The subroutines used in this program are primarily those listed in Reference (12). The only exceptions are modified versions of the subroutines RMATNZ and WRTMAT.

Modifications of RMATNZ

A counter (IENT) has been added to this subroutine to keep track of which call the subroutine is in. According to the time of entry, the appropriate heading for the matrix that is read is printed with its title; i.e., when IENT is 1, the computed GO TO statement number 1000 sends control to statement number 4, which prints out the name [ALPIJ] with Format 103. To adjust this subroutine for different programs, the order of the matrices to be read in must be known. A numbered write statement must be set up for each matrix with the appropriate format

for that matrix. With these statements in order, statement 1000 must be altered to send control to the proper write statement according to the current entry the subroutine is in.

Also, statement 102 has been changed from

```
102 FORMAT (6X,I4,6X,I4,E10.4)
```

to

```
102 FORMAT (6X,I4,6X,I4,E14.7).
```

Modifications of WRTMAT

This subroutine has been altered in the same manner as was RMATNZ. A numbered write statement is needed for each matrix that is to be printed. A format is needed with the name of a matrix for each matrix that is to be printed. With these statements added, the computed GO TO statement must be changed to send control to the proper write statement depending upon the time of entry which determines the matrix that is printed.

Additional Matrix Designations

The following matrices are defined as

$$[a_{rs}] \equiv [ARS],$$

$$[A_{MN}] \equiv [CAMN],$$

$$[a_{rn}] \equiv [ARN],$$

$$[G_{MN}] \equiv [GNN],$$

$$[G_{im}] \equiv [CGIM],$$

$$[g_{ir}][\alpha_{ij}] \equiv [GRIALP],$$

$$[G_{sn}] \equiv [GSN],$$

$$[g_{im}][\alpha_{ij}] \equiv [GMIALP],$$

$$\begin{aligned} [G_{MP}] &\equiv [GMP], & [I] &\equiv [XIDM], \\ [a_{MN}] &\equiv [AMN], & [ars]^{-1} &\equiv [ARSINV]. \end{aligned}$$

With the above definitions and those made in prior topics, the equations given in Chapter II are converted to computer language and a description of the computer program may now be given.

Program Description

This package program is made up of a main program and several subroutines. The main program serves only to prepare arrays for operations which are carried out in subroutines. The flow of manipulations of the matrices can be followed through the main program.

Since the input/output assignments are held in common for all the subroutines, KIN (input) and KOUT (output) must be established. On the IBM 7040 KIN is set to 5, and KOUT is set to 6. This causes all data to be read in from the card reader and all output to be printed on the printer.

Two calls to RMATNZ read in $[ALPIJ]$ and $[GIR]$. Each call reads the matrix and prints the matrix with the appropriate title. $[ALPIJ]$ and $[GIR]$ are manipulated as AXB giving $[GRIALP]$ which is printed by a call to WRMAT. Then $[GRIALP]$ is multiplied by $[GIR]$ giving $[ARS]$. This multiplication is initiated by a call to MXM. The resulting $[ARS]$ is printed with WRMAT. A DO-loop is inserted to save $[ARS]$ in STORE as it is desired later to invert $[ARS]$ and then multiply back to obtain an identity matrix. (The inversion subroutine destroys the input matrix.)

After storing $[ARS]$, $[ARSINV]$ is obtained and is printed with a call to $[INVERX]$ and a call to $WRTMAT$. To check the condition of $[ARS]$, the identity matrix $[XIDM]$ is computed by MXM and then printed with $WRTMAT$.

After printing $[XIDM]$, $[GIM]$ is read and printed via $RMATNZ$ and the $[GRIALP]$ and $[GIM]$ are multiplied giving $[ARN]$, which is printed with $WRTMAT$. To obtain $[GSN]$, MXM is called to multiply $[ARSINV]$ by $[ARN]$. The result is then printed. Another multiplication is performed obtaining $[GSN]$ from $[ARSINV] \times [ARN]$. Following the printing of $[GSN]$, $[GIR]$ is multiplied by $[GSN]$ to get $[GMP]$. Since $[ARSINV]$ is no longer needed, $[GMP]$ could have been stored in $[ARSINV]$. Next $[GMP]$ is subtracted from $[GIM]$ giving $[CGIM]$ which is then printed. The subtraction is done with a call to MSM . $[FORCE]$ is read in and printed with a call to $RMATNZ$ and is then multiplied by $[CGIM]$ to give the desired $[QI]$. $[QI]$ is printed by a call to $WRTMAT$. To find the stresses, the matrix $[AREINV]$ is printed and then $[STRESS (1)]$ is set equal to $[QI (1)]$ and $[STRESS (2)]$ equal to $[QI (2)]$. This is done because the first two elements of any array in this program are the number of rows and the number of columns. Following the multiplication of $[AREINV]$ and $[QI]$ which is done element-wise, the result, $[STRESS]$, will be the same size as $[QI]$. The actual multiplication is done with a double DO-loop. Following the multiplication, $[STRESS]$ is printed with $WRTMAT$ and punched which gives output capable of being read with $RMATNZ$.

To obtain deflections, the transpose of $[GIM]$ is multiplied times $[ALPIJ]([GIM] \times [ALPIJ])$ giving $[GMIALP]$ which is then printed with $WRTMAT$. MXM is used to obtain $[GMIALP] \times [GIM]$ resulting in $[AMN]$.

$[AMN]$ is printed. Next, another transposed multiplication is

performed giving $[GNN]$, which is printed. A subtraction $[AMN] - [GNN]$ is performed, giving $[CAMN]$, which is also printed with WRTMAT. The deflection matrix, $[DELTAM]$ is computed by multiplying $[CAMN]$ by $[FORCE]$. $[DELTAM]$ is then printed with WRTMAT.

To obtain a check on the final results of a redundant force calculation, a multiplication of $[GRIALP]$ and $[CGIM]$ is performed giving $[ARNTR]$. $[ARNTR]$ could have been stored in $[GMIALP]$ or almost anywhere since the program is so near completion. $[ARNTR]$ is then printed and a CALL EXIT concludes processing of the program.

Example Listing

A complete listing of the main program, required subroutines and input matrices is given in Table XXIII.

TABLE XXIII

FORTRAN PROGRAM FOR IMPLEMENTING THE
MATRIX FORCE METHOD

```

SIBFTC MAIN DECK
C FORTRAN IV MATRIX PACKAGE FOR STRUCTURAL ANALYSIS
C ARMY RESEARCH OFFICE CONTRACT PROF. R. E. CHAPEL, PROJECT LEADER
COMMON KIN, KOUT
DIMENSION ALPIJ(2650),GIR(350),GRIALP(350),ARS(100),ARSINV(100),
1STORE(100),XIDM(100),GIM(999),ARN(100),GSN(100),GMP(350),CGIM(350),
1,FORCE(200),QI(1000),AREINV(100),STRESS(1000),GMIALP(402),AMN(350),
1*
IGNN(350),CAMN(350),DELTAM(350),ARNTR(350)
KIN=5
KOUT=6
ICT=0
100 READ(5,100)IPCH
FORMAT(11)
CALL RMATNZ(ALPIJ)
CALL RMATNZ(GIR)
CALL MTXM(GIR, ALPIJ, GRIALP)
CALL WRTMAT(GRIALP)
CALL MXM(GRIALP, GIR, ARS)
CALL WRTMAT(ARS)
DO1I=1,38
1 STORE(I)=ARS(I)
CALL INVERX(ARS,ARSINV,DET,IE)
CALL WRTMAT(ARSINV)
CALL MXM(ARSINV,STORE,XIDM)
CALL WRTMAT(XIDM)
CALL RMATNZ(GIM)
CALL MXM(GRIALP, GIM, ARN)
CALL WRTMAT(ARN)
CALL MXM(ARSINV, ARN, GSN)
CALL WRTMAT(GSN)
CALL MXM(GIR, GSN, GMP)
CALL WRTMAT(GMP)
CALL MSM(GIM,GMP,CGIM)
CALL WRTMAT(CGIM)
CALL RMATNZ(FORCE)
CALL MXM(CGIM, FORCE, QI)
CALL WRTMAT(QI)
11 ICT=ICT+1
IELM=QI(1)*QI(2)+2.
DO12I=1,IELM
12 STRESS(I)=0.0
CALL RMATNZ(AREINV)
STRESS(1)=QI(1)
STRESS(2)=QI(2)
IROWS=STRESS(1)+2.
ICOLS=STRESS(2)
DO1J=1,ICOLS
DO2J=3,IROWS
K=(J-3)*FIX(QI(2))+1
L=K+2
2 STRESS(L)=AREINV(J)*QI(L)
3 CONTINUE
CALL WRTMAT(STRESS)
IF(IPCH.EQ.0)GO TO 9993
CALL PUNCH(STRESS)
9993 IF(1CT.LE.1)GO TO 11
C DEFLECTIONS
CALL MTXM(GIM,ALPIJ,GMIALP)
CALL WRTMAT(GMIALP)
CALL MXM(GMIALP,GIM,AMN)
CALL WRTMAT(AMN)

```

```

CALL MTXM(ARN,GSN,GNN)
CALL WRTMAT(GNN)
CALL MSM(AMN,GNN,CAMN)
CALL WRTMAT(CAMN)
CALL MXM(CAMN,FORCE,DELTAM)
CALL WRTMAT(DELTAM)
C REDUNDANCY
CALL MXM(GRIALP,CGIM,ARNTR)
CALL WRTMAT(ARNTR)
CALL EXIT
END
SIBFTC RMATNZ
SUBROUTINE RMATNZ (A)
C READ NONZERO ELEMENTS ONLY AND STORE AS FULL MATRIX
C LAST DATA CARD OF MATRIX MUST BE FOLLOWED BY END CARD
DIMENSION A(1)
COMMON KIN, KOUT
101 FORMAT(6X,14,6X,14,E14.7)
103 FORMAT(7H1ALPIJ,14,3X,1HX,14)
104 FORMAT(10X,3HROW,16)
105 FORMAT(25X,6E15.4)
106 FORMAT(4H1GIR,14,3X,1HX,14)
107 FORMAT(4H1GIM,14,3X,1HX,14)
108 FORMAT(6H1FORCE,14,3X,1HX,14)
109 FORMAT(7H1AREINV,14,3X,1HX,14)
IENT=IENT+1
READ(KIN,101)L,L1
A(1)=L
A(2)=L1
IJMAX=L*L1+2
DO 1 I = 3, IJMAX
1 A(I) = 0.0
2 READ(KIN,101)M,N,DATA
IF (N .LE. 0) GO TO 1000
I=(M-1)*L1+N+2
A(I) = DATA
GO TO 2
C PRINT INPUT MATRIX
1000 GO TO (4,5,6,7,9,9),IENT
4 WRITE(KOUT,103)L,L1
8 L2=3
DO3K=1,L
L3=L1+L2-1
WRITE (KOUT, 104) K
WRITE (KOUT, 105)(A(I), I =L2, L3)
L2 = L3 + 1
3 CONTINUE
RETURN
5 WRITE(KOUT,106)L,L1
GO TO 8
6 WRITE(KOUT,107)L,L1
GO TO 8
7 WRITE(KOUT,108)L,L1
GO TO 8
9 WRITE(KOUT,109)L,L1
GO TO 8
END
SIBFTC WRTMAT DECK
SUBROUTINE WRTMAT(A)
DIMENSION A(1)
COMMON KIN, KOUT
100 FORMAT(7H1GRIALP,14,3X,1HX,14)

```

TABLE XXIII (Continued)

```

101 FORMAT(4HIARS,I4,3X,1HX,I4)
102 FORMAT(4HIARN,I4,3X,1HX,I4)
103 FORMAT(4HIGSN,I4,3X,1HX,I4)
104 FORMAT(4HIGMP,I4,3X,1HX,I4)
105 FORMAT(5HICGIM,I4,3X,1HX,I4)
106 FORMAT(3HIQI ,I4,3X,1HX,I4)
107 FORMAT(20X,1P6E16.5)
108 FORMAT(10X,5H ROW ,I4)
109 FORMAT(7HIARSINV,I4,3X,1HX,I4)
110 FORMAT(4HIAMN,I4,3X,1HX,I4)
111 FORMAT(4HIGNN,I4,3X,1HX,I4)
112 FORMAT(7HIDELTAM,I4,3X,1HX,I4)
113 FORMAT(6HIARNTR,I4,3X,1HX,I4)
114 FORMAT(5HIXIDM,I4,3X,1HX,I4)
115 FORMAT(7HIGMIALP,I4,3X,1HX,I4)
116 FORMAT(5HICAMN,I4,3X,1HX,I4)
117 FORMAT(7HISTRESS,I4,3X,1HX,I4)
    IENT=IENT+1
    L = A(1)
    L1 = A(2)
    L2 = 3
    GO TO (3,4,10,15,5,6,7,8,9,18,18,16,11,12,17,13,14),IENT
1  DO2K=1,L
    L3 = L2 + L1 - 1
    WRITE(KOUT,108)K
    WRITE(KOUT,107)(A(I),I=L2,L3)
    L2 = L3 + 1
2  CONTINUE
    RETURN
3  WRITE(KOUT,100)L,L1
    GO TO 1
4  WRITE(KOUT,101)L,L1
    GO TO 1
5  WRITE(KOUT,102)L,L1
    GO TO 1
6  WRITE(KOUT,103)L,L1
    GO TO 1
7  WRITE(KOUT,104)L,L1
    GO TO 1
8  WRITE(KOUT,105)L,L1
    GO TO 1
9  WRITE(KOUT,106)L,L1
    GO TO 1
10 WRITE(KOUT,109)L,L1
    GO TO 1
11 WRITE(KOUT,110)L,L1
    GO TO 1
12 WRITE(KOUT,111)L,L1
    GO TO 1
13 WRITE(KOUT,112)L,L1
    GO TO 1
14 WRITE(KOUT,113)L,L1
    GO TO 1
15 WRITE(KOUT,114)L,L1
    GO TO 1
16 WRITE(KOUT,115)L,L1
    GO TO 1
17 WRITE(KOUT,116)L,L1
    GO TO 1
18 WRITE(KOUT,117)L,L1
    GO TO 1
    END

```

```

$IBFTC PUNCH DECK
SUBROUTINE PUNCH(A)
DIMENSION A(1)
100 FORMAT(6X,I4,6X,I4,E14.7)
INROW=1
ICOLCT=0
L=A(1)
L1=A(2)
L2=L*L1+2
DO3I=3,L2
ICOLCT=ICOLCT+1
IF(ICOLCT.EQ.L1+1)GO TO 2
IF(A(I).EQ.0.0)GO TO 3
1  WRITE(7,100)INROW,ICOLCT,A(I)
    GO TO 3
2  INROW=INROW+1
    ICOLCT=1
    GO TO 1
3  CONTINUE
    RETURN
    END
$IBFTC INVERX
SUBROUTINE INVERX(A,B,DET,IE)
DIMENSION A(1),B(1)
DET = 1.0
N = A(1)
L10 = N**2 + 2
DO 1 I = 1,L10
1  B(I) = 0.
    B(1) = N
    B(2) = N
    L9 = N + 1
    DO 2 I = 3,L10,L9
2  B(I) = 1.0
    JK = N - 1
    J = 3
    N1 = 3
    N2 = N + 2
    JO = N - 1
    J2 = N + 3
    J4 = 3
    DO 300 L1 = 1,JK
    NR = (J + N - 2)/(N + 1)
    NRI = NR
    NRI = N - NR
    JN1 = J + N
    IF (NRI .LT. 1) GO TO 900
    IF (NRI .GT. 1) GO TO 804
800 AMAX = ABS (A(J))
    AMXA = ABS (A(JN1))
    IF (AMAX .GE. AMXA) GO TO 900
801 N5 = J - NR + 1
    N6 = N5 + N - 1
    IAD = N
802 DO 803 IT = N5,N6
    IT6 = IT + IAD
    ATEM = A(IT)
    A(IT) = A(IT6)
    A(IT6) = ATEM
    ATEM = B(IT)
    B(IT) = B(IT6)
803 B(IT6) = ATEM

```

TABLE XXIII (Continued)

```

GO TO 900
804 J11 = J + N + 1
      J10 = J + N
          AMAX = ABS (A(J))
          DO 807 IT = 1, NRI
              AMXA = ABS (A(J10))
          IF (AMAX .GE. AMXA) GO TO 806
805 AMAX = AMXA
      NR1 = (J11 + N - 2)/(N + 1)
806 J10 = J10 + N
807 J11 = J11 + N + 1
      N5 = J - NR + 1
      N6 = N5 + N - 1
      ITEM = NR1 - NR
      IAD = ITEM*N
      IF (IAD .GT. 0 ) GO TO 802
900 CONTINUE
      DENOM = A(J)
      IF (DENOM .EQ. 0.0) GO TO 51
50 IF (IAD .GT. 0 ) GO TO 701
700 DET = DET*DENOM
      GO TO 702
701 DET = DET*(-DENOM)
702 DO 100 J1 = N1, N2
      A(J1) = A(J1)/DENOM
100 B(J1) = B(J1)/DENOM
      J3 = J4
      N3 = N2 + 1
      N4 = N2 + N
      DO 200 L = 1, JO
          AMULT = A(J2)
          DO 101 J1 = N3, N4
              A(J1) = A(J1) - AMULT*A(J3)
              B(J1) = B(J1) - AMULT*B(J3)
101 J3 = J3 + 1
      J2 = J2 + N
      J3 = J4
      N3 = N3 + N
200 N4 = N4 + N
      N1 = N1 + N
      N2 = N2 + N
      JO = JO - 1
      J = J + N + 1
      J2 = J + N
300 J4 = J4 + N
      DENOM = A(J)
      IF (DENOM .EQ. 0.0) GO TO 51
60 A(J) = A(J)/DENOM
      DET = DET*DENOM
      LT = J - N + 1
      DO 400 J1 = LT, J
400 B(J1) = B(J1)/DENOM
      JO = JK
      J2 = J - N
      J4 = J - N + 1
      N2 = J2 - N
      DO 600 L1 = 1, JK
          J3 = J4
          N3 = N2 + 1
          N4 = N2 + N
          DO 500 L = 1, JO
              AMULT = A(J2)
              DO 401 J1 = N3, N4
                  A(J1) = A(J1) - AMULT*A(J3)
                  B(J1) = B(J1) - AMULT*B(J3)
401 J3 = J3 + 1
          J3 = J4
          J2 = J2 - N
          N3 = N3 - N
500 N4 = N4 - N
          N2 = N2 - N
          JO = JO - 1
          J = J - N - 1
          J2 = J - N
600 J4 = J4 - N
          IE = 1
703 RETURN
51 IE = 0
      GO TO 703
      END
$IBFIC MXM
SUBROUTINE MXM (A,B,C)
DIMENSION A(1), B(1), C(1)
COMMON KIN, KOUT
100 FORMAT(1H0,I4,41HMATRICES NOT CONFORMAL FOR MULTIPLICATION,I4,1HX,
114,4HMULT,I4,1HX,I4)
MATCON = MATCON + 1
IROWA = A(1)
ICOLA = A(2)
IROWB = B(1)
ICOLB = B(2)
IF (ICOLA.EQ.IROWB)GOTO4
WRITE (KOUT, 100) MATCON, IROWA, ICOLA, IROWB, ICOLB
GO TO 6
4 N = IROWA * ICOLB + 2
DO 5 I = 1, N
5 C(I) = 0.0
IX = 3
I = 3
J = 3
K = 3
KX = 3
DO 10 M = 1, IROWA
DO 9 N = 1, ICOLB
DO 8 NX = 1, ICOLA
C(J) = C(J) + A(I) * B(K)
I = I+1
K = K + ICOLB
I = IX
J = J+1
KX = KX+1
9 K = KX
IX = IX + ICOLA
I = IX
K = 3
10 KX = 3
6 C(1) = A(1)
C(2) = B(2)
RETURN
END
$IBFIC MTXM
SUBROUTINE MTXM (A, B, C)
C READ MATRIX A BY ROWS WITH READ SUBROUTINE
C PREMULTIPLY THE MATRIX (B) BY THE TRANSPOSE OF MATRIX (A)

```

TABLE XXIII (Continued)

```

1      2 0.6741249E 01
1      25 0.2100000E 02
2      1 0.6741249E 01
2      2 0.1348250E 02
2      25 0.1800000E 02
2      34-0.7100246E 01
3      3 0.1348250E 02
3      4 0.6741249E 01
3      26 0.1800000E 02
3      34-0.7100246E 01
4      3 0.6741249E 01
4      4 0.1348250E 02
4      26 0.1500000E 02
4      40-0.5916872E 01
5      5 0.1348250E 02
5      6 0.6741249E 01
5      27 0.1500000E 02
5      40-0.5916872E 01
6      5 0.6741249E 01
6      6 0.1348250E 02
6      27 0.1200000E 02
6      46-0.2366748E 01
7      7 0.2669969E 02
7      8 0.1334985E 02
7      25 0.1400000E 02
7      28-0.1400000E 02
8      7 0.1334985E 02
8      8 0.2669969E 02
8      25 0.1200000E 02
8      28-0.1200000E 02
8      35-0.1544173E 02
8      36-0.1544173E 02
9      9 0.2669969E 02
9      10 0.1334985E 02
9      26 0.1200000E 02
9      29-0.1200000E 02
9      35-0.1544173E 02
9      36-0.1544173E 02
10     9 0.1334985E 02
10     10 0.2669969E 02
10     26 0.1000000E 02
10     29-0.1000000E 02
10     41-0.1286811E 02
10     42-0.1286811E 02
11     11 0.2669969E 02
11     12 0.1334985E 02
11     27 0.1000000E 02
11     30-0.1000000E 02
11     41-0.1286811E 02
11     42-0.1286811E 02
12     11 0.1334985E 02
12     12 0.2669969E 02
12     27 0.8000000E 01
12     30-0.8000000E 01
12     47-0.5147242E 01
12     48-0.5147242E 01
13     13 0.2669969E 02
13     14 0.1334985E 02
13     28 0.1400000E 02
13     31 0.1400000E 02
14     13 0.1334985E 02
14     14 0.2669969E 02

```

```

DIMENSION A(1), B(1), C(1)
COMMON KIN, KOUT
100 FORMAT(1H0,I4,41HMATRICES NOT CONFORMAL FOR MULTIPLICATION,I4,2HX,I4
114,5HMULT,I4,2HX,I4)
MATCON = MATCON + 1
ICOLA = A(1)
IROWA = A(2)
IROWB = B(1)
ICOLB = B(2)
IF(ICOLA.EQ.IROWB)GO TO 4
WRITE (KOUT,100) MATCON, IROWA, ICOLA, IROWB, ICOLB
GO TO 6
4 N = IROWA * ICOLB + 2
DO 5 I = 1,N
5 C(I) = 0.0
IX = 3
I = 3
J = 3
K = 3
KX = 3
DO 10 M = 1, IROWA
DO 9 N = 1, ICOLB
DO 8 NX = 1, ICOLA
C(J) = C(J) + A(I) * B(K)
I = I + IROWA
8 K = K + ICOLB
I = IX
J = J+1
KX = KX+1
9 K = KX
IX = IX + 1
I = IX
K = 3
10 KX = 3
6 C(1) = A(2)
C(2) = B(2)
RETURN
END
$1BFTC MSM
SUBROUTINE MSM (A,B,C)
DIMENSION A(1), B(1), C(1)
COMMON KIN, KOUT
100 FORMAT(1HL,38HMATRICES NOT CONFORMAL FOR SUBTRACTION,2X,6HIROWA=,I
12,6H4IROWB=,I2)
101 FORMAT(1HL,38HMATRICES NOT CONFORMAL FOR SUBTRACTION,2X,6HJCOLA=,I2,
12,6HJCOLB=,I2)
IF(A(1)-NE.B(1))GOTO40
IF(A(2)-NE.B(2))GOTO41
L=IFIX(A(1))*IFIX(A(2))+2
DO10I=3,L
10 C(I)=A(I)-B(I)
C(1)=B(1)
C(2)=B(2)
20 RETURN
40 WRITE(KOUT,100)A(1),B(1)
GO TO 20
41 WRITE(KOUT,101)A(2),B(2)
GO TO 20
END
0
51      51
1      1 0.1348250E 02

```

APPENDIX D

A DIGITAL COMPUTER PROGRAM FOR CALCULATING

[GIM] AND [GIR]

This digital computer program solves the twenty-one simultaneous equations described in Chapter II. Then, it reindexes the solution values such that for [GIM] the selected redundant internal forces are zero and the remainder of the [GIM] matrix is made up of the solution values. For [GIR], the selected redundant internal forces are set equal to unity with the solution values making up the remaining positions.

The input to this program consists of the [COEF] and [CONST] matrices, both of which are described in Chapter II, placed side-by-side and listed as one large matrix. The solution matrix is found by the Gaussian elimination process and listed. The solution matrix is then broken apart and a zero matrix inserted at the appropriate locations for the formation of [GIM]. This process is repeated except that an identity matrix is inserted at the appropriate locations to form [GIR].

The subroutines included in this program are as listed:

1. The READ 3 Subroutine, which reads in all input data.
2. The SOLVE Subroutine, which determines the solution values.
3. The MOVE Subroutine, which breaks apart the solution

matrix for the insertion of the identity and zero matrices.

4. The IDENT Subroutine, which places the identity and zero matrices in the appropriate locations in the solution matrix.
5. The PRINT 1 Subroutine, which prints the final results.

A complete Fortran listing of the main program and the required subroutines are given in Table XXIV.

TABLE XXIV (Continued)

	ICOLCT=ICOLCT+1	MP070170	END	MP070710
	IF(ICOLCT.EQ.IDCOL+1)GO TO 50	MP070180	\$IBFTC PRINT1 NODECK	
1	GO TO (2,3+6,3,11),KDEL	MP070190	SUBROUTINE PRINT1(A,IUNT,IROW,ICOL,IDEL,IDROW,IDCOL,ICTLR,ICTLC	MP040010
2	JK=I	MP070200	1,IDI)	MP040020
	GO TO 20	MP070210	DIMENSION A(1),ICTLR(1),ICTLC(1),ID(12),T(10)	MP040030
50	INROW=INROW+1	MP070220	C A SUBROUTINE OF THE MATRIX PACKAGE DECK WRITTEN BY BILL ACCOLA	MP040040
	ICOLCT=1	MP070230	C THIS SUBROUTINE IS DESIGNED TO PRINT A WITH TEN COLUMNS PER PAGE.	MP040050
	GO TO 1	MP070240	2001 FORMAT(1H1,12A6,10X,4HPAGE,13)	MP040060
3	IF(ICOLCT.NE.1)GO TO 5	MP070250	2002 FORMAT(1X,10I12)	MP040070
	DO4J=1,IROWA	MP070260	2003 FORMAT(1X,14,10E12.5)	MP040080
	IF(J.EQ.ICTLR(INROW))GO TO 5	MP070270	2004 FORMAT(1HK,6HERROR ,13,10H IN ENTRY ,12,10H OF PRINT1)	MP040090
4	CONTINUE	MP070280	IPG = 1	MP040100
	GO TO 9999	MP070290	JSTR = 1	MP040110
5	JK=(J-1)*ICOLA+ICOLCT	MP070300	IERR=903	MP040120
	IF(KDEL.EQ.4)GO TO 9	MP070310	IENT=IENT+1	MP040130
	GO TO 20	MP070320	JSTP2=IDCOL	MP040140
6	DO7JJ=1,ICOLA	MP070330	Istp=IROW	MP040150
	IF(JJ.EQ.ICTLC(ICOLCT))GO TO 8	MP070340	IF(IDEL-IDROW-IDCOL.EQ.IDEL)GO TO 25	MP040160
7	CONTINUE	MP070350	10 KDEL=IDEL+1	MP040170
	GO TO 9999	MP070360	GO TO (17,23+11,24,24),KDEL	MP040180
8	IF(KDEL.EQ.4)GO TO 10	MP070370	17 JSTP2=ICOL	MP040190
	JK=(INROW-1)*ICOLA+JJ	MP070380	1 JSTP1=ICOL	MP040200
	GO TO 20	MP070390	GOTO3	MP040210
9	JK1=JK	MP070400	11 IF(IDCOL.EQ.0)GO TO 99	MP040220
	GO TO 6	MP070410	2 JSTP1=IDCOL	MP040230
10	JK=JK+JJ-ICOLCT	MP070420	3 JSTP = JSTR+9	MP040240
	GO TO 20	MP070430	IF(JSTP.GT.JSTP1)JSTP=JSTP1	MP040250
11	DO12J=1,IROWA	MP070440	WRITE(IUNT,2001) ID,IPG	MP040260
	IF(ISWTCH.EQ.2)GO TO 17	MP070450	WRITE(IUNT,2002) (J,J=JSTR,JSTP)	MP040270
	IF(J.EQ.ICTLR(INROW))GO TO 13	MP070460	DO3GI=1,ISTP	MP040280
17	IF(ISWTCH.EQ.3)GO TO 15	MP070470	DO 5 K=1,10	MP040290
	IF(J.EQ.ICTLR(ICOLCT))GO TO 14	MP070480	5 T(K) = 0.0	MP040300
	GO TO 12	MP070490	GO TO (12,7,12,7,7),KDEL	MP040310
13	JK1=J	MP070500	12 IK=I	MP040320
	ISWTCH=ISWTCH+2	MP070510	GO TO 8	MP040330
	GO TO 17	MP070520	7 IK=ICTLR(I)	MP040340
14	ISWTCH=ISWTCH+3	MP070530	IF(IK.GT.IROW)GO TO 97	MP040350
	JK2=J	MP070540	IF(IK.LE.0) GO TO 21	MP040360
15	IF(ISWTCH.EQ.5)GO TO 16	MP070550	8 IK=(IK-1)*ICOL	MP040370
12	CONTINUE	MP070560	DO 20 J=JSTR,JSTP	MP040380
	ISWTCH=0	MP070570	GO TO (13,13,14,14,16),KDEL	MP040390
	GO TO 9999	MP070580	13 JK=J	MP040400
16	JK=(JK1-1)*ICOLA+JK2	MP070590	GO TO 18	MP040410
	ISWTCH=0	MP070600	14 JK=ICTLC(J)	MP040420
20	BIT=A(JK)	MP070610	IF(IJK.GT.ICOL)GO TO 96	MP040430
9999	CONTINUE	MP070620	GO TO 19	MP040440
	RETURN	MP070630	16 JK=ICTLR(J)	MP040450
30	IF(IDEL.EQ.0)GO TO 1	MP070640	IF(IJK.GT.ICOL)GO TO 96	MP040460
	IERR=IERR+1	MP070650	19 IF(IJK.LE.0)GOTO20	MP040470
97	IERR=IERR+1	MP070660	18 IK1=IK+JK	MP040480
98	IERR=IERR+1	MP070670	15 JK=J-JSTR+1	MP040490
99	IERR=IERR+1	MP070680	T(JK)=A(IK1)	MP040500
	WRITE(6,2001)IERR,IENT	MP070690	20 CONTINUE	MP040510
	RETURN	MP070700	21 IF(JSTP.GT.10)GO TO 22	MP040520

TABLE XXIV (Continued)

WRITE(IUNT,2003)I,(I(J),J=1,JSTP)	MP040530	12	6 1.0000000E+00	21SIMEQNSTAPFARDC1
30 CONTINUE	MP040540	12	15-1.0111873E+01	21SIMEQNSTAPFARDC1
IF(JSTP.EQ.JSTP2)RETURN	MP040550	13	7 7.0000000E+00	21SIMEQNSTAPFARDC1
IF(JSTP.EQ.IDCOL) RETURN	MP040560	13	8-5.0000000E+00	21SIMEQNSTAPFARDC1
IPG = IPG+1	MP040570	13	16 1.0000000E+00	21SIMEQNSTAPFARDC1
JSTR = JSTP+1	MP040580	14	8 6.0000000E+00	21SIMEQNSTAPFARDC1
GO TO 3	MP040590	14	9-4.0000000E+00	21SIMEQNSTAPFARDC1
22 JSTP3=JSTP-(IPG-1)*10	MP040600	14	18 1.0000000E+00	21SIMEQNSTAPFARDC1
WRITE(IUNT,2003)I,(I(J),J=1,JSTP3)	MP040610	15	9 5.0000000E+00	21SIMEQNSTAPFARDC1
GO TO 30	MP040620	15	20 1.0000000E+00	21SIMEQNSTAPFARDC1
23 ISTP=IDROW	MP040630	16	10 7.0000000E+00	21SIMEQNSTAPFARDC1
IF(IDROW.EQ.0)GO TO 98	MP040640	16	11-5.0000000E+00	21SIMEQNSTAPFARDC1
JSTP2=ICOL	MP040650	16	16-1.0000000E+00	21SIMEQNSTAPFARDC1
GOTO1	MP040660	16	17 1.0000000E+00	21SIMEQNSTAPFARDC1
24 ISTP=IDROW	MP040670	17	11 6.0000000E+00	21SIMEQNSTAPFARDC1
GOTO2	MP040680	17	12-4.0000000E+00	21SIMEQNSTAPFARDC1
25 IF(IDEL.NE.0)GO TO 100	MP040690	17	18-1.0000000E+00	21SIMEQNSTAPFARDC1
GO TO 10	MP040700	17	19 1.0000000E+00	21SIMEQNSTAPFARDC1
96 IERR=IERR+1	MP040710	18	12 5.0000000E+00	21SIMEQNSTAPFARDC1
97 IERR=IERR+1	MP040720	18	20-1.0000000E+00	21SIMEQNSTAPFARDC1
98 IERR=IERR+1	MP040730	18	21 1.0000000E+00	21SIMEQNSTAPFARDC1
99 IERR=IERR+1	MP040740	19	13 7.0000000E+00	21SIMEQNSTAPFARDC1
100 IERR=IERR+1	MP040750	19	14-5.0000000E+00	21SIMEQNSTAPFARDC1
WRITE(6,2004)IERR,IENT	MP040760	19	17-1.0000000E+00	21SIMEQNSTAPFARDC1
RETURN	MP040770	20	14 6.0000000E+00	21SIMEQNSTAPFARDC1
END	MP040780	20	15-4.0000000E+00	21SIMEQNSTAPFARDC1
SENTRY		20	19-1.0000000E+00	21SIMEQNSTAPFARDC1
INPUT MATRIX		21	15-5.0000000E+00	21SIMEQNSTAPFARDC1
1 1 1.0000000E+00	21SIMEQNSTAPFARDC1	21	21 1.0000000E+00	21SIMEQNSTAPFARDC1
1 2-1.0000000E+00	21SIMEQNSTAPFARDC1	3	22 1.0111873E+00	21SIMEQNS,CORR-C,NST,RDC1
1 7 1.0111873E+01	21SIMEQNSTAPFARDC1	4	30 1.0012385E+00	21SIMEQNS,CORR-C,NST,RDC1
2 2 1.0000000E+00	21SIMEQNSTAPFARDC1	4	31-1.0000000E+00	21SIMEQNS,CORR-C,NST,RDC1
2 3-1.0000000E+00	21SIMEQNSTAPFARDC1	4	32 1.0000000E+00	21SIMEQNS,CORR-C,NST,RDC1
2 8 1.0111873E+01	21SIMEQNSTAPFARDC1	5	32-1.0000000E+00	21SIMEQNS,CORR-C,NST,RDC1
3 3 1.0000000E+00	21SIMEQNSTAPFARDC1	5	33 1.0000000E+00	21SIMEQNS,CORR-C,NST,RDC1
3 9 1.0111873E+01	21SIMEQNSTAPFARDC1	6	23 1.0012385E+00	21SIMEQNS,CORR-C,NST,RDC1
4 7-1.0012385E+01	21SIMEQNSTAPFARDC1	6	33-1.0000000E+00	21SIMEQNS,CORR-C,NST,RDC1
4 10 1.0012385E+01	21SIMEQNSTAPFARDC1	7	34-1.0000000E+00	21SIMEQNS,CORR-C,NST,RDC1
5 8-1.0012385E+01	21SIMEQNSTAPFARDC1	7	35 1.0000000E+00	21SIMEQNS,CORR-C,NST,RDC1
5 11 1.0012385E+01	21SIMEQNSTAPFARDC1	8	35-1.0000000E+00	21SIMEQNS,CORR-C,NST,RDC1
6 9-1.0012385E+01	21SIMEQNSTAPFARDC1	8	36 1.0000000E+00	21SIMEQNS,CORR-C,NST,RDC1
6 12 1.0012385E+01	21SIMEQNSTAPFARDC1	9	24 1.0012385E+00	21SIMEQNS,CORR-C,NST,RDC1
7 4 1.0000000E+00	21SIMEQNSTAPFARDC1	9	36-1.0000000E+00	21SIMEQNS,CORR-C,NST,RDC1
7 10-1.0012385E+01	21SIMEQNSTAPFARDC1	12	25 1.0111873E+00	21SIMEQNS,CORR-C,NST,RDC1
7 13 1.0012385E+01	21SIMEQNSTAPFARDC1	13	30 2.5000000E-02	21SIMEQNS,CORR-C,NST,RDC1
8 11-1.0012385E+01	21SIMEQNSTAPFARDC1	15	22 1.5000000E-01	21SIMEQNS,CORR-C,NST,RDC1
8 14 1.0012385E+01	21SIMEQNSTAPFARDC1	15	23 2.5000000E-02	21SIMEQNS,CORR-C,NST,RDC1
9 12-1.0012385E+01	21SIMEQNSTAPFARDC1	15	28 5.0000000E-01	21SIMEQNS,CORR-C,NST,RDC1
9 15 1.0012385E+01	21SIMEQNSTAPFARDC1	15	29 1.0000000E+00	21SIMEQNS,CORR-C,NST,RDC1
10 4 1.0000000E+00	21SIMEQNSTAPFARDC1	16	30 2.5000000E-02	21SIMEQNS,CORR-C,NST,RDC1
10 5-1.0000000E+00	21SIMEQNSTAPFARDC1	18	23 2.5000000E-02	21SIMEQNS,CORR-C,NST,RDC1
10 13-1.0111873E+01	21SIMEQNSTAPFARDC1	18	24-2.5000000E-02	21SIMEQNS,CORR-C,NST,RDC1
11 5 1.0000000E+00	21SIMEQNSTAPFARDC1	18	27-5.0000000E-01	21SIMEQNS,CORR-C,NST,RDC1
11 6-1.0000000E+00	21SIMEQNSTAPFARDC1	18	28 5.0000000E-01	21SIMEQNS,CORR-C,NST,RDC1
11 14-1.0111873E+01	21SIMEQNSTAPFARDC1	18		

TABLE XXIV (Continued)

21	24	2.5000000E-02
21	25	1.5000000E-01
21	26	1.0000000E+00
21	27	5.0000000E-01

21SIMEQNS,CORR-CNST,RDC1
21SIMEQNS,CORR-CNST,RDC1
21SIMEQNS,CORR-CNST,RDC1
21SIMEQNS,CORR-CNST,RDC1

9
SOLUTION MATRIX
GIM FROM SOLUTIONS
GIR FROM SOLUTIONS
SIBSYS

APPENDIX E

TREATMENT OF EXPERIMENTAL DATA

The experimental strain data were processed by the IBM 7040 Digital Computer. The basic data obtained from the strain gages are reduced to values per unit load for each of the load conditions.

The strain values are obtained by finding the most reliable linear relationship using the least-squares criterion. The method of least squares provides that the most probable function for a quantity obtained from a set of measurements is the function which minimizes the sum of the squares of the deviations or errors of these measurements. In a statistical sense, the equation of a line giving the "best" fit to a set of paired values of two variables x and y is desired. Predictions of a value of y can then be based upon an assumed or observed value of x . The word "best" is synonymous with the method of least squares (14).

It is assumed that (y_i, x_i) which are the data (y_i being a strain value and x_i being a corresponding value of load cell load), such that $i = 1, 2, \dots, n$, satisfy the simple linear model,

$$y_i = \alpha + \beta x_i + e_i,$$

where α and β are unknown parameters and e_i is the error present for each observation. Least squares estimators are found for α and β by minimizing the sum of squares of the errors, $\sum_{i=1}^n e_i^2$.

The linear model can be solved for e_i to give

$$\sum_{i=1}^n e_i^2 = \sum_{i=1}^n (Y_i - \alpha - \beta X_i)^2 = \sum_{i=1}^n (\alpha + \beta X_i - Y_i)^2.$$

A function of two variables is minimized by taking the partial derivative of the function with respect to each of the variables in turn and setting each derivative equal to zero.

Thus, the first partial derivative is

$$\frac{\partial}{\partial \alpha} \sum e_i^2 = \sum 2(\alpha + \beta X_i - Y_i) = 0,$$

or expressed differently, it is

$$n\alpha + \beta \sum X_i = \sum Y_i.$$

The second partial derivative is

$$\frac{\partial}{\partial \beta} \sum e_i^2 = \sum 2X_i(\alpha + \beta X_i - Y_i) = 0,$$

or expressed differently

$$\alpha \sum X_i + \beta \sum X_i^2 = \sum X_i Y_i.$$

The equations

$$\alpha n + \beta \sum X_i = \sum Y_i,$$

$$\alpha \sum X_i + \beta \sum X_i^2 = \sum X_i Y_i,$$

are simultaneous for α and β .

The two equations above can be solved for α and β to give

$$\hat{\alpha} = \frac{(\sum Y_i)(\sum X_i^2) - (\sum Y_i X_i)(\sum X_i)}{n(\sum X_i^2) - (\sum X_i)^2} = \bar{Y} - \hat{\beta} \bar{X},$$

$$\hat{\beta} = \frac{n(\sum Y_i X_i) - (\sum Y_i)(\sum X_i)}{n(\sum X_i^2) - (\sum X_i)^2},$$

where:

$\hat{\alpha}$ is defined as the least squares estimator of α .

$\hat{\beta}$ is defined as the least squares estimator of β .

$$\sum \equiv \sum_{i=1}^n$$

\bar{y} = mean of y_i 's.

\bar{x} = mean of x_i 's.

$\hat{\alpha}$, now, is the intercept and $\hat{\beta}$ is the slope of the "best" straight line positioned among the data points. $\hat{\beta}$, then, is the unit strain per unit load cell load and is the ultimate objective of the above calculations. $\hat{\alpha}$, the intercept, is merely a function of the value at which the strain indicators are initially balanced or zeroed. See Figure 52.

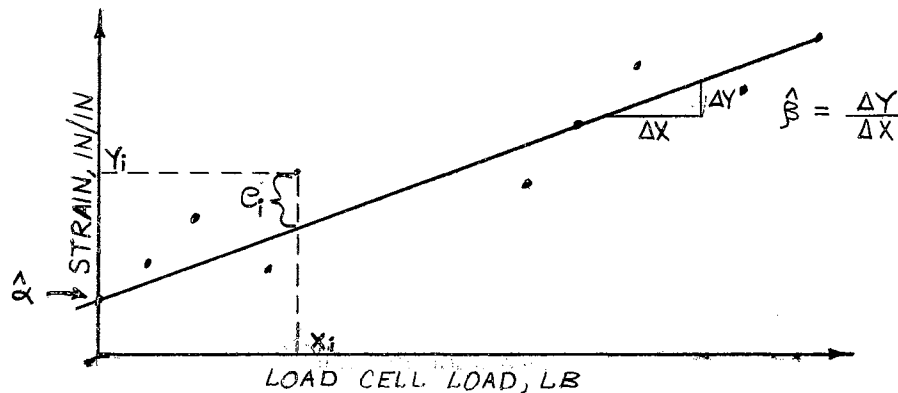


Figure 52. Typical Experimental Data

Correlation of Experimental Data

In the previous section, constants in a linear equation relating two variables, x and y , were determined by using pairs of observations

(x_i, y_i) of these variables. The determination of these constants was based entirely upon the assumption that a linear relationship exists between x and y . This assumption is quite reasonable as the experimental model is loaded only within its elastic range which implies Hookean stress-strain behavior.

The situation may arise such that it is not known in advance whether the two variables x and y are related. Furthermore, if pairs of observations (x_i, y_i) are taken as before, the data may be scattered so widely because of experimental errors that it is not clear whether or not there is any relation between x and y . By representing the observations (x_i, y_i) graphically, a picture (Figure 53) similar to Figure 52 might be obtained. Are x and y related, or are they not? Is there any "correlation" between x and y ?

There are an infinite variety of possible functional relationships between x and y . There is no general way of investigating all possible relationships but the simpler ones can be checked. The simplest one, of course, is a linear equation. Therefore, a reasonable place to begin is to ask whether there is a linear relationship between x and y , i.e., a "linear correlation."

This question can at least be answered partially by taking a special case of the method of least squares for two unknowns. A linear relationship between x and y can be assumed

$$Y = mx + b,$$

and the constants m and b can be determined from observations (x_i, y_i) in the same manner as in the previous section. In particular,

$$m = \frac{n(\sum xy) - (\sum x)(\sum y)}{n(\sum x^2) - (\sum x)^2}.$$

The scattered points are represented by drawing the "best straight line" through them. Then, the expression for e_i is

$$e_i = mx_i + b - y_i.$$

e_i represents the vertical distance between the point (x_i, y_i) and the straight line described by the constants m and b . In this case, the method of least squares minimizes the sum of the squares of the vertical distances between the point and the straight line. The line determined by this procedure is sometimes called the "line of regression of y on x ."

If there is no correlation at all between x and y , the sum of squares will be minimized by a horizontal line, or $m = 0$.

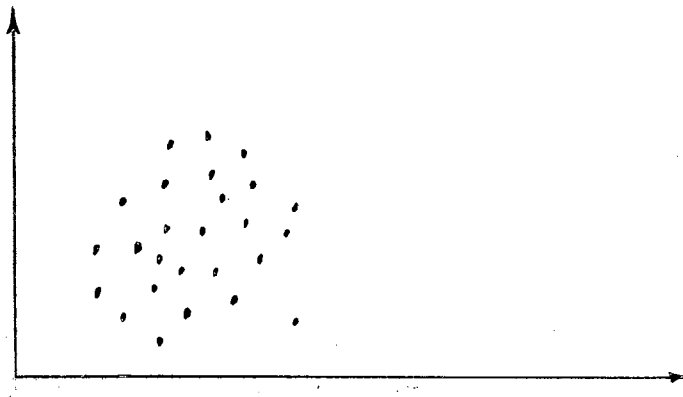


Figure 53. Scattering of Data Points

There is no particular reason for writing the assumed relationship between x and y in the form

$$Y = mx + b.$$

It could just as well have been written

$$X = m'Y + b',$$

in which case the roles of x and y have been reversed. In this case, the error used in the method of least squares is given by

$$e_i = m'Y_i + b' - X_i.$$

The method of least squares now minimizes the sum of the squares of the horizontal distance between the line

$$X = m'Y + b',$$

and the points (x_i, y_i) representing the observations. The result is the line of regression of x on y . The expression for m' would be

$$m' = \frac{n(\sum XY) - (\sum X)(\sum Y)}{n(\sum Y^2) - (\sum Y)^2}.$$

Then m' is the reciprocal of m .

If there is no correlation between x and y , the method of least squares will give the value $m' = 0$, a vertical line. If, on the other hand, all points lie exactly on the line, i.e., the correlation is perfect, then the same line as the previous one must result. Therefore, in the case of perfect correlation, $\frac{1}{m} = m$ or $mm' = 1$. If there is no correlation between x and y , $mm' = 0$. The product mm' , then, has something to do with the extent to which the variables x and y are correlated.

It follows, then, that a "correlation coefficient," R , can be defined as:

$$R = \sqrt{mm'} = \frac{n(\sum XY) - (\sum X)(\sum Y)}{[n(\sum X^2) - (\sum X)^2]^{1/2} \cdot [n(\sum Y^2) - (\sum Y)^2]^{1/2}}.$$

Rewritten, R sometimes appears as

$$R = \hat{\beta} \frac{\sqrt{\sum_{i=1}^n (x_i - \bar{x})^2}}{\sqrt{\sum_{i=1}^n (y_i - \bar{y})^2}} .$$

Thus, $R = 1$ means perfect correlation, and $R = 0$ means no correlation.

Consequently, for imperfect correlation, $0 \geq |R| \geq -1$.

Suppose, now, that R has been calculated for a set of observations. How is this result interpreted? The interpretation of the correlation coefficient R is based on experience. The question is how large a value of R indicates a significant correlation between the variables x and y. Because of random fluctuations in the experimental data, R would not be exactly equal to zero, even if the data were completely erroneous. Similarly, due to experimental fluctuations, R would not be exactly equal to one. However, since the nature of the problem dictates that a linear relationship exists and the experimental errors are hopefully minimized, then one should expect to get values in the neighborhood of $R = 1$. The criterion used to determine whether the linear correlation is substantial is to consider the probability of obtaining a value of R as large as possible purely by chance from the observations of two variables which are not related. Table XXV has been calculated to give the probability of obtaining a given value of R for various numbers of pairs of observations (16).

From Table XXV for ten observations, N equals ten. The probability P is 0.10 of finding a correlation coefficient of 0.549 or larger and a probability of 0.01 of finding R greater than or equal to 0.765 if the

TABLE XXV
CORRELATION COEFFICIENTS*

N	Probability				
	0.10	0.05	0.02	0.01	0.001
3	0.988	0.997	0.999	1.000	1.000
4	0.900	0.950	0.980	0.990	0.999
5	0.805	0.878	0.934	0.959	0.992
6	0.729	0.811	0.882	0.917	0.974
7	0.669	0.754	0.833	0.874	0.951
8	0.621	0.707	0.789	0.834	0.925
10	0.549	0.632	0.716	0.765	0.872
12	0.497	0.576	0.658	0.708	0.823
15	0.441	0.514	0.592	0.641	0.760
20	0.378	0.444	0.516	0.561	0.679

*This table is adapted from Table V of H. Young, Statistical Treatment of Experimental Data published by McGraw-Hill Book Company, Inc., New York.

variables are not related. If, for ten observations, the correlation coefficient $R = 0.9$, there is reasonable assurance that this indicates a true correlation and not an accident. Conversely, if $R = 0.5$, this would mean that the data were questionable since there is more than a ten per cent chance that this value would occur for random data. A commonly used rule of thumb for interpreting values of the correlation coefficient is to regard the correlation as significant if there is less than one chance in twenty, $P = 0.05$, that the value will occur by chance (16). For any value of the correlation coefficient greater than the value given in the Table II for $P = 0.05$, the experimental data should be regarded as showing a significant correlation.

R , then, is a measure of how well the straight line based on $\hat{\alpha}$ and $\hat{\beta}$ "fits" the data. But it is only a measure of the "best fit" of a linear relationship to the experimental data and is in no way an indication that the experimental data accurately represent the physical phenomena. It is merely an indication that a linear correlation exists between the variables x and y .

Stress-Strain Relations

For the single legged axial strain gage, the stress-strain relation is:

$$\sigma_{axial} = E \cdot \epsilon_{axial},$$

where:

E = Modulus of elasticity.

The development of stresses from strain values for the delta or "y" pattern rosette strain gage is as follows.

From reference (17), the general equation for finding ϵ_x , ϵ_y and γ_{xy} from ϵ_1 , ϵ_2 , and ϵ_3 is

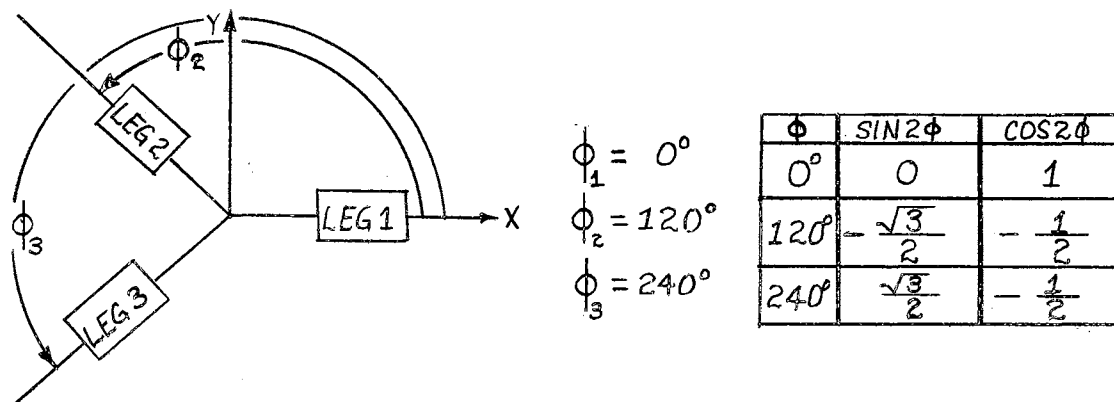


Figure 54. Leg Locations and Reading Sequence

$$\epsilon_\phi = \frac{\epsilon_x + \epsilon_y}{2} + \frac{\epsilon_x - \epsilon_y}{2} \cos 2\phi + \frac{\gamma_{xy}}{2} \sin 2\phi,$$

(cf. Figure 54).

By substituting in ϵ_1 , ϵ_2 , ϵ_3 , ϕ_1 , ϕ_2 , and ϕ_3 , ϵ_ϕ becomes

$$\epsilon_1 = \frac{\epsilon_x + \epsilon_y}{2} + \frac{\epsilon_x - \epsilon_y}{2} \cos 2\phi_1 + \frac{\gamma_{xy}}{2} \sin 2\phi_1,$$

$$\epsilon_2 = \frac{\epsilon_x + \epsilon_y}{2} + \frac{\epsilon_x - \epsilon_y}{2} \cos 2\phi_2 + \frac{\gamma_{xy}}{2} \sin 2\phi_2,$$

$$\epsilon_3 = \frac{\epsilon_x + \epsilon_y}{2} + \frac{\epsilon_x - \epsilon_y}{2} \cos 2\phi_3 + \frac{\gamma_{xy}}{2} \sin 2\phi_3.$$

By substituting in values of $\cos 2\phi$ and $\sin 2\phi$, ϵ_1 , ϵ_2 , and ϵ_3 become

$$\epsilon_1 = \epsilon_x,$$

$$\epsilon_2 = \frac{\epsilon_x}{4} + \frac{3\epsilon_y}{4} - \frac{\sqrt{3}}{4} \gamma_{xy},$$

$$\epsilon_3 = \frac{\epsilon_x}{4} + \frac{3\epsilon_y}{4} + \frac{\sqrt{3}}{4} \gamma_{xy}.$$

If ϵ_x , ϵ_y , and γ_{xy} are solved for in terms of ϵ_1 , ϵ_2 , and ϵ_3 , ϵ_x , ϵ_y , and σ_{xy} become

$$\epsilon_x = \epsilon_1,$$

$$\epsilon_y = \frac{-\epsilon_1 + 2\epsilon_2 + 2\epsilon_3}{3},$$

$$\gamma_{xy} = \frac{-2\epsilon_2 + 2\epsilon_3}{\sqrt{3}}.$$

For plane stress distribution for isotropic material obeying Hooke's law, the expression for σ_x , σ_y , and τ_{xy} are

$$\sigma_x = \frac{E}{1-\nu^2} (\epsilon_x + \nu\epsilon_y),$$

$$\sigma_y = \frac{E}{1-\nu^2} (\nu\epsilon_x + \epsilon_y),$$

$$\tau_{xy} = \frac{E}{2(1+\nu)} \gamma_{xy},$$

where ν = Poisson's Ratio.

If ϵ_x , ϵ_y , and γ_{xy} are substituted in terms of ϵ_1 , ϵ_2 , and ϵ_3 , σ_x , σ_y , and τ_{xy} become

$$\sigma_x = \frac{E}{3(1-\nu^2)} [(3-\nu)\epsilon_1 + 2\nu(\epsilon_2 + \epsilon_3)],$$

$$\sigma_y = \frac{E}{3(1-\nu^2)} [(3\nu-1)\epsilon_1 + 2(\epsilon_2 + \epsilon_3)],$$

$$\tau_{xy} = \frac{E}{(1+\nu)} \left[\frac{-\epsilon_2 + \epsilon_3}{\sqrt{3}} \right].$$

The principle stresses are given by:

$$\sigma_{\text{MAX}} = \frac{\sigma_x + \sigma_y}{2} + \frac{1}{2} \sqrt{(\sigma_x - \sigma_y)^2 + 4\tau_{xy}^2},$$

$$\tau_{\text{MAX}} = \frac{1}{2} \sqrt{(\sigma_x - \sigma_y)^2 + 4\tau_{xy}^2},$$

$$\phi = \frac{1}{2} \text{TAN}^{-1} \left[\frac{(\sigma_x - \sigma_y)}{2\tau_{xy}} \right].$$

Data Reduction Computer Program

A digital computer program has been developed to calculate the required stress results for each axial gage and "y" pattern rosette. The strain data are copied onto the special data sheet shown in Table XXVI and then keypunched on IBM cards. All axial gage data are processed first followed by the rosette gage data. Each three sets of rosette gage data is used for the required calculations above. The program prints the test data in tabular form for each indicator. The correlation coefficient and stress data are summarized at the end of the analysis to provide a more rapid analysis of the experimental results. The validity of the data is indicated by the correlation coefficient. A Fortran listing of the digital computer program is shown in Table XXVII.

TABLE XXVII

AXIAL AND ROSETTE STRAIN GATE DATA
REDUCTION PROGRAM

```

SID          B-0001 ACCOLA
SIBJOB NAMEPR
SIBFTC DKNAME NODECK
          INTEGER GAGE1,GAGE2,GAGE3,GAGE4,CARD1,CARD2,TYPE1,TYPE2,TYPE3,TYPE4
          14
          DIMENSION X(10)
          DIMENSION AVE(10),ID(4)
100        FORMAT(11,13,11,5E12.1,4A5)
101        FORMAT(1HK,14HERROR IN CARD1,8HGAGE NO.,14)
102        FORMAT(1HK,14HERROR IN CARD2,8HGAGE NO.,14)
104        FORMAT(62HKSECOND GAGE OF THIS SET DOES NOT AGREE IN TYPE TO FIRST
          IGAGE.,14)
105        FORMAT(1H1)
106        FORMAT(1HK,7X,8HGAGE NO.,13,6H AXIAL,1X,4A5)
107        FORMAT(1HK,7X,8HGAGE NO.,13,8H ROSETTE,1X,4A5)
109        FORMAT(1H ,3(5X,E15.8))
110        FORMAT(9HKSLOPE IS,E12.5,5X,14HY-INTERCEPT IS,E10.3)
111        FORMAT(15H SIGMA(AXIAL) =,E12.5,6HPSI/LB)
112        FORMAT(11H SIGMA(X) =,E12.5,6HPSI/LB)
113        FORMAT(11H SIGMA(Y) =,E12.5,6HPSI/LB)
114        FORMAT(2X,9HTAU(XY) =,E12.5,6HPSI/LB)
115        FORMAT(13H SIGMA(MAX) =,E12.5,6HPSI/LB)
116        FORMAT(13H SIGMA(MIN) =,E12.5,6HPSI/LB)
117        FORMAT(11H TAU(MAX) =,E12.5,6HPSI/LB)
118        FORMAT(14H PHI(SIGMAX) =,E12.5,7HDEGREES)
119        FORMAT(14H PHI(TAUMAX) =,E12.5,7HDEGREES)
120        FORMAT(16H SIGMA(TAUMAX) =,E12.5,6HPSI/LB)
121        FORMAT(26H CORRELATION COEFFICIENT =,F9.6)
122        FORMAT(3F10.5)
123        FORMAT(6H GFR =,F7.4)
          READ(5,122)BEGIN,XINCR,GFR
          BEGIN=BEGIN/1000.
          XINCR=XINCR/1000.
          X(1)=BEGIN
          SUMX=X(1)
          SUMXSQ=BEGIN*BEGIN
          DO11=2,10
          X(1)=X(1-1)+XINCR
          SUMX+SUMX+X(1)
11        SUMXSQ=SUMXSQ+X(1)*X(1)
          SUMSQX=SUMX*SUMX
          DENOM=10.*SUMXSQ-SUMSQX
          XBAR=SUMX/10.
          NUMROS=0
          ICT=0
          E=10.6E+06
          TERM=E/2.683125
1          CONTINUE
          XMXBSQ=0.0
          ICT=ICT+1
          READ(5,100)TYPE1,GAGE1,CARD1,(AVE(I),I=1,5),ID
          IF(CARD1.NE.1)GO TO 99
          READ(5,100)TYPE2,GAGE2,CARD2,(AVE(I),I=6,10)
          IF(CARD2.NE.2)GO TO 98
          IF(GAGE2.NE.GAGE1).OR.(TYPE1.NE.TYPE2)GO TO 98
          IF((TYPE1.EQ.3).AND.(NUMROS.EQ.0))ICT=4
          IF(ICT.GE.4)WRITE(6,105)
          IF(ICT.GE.4)ICT=1
          SUMXY=0.0
          SUMY=0.
          SUMYSQ=0.0
          YMYBSQ=0.0
          DO31=1,10
          AVE(1)=AVE(1)/1000.
          SUMXY=X(1)+AVE(1)+SUMXY
          SUMY=SUMY+AVE(1)
          SUMYSQ=SUMYSQ+AVE(1)*AVE(1)
          SQSUMY=SUMY*SUMY
          BETA=(10.*SUMXY-SUMX*SUMY)/DENOM
          BETA=BETA*GFR
          ALPHA=(SUMY/10.)-BETA*XBAR
          DO41=1,10
          XMXBSQ=XMXBSQ+((X(1)-XBAR)**2)
          YMYBSQ=YMYBSQ+((AVE(1)-SUMY/10.)**2)
          CCEFF=BETA*SQRT(XMXBSQ/YMYBSQ)
          IF(TYPE1.EQ.3)GO TO 50
          WRITE(6,106)GAGE1,ID
          DO51=1,10
          WRITE(6,109)                                AVE(I)
          WRITE(6,110)BETA,ALPHA
          WRITE(6,123)GFR
          WRITE(6,121)CCEFF
          SIGAXL=BETA*E
          WRITE(6,111)SIGAXL
          GO TO 1
50        NUMROS=NUMROS+1
          WRITE(6,107)GAGE1,ID
          DO61=1,10
          WRITE(6,109)                                AVE(I)
          WRITE(6,110)BETA,ALPHA
          WRITE(6,123)GFR
          WRITE(6,121)CCEFF
          IF(NUMROS.EQ.1)BETA1=BETA
          IF(NUMROS.EQ.2)BETA2=BETA
          IF(NUMROS.EQ.3)BETA3=BETA
          IF(NUMROS.NE.3)GO TO 1
          IF(NUMROS.EQ.3)NUMROS=0
          SIGX=TERM*(2.675*BETA1)+0.650*(BETA2+BETA3)
          SIGY=TERM*(-.025*BETA1+2.*(BETA2+BETA3))
          TAUXY=(E/1.325)*(-BETA2+BETA3)/1.732
          STMAX=(SIGX+SIGY)/2.
          TAUMAX=SQRT((SIGX-SIGY)**2+4.*TAUXY*TAUXY)/2.
          SIGMAX=STMAX+TAUMAX
          SIGMIN=STMAX-TAUMAX
          PSMAX=ATAN(2.*TAUXY/(SIGX-SIGY))/2.
          PTMAX=ATAN(-(SIGX-SIGY)/2.*TAUXY)/2.
          WRITE(6,112)SIGX
          WRITE(6,113)SIGY
          WRITE(6,114)TAUXY
          WRITE(6,115)SIGMAX
          WRITE(6,116)SIGMIN
          WRITE(6,117)TAUMAX
          WRITE(6,118)PSMAX
          WRITE(6,119)PTMAX
          WRITE(6,120)STMAX
          GO TO 1
99        WRITE(6,101)
          GO TO 1
98        WRITE(6,102)
          GO TO 1
97        WRITE(6,104)
          GO TO 1
          END
          SENTRY

```

APPENDIX F

LIST OF MAJOR INSTRUMENTATION

Strain Indicator (4)	Budd Model P350
Switch and Balance Unit (25)	Budd Model SB-1
Switch and Balance Unit	BLH Type PSBA20 Model 3
Switch and Balance Unit	BLH Type 225
SR-4 Strain Indicator	BLH Type N
10,000-lb. Load Cell	BLH Type U3G1
5,000-lb. Load Cell	BLH Type U3G1
Dial Indicators (10)	Starrett No. 656-617
Calibration Unit	BLH Model 625

APPENDIX G

CALIBRATION OF STRAIN GAGE SYSTEMS

Once the strain gages are attached to the panel, it is not possible to attain a calibration by the use of a known strain situation. The strain gages are manufactured under carefully controlled conditions, and the gage factor for each lot of gages is within about ± 0.27 per cent. The gage factor and the gage resistance make possible a simple method for calibrating the resistance strain gage system. This method consists of determining the system's response to the introduction of a specific small resistance change at the gage and of calculating the resulting equivalent strain. The resistance change is introduced by shunting a relatively high value precision resistor across the gage as shown in the following figure.

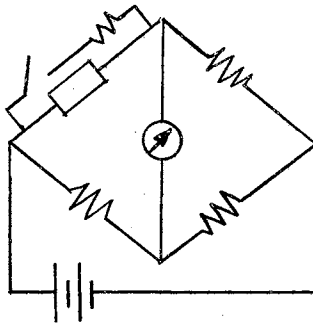


Figure 55. Strain Gage Bridge
With Calibration
Resistor

The equivalent strain for the shunt resistor in parallel with the active gage is

$$\epsilon = \frac{1}{GF} \left(\frac{r_g}{r_g + r_s} \right),$$

where GF = gage factor,

r_g = gage resistance, ohms,

r_s = shunt resistance, ohms.

The Budd portable strain indicator systems were calibrated with a 60K ohm resistor. The resistor was shunted across each active gage.

Direct calibration of an external bridge input by using a known resistance assures maximum accuracy if the gage resistances are known accurately and load resistances are insignificant. The shunt calibration circuit is also helpful to ascertain the error caused by load resistance when long input leads are used.

The maximum variation for any single gage was well within its required accuracy, and 70 per cent of gages were within 2 per cent of the calibration value. Results from the calibration tests are shown in the following table.

TABLE XXVIII
TYPICAL INDICATOR READINGS DURING
CALIBRATION TESTS

Gage Number	Indicator Reading Zero Level	Indicator Reading With Shunt Resistor	Net Change
1004	2770	1757	1013
1010	3757	2747	1010
1014	-39	-1050	1011
1017	795	-222	1017
1022	1507	495	1012
1040	362	-650	1012
1058	-530	-1545	1015
3073	8010	7005	1005
3091	1806	800	1006
2095	-216	-1227	1011

Calibration of Load Recording Equipment

A calibration of the load recording equipment was performed to determine the accuracy of the load application system. The BLH U-3G1 type load cells have strain gages with a gage factor of 2.0 and a resistance of 350 ohms. With a 60K Ω calibration resistor, the computed strain should be 2900.

The calibration was performed from the zero reading for the 5000-pound load cell of 11050. The 60K Ω resistor was shunted across each leg of the strain gage bridge, and the following records were obtained:

<u>Shunt</u>	<u>Dial Reading</u>	<u>Net Change</u>
P ₁ to S ₁	13915	2865
P ₁ to S ₂	8240	2810
P ₂ to S ₁	8180	2870
P ₂ to S ₂	13860	2810

The same procedure was used in calibrating the system for the 10,000-pound load cell. Again, the gage factor of 2.0 and a gage resistance of 350 ohms provide a strain input of 2900. The 60K Ω resistor was shunted across the four arms of the bridge, one arm at a time. The following records were obtained:

<u>Shunt</u>	<u>Dial Reading</u>	<u>Net Change</u>
P ₁ to S ₁	13770	2870
P ₂ to S ₂	8100	2800
P ₂ to S ₁	8030	2870
P ₂ to S ₂	13715	2815

In general, a value of approximately 2800 to 2870 was obtained for each leg of the strain gage bridge. This is a variation of approximately three per cent or corresponds to a gage factor change of from 2.00 to 2.07, which might actually be the gage factor for the strain gages used in the load cell.

The load indicator system was subsequently calibrated with a BLH Model 625 voltage divider unit. A linear change in indicator reading was obtained for a linear change in MV/V input. The load cells have a 3MV/V full scale output which corresponds to 6000 units on the BLH SR-4 indicator.

As a further calibration of the complete load application system, the testing facilities of Halliburton Oil Company, Duncan, Oklahoma,

were utilized.

The author is indebted to Mr. Elwin Seay, Project Engineer, Halliburton Oil Company, and his assistants for their aid in completing the tests.

Both the 5000 LB and 10,000 LB load cells were hooked into a hydraulic testing machine and corresponding readings were made from the BLH Strain Indicator at certain known load values.

Typical load versus indicator readings are shown for the 5000 LB and 10,000 LB load cells in Tables XXIX and XXX.

TABLE XXIX

CALIBRATION OF 5000 LB BLH U-3G1
TYPE LOAD CELL

Bridge Hookup: Full; Resistance Capacity: 350 Ω ; GF = 2.00; Channel: 1

Date: 26 May 66

Known Load From Hydraulic Testing Machine (LB)	BLH Strain Indicator Reading
0	13,370
1,145	14,725
2,170	15,940
3,210	17,175
4,255	18,400
4,775	19,015

TABLE XXX

CALIBRATION OF 10,000 LB BLH U-3G1
TYPE LOAD CELL

Bridge Hookup: Full; Resistance Capacity: 350Ω , GF = 2.00; Channel: 1

Date: 26 May 66

Known Load From Hydraulic Testing Machine (LB)	BLH Strain Indicator Reading
0	17,320
995	17,910
2,995	19,099
5,000	20,291
7,005	21,491
9,500	23,000

APPENDIX H

CALIBRATION OF DIAL INDICATORS

The Starrett Dial Indicators were calibrated with the "0.05" thick size of Fonda Gage Blocks, Unit Set 845, Serial Number N-154, manufactured by the Fonda Gage Company, Inc., Stamford, Connecticut. These blocks are rated at $\pm .000008$ in. accuracy.

Typical readings before and after block insertion and the difference in readings are shown in Table XXXI.

TABLE XXXI

CALIBRATION OF STARRETT DIAL INDICATORS USING A "0.05" THICK FONDA GAGE BLOCK

Dial Gage No.	Reading Before Block Insertion	Reading After Block Insertion	Difference
5	0.1000	0.1506	0.0506
6	0.3140	0.3645	0.0505
7	0.0205	0.0706	0.0501
8	0.1500	0.2003	0.0503
9	0.1000	0.1503	0.0503
10	0.0400	0.0900	0.0500

The maximum error is 1.2 per cent.

VITA

Gordon Campbell Stone

Candidate for the Degree of

Doctor of Philosophy

Thesis: STRESS AND DISPLACEMENT ANALYSIS OF PLANAR STIFFENED SHELL
STRUCTURES

Major Field: Mechanical Engineering

Biographical:

Personal Data: Born in Big Spring, Texas, November 1, 1936, the son of Gordon and Inez Campbell Stone. Married to Martha Gay Fuqua on February 4, 1961. Father of a daughter, Mary Kathryn, born August 26, 1963 and a son, Wilson Gordon, born September 7, 1966.

Education: Attended grade school in Stanton, Texas; graduated from Stanton High School in 1955; received the Bachelor of Science degree in Mechanical Engineering with an Aeronautical option from Southern Methodist University in June, 1960; received the Master of Science degree from Oklahoma State University, with a major in Mechanical Engineering, in May, 1963; completed requirements for the Doctor of Philosophy degree in October, 1966.

Professional Experience: Employed as Junior Engineer by Convair, a Division of General Dynamics Corporation, Ft. Worth, Texas for 18 months during the period September, 1956 through March, 1959 in compliance with the SMU Engineering School's Co-op Plan. Employed as Design Engineer by Standard Manufacturing Co., Inc., Dallas, Texas from June, 1960 to August, 1961. Served as Graduate Assistant in the School of Mechanical Engineering at Oklahoma State University from September, 1962 to August, 1963; Research Assistant in the School of Mechanical Engineering at Oklahoma State University from September, 1964 to September, 1965; Staff Assistant in the School of Mechanical Engineering at Oklahoma State University from September, 1965 to October, 1966.

Organizations: American Institute of Aeronautics and Astronautics